

University of Groningen

Pharmacokinetics and biotransformation of biopharmaceuticals

Bults, Peter

DOI:
[10.33612/diss.206613225](https://doi.org/10.33612/diss.206613225)

IMPORTANT NOTE: You are advised to consult the publisher's version (publisher's PDF) if you wish to cite from it. Please check the document version below.

Document Version
Publisher's PDF, also known as Version of record

Publication date:
2022

[Link to publication in University of Groningen/UMCG research database](#)

Citation for published version (APA):
Bults, P. (2022). *Pharmacokinetics and biotransformation of biopharmaceuticals: by liquid chromatography with unit-mass and high-resolution mass spectrometric detection*. University of Groningen.
<https://doi.org/10.33612/diss.206613225>

Copyright

Other than for strictly personal use, it is not permitted to download or to forward/distribute the text or part of it without the consent of the author(s) and/or copyright holder(s), unless the work is under an open content license (like Creative Commons).

The publication may also be distributed here under the terms of Article 25fa of the Dutch Copyright Act, indicated by the "Taverne" license. More information can be found on the University of Groningen website: <https://www.rug.nl/library/open-access/self-archiving-pure/taverne-amendment>.

Take-down policy

If you believe that this document breaches copyright please contact us providing details, and we will remove access to the work immediately and investigate your claim.

Downloaded from the University of Groningen/UMCG research database (Pure): <http://www.rug.nl/research/portal>. For technical reasons the number of authors shown on this cover page is limited to 10 maximum.

Pharmacokinetics and biotransformation of biopharmaceuticals

by liquid chromatography with unit-mass and high-resolution mass
spectrometric detection

Peter Bults

The research described in this thesis was supported by ICON and partly by the Samenwerkingsverband Noord-Nederland (SNN, grant T3041); the experimental work was carried out at the department of Analytical Biochemistry from the University of Groningen and at the Bioanalytical Laboratory NL - Early Development Services of ICON, located in Assen, The Netherlands.

The author gratefully acknowledges the financial support of the University Library, the Graduate School of Science and Engineering from the University of Groningen, SCIEX and ICON for the printing of this thesis.

© Peter Bults, 2022 All rights reserved. No part of this thesis may be reproduced or transmitted in any form, by any means, without permission of the author.

Provided by thesis specialist Ridderprint, ridderprint.nl

Printing : Ridderprint

Layout and design : Eduard Boxem, persoonlijkproefschrift.nl

ISBN : 978-94-6458-068-6

ISBN (digital) : 978-94-6458-074-7



university of
 groningen

Pharmacokinetics and biotransformation of biopharmaceuticals

by liquid chromatography with unit-mass and high-resolution mass
spectrometric detection

PhD thesis

to obtain the degree of PhD at the
University of Groningen
on the authority of the
Rector Magnificus Prof. C. Wijmenga
and in accordance with
the decision by the College of Deans.

This thesis will be defended in public on

Monday 11 April 2022 at 14:30 hours

by

Peter Bults

born on 15 September 1977

in Borger

Promotores

Prof. dr. N.C. van de Merbel

Prof. dr. R.P.H. Bischoff

Assessment committee

Prof. dr. E.M.J. Verpoorte

Prof. dr. G.W. Somsen

Prof. dr. L. Reubsæet

TABLE OF CONTENTS

Chapter I	General introduction and scope of this thesis.	7
Chapter II	Quantification of biopharmaceuticals and biomarkers in complex biological matrices: a comparison of LC-MS/MS and ligand binding assays. Expert Rev. Proteomics, 2015, 12(4), 355-374, DOI: 10.1586/14789450.2015.1050384	15
Chapter III	LC-MS/MS based monitoring of in vivo protein biotransformation: quantitative determination of trastuzumab and its deamidation products in human plasma. Anal. Chem., 2016, 88(3), 1871-1877, DOI: 10.1021/acs.analchem.5b04276	55
Chapter IV	Analytical and pharmacological consequences of the in vivo deamidation of trastuzumab and pertuzumab. Anal. Bioanal. Chem. (2022), DOI:10.1007/s00216-021-03756-z	95
Chapter V	Intact protein bioanalysis by liquid chromatography – high-resolution mass spectrometry. J. Chromatogr. B-Analyt. Technol. Biomed. Life Sci., 2019, 1110-1111, 155-167, DOI: 10.1016/j.jchromb.2019.01.032	153
Chapter VI	Improving selectivity and sensitivity of protein quantitation by LC-HR-MS/MS: determination of somatropin in rat plasma. Bioanalysis, 2018, 10(13), 1009-1021, DOI: 10.4155/bio-2018-0032	187
Chapter VII	Intact protein quantification in biological samples by liquid chromatography – high resolution mass spectrometry: somatropin in rat plasma. J. Chromatogr. B, 2020, 1144, 122079, DOI: 10.1016/j.jchromb.2020.122079	215
Chapter VIII	Summary	243
Chapter IX	Nederlandse samenvatting	256
	List of publications	264
	Curriculum vitae	266
	Acknowledgments	268

CHAPTER I

General introduction and scope of this thesis

In the past two decades, there has been a considerable increase in the development, marketing and use of protein-based drugs, or biopharmaceuticals, for the treatment of a variety of diseases, such as different types of cancer, auto-immune diseases, growth hormone deficiency, diabetes and cardiovascular disorders. These biopharmaceuticals vary in molecular weight from approximately 5000 dalton (Da) up to several hundred kDa and range from relatively simple linear peptides to structurally complicated, multi-unit proteins, such as enzymes, hormones and antibodies.

To support drug development, patient care and clinical research with biopharmaceuticals, the availability of reliable analytical methods for the quantification of their concentrations in biological samples is essential. While chromatographic methods, and notably liquid chromatography coupled to mass spectrometry (LC-MS), are typically being used for quantification of traditional small-molecule drugs and metabolites, historically ligand binding assays (LBAs) are the gold standard for the analysis of biopharmaceuticals. LBAs are based on the selective recognition of a protein analyte by one or more binding reagents, such as endogenous receptors or (recombinant) antibodies raised against the analyte, and the reason for their popularity is the fact that LBAs are highly sensitive and specific, often fast and easy to use without the need for expensive equipment. There are, however, also several down-sides to the use of LBAs, which are becoming more and more evident. Next to having analytical disadvantages, such as difficulties with multiplexing, limited linear dynamic ranges and less favorable precision and accuracy, LBAs rely on critical binding reagents which may be difficult to obtain or vary in batch-to-batch quality. From a scientific perspective, LBA is essentially a black-box technology and more often than not it is unknown to which part of a protein analyte the reagents exactly bind. Therefore, it is generally difficult to control the consistency of the analytical response of an LBA and to predict or even assess the effect of variations in the composition of critical reagent solutions and sample-to-sample differences with regard to e.g. protein binding or structural modification of the biopharmaceutical protein of interest.

To overcome some of these limitations, over the past ten years much effort has been put into developing LC-MS as a complementary technique for the quantification of biopharmaceuticals in biological matrices. So far, most attention has been devoted to the technical aspects of the analysis of biopharmaceuticals using LC-MS, and mainly to sample preparation, to address the most important limitation of the technique, its relatively unfavorable detection sensitivity. In the vast majority of cases, the LC-MS quantification of biopharmaceuticals is achieved by enzymatically digesting the protein into a series of

peptides and determining the concentration of one or more of these, the so-called signature or surrogate peptides, as a measure for the original, intact protein. By optimization of the sample processing procedure, such as the digestion and extraction steps, the selection of unique surrogate peptides with favorable LC-MS properties, and the use of appropriate internal standards for response normalization, it is now generally possible to accurately quantify biopharmaceuticals in complex biological samples down to low ng/mL levels or below [1-11]. Still, there are some aspects of biopharmaceutical analysis by LC-MS, that have been somewhat neglected over the years and that deserve more attention for further advancement of the field. This thesis focuses on a few of these aspects.

First, now that LC-MS is becoming an established technology for protein quantification, it is increasingly evident that its fundamentally different analytical principle compared to LBAs often leads to different concentration results when both techniques are used to analyze the same samples. Since LC-MS is capable of obtaining detailed structural information, it is ideally suited to investigate the underlying root cause for these differences and to shed more light on the actual meaning of a concentration result for a protein analyte. Chapters II – IV, in the first part of the thesis, focus on the *in vivo* effects that a biopharmaceutical may undergo and on the consequences this has for the concentration result, as determined by LBA and LC-MS. Unlike the situation for small-molecule drugs, where metabolism is extensively studied, protein quantification by LC-MS and LBA has disregarded biotransformation to a large extent and at the start of the research described in this thesis there were hardly any papers to be found about *in-vivo* biotransformation of biopharmaceuticals. The response of both LBA and LC-MS methods, by nature of the technique, is based on specific parts of the protein and does not represent the entire molecule. With LBA analysis, a single read-out is obtained, the magnitude of which depends on the accessibility and intactness of the binding epitope of the analyte of interest. LC-MS uses an enzyme, to cleave the protein into a series of peptides and quantifies just one or a few of these, which may represent only a few percent of the original intact molecule. It is, therefore, not surprising that the concentrations obtained by LC-MS and LBA may differ considerably, depending on the part(s) of the protein to which the methods are directed and on whether or not any structural modifications occur in these parts of the molecule. From the field of biopharmaceutical development, it is well-known that proteins undergo chemical reactions *in vitro* (such as deamidation, isomerization and oxidation) that may very well also occur *in vivo*, thereby changing the molecular structure and possibly also the concentration result.

Chapter II gives an overview of the scientific literature on the differences between LBA and LC-MS for protein quantification. It describes the fundamental analytical principles of both technologies and reviews the sources of protein heterogeneity and the different biotransformation reactions that can take place *in vivo* and *in vitro*. By evaluating published examples, the possible effects are discussed that protein heterogeneity and biotransformation can have on the analytical outcome of a quantitative LBA or LC-MS analysis. Where possible, the discrepancies are explained between LBA and LC-MS results for the same samples, but also between the results obtained with two different LBA or two different LC-MS methods.

This sets the stage for the next two chapters, III and IV, in which one specific but important biotransformation reaction was studied in more detail: the *in vitro* and *in vivo* deamidation of an asparagine (Asn) in the heavy chain of two therapeutic monoclonal antibodies: Asn55 in trastuzumab and Asn54 in pertuzumab. This is relevant because these amino acids are in the center of a complementarity determining region (CDR), which is involved in receptor binding, and their deamidation may therefore influence the pharmacological activity of the proteins. Chapter III focuses on trastuzumab and reports the development and validation of an LC-MS method that is capable of assessing the degree of deamidation of Asn55 to the corresponding aspartate (Asp55) and isoaspartate (isoAsp55) and the reaction intermediate: a succinimide (Asu55). It is shown that substantial *in vivo* deamidation of Asn55 occurs after dosing this biopharmaceutical to breast cancer patients and that all three biotransformation products are present in their plasma samples. Analysis of these samples by an LBA (an anti-idiotypic ELISA) reveals that deamidation of Asn55 in trastuzumab leads to a complete loss of recognition by the assay reagents and, therefore, to a reduced response compared to the responses found by LC-MS. A second, more extensive investigation is described in chapter IV. Since (HER2 positive) breast cancer is increasingly treated by a combination of trastuzumab and pertuzumab, the quantification of these two biopharmaceuticals is reported and a comparison of three analytical platforms is provided: a multiplexed LC-MS method and two LBAs: a receptor-binding assay and an anti-idiotypic ELISA. *In vitro* and *in vivo* deamidation of both biopharmaceutical proteins is demonstrated and, again, a loss of LBA response for the deamidated protein forms. In addition, the results of a cell-based activity assay show that along with the deamidation, the biopharmaceuticals lose their ability to inhibit breast cancer cell growth. In both chapters, full validation of the LC-MS methods according to international bioanalytical guidelines is

reported, showing the feasibility and usefulness of LC-MS as a quantification method for biopharmaceuticals in patient samples.

The second part of the thesis focuses on the instrumental aspects of biopharmaceutical analysis. So far, most protein LC-MS methods are being performed using triple-quadrupole mass spectrometry after sample digestion and further sample processing. This type of mass spectrometry has unit-mass resolution and its use for protein quantification essentially is an extension of the typical approach for small-molecule analysis, which has been routinely applied in laboratories around the globe for the past 25 years. Very little is known about the quantitative possibilities of other, high-resolution mass spectrometry (HRMS) approaches for biopharmaceuticals. HRMS is widely used for qualitative purposes, such as the structural elucidation or confirmation of both small and large molecules, because of its high mass accuracy, but it also offers the option for quantitative analysis. It can thus be used as an alternative detection technique for digested protein analysis with improved selectivity compared to unit-mass resolution MS, and it also is capable of quantifying intact proteins, which is virtually impossible on triple-quadrupole instrumentation. In chapter V, a second review paper is presented which explores the (theoretical) options for intact protein quantification by HRMS. This field is still clearly in its infancy and although the first reports have started to appear, many aspects need to be further developed, from sample preparation to the separation of protein species and the use and interpretation of the highly complex mass spectra.

The final two chapters of this thesis report the results of quantitative LC-MS methods using one particular type of HRMS, a quadrupole-time of flight (Q-TOF) instrument. Chapter VI focuses on the quantification of somatropin (recombinant human growth hormone, rhGH, 22 kDa) in rat plasma after digestion, and focusses especially on the selectivity and sensitivity gains. Reducing the width of the mass-extraction window during data-processing from about 0.7 Da down to 0.01 Da for HRMS considerably decreases the interference of tryptic peptides generated from endogenous matrix proteins. As a result of the better selectivity, four-fold enhanced sensitivity (a lower limit of quantification of 25 ng/mL as compared to 100 ng/mL) was obtained, as well as improved accuracy and precision. The LC-HRMS methodology was validated and used to support a preclinical trial in which somatropin was dosed to rats. In general, it can be concluded that the use of HRMS may lead to a reduced length and complexity of extraction procedures, which are normally needed to remove interfering peptides and/or endogenous compounds from sample digests, and thus to faster sample preparation and results generation.

By using HRMS, somatropin can also be quantified in its intact form in complex biological samples, which is the topic of chapter VII. Intact protein analysis is more challenging for a number of reasons. Traditional sample processing procedures, such as solid phase extraction, are less suitable for intact proteins and the analysis often requires antibody-based capture to selectively isolate the protein of interest. Chromatographic separation and also data processing are more complicated compared with peptide analysis, but it is shown that by optimizing these aspects, intact somatropin can be reliably quantified down to 10 ng/mL in rat plasma. By dedicated software HR mass spectra can be deconvoluted into the corresponding theoretical neutral spectrum, which can also be used as the basis for quantification with equally acceptable method performance. The final method, based on immunocapture of intact somatropin and subsequent LC-HRMS analysis, was validated and applied to the analysis of plasma samples from a pre-clinical study.

REFERENCES

1. Bronsema, K. J.; Bischoff, R.; Pijnappel, W. W. M. P.; Ploeg, A. T. van der; van de Merbel, N. C. Absolute Quantification of the Total and Anti-Drug Antibody-Bound Concentrations of Recombinant Human α -Glucosidase in Human Plasma Using Protein-G Extraction and LC-MS/MS. *Analytical Chemistry*, 2015, 87(8), 4394-4401.
2. Wilffert, D.; Asselman, A.; Donzelli, R.; Hermans, J.; Govorukhina, N.; Quax, W. J.; van de Merbel, N. C.; Bischoff, R. Highly Sensitive Antibody-Free Micro LC-MS/MS Quantification of rhTRAIL in Serum. *Bioanalysis*, 2016, 8(9), 881-890.
3. Wilffert, D. Antibody-Free Workflows for Protein Quantification by LC – MS / MS. *Bioanalysis*, 2015, 7(6), 763-779.
4. Bronsema, K.; Bischoff, R.; Merbel, N. van de. High- Sensitivity LC-MS/MS Quantification of Peptides and Proteins in Complex Biological Samples: The Impact of Enzymatic Digestion and Internal Standard Selection on Method Performance. *Analytical Chemistry*, 2013, 85(20), 9528-9535.
5. Klont, F.; Pouwels, S. D.; Hermans, J.; van de Merbel, N. C.; Horvatovich, P.; ten Hacken, N. H. T.; Bischoff, R. A Fully Validated Liquid Chromatography-Mass Spectrometry Method for the Quantification of the Soluble Receptor of Advanced Glycation End-Products (SRAGE) in Serum Using Immunopurification in a 96-Well Plate Format. *Talanta*, 2018, 182, 414-421.
6. Klont, F.; Hadderingh, M.; Horvatovich, P.; ten Hacken, N. H. T.; Bischoff, R. Affimers as an Alternative to Antibodies in an Affinity LC-MS Assay for Quantification of the Soluble Receptor of Advanced Glycation End-Products (SRAGE) in Human Serum. *Journal of Proteome Research*, 2018, 17(8), 2892-2899.
7. Furlong, M.; Zhao, S.; Mylott, W.; Jenkins, R. Dual Universal Peptide Approach to Bioanalysis of Human Monoclonal Antibody Protein Drug Candidates in Animal Studies. *Bioanalysis*, 2013, 5(11), 1363-1376.
8. Heinig, K.; Wirz, T.; Schick, E.; Guenzi, A. Bioanalysis of Therapeutic Peptides: Differentiating between Total and Anti-Drug Antibody Bound Drug Using Liquid Chromatography-Tandem Mass Spectrometry Quantitation. *Journal of chromatography A*, 2013, 1316, 69-77.
9. Anderson, N. L.; Anderson, N. G.; Haines, L. R.; Hardie, D. B.; Olafson, R. W.; Pearson, T. W. Mass Spectrometric Quantitation of Peptides and Proteins Using Stable Isotope Standards and Capture by Anti-Peptide Antibodies (SISCAPA). *Journal of Proteome Research*, 2004, 3(2), 235-244.
10. Ewles, M.; Goodwin, L. Bioanalytical Approaches to Analyzing Peptides and Proteins by LC-MS/MS. *Bioanalysis*, 2011, 3(12), 1379-1397.
11. van den Broek, I.; Sparidans, R. W.; Schellens, J. H. M.; Beijnen, J. H. Quantitative Bioanalysis of Peptides by Liquid Chromatography Coupled to (Tandem) Mass Spectrometry. *Journal of chromatography B, Analytical technologies in the biomedical and life sciences*, 2008, 872 (1-2), 1-22.

CHAPTER II

Quantification of biopharmaceuticals and biomarkers in complex biological matrices: a comparison of LC-MS/MS and ligand binding assays

Peter Bults^{1,2}, Nico C. van de Merbel^{1,2} and Rainer Bischoff²

¹ *Bioanalytical Laboratory, PRA Health Sciences, Early Development Services, Westerbrink 3, 9405 BJ Assen, The Netherlands*

² *Analytical Biochemistry, Department of Pharmacy, University of Groningen, A. Deusinglaan 1, 9713 AV Groningen, The Netherlands*

Expert Rev. Proteomics, 2015, 12(4), 355-374

ABSTRACT

The quantification of proteins (biopharmaceuticals or biomarkers) in complex biological samples such as blood plasma requires exquisite sensitivity and selectivity, as all biological matrices contain myriads of proteins that are all made of the same 20 proteinogenic amino acids, notwithstanding post-translational modifications. In this review we describe and compare the two main approaches notably ligand binding assays (LBAs) and liquid chromatography coupled to tandem mass spectrometry (LC-MS/MS) in the selected reaction monitoring (SRM) mode. While LBAs remain the most widely used approach, SRM assays are gaining interest up due to their generally better analytical performance (precision & accuracy) and their capacity for multiplex analyses. In this article we focus on the possible reasons for discrepancies between results obtained by LBAs and SRM assays.

2.1 INTRODUCTION

Protein bioanalysis plays an important role in the development of novel biopharmaceuticals, the measurement of clinically relevant biomarkers and many other areas where precise and accurate protein quantification is needed [1-65]. There is, however, a major difference between proteins and low-molecular-weight pharmaceuticals or biomarkers, because proteins are not homogenous single molecules but comprise families of molecules that are grouped under a single denominator. This means that measuring a “protein” is in itself not a meaningful description unless one defines the method it is measured with and the molecular property this method responds too. Recent work in proteomics has shown that proteins occur as “species” or “proteoforms” depending on the nomenclature and definition used [66-73]. This is in itself not new, since work on protein separation by two-dimensional gel electrophoresis (2D-GE) showed that there is hardly any protein in nature that occurs as a single form [66,74-92]. How then to deal with protein heterogeneity when it comes to protein bioanalysis, where regulatory authorities and clinicians expect single defined values for approval of biopharmaceuticals or decision-making based on biomarkers? This conundrum is well-known to proteomics researchers, who experience regularly that LC-MS/MS analyses in the data-dependent, so-called “shotgun proteomics” mode, result in different values for individual peptides regrouped as belonging to a “single protein” according to the database that has been searched. While some proteomics studies resolve this dilemma by defining that the three most intense peptides are representative for the corresponding protein [93-96], this is not always based on sound scientific evidence and rather an “easy way out” to avoid having to deal with protein heterogeneity. Such an approach is not tolerated in regulated bioanalysis of proteins.

2.2 The basis of protein heterogeneity

There are many reasons why proteins are not single-species, homogenous molecules. First of all, there are more than 350 post-translational modifications (PTMs) that have been described, which may affect the physical and chemical properties of proteins [97-99]. Many of these PTMs have an effect on biological activity and function and are thus not only complicating protein bioanalysis but more importantly may have a bearing on the biological function of biopharmaceuticals and biomarkers alike. Next to biologically-induced PTMs, there is also ample opportunity for chemically-induced modifications, since most amino acids contain potentially reactive side chains. Notable examples are the deamidation of

Asn and Gln [100-127], the oxidation of the sulfur-containing amino acids Cys and Met [116,128-145], oxidative modifications of Tyr, Trp or His [130,133,134,146-155] or Tyr and Trp nitration [134,150,151,156-184]. Taken together it is thus not at all surprising that proteins occur as families of molecules rather than single species. In the following we will highlight a few examples to exemplify the versatile chemistry and biochemistry of proteins in view of their analysis. For a more complete overview over PTMs we refer the reader to the excellent book of Walsh [97].

2.2.1 Glycosylation

Protein glycosylation has been widely studied, notably in the context of biopharmaceuticals [88,115,116,136,185-212] and biomarkers for cancer [213-245]. Detailed studies have shown that protein glycosylation may have a significant effect on *in vivo* half-life, the effector function of monoclonal antibodies or the biological activity of hormones such as erythropoietin (EPO) or follicle-stimulating hormone (FSH). Most bioanalytical methods try to avoid targeting regions containing glycosylation sites (e.g. signature peptides for LC-MS/MS or epitopes for antibody recognition) but they must be considered in cases where pharmacodynamic data are required from proteins that depend on proper glycosylation for activity.

While there is a considerable body of literature concerning protein glycosylation when it comes to the detailed characterization of biopharmaceuticals, there is very little about the change in glycosylation and thus in activity or function once a biopharmaceutical protein has been administered. This so-called “protein metabolism” has only recently caught the attention of researchers and regulators alike [246]. Protein metabolism may also influence the results of bioanalytical assays. Changes in glycosylation due to *in vivo* metabolism may, for example, affect the binding of the first and/or second antibody in an ELISA leading to a changed response independent of the absolute protein concentration. On the other hand, an LC-MS/MS assay in the Selected Reaction Monitoring (SRM) mode may not suffer from this change, since the protein is first proteolytically digested and a signature peptide measured that has no glycosylation site. However, LC-MS/MS assays may also be affected, since proteolytic digestion may be affected by whether the protein is glycosylated or not. It is thus not uncommon to find different results for a given “protein” when using an LBA or an SRM assay on the exact same sample. In fact each assay measures part of the family of protein species and these parts may not be congruent as schematically shown in **Figure 1**. Examples will be discussed in the section on Ligand Binding Assays.

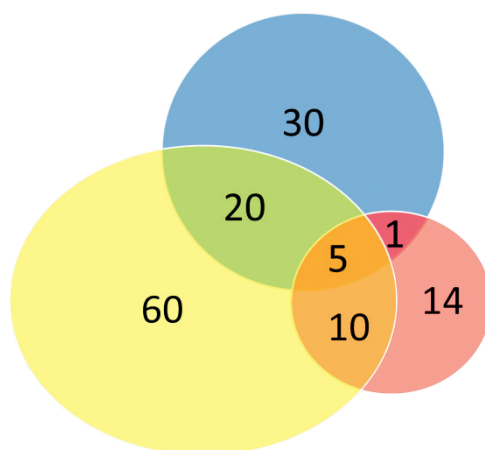


Figure 1: Schematic representation of the hypothetical results of three different assays to quantify a “protein” in a complex biological sample. Blue (Ligand Binding Assay, LBA); Yellow (LC-MS/MS assay, SRM); Red (functional assay, for example a bioassay). The scheme shows that each assay measures a different fraction of the entire group of protein species with more or less overlap between them. This results in different results for different assays for the same sample. There is thus no single value that “quantifies” this protein unless one is sure that an assay covers all protein species.

2.2.2 Deamidation

Deamidation is the conversion of Asn or Gln into Asp or Glu (see **Figure 2**).

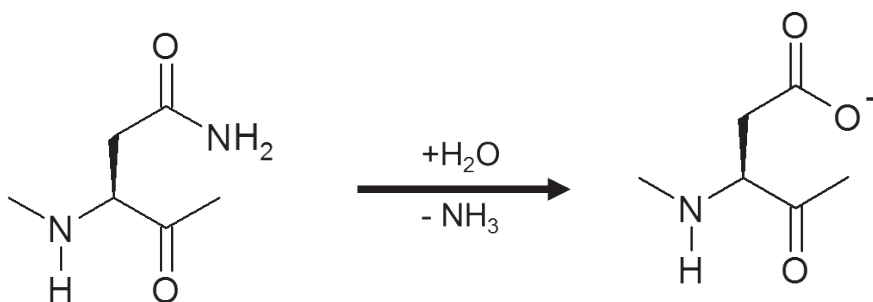


Figure 2: Chemical reaction converting Asn to Asp (deamidation). This conversion introduces an additional negative charge and increases the molecular mass by 1 amu.

Deamidations may occur at basic and at acidic pH values and are facilitated by a sequence context where the amino acid C-terminal to Asn or Gln is small and/or hydrophilic (e.g. Gly or Ser). Most proteins contain sites that are prone to deamidation either *in vivo* or *in vitro*. *In vivo* deamidations, which may be considered part of protein metabolism, have been studied in long-lived proteins such as eye lens crystallines [112,119,120]. There is, however, rather little literature on *in vivo* deamidation, which is likely much more frequent

than reported due to the limited number of studies on *in vivo* protein metabolism. *In vitro* deamidation, on the contrary, has been the subject of many reports including some reviews [100-111,113,114,117,118,121-127]. One of the main reasons is that deamidation forms an “Achilles heel” for many biopharmaceutical proteins with respect to stability during production and storage. The deamidation reaction proceeds via a cyclic imide intermediate and may lead to formation of Asp or iso-Asp (see **Figure 3**). Notably the formation of iso-Asp has been shown to be detrimental to biological activity as reported for the anti-cancer agent Trastuzumab (Herceptin®) [123,136]. We recently showed that this may occur *in vivo* after Trastuzumab administration [247].

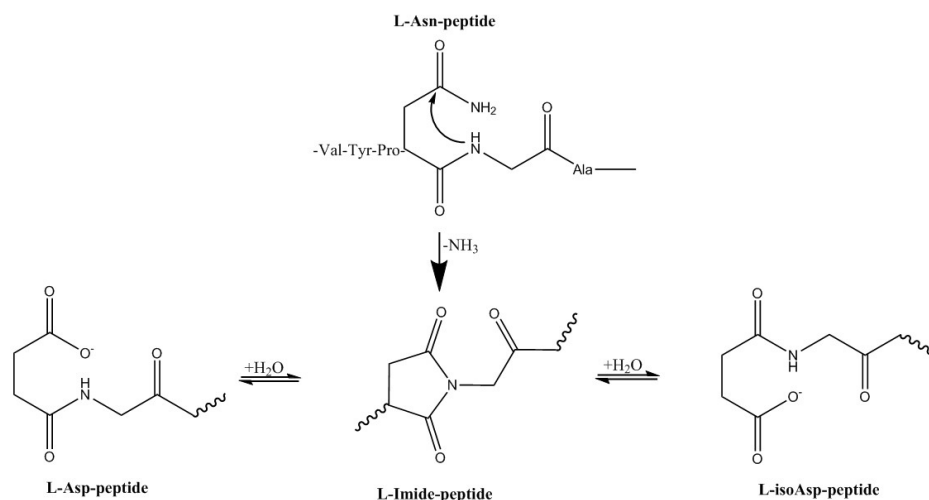


Figure 3: Reaction scheme of the deamidation of a protein or peptide (... - Val-Tyr-Pro-Asn-Ala- ...) to the corresponding Asp- or iso-Asp-containing product. Deamidation proceeds via a cyclic imide intermediate that can open its ring to form Asp or the non-natural iso-Asp. Notably formation of iso-Asp is often detrimental to protein activity and function (reprinted from [127] with permission of the publisher).

2.2.3 Oxidation

There are a number of oxidation-sensitive amino acid residues in proteins [98]. The most notable ones are the sulfur-containing amino acids Cys and Met. Numerous *in vivo* PTMs have been described for Cys including 1- and 2-electron oxidations and alkylations (**Figure 4**).

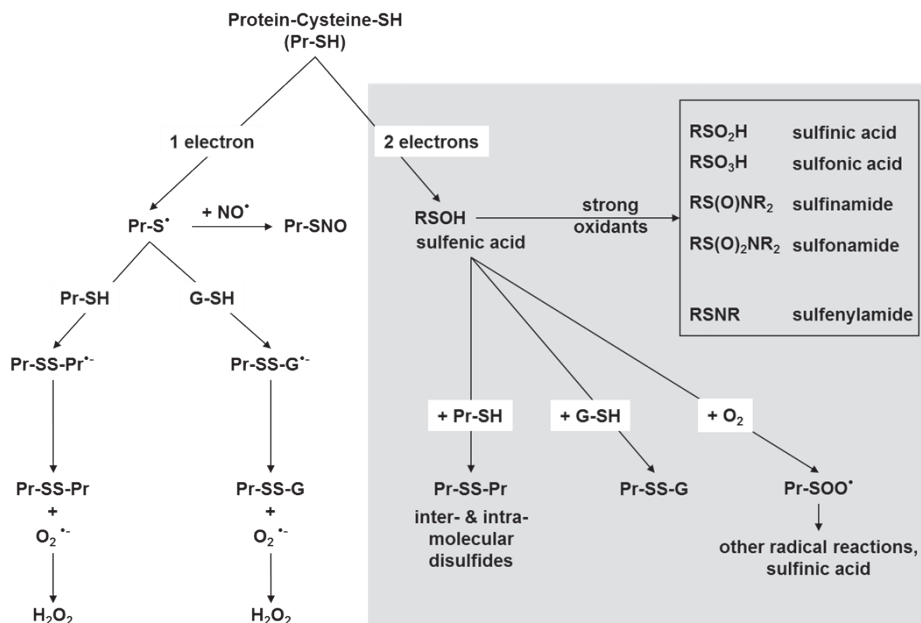


Figure 4: The chemistry of the thiol group of cysteine. Two electron oxidations of a protein thiol (Pr-SH), yield sulfenic acid (Pr-SOH), which is a transient intermediate. With glutathione (GSH) it forms a mixed disulfide (Pr-SS-G), with other cysteines intramolecular or intermolecular disulfides and with adjacent amides it yields a sulfenylamide by condensation. Hypohalous acids, which can be produced *in vivo* by peroxidase-catalyzed reactions of halide ions with H₂O₂, first give rise to sulfenyl halides, which hydrolyze to the sulfenic acid. One electron oxidants, such as radicals or transition metal ions, form the thiyl radical (Pr-S•). The most preferred reaction of this radical under aerobic conditions with a thiolate anion (GSH or protein-SH) yields the disulfide anion radical, which perpetuates the reaction with oxygen forming superoxide. The thiyl radical can also transmit radical reactions or be quenched by scavengers (reproduced from [98] with permission of the publisher).

Tyr and Trp are also sensitive to oxidative conditions that may lead to protein-protein crosslinks and colored amino acid derivatives. A recent report described that the coloring of monoclonal antibodies upon storage may be due to Trp modifications [146]. Oxidations may occur *in vivo* as part of protein metabolism or *in vitro* during production, down-stream processing and storage. The oxidation of Met may occur *in vivo* or *in vitro* and its level is hard to control. That is why Met-containing peptides are generally avoided as signature peptides for LC-MS/MS assays. Deliberate oxidation of Met to its sulfoxide with H₂O₂ may, however, overcome this limitation [55].

2.2.4 Proteolysis

Proteolysis is a common problem during sample preparation of complex protein mixtures and may be avoided by rapid denaturation of all proteases in the sample by heat treatment in the presence of a strong denaturant or by adding a so-called “cocktail” of protease inhibitors. *In vivo* proteolysis is often part of the activation or inactivation of hormones (e.g. the conversion of pro-insulin to insulin) as well as the degradation of proteins back to amino acids. Indeed it is conceivable that most biopharmaceuticals will be metabolized by *in vivo* proteolysis some time after administration but this has not been studied in detail. Proteolysis often commences from the N- or C-termini of proteins by the action of exopeptidases and may occur during protein production in cell culture or microorganisms [185,190,195,205,248]. **Figure 5** shows a trace of the anti-thrombotic agent recombinant hirudin produced in *Saccharomyces cerevisiae*. The earlier and later eluting peaks correspond to C-terminal degradation products missing amino acids 65 and 65 + 64, respectively. There is no indication that these C-terminally truncated products have lower anti-thrombin activity. A notable example of proteolysis is the C-terminal clipping of Lys in the case of monoclonal antibodies [249].

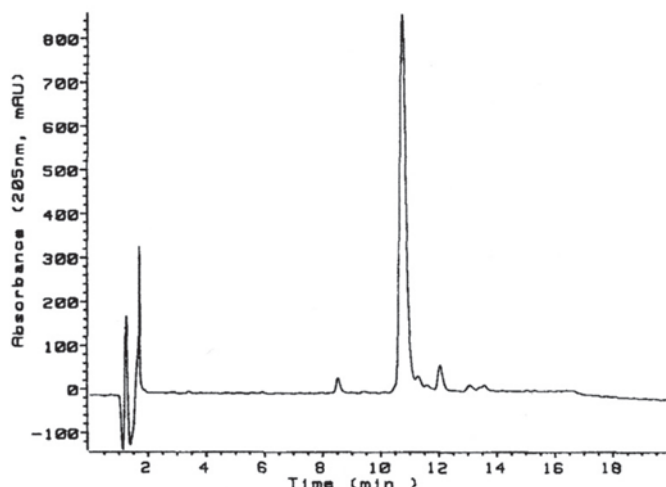


Figure 5: Reversed-phase analysis of recombinant hirudin secreted from *Saccharomyces cerevisiae*. The peaks at 8.5 and 12 min correspond to C-terminal degradation products (reproduced from [248] with permission of the publisher).

2.3 Ligand Binding Assays

Protein bioanalysis in regulated environments is most widely performed by Ligand Binding Assays (LBAs). The fundamental principle of all types of LBAs is similar. The protein of

interest is bound by a capturing agent, often an analyte-directed antibody, which has a high specificity towards a particular part of the analyte structure, called the epitope. The other, non-bound components of the sample are removed by washing steps and the presence of the capturing agent-analyte complex is subsequently detected as a measure for the original analyte concentration in the sample. Detection takes place either via a modified and easily detectable form of the protein analyte, which competes with the analyte for the binding sites on the capturing reagent (single-site or competitive LBA) or by a further complex formation with a detection reagent (two-site or sandwich LBA). In the latter case, the detection reagent typically is a protein that binds with high specificity to the analyte and that is labeled with a detectable tag or with an enzyme, which converts a substrate into a detectable product. Over the years, a variety of LBA formats have been developed, that differ in analytical design, the nature of the capturing and detection reagents and the detection principle. The concentration results for a protein in a biological sample may vary considerably between assays, as they are strongly dependent on the actual LBA format and the reagents that are used for quantitation as well as on the composition of the sample in which the analyte is present.

The capturing and detection reagents in an LBA appear to have the largest effect on the obtained concentrations. Although the detection principle can have a considerable impact on the dynamic range and the sensitivity of an assay as well as on the operational costs, it does not seem to have a large influence on the actual concentration result. In a comparison of two LBA platforms for PEGylated human insulin, for example, essentially similar plasma concentrations were found in a pharmacokinetic study in rats, for an enzyme-linked immunosorbent assay (ELISA) using colorimetric detection and an electrochemiluminescent assay (ECLA) [11]. In both cases, an anti-PEG monoclonal antibody was used as a capturing reagent and a biotinylated anti-insulin antibody as a detection reagent, which was further bound to streptavidin-horseradish peroxidase (ELISA) or streptavidin-SulfoTag (ECLA). Similarly, four LBA platforms were compared for human IgG1 in mouse plasma, using monoclonal antibodies against the constant region of human IgG as both capturing and detection reagents [250]. Colorimetric detection via horseradish peroxidase (ELISA), electrochemiluminescence detection via a ruthenium label (ECLA), fluorescence detection via a fluorophore label and luminescence detection via laser-excitable donor beads all gave the same results for spiked samples.

Sandwich assays are generally considered more specific than competitive assays, because they use two analyte epitopes for binding rather than one. This was clearly

demonstrated for the 28-amino acid peptide ghrelin and its deacylated form in human plasma, for which two competitive and two sandwich assays were compared [251]. The sandwich ELISAs for ghrelin and des-acyl ghrelin yielded concentration values that were up to two-fold lower than those obtained by the corresponding competitive assays, which used comparable capturing reagents. It was suggested that degraded forms of ghrelin and des-acyl ghrelin might be responsible for the difference. These would be bound by the capturing reagents of both assay formats and thus contribute to the response in the competitive assay, but would not be recognized by the detection reagent and thus remain undetected by the sandwich assay. This was confirmed by a forced degradation study, in which full-length ghrelin and des-acyl ghrelin were converted to degradation products by plasma proteases and were undetectable by sandwich assay, but still gave quantifiable results by the competitive LBAs.

The nature of the capturing reagent can also have a considerable effect on protein quantitation, as was shown for a number of therapeutic monoclonal antibodies using LBAs in sandwich format [252]. For ocrelizumab, an assay using a monoclonal antibody for capturing (MAC) and one using a polyclonal antibody for capturing (PAC) were compared and found to give considerably different results, with concentrations being typically two-fold higher for the PAC assay (**Figure 6**). This was attributed to the presence of the pharmacological target CD20 in patient serum, which binds to the exact same epitope of the protein analyte as the capturing monoclonal antibody and thus reduces its detectable concentration. With this assay format the unbound fraction of the drug is therefore detected. The polyclonal capturing antibodies, however, have multiple binding epitopes and will form an immune complex with the analyte not only when it is free but also when it is bound to its target, resulting in the determination of the total drug concentration. A decrease of more than 60% in the observed ocrelizumab concentration was found when recombinant CD20 was added to plasma in a 1000-fold excess and the samples were analyzed using the MAC format. The decrease was negligible when the same samples were analyzed using the PAC assay. Interestingly, no differences were found between the two assay formats for another therapeutic antibody of the same class, v114, suggesting that CD20 and the monoclonal antibody raised against this drug bind to different epitopes on the drug molecule. This example clearly shows that the nature of the capturing reagent and the exact epitope to which it binds determine the concentration result that is obtained by an LBA.

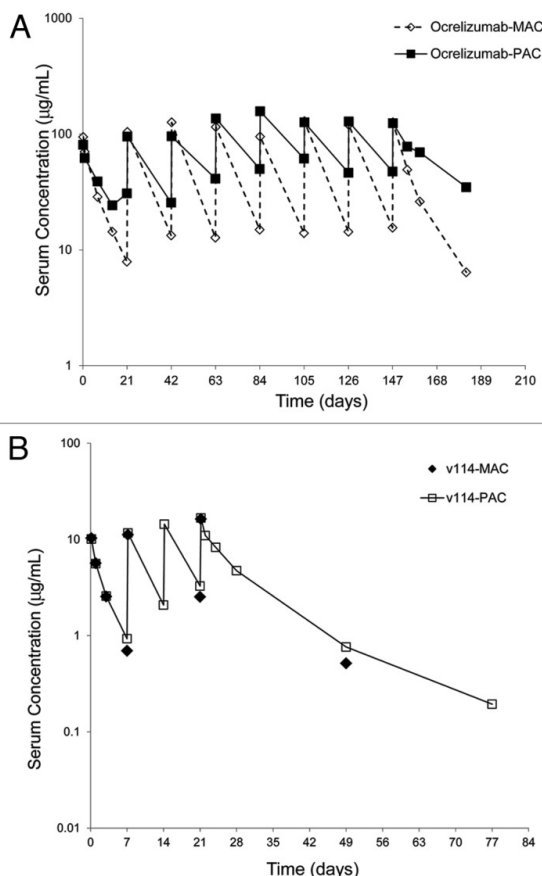


Figure 6: Concentration-time profiles of ocrelizumab (A) and v114 (B) in a clinical study with non-Hodgkin lymphoma patients, obtained by monoclonal (MAC) or polyclonal (PAC) antibody capturing reagents. Capturing ocrelizumab with a MAC suffers from interference due to competition with the pharmacological target CD20 while capturing with a PAC does not suffer from this limitation. Reproduced with permission from [252].

A similar situation was encountered for the therapeutic monoclonal antibody rituximab [270]. Two sandwich ELISAs were performed, the first using the pharmacological target (also CD20) as the capturing reagent and the second an analyte-specific monoclonal antibody. In both cases, the detection reagent was the same: an enzyme-linked monoclonal antibody directed against the constant part (Fc) of human IgG. Diverging results were obtained when pharmacokinetic samples were analyzed, with concentrations generated by the antibody-based method being systematically higher than those obtained by the CD20-based method. Again, circulating CD20, which is elevated in patients, was held responsible

for the discrepancy. By forming a complex with rituximab, it reduces the fraction that is recognized by the capturing reagents. Although this effect plays a role for both ELISAs, the interaction between the capturing monoclonal antibody and rituximab is much stronger than that between CD20 and rituximab and it was speculated that the antibody reagent is able to capture rituximab, even if it is already bound to CD20, probably by displacing CD20. In contrast, the target reagent-based method cannot displace circulating CD20 from rituximab and was concluded to detect only the free fraction of the drug. The presence of CD20 in patient samples may not be the only reason for the higher concentrations obtained with the antibody-based ELISA. Also when rituximab was dosed to healthy mice, whose serum is free from human CD20, about two-fold higher drug levels were obtained than with the CD20-based assay. This was attributed to a possible formation of drug aggregates, which would not be able to bind to the CD20-based capturing reagent. The high affinity of the capturing antibody towards rituximab, on the other hand, might partly or completely overcome this effect. Although it was concluded that the antibody-based method may determine the total concentration of rituximab, it remains unclear whether circulating CD20-bound or aggregated rituximab is really completely captured by this ELISA.

That the detection reagents can also influence the concentration results for a protein was reported for the quantitation of human parathyroid hormone (PTH) in human plasma [253]. Three commercial sandwich assays were compared which used different detection reagents. Two of these employed ^{125}I -labeled anti-PTH antibodies for radioactivity detection and the third an acridinium labeled anti-PTH antibody for luminescence detection. All three assays used the same capturing reagent, polyclonal antibodies against the C-terminal region of PTH, but the detection antibodies had different specificities, as they were raised against different N-terminal parts of the analyte: amino acids 1-34 (method A), 1-6 (method B) and 1-12 (method C), respectively. It was found that the PTH fragments (3-84) and (7-84), which are truncated at the molecule's N-terminus and can be present in plasma at higher concentrations than full-length PTH itself, showed different degrees of cross-reactivity. Both fragments are bound by the capturing reagent and, additionally, recognized by the detection antibody of method A, causing an overestimation of PTH concentrations of about 100% when equal concentrations of PTH and the fragments were present in the sample. Likewise, method C overestimated PTH concentrations by approximately 60% in the presence of an equal concentration of fragment 3-84, but fragment 7-84 only affected PTH concentrations when substantially higher amounts were added. Method B showed no

interference by either of the fragments up to a 50-fold excess and was thus concluded to be the most specific for PTH quantitation.

The selected examples discussed above show that the results obtained by LBAs, which are based on molecular interactions between analyte and reagent(s), may be significantly biased in case a relatively large fraction of the analyte molecules is bound to one or more sample constituents and/or when other molecules, for example proteolytic degradation products, are present in the sample that are also recognized by the capturing or detection reagents. Therefore, proper attention has to be paid to the reagents that are used, in order to guarantee that the obtained concentration results accurately reflect the actual concentrations in the biological samples.

2.4 LC-MS/MS in the SRM mode

The use of LC-MS-based techniques for protein quantification has sharply increased over the past few years. With the development of increasingly sensitive mass spectrometers, LC-MS has become a useful alternative to LBAs for many bioanalytical applications [64,65]. This is mainly driven by its generally better accuracy and precision and the fact that it does not necessarily require immunochemical reagents, which, as illustrated above, may vary in quality and specificity and may thus be the cause of limited comparability of results between or even within LBA platforms [26]. The highest concentration sensitivity is currently still obtained by using triple quadrupole (MS/MS) mass spectrometry, the traditional workhorse for small-molecule quantification, employed in the SRM mode. With this approach, the analyte of interest, after eluting off the LC column, is ionized and based on its mass-to-charge ratio selectively transferred to a collision cell, where it is fragmented and from where a structure-specific fragment is further selected for detection.

This detection principle ensures high selectivity and works very well for relatively small molecular species, up to around 5000 Da, but is inherently less suitable for larger analytes, mainly because their ions are distributed over many different charge states and these also tend to fragment less readily, which reduces sensitivity considerably. An important consequence for protein quantification is that any macromolecular analyte needs to be converted to a smaller compound to allow quantification by LC-MS/MS. This is usually accomplished by digestion of the analyte with an enzyme such as trypsin into a series of peptides. One of these, the so-called proteotypic or signature peptide, is then quantified as a surrogate for the intact protein.

With this approach, the obtained concentration result for a protein depends on the physicochemical and analytical properties of the selected signature peptide. An important feature is the requirement that the signature peptide may not be released from any other protein present in the sample, endogenous or otherwise, as this would lead to overestimation of the concentration of the protein of interest. In addition, many researchers apply rather strict selection criteria for signature peptides to ensure sufficient robustness of the LC-MS/MS assay. Peptides containing amino acids that are unstable or post-translationally modified are typically disregarded, as they would require additional analytical efforts for stabilization or might introduce undesirable heterogeneity. Likewise, peptides that are too small, too large or too hydrophobic may also cause analytical issues because of selectivity or sensitivity limitations or adsorption problems. In everyday practice, it is not uncommon that just a few peptides are considered suitable for LC-MS/MS analysis, out of the several dozens of peptides that may result from the digestion of a typical protein analyte.

Because of all these practical, assay-related limitations, the suitability of the selected signature peptide to properly represent the intact analyte may be compromised. A good way to increase confidence in the result and obtain more detailed information of the *in vivo* fate of a protein is the quantification of multiple signature peptides for a single protein. While common in targeted proteomics, this approach is not widespread in the field of regulated bioanalysis, where scientists are often reluctant to report multiple and potentially diverging concentrations for the same sample to regulatory agencies. An example of good concordance between the results for two signature peptides was reported by Ouyang *et al.* [254], who quantified a large therapeutic protein in monkey plasma after precipitation of plasma proteins with methanol and tryptic digestion of the isolated protein pellet, followed by direct LC-MS/MS analysis of the digest. The average difference between their primary signature peptide and the second, confirmatory peptide was just 0.83% with 39 out of 41 study samples having a relative difference below 15%. They concluded that the almost identical PK profiles obtained using the two peptides suggest that the protein remained intact *in vivo*. In another paper from the same group [19], the general use of a second peptide was proposed to address the inability of a single signature peptide to reliably distinguish between intact and degraded forms of a protein. If the concentrations obtained for two peptides from different regions of the protein remain consistent, it could be concluded that the protein is structurally intact (**Fig. 7A**). Diverging concentrations could be indicative of *in vivo* degradation over time, during which the protein is cleaved

into (at least) two fragments, each containing one of the peptides, which are cleared from the plasma at different rates (**Fig. 7B**). It should be realized, however, that concordant PK profiles could also occur in the case of protein degradation if the resulting fragments with the two signature peptides are cleared at the same rate or if degradation takes place outside the regions containing the signature peptides.

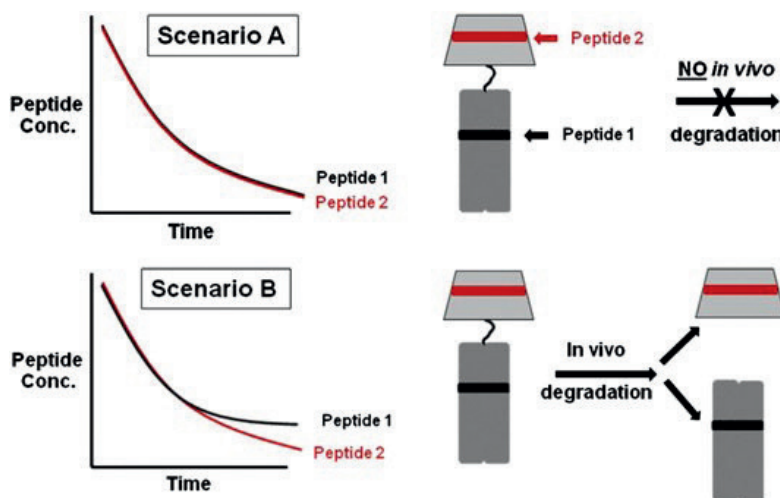


Figure 7: Hypothetical concentration-time profiles obtained by simultaneous quantification of two signature peptides. A: little or no *in vivo* degradation over time, resulting in concordant PK profiles; B: *in vivo* degradation and more rapid clearance of the fragment containing peptide 2, resulting in diverging PK profiles. Reproduced with permission from [19].

The potential disadvantage of protein analysis by a single peptide was demonstrated in a study with a PEGylated therapeutic peptide in human plasma, using the N-terminal (1-12)-peptide for quantification [58]. Sample treatment by protein precipitation and trypsin digestion of the supernatant (in which the analyte was recovered) was compared to immunoaffinity purification with an anti-PEG directed antibody coupled to magnetic beads, followed by on-bead trypsin digestion. Consistently (15-30%) higher concentrations were found with the protein precipitation approach, which was speculated to be caused by *in vivo* dePEGylation to a molecule that contains the same signature peptide as the PEGylated form and which was thus co-quantified with the analyte. Accurate determination of levels of the PEGylated peptide, therefore, requires an extra level of selectivity and this was provided by the immunoaffinity extraction directed towards the PEG moiety of the molecule. Our own group recently showed the usefulness of monitoring two signature peptides for the investigation of the metabolism of the therapeutic monoclonal antibody trastuzumab [247]. One peptide was a metabolically stable part of the protein, while the other contained

an asparagine, which is sensitive to *in vivo* deamidation. Plasma proteins, including the analyte, were precipitated with methanol and subjected to trypsin digestion at a relatively low pH of 7 to prevent *in vitro* deamidation during analysis; the two signature peptides were subsequently quantified by LC-MS/MS. Notable differences for the trastuzumab plasma concentrations were derived from the two peptides, both in an *in vitro* stress test and in samples collected from patients on long-term treatment with trastuzumab. Considerably lower levels were found for the asparagine-containing peptide and this was accompanied by an increase in the concentrations of two deamidated (aspartate and isoaspartate-containing) forms. This result shows that it is an oversimplification to refer to “the” trastuzumab concentration in plasma. In this case, the concentrations obtained using the stable peptide can be considered representative for the total amount of circulating trastuzumab, while the concentrations found with the other peptide represent the amount of drug that remained non-deamidated in this part of the molecule.

2.5 Comparison of LBA and LC-MS/MS

In various papers, newly developed LC-MS/MS methods have been compared to existing LBAs for the same protein. In a few cases, a relatively small (<20%) difference was found between the obtained concentration results. Li *et al.* [255] applied an immunocapture step with an anti-human Fc antibody to selectively extract two therapeutic monoclonal antibodies from rat plasma, prior to reduction, alkylation, digestion and LC-MS/MS analysis of one signature peptide per antibody. The pharmacokinetic results for both analytes corresponded very well to those obtained using an ELISA, with an average deviation of <3%. It was speculated that the similarity of the data could be the result of the same immunocapture reagent that was used for both the LC-MS/MS method and the ELISA. That a good concordance between LC-MS/MS and ELISA can also be found when the extraction principles differ was demonstrated for another monoclonal antibody [18]. Two LC-MS/MS methods were developed, one of which employed an anti-idiotypic antibody and the other protein G to extract the analyte from human serum in samples from a first in human study. The capture reagent used in the ELISA was the pharmacological target mucosal addressin cell adhesion molecule (MAdCAM). Even though all three extraction methods were thus based on different molecular interactions, the concentration results showed a high correlation with an overall bias of <3%. Also when a biological sample is directly digested and analyzed by LC-MS/MS with no prior isolation of the protein analyte, LC-MS/MS and ELISA results can be very similar. A therapeutic nanobody® (28 kDa) was quantified in

rabbit plasma and aqueous humor by digestion of untreated sample, followed by enrichment of the signature peptide by two-dimensional solid-phase extraction (SPE) and LC-MS/MS. Concentration results were on average 3% (plasma) or 16% (aqueous humor) higher than found with a sandwich ELISA which used a monoclonal antibody and a horse radish peroxidase coupled nanobody raised against the therapeutic nanobody as the capture and detection reagents, respectively. As a possible cause for the slightly lower concentrations as determined by ELISA, the potential binding of the analyte to its pharmacological target in the samples was suggested, which might reduce analyte recognition in the ELISA. Likewise, the comparison of an LC-MS/MS method for endogenous insulin-like growth factor-1 (7.7 kDa) in human plasma to a commercial LBA-based clinical analyzer showed similar results [256]. The LC-MS/MS method involved reduction, alkylation, digestion and solid-phase extraction of two signature peptides. The concentrations results for both peptides were typically within 5% from those obtained by the LBA.

More often, there is a higher discrepancy between LBA and LC-MS/MS results. A monoclonal antibody was quantified by ELISA using anti-idiotypic antibodies as both capture and detection reagents and concentrations in monkey plasma were obtained that were about three-fold lower than with an LC-MS/MS method, which was based on immunocapture with an anti-Fc directed antibody (**Figure 8**) [62]. A possible explanation that was advanced was the difference in the capturing reagents. While the anti-Fc reagent in the LC-MS/MS assay captures the analyte both in its free form and when it is bound to its target, the anti-idiotypic antibody used in the ELISA only binds to the analyte when it does not have the target bound to it. Additional experiments showed that the target was present in the sample after the anti-Fc immunocapture step, suggesting that at least part of the captured monoclonal antibody was indeed bound to its target.

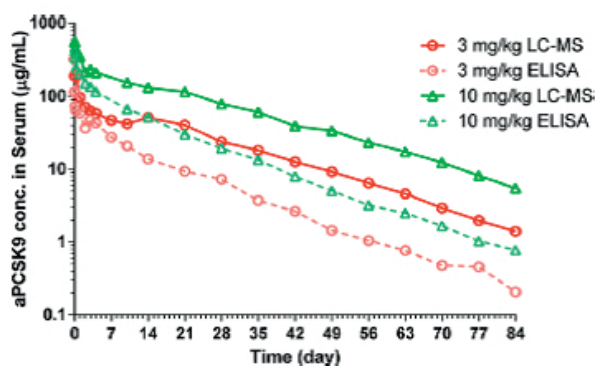


Figure 8: Concentration-time profiles for a monoclonal antibody, administered at two different doses to a monkey, as obtained by ELISA and LC-MS/MS. Reproduced with permission from [62].

The reverse situation was encountered with a method for the endogenous pharmacological target RANKL in preclinical PK studies with the human monoclonal antibody drug denosumab [46]. The commercial ELISA kit that was employed used anti-human RANKL antibodies for capture and detection. The LC-MS method involved addition of an excess of denosumab, extraction of the immune complex of RANKL and denosumab by an immobilized anti-human Fc antibody and subsequent digestion and quantification of a RANKL-specific peptide. While the ELISA provided accurate results in the absence of denosumab, the addition of clinically relevant levels of the drug reduced the response more than 25-fold, very probably because the formed immune complex does no longer bind to the antibodies used as capture and detection reagents. The LC-MS/MS assay, on the other hand, captures the complex via the Fc part of the denosumab molecule and thus actually needed an excess of the drug to completely extract all RANKL from the sample and obtain a reliable estimate of the total concentration of this compound.

The *in vivo* formation of anti-drug antibodies (ADAs) in response to the administration of an exogenous protein drug is a well-known phenomenon, which can have a large impact on the accuracy of concentration results, as has been reported in multiple studies. A monoclonal antibody was quantified in marmoset serum by reduction, alkylation, trypsin digestion and LC-MS/MS analysis of a signature peptide and concentrations were compared to a competitive ELISA, which used an anti-idiotypic antibody for capture [24]. The PK curves obtained after analysis of serum samples from a preclinical study displayed similar profiles but with the LC-MS/MS results being on average 60% higher than the corresponding ELISA results. This was concluded to be due to the presence of ADAs, which form a complex with the drug and thereby reduce its recognition by the ELISA capture

reagent, while >80% of the drug was demonstrated to be digested also in the presence of elevated concentrations of added ADAs. This may not be the only explanation for the discrepancy of the serum concentrations, since the difference was found throughout the PK sampling period after a single dose and ADAs reportedly take some time to be formed after exposition of an organism to exogenous proteins. A more conceivable divergence in the PK profiles as obtained by LC-MS/MS and ELISA was reported for a PEGylated scaffold protein in monkey plasma [257]. In the LC-MS/MS approach, the sample was subjected to differential protein precipitation with isopropanol, digested and analyzed. The ELISA used the pharmacological target as a capture reagent and an anti-PEG directed antibody for detection. The drug concentrations measured by ELISA and LC-MS/MS were very similar (bias <10%) up to 24 hours after a single drug dose to cynomolgus monkeys, but started to diverge for later time-points (**Figure 9**). After 96 hours, the LC-MS/MS results were consistently >30% higher than the ELISA data with the difference increasing to a factor 8 at 504 hours post-dose. The presence of ADAs specific to the antigen-binding region in the PEGylated drug was demonstrated in all samples collected later than 168 hours post-dose and, hence, the discrepancy between ELISA and LC-MS/MS was attributed to the interference of these ADAs with the analyte capture step in the ELISA.

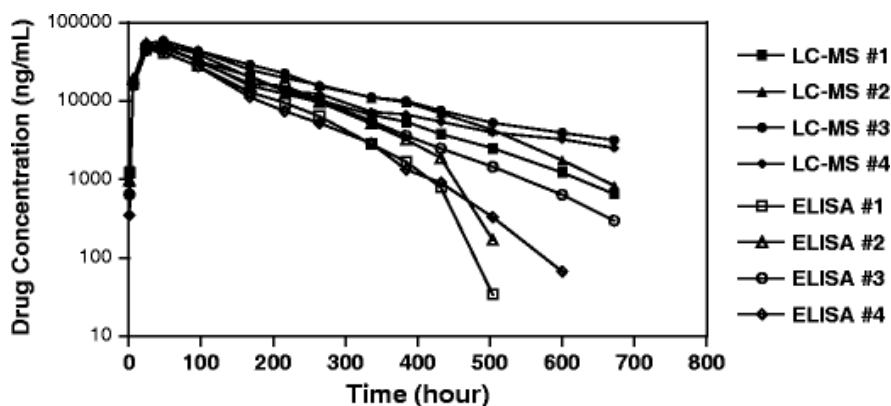


Figure 9: Plasma concentration-time profiles of a PEGylated scaffold protein obtained by LC-MS/MS (closed symbols) or ELISA (open symbols) in four cynomolgus monkeys. Reproduced with permission from [257].

The formation of anti-analyte antibodies does not only play a role for the quantification of biopharmaceuticals but can also be of importance for endogenous biomarkers. The serum concentrations of thyroglobulin (Tg), a biomarker for thyroid carcinoma, increase in the case of (recurring) cancer and can give rise to the development of endogenous anti-

Tg autoantibodies. It has been known for some time that these autoantibodies can mask the Tg epitopes that are involved in binding to the reagent antibodies in immunoassays and thereby lead to falsely low concentration results. A comparison of a commercial immunoanalyzer for Tg and a newly developed LC-MS/MS method showed very similar results for Tg-autoantibody negative serum, but 50% lower levels for the immunoassay when autoantibodies were present. The LC-MS/MS method involved addition of an excess of rabbit anti-Tg antibody to all serum samples and precipitation of the formed complex with ammonium sulfate, followed by the usual reduction, alkylation and digestion steps and purification of the digest with an immunocapture reagent directed towards the signature peptide. In this way, differences between Tg-autoantibody-negative and -positive serum were overcome [34]. These examples illustrate that ELISA often is incapable of measuring the total (free plus target- or ADA-bound) concentration of a protein-based drug or biomarker because the bound fraction typically is not recognized by the reagents in the assay, unless these are specifically designed to bind to parts of the analyte molecule that are not involved in target or ADA binding or the binding is disrupted by some form of manipulation of the sample. LC-MS/MS virtually always contains a digestion step and will break the interaction between the analyte and any other protein present in the sample and this technique therefore gives the total concentration. Large deviations between results obtained with both platforms are, therefore, often related to some sort of *in vivo* binding of the analyte.

There are, however, also other explanations for divergence between LBA and LC-MS/MS. Three commercial LBAs for C-peptide (3.6 kDa) in human plasma showed 50-90% higher concentration levels than a method, which extracted the intact analyte from the sample by SPE and quantified it by LC-MS/MS [258]. In this case, the difference was explained by the heterogeneity in circulating forms, which should be understood as the presence of structurally related molecules, which cross-react with the LBA antibodies and cause an overestimation of the C-peptide concentration. A similar situation was encountered for the iron-regulatory peptide hepcidin, which consists of three isoforms: one bioactive and two truncated, inactive forms [259]. The anti-human hepcidin antibodies employed in a competitive ELISA were unable to discriminate between the three isoforms and overestimated the plasma concentrations about four-fold, when compared to an immunocapture MS-based method. Situations like these are likely to occur in case of insufficiently specific LBA reagents and when significant levels of structurally related peptides or proteins occur in the sample. LC-MS/MS may be expected to provide more

accurate results for peptide analytes, which can be quantified intact, but for proteins this will depend on the choice of the signature peptide. Obviously, if such a peptide occurs in all structurally related molecules, LC-MS/MS will also give a concentration that represents the sum of all these compounds.

Biotransformation of a protein analyte at a critical site in its structure may also be the reason for differing ELISA and LC-MS/MS results. A sandwich ELISA using an anti-idiotypic antibody for both capture and detection of trastuzumab was compared to an LC-MS/MS assay employing two signature peptides [247]. After 56 days of incubation in human plasma at 37°C of 400 µg/mL of trastuzumab, a remaining concentration of just 100 µg/mL was found with the ELISA, while 250 µg/mL was measured by LC-MS/MS using a deamidation-sensitive peptide and the original concentration was still obtained with LC-MS/MS using a stable peptide. It was concluded that the part of the molecule represented by the deamidation-sensitive peptide apparently needs to remain unmodified to effect complete binding to the ELISA reagents. The decrease in the ELISA response was two-fold larger than that of the deamidation-sensitive peptide in the LC-MS/MS method, which was explained by the fact that, like any monoclonal antibody, trastuzumab contains two similar binding sites, that both need to be unmodified to obtain a stable immune-complex and an unaffected response in the ELISA.

Finally, there are situations in which the reason for the differences remains unclear. An example is the measurement of a PEGylated form of insulin, for which about 40% lower results were obtained using two types of LBA than for an LC-MS/MS method [11]. It may be difficult to exactly pinpoint the underlying reason for such discrepancies but the inherent difference in the analytical approach between LBA and LC-MS/MS will certainly play a role. LC-MS/MS is an absolute technique that, for proteins, determines the concentration of a signature peptide, which is a small linear chain of amino acids, typically between 500 and 2000 Da. The concentration result obtained therefore only reflects the unmodified presence of the peptide within the total structure of the protein analyte, or any other protein present in the sample. The intact protein, on the other hand, which may be as large as several 100,000 Da, has a complex three-dimensional and potentially heterogeneous structure, which not only determines its biological activity but also its response in an LBA. Changes in the secondary, tertiary or quaternary structure of the protein may thus very well lead to a modified LBA signal, which would not be seen by LC-MS/MS. Likewise, protein metabolism may also influence the results of bioanalytical assays. For example, an LBA may depend on the recognition of a structural epitope that is stabilized by glycosylation.

Changes in glycosylation due to *in vivo* metabolism may thus affect the binding of the first and/or second antibody in an ELISA. An LC-MS/MS assay may not suffer from this change, since unglycosylated signature peptides are typically selected.

2.6 Final conclusions

Ligand Binding Assays (LBAs) are still the main approach towards quantifying proteins and peptides in complex biological samples, notably blood plasma or serum. However, recent developments in the area of Liquid Chromatography coupled to Tandem Mass Spectrometry (LC-MS/MS) in the Selected Reaction Monitoring (SRM) mode make this technique a viable alternative to LBAs with advantages in terms of performance (accuracy, precision) and the fact that antibodies may not be required. As outlined in this article, there is no right or wrong when it comes to results obtained with LBAs or SRM, since proteins are not single-species analytes but composed of families of molecules. Each analytical technique will therefore give information about one of the many aspects of the protein of interest and, depending on the question that needs to be answered, either LC-MS/MS or LBA will give the most relevant and meaningful readout. Here, it should be realized that two different LC-MS/MS assays or two different LBAs may very well also give different results, depending on the analytical principle of the method. In many cases, a combination of several different methods may be desirable to obtain the required information. In general, LBAs rely on the recognition between an antibody and the target analyte while SRM relies on signature peptides as surrogates for the protein to be analyzed. Chemical or biochemical modifications affecting either the binding site or the signature peptide will thus affect the results of LBAs or SRM assays often to different extents. Interactions of target analytes such as biopharmaceuticals or biomarkers with anti-analyte antibodies or targeted receptors will also affect the results as shown for a number of examples in this review. It is likely that LC-MS/MS will be increasingly used in the bioanalysis of macromolecular pharmaceuticals and biomarkers providing a richer chemical knowledge about these molecules, their *in vivo* fate and the relation between activity and concentration.

Expert commentary: 'vision of the author'

Regulated bioanalysis relies on accurate and reproducible measurements of biologically relevant molecules. Both LBAs and SRM assays can provide such data but it is critical that the limitations and possible interferences are taken into consideration and that results are interpreted with caution. The fact that proteins, be they biomarkers or biopharmaceuticals,

are not homogeneous compounds but comprise families of molecules with different physicochemical properties means that not all members of a given protein family may be detected with an LBA or SRM assay and that results between these assays may differ for the same sample.

Five-year view

As mass spectrometers and chromatography columns continue to improve in terms of sensitivity and efficiency, it is conceivable that LC-MS/MS (e.g. SRM) will play an increasing role in clinical and biopharmaceutical analysis driven by developments in the proteomics community. Notably the capacity of LC-MS/MS to quantify multiple analytes in a single run opens the possibility of measuring patterns of molecules rather than single compounds. This development is already affecting how diagnostic and prognostic assays are set up in clinical chemistry laboratories as well as how the discovery of new predictive molecular signatures is being performed in multifactorial diseases having genetic and environmental influences (e.g. lifestyle-related). Such approaches must be accompanied by corresponding data processing and statistical approaches to arrive at clinical scores that can be translated into routine practice at hospitals across the world. While we are not there yet, it is conceivable that the future will show that personalized medicine will thrive based on such more refined measurements.

On the instrumental level, there is a rapid development of high-sensitivity and fast high-resolution mass spectrometers that may rival currently used triple quadrupole instruments. This has already led to the development of more comprehensive analytical approaches in the protein and metabolite analysis areas [260-266]. Recent comparisons between standard SRM approaches and extracting SRM-like data from comprehensive high-resolution LC-MS/MS analyses that do not rely on precursor ion selection, have shown that the sensitivity gap is narrowing [267].

While mass spectrometry often receives much attention when it comes to innovative analytical approaches, LBAs are also improving and moving ahead in many ways. A number of LBA formats allow the multiplex analysis of a range of analytes (e.g. cytokines) at high throughput and with high sensitivity. LBAs further form the basis for the many formats of biosensors that generate an optical or electric signal upon ligand binding to a target molecule. Biosensors may form the basis for future on-site diagnostics and the rapidly developing market for remote diagnostics via mobile data networks. Last not least LBAs try to enter concentration ranges far beyond current LC-MS/MS approaches based on single molecule detection [268].

REFERENCES

1. An B, Zhang M, Qu J. Toward sensitive and accurate analysis of antibody biotherapeutics by liquid chromatography coupled with mass spectrometry. *Drug Metabolism and Disposition* 42, 1858-1866 (2014).
2. Barton C, Kay RG, Gentzer W. Development of high-throughput chemical extraction techniques and quantitative HPLC-MS/MS (SRM) assays for clinically relevant plasma proteins. *Journal of Proteome Research*, 333-340 (2009).
3. Becker JO, Hoofnagle AN. Replacing immunoassays with tryptic digestion-peptide immunoaffinity enrichment and LC-MS/MS. *Bioanalysis*, 4, 281-290 (2012).
4. Bronsema KJ, Bischoff R, Merbel NCvd. Internal standards in the quantitative determination of protein biopharmaceuticals using liquid chromatography coupled to mass spectrometry. *Journal of Chromatography B*, 893-894, 1-14 (2012).
5. Bronsema KJ, Bischoff R, van de Merbel NC. High-Sensitivity LC-MS/MS Quantification of Peptides and Proteins in Complex Biological Samples: the Impact of Enzymatic Digestion and Internal Standard Selection on Method Performance. *Analytical Chemistry*, 85, 9528-9535 (2013).
6. Bystrom CE, Salameh W, Reitz R, Clarke NJ. Plasma renin activity by LC-MS/MS: development of a prototypical clinical assay reveals a subpopulation of human plasma samples with substantial peptidase activity. *Clinical Chemistry*, 56, 1561-1569 (2010).
7. Campbell JL, Blanc JCYL. Peptide and protein drug analysis by MS: challenges and opportunities for the discovery environment. *Bioanalysis*, 3, 645-657 (2011).
8. Chappell DL, Lassman ME, McAvoy T, Lin M, Spellman DS, Laterza OF. Quantitation of human peptides and proteins via MS: review of analytically validated assays. *Bioanalysis*, 6, 1843-1857 (2014).
9. Damen CWN, Schellens JHM, Beijnen JH. Bioanalytical methods for the quantification of therapeutic monoclonal antibodies and their application in clinical pharmacokinetic studies. *Human Antibodies*, 18, 47-73 (2009).
10. Dawes ML, Gu H, Wang J, Schuster AE, Haulenbeek J. Development of a validated liquid chromatography tandem mass spectrometry assay for a PEGylated adnectin in cynomolgus monkey plasma using protein precipitation and trypsin digestion. *Journal of Chromatography B*, 934, 1-7 (2013).
11. de Dios K, Manibusan A, Marsden R, Pinkstaff J. Comparison of bioanalytical methods for the quantitation of PEGylated human insulin. *Journal of Immunological methods*, 396, 1-7 (2013).
12. Delinsky DC, Hill KT. Quantitation of the large polypeptide glucagon by protein precipitation and LC/MS. *Biomedical Chromatography*, 18, 700-705 (2004).
13. Dillen L, Cools W, Vereyken L. Comparison of triple quadrupole and high-resolution TOF-MS for quantification of peptides. *Bioanalysis*, 4, 565-579 (2012).
14. Dufield DR, Radabaugh MR. Online immunoaffinity LC/MS/MS. A general method to increase sensitivity and specificity: How do you do it and what do you need? *Methods*, 56, 236-245 (2012).
15. Ewles M, Goodwin L. Bioanalytical approaches to analyzing peptides and proteins by LC-MS/MS. *Bioanalysis*, 3, 1379-1397 (2011).
16. Ezan E, Bitsch F. Critical comparison of MS and immunoassays for the bioanalysis of therapeutic antibodies. *Bioanalysis*, 1375-1388 (2009).
17. Ezan E, Dubois M, Becher F. Bioanalysis of recombinant proteins and antibodies by mass spectrometry. *The Analyst*, 134, 825-834 (2009).
18. Fernández Ocaña M, James IT, Kabir M *et al.* Clinical pharmacokinetic assessment of an anti-MAdCAM monoclonal antibody therapeutic by LC-MS/MS. *Analytical Chemistry*, 84, 5959-5967 (2012).

19. Furlong MT, Ouyang Z, Wu S *et al.* A universal surrogate peptide to enable LC-MS/MS bioanalysis of a diversity of human monoclonal antibody and human Fc-fusion protein drug candidates in pre-clinical animal studies. *Biomedical Chromatography*, 26, 1024-1032 (2012).
20. Furlong MT, Titsch C, Xu W, Jiang H, Jemal M, Zeng J. An exploratory universal LC-MS/MS assay for bioanalysis of hinge region-stabilized human IgG4 mAbs in clinical studies. *Bioanalysis*, 6, 1747-1758 (2014).
21. Furlong MT, Zhao S, Mylott W, Jenkins R. Dual universal peptide approach to bioanalysis of human monoclonal antibody protein drug candidates in animal studies. *Bioanalysis*, 5, 1363-1376 (2013).
22. Halquist MS, Karnes HT. Quantification of Alefacept, an immunosuppressive fusion protein in human plasma using a protein analogue internal standard, trypsin cleaved signature peptides and liquid chromatography tandem mass spectrometry. *Journal of Chromatography B*, 879, 789-798 (2011).
23. Heinig K, Wirz T, Schick E, Guenzi A. Bioanalysis of therapeutic peptides: differentiating between total and anti-drug antibody bound drug using liquid chromatography-tandem mass spectrometry quantitation. *Journal of Chromatography. A*, 1316, 69-77 (2013).
24. Heudi O, Barteau S, Zimmer D *et al.* Towards absolute quantification of therapeutic monoclonal antibody in serum by LC-MS/MS using isotope-labeled antibody standard and protein cleavage isotope dilution mass spectrometry. *Analytical Chemistry*, 80, 4200-4207 (2008).
25. Hoofnagle AN, Becker JO, Wener MH, Heinecke JW. Quantification of thyroglobulin, a low-abundance serum protein, by immunoaffinity peptide enrichment and tandem mass spectrometry. *Clinical Chemistry*, 54(11), 1796-1804 (2008).
26. Hoofnagle AN, Wener MH. The fundamental flaws of immunoassays and potential solutions using tandem mass spectrometry. *Journal of Immunological Methods*, 347, 3-11 (2009).
27. Ji C, Sadagopan N, Zhang Y, Lepsy C. A universal strategy for development of a method for absolute quantification of therapeutic monoclonal antibodies in biological matrices using differential dimethyl labeling coupled with ultra performance liquid chromatography-tandem mass spectrometry. *Analytical Chemistry*, 81, 9321-9328 (2009).
28. Ji QC, Rodila R, Gage EM, El-Shourbagy Ta. A strategy of plasma protein quantitation by selective reaction monitoring of an intact protein. *Analytical Chemistry*, 75, 7008-7014 (2003).
29. Jiang H, Zeng J, Titsch C *et al.* Fully validated LC-MS/MS assay for the simultaneous quantitation of coadministered therapeutic antibodies in cynomolgus monkey serum. *Analytical Chemistry*, 85, 9859-9867 (2013).
30. Kirsch S, Widart J, Louette J, Focant J-F, De Pauw E. Development of an absolute quantification method targeting growth hormone biomarkers using liquid chromatography coupled to isotope dilution mass spectrometry. *Journal of Chromatography. A*, 1153, 300-306 (2007).
31. Kleemann GR, Beierle J, Nichols AC, Dillon TM, Pipes GD, Bondarenko PV. Characterization of IgG1 immunoglobulins and peptide-Fc fusion proteins by limited proteolysis in conjunction with LC-MS. *Analytical Chemistry*, 80, 2001-2009 (2008).
32. Knutsson M, Schmidt R, Timmerman P. LC-MS/MS of large molecules in a regulated bioanalytical environment - which acceptance criteria to apply? *Bioanalysis*, 5, 2211-2214 (2013).
33. Kumar V, Barnidge DR, Chen L-S *et al.* Quantification of serum 1-84 parathyroid hormone in patients with hyperparathyroidism by immunocapture in situ digestion liquid chromatography-tandem mass spectrometry. *Clinical Chemistry*, 56, 306-313 (2010).
34. Kushnir MM, Rockwood AL, Roberts WL, Abraham D, Hoofnagle AN, Meikle aW. Measurement of thyroglobulin by liquid chromatography-tandem mass spectrometry in serum and plasma in the presence of antithyroglobulin autoantibodies. *Clinical Chemistry*, 59, 982-990 (2013).
35. Lee JW, Kelley M, King LE *et al.* White Paper Bioanalytical Approaches to Quantify "Total" and "Free" Therapeutic Antibodies and Their Targets : Technical Challenges and PK / PD Applications Over the Course of Drug Development. *The AAPS Journal*, 13, 99-110 (2011).

36. Li F, Fast D, Michael S. Absolute quantitation of protein therapeutics in biological matrices by enzymatic digestion and LC-MS. *Bioanalysis*, 3, 2459-2480 (2011).
37. Li H, Ortiz R, Tran L *et al.* General LC-MS/MS method approach to quantify therapeutic monoclonal antibodies using a common whole antibody internal standard with application to preclinical studies. *Analytical Chemistry*, 84, 1267-1273 (2012).
38. Li H, Ortiz R, Tran LTB, Salimi-Moosavi H. Simultaneous Analysis of Multiple Monoclonal Antibody Biotherapeutics by LC-MS/MS Method in Rat Plasma Following Cassette-Dosing. *The AAPS Journal*, 15, 1267-1273 (2013).
39. Lin M, Lassman ME, Weiner R, Laterza OF. Development and fit-for-purpose validation of a LC-MS/MS assay for fibrinogen peptide A quantitation in human plasma. *Bioanalysis*, 6, 1759-1766 (2014).
40. Liu H, Manuilov AV, Chumsae C, Babineau ML, Tarcza E. Quantitation of a recombinant monoclonal antibody in monkey serum by liquid chromatography-mass spectrometry. *Analytical Biochemistry*, 414, 147-153 (2011).
41. Lu Q, Zheng X, McIntosh T *et al.* Development of different analysis platforms with LC-MS for pharmacokinetic studies of protein drugs. *Analytical Chemistry*, 81, 8715-8723 (2009).
42. Mekhssian K, Mess J-N, Garofolo F. Application of high-resolution MS in the quantification of a therapeutic monoclonal antibody in human plasma. *Bioanalysis*, 6, 1767-1779 (2014).
43. Nelson RW, Nedelkov D, Tubbs KA, Kiernan UA. Quantitative Mass Spectrometric Immunoassay of Insulin Like Growth Factor 1 research articles. *Journal of Proteome Research*, 3, 851-855 (2004).
44. Nouri-Nigjeh E, Zhang M, Ji T, Yu H. Effects of Calibration Approaches on the Accuracy for LC-MS Targeted Quantification of Therapeutic Protein. *Analytical Chemistry*, 86, 3575-3584 (2014).
45. Nowatzke WL, Rogers K, Wells E, Bowsher RR, Ray C, Unger S. Unique challenges of providing bioanalytical support for biological therapeutic pharmacokinetic programs. *Bioanalysis*, 3, 509-521 (2011).
46. Onami I, Ayabe M, Murao N, Ishigai M. A versatile method for protein-based antigen bioanalysis in non-clinical pharmacokinetics studies of a human monoclonal antibody drug by an immunoaffinity liquid chromatography-tandem mass spectrometry. *Journal of Chromatography A*, 1334, 64-71 (2014).
47. Pan S, Aebersold R, Chen R. Mass spectrometry based targeted protein quantification: methods and applications. *Journal of Proteome Research*, 8, 787-797 (2008).
48. Rauh M. LC-MS/MS for protein and peptide quantification in clinical chemistry. *Journal of Chromatography B*, 883-884, 59-67 (2012).
49. Sandra K, Mortier K, Jorge L *et al.* LC-MS/MS quantification of next-generation biotherapeutics: a case study for an IgE binding Nanobody in cynomolgus monkey plasma. *Bioanalysis*, 6, 1201-1213 (2014).
50. van de Merbel NC, Bronsema KJ, Nemansky M. Protein quantification using LC-MS: can it make a difference? *Bioanalysis*, 4, 2113-2116 (2012).
51. van den Broek I, Sparidans RW, Schellens JHM, Beijnen JH. Quantitative bioanalysis of peptides by liquid chromatography coupled to (tandem) mass spectrometry. *Journal of Chromatography B*, 872, 1-22 (2008).
52. Vazvaei F, Duggan JX. Validation of LC-MS/MS bioanalytical methods for protein therapeutics. *Bioanalysis*, 6, 1739-1742 (2014).
53. Wang Y, Qu Y, Bellows CL, Ahn JS, Burkey JL, Taylor SW. Simultaneous quantification of davalintide, a novel amylin-mimetic peptide, and its active metabolite in beagle and rat plasma by online SPE and LC-MS/MS. *Bioanalysis*, 4, 2141-2152 (2012).
54. Whiteaker JR, Zhao L. An automated and multiplexed method for high throughput peptide immunoaffinity enrichment and multiple reaction monitoring mass spectrometry-based quantification. *Molecular & Cellular Proteomics*, 9, 184-196 (2010).

55. Wilffert D, Reis CR, Hermans J *et al.* Antibody-free LC-MS/MS quantification of rhTRAIL in human and mouse serum. *Analytical Chemistry*, 85, 10754-10760 (2013).
56. Wright K, Dufield D. Minimalistic sample preparation strategies for LC-MS quantification of large molecule biopharmaceuticals: a case study highlighting alpha-1 antitrypsin protein. *Bioanalysis*, 6, 1813-1825 (2014).
57. Xu K, Liu L, Maia M *et al.* A multiplexed hybrid LC-MS/MS pharmacokinetic assay to measure two co-administered monoclonal antibodies in a clinical study. *Bioanalysis*, 6, 1781-1794 (2014).
58. Xu Y, Mehl JT, Bakhtiar R, Woolf EJ. Immunoaffinity purification using anti-PEG antibody followed by two-dimensional liquid chromatography/tandem mass spectrometry for the quantification of a PEGylated therapeutic peptide in human plasma. *Analytical Chemistry*, 82, 6877-6886 (2010).
59. Yang Z, Hayes M, Fang X, Daley MP, Ettenberg S, Tse FLS. LC-MS/MS approach for quantification of therapeutic proteins in plasma using a protein internal standard and 2D-solid-phase extraction cleanup. *Analytical Chemistry*, 79, 9294-9301 (2007).
60. Yang Z, Ke J, Hayes M, Bryant M, Tse FLS. A sensitive and high-throughput LC-MS/MS method for the quantification of pegylated-interferon-alpha2a in human serum using monolithic C18 solid phase extraction for enrichment. *Journal of Chromatography B*, 877, 1737-1742 (2009).
61. Yuan L, Aubry A-F, Arnold ME, Ji QC. Systematic investigation of orthogonal SPE sample preparation for the LC-MS/MS bioanalysis of a monoclonal antibody after pellet digestion. *Bioanalysis*, 5, 2379-2391 (2013).
62. Zhang Q, Spellman DS, Song Y *et al.* Generic automated method for liquid chromatography-multiple reaction monitoring mass spectrometry based monoclonal antibody quantitation for preclinical pharmacokinetic studies. *Analytical Chemistry*, 86, 8776-8784 (2014).
63. Zheng J, Mehl J, Zhu Y, Xin B, Olah T. Application and challenges in using LC-MS assays for absolute quantitative analysis of therapeutic proteins in drug discovery. *Bioanalysis*, 6, 859-879 (2014).
64. Bischoff R, Bronsema KJ, van de Merbel NC. Analysis of biopharmaceutical proteins in biological matrices by LC-MS/MS I. Sample preparation. *TrAC Trends in Analytical Chemistry*, 48, 41-51 (2013).
65. Hopfgartner G, Lesur A, Varesio E. Analysis of biopharmaceutical proteins in biological matrices by LC-MS/MS II. LC-MS/MS analysis. *TrAC Trends in Analytical Chemistry*, 48, 52-61 (2013).
66. Jungblut PR, Holzthutter HG, Apweiler R, Schluter H. The speciation of the proteome. *Chemistry Central Journal*, 2:16, doi:10.1186/1752-153X-2-16 (2008).
67. Schluter H, Apweiler R, Holzthutter HG, Jungblut PR. Finding one's way in proteomics: a protein species nomenclature. *Chem Cent.J.*, 3:11, doi:10.1186/1752-153X-3-11 (2009).
68. Foster MW, Thompson JW, Ledford JG *et al.* Identification and Quantitation of Coding Variants and Isoforms of Pulmonary Surfactant Protein A. *Journal of Proteome Research*, 13, 3722-3732 (2014).
69. Lisitsa A, Moshkovskii S, Chernobrovkin A, Ponomarenko E, Archakov A. Profiling proteoforms: Promising follow-up of proteomics for biomarker discovery. *Expert Review of Proteomics*, 11, 121-129 (2014).
70. Yang Y, Barendregt A, Kamerling JP, Heck AJR. Analyzing Protein Micro-Heterogeneity in Chicken Ovalbumin by High-Resolution Native Mass Spectrometry Exposes Qualitatively and Semi-Quantitatively 59 Proteoforms. *Analytical Chemistry*, 85, 12037-12045 (2013).
71. Smith LM, Kelleher NL. Proteoform: a single term describing protein complexity. *Nature Methods*, 10, 186-187 (2013).
72. Vegvari A, Sjodin K, Rezeli M *et al.* Identification of a Novel Proteoform of Prostate Specific Antigen (SNP-L132I) in Clinical Samples by Multiple Reaction Monitoring. *Molecular & Cellular Proteomics*, 12, 2761-2773 (2013).
73. Liu X, Hengel S, Wu S, Tolic N, Pasa-Tolic L, Pevzner PA. Identification of Ultramodified Proteins Using Top-Down Tandem Mass Spectra. *Journal of Proteome Research*, 12(12), 5830-5838 (2013).

74. Steel LF, Haab BB, Hanash SM. Methods of comparative proteomic profiling for disease diagnostics. *Journal of Chromatography B*, 815, 275-284 (2005).
75. Huang X, Wei Y, Li L *et al.* Serum proteomics study of the squamous cell carcinoma antigen 1 in tongue cancer. *Oral Oncology*, 42, 26-31 (2005).
76. Yoo BS, Regnier FE. Proteomic analysis of carbonylated proteins in two-dimensional gel electrophoresis using avidin-fluorescein affinity staining. *Electrophoresis*, 25(9), 1334-1341 (2004).
77. Terry DE, Desiderio DM. Between-gel reproducibility of the human cerebrospinal fluid proteome. *Proteomics*, 3, 1962-1979 (2003).
78. Garfin DE. Two-dimensional gel electrophoresis: an overview. *TrAC Trends in Analytical Chemistry*, 22, 263-272 (2003).
79. Caldini A, Moneti G, Fanelli A *et al.* Epoetin alpha, epoetin beta and darbepoetin alfa: two-dimensional gel electrophoresis isoforms characterization and mass spectrometry analysis. *Proteomics*, 3, 937-941 (2003).
80. Beranova-Giorgianni S. Proteome analysis by two-dimensional gel electrophoresis and mass spectrometry: strengths and limitations. *TrAC Trends in Analytical Chemistry*, 22, 273-281 (2003).
81. Galeva N, Altermann M. Comparison of one-dimensional and two-dimensional gel electrophoresis as a separation tool for proteomic analysis of rat liver microsomes: Cytochromes P450 and other membrane proteins. *Proteomics*, 2, 713-722 (2002).
82. Pan T, Colucci M, Wong BS *et al.* Novel Differences between Two Human Prion Strains Revealed by Two-dimensional Gel Electrophoresis. *Journal of Biological Chemistry*, 276, 37284-37288 (2001).
83. Gygi SP, Corthals GL, Zhang Y, Rochon Y, Aebersold R. Evaluation of two-dimensional gel electrophoresis-based proteome analysis technology. *Proceedings of the National Academy of Sciences*, 97, 9390-9395 (2000).
84. Cordwell SJ, Nouwens AS, Verrills NM, Basseal DJ, Walsh BJ. Subproteomics based upon protein cellular location and relative solubilities in conjunction with composite two-dimensional electrophoresis gels. *Electrophoresis*, 21, 1094-1103 (2000).
85. Celis JE, Gromov P. 2D protein electrophoresis: can it be perfected? *Current Opinion in Biotechnology*, 10, 16-21 (1999).
86. Wilkins MR, Gasteiger E, Sanchez JC, Bairoch A, Hochstrasser DF. Two-dimensional gel electrophoresis for proteome projects: The effects of protein hydrophobicity and copy number. *Electrophoresis*, 19, 1501-1505 (1998).
87. Rabilloud T. Use of thiourea to increase the solubility of membrane proteins in two-dimensional electrophoresis. *Electrophoresis*, 19, 758-760 (1998).
88. Packer NH, Lawson MA, Jardine DR, Sanchez JC, Gooley A. Analyzing glycoproteins separated by two-dimensional gel electrophoresis. *Electrophoresis*, 19, 981-988 (1998).
89. Fountoulakis M, Takacs B, Langen H. Two-dimensional map of basic proteins of Haemophilus influenzae. *Electrophoresis*, 19, 761-766 (1998).
90. Rosenfeld J, Capdevielle J, Guillemot JC, Ferrara P. In-gel digestion of proteins for internal sequence analysis after one- or two-dimensional gel electrophoresis. *Analytical Biochemistry*, 203, 173-179 (1992).
91. Schubach J, Ammann RW, Freiburghaus AU. A universal method for two-dimensional polyacrylamide gel electrophoresis of membrane proteins using isoelectric focusing on immobilized pH gradients in the first dimension. *Analytical Biochemistry*, 196, 337-343 (1991).
92. Hochstrasser DF, Harrington MG, Hochstrasser AC, Miller MJ, Merril CR. Methods for increasing the resolution of two-dimensional protein electrophoresis. *Analytical Biochemistry*, 173, 424-435 (1988).

93. Silva JC, Gorenstein MV, Li GZ, Vissers JPC, Geromanos SJ. Absolute Quantification of Proteins by LCMSE: A Virtue of Parallel ms Acquisition. *Molecular Cellular Proteomics*, 5, 144-156 (2006).
94. Fabre B, Lambour T, Bouyssie D *et al.* Comparison of label-free quantification methods for the determination of protein complexes subunits stoichiometry. *EuPA Open Proteomics*, 4, 82-86 (2014).
95. Krey JF, Wilmarth PA, Shin JB *et al.* Accurate label-free protein quantitation with high- and low-resolution mass spectrometers. *Journal of Proteome Research*, 13, 1034-1044 (2014).
96. Ahrne E, Molzahn L, Glatter T, Schmidt A. Critical assessment of proteome-wide label-free absolute abundance estimation strategies. *Proteomics*, 13, 2567-2578 (2013).
97. Walsh CT. *Posttranslational modifications of proteins: expanding nature's inventory* (Roberts and Company Publishers, 2006).
98. Bischoff R, Schlüter H. Amino acids: Chemistry, functionality and selected non-enzymatic post-translational modifications. *Journal of Proteomics*, 75, 2275-2296 (2012).
99. Walsh CT, Garneau-Tsodikova S, Gatto J. Protein posttranslational modifications: The chemistry of proteome diversifications. *Angewandte Chemie - International Edition*, 44, 7342-7372 (2005).
100. Wang S, Kaltashov IA. An 18O-Labeling Assisted LC/MS Method for Assignment of Aspartyl/Isoaspartyl Products from Asn Deamidation and Asp Isomerization in Proteins. *Analytical Chemistry*, 85, 6446-6452 (2013).
101. Shimura K, Hoshino M, Kamiya K *et al.* Estimation of the Deamidation Rates of Major Deamidation Sites in a Fab Fragment of Mouse IgG1-k by Capillary Isoelectric Focusing of Mutated Fab Fragments. *Analytical Chemistry*, 85, 1705-1710 (2013).
102. Nepomuceno AI, Gibson RJ, Randall SM, Muddiman DC. Accurate Identification of Deamidated Peptides in Global Proteomics Using a Quadrupole Orbitrap Mass Spectrometer. *Journal of Proteome Research*, 13, 777-785 (2013).
103. Palmisano G, Melo-Braga MN, Engholm-Keller K, Parker BL, Larsen MR. Chemical Deamidation: A Common Pitfall in Large-Scale N-Linked Glycoproteomic Mass Spectrometry-Based Analyses. *Journal of Proteome Research*, 11, 1949-1957 (2012).
104. Du Y, Wang F, May K, Xu W, Liu H. Determination of Deamidation Artifacts Introduced by Sample Preparation Using 18O-Labeling and Tandem Mass Spectrometry Analysis. *Analytical Chemistry*, 84, 6355-6360 (2012).
105. Wang S, Bobst CE, Kaltashov IA. Pitfalls in Protein Quantitation Using Acid-Catalyzed O18 Labeling: Hydrolysis-Driven Deamidation. *Analytical Chemistry*, 83(18), 7227-7232 (2011).
106. Liu M, Cheetham J, Cauchon N *et al.* Protein Isoaspartate Methyltransferase-Mediated 18O-Labeling of Isoaspartic Acid for Mass Spectrometry Analysis. *Analytical Chemistry*, 84, 1056-1062 (2011).
107. Hao P, Ren Y, Alpert AJ, Sze SK. Detection, Evaluation and Minimization of Nonenzymatic Deamidation in Proteomic Sample Preparation. *Molecular & Cellular Proteomics*, 10, 10.1074/mcp.O111.009381 (2011).
108. Zhang X, Hojrup P. Cyclization of the N-Terminal X-Asn-Gly Motif during Sample Preparation for Bottom-Up Proteomics. *Analytical Chemistry*, 82, 8680-8685 (2010).
109. Yang H, Zubarev RA. Mass spectrometric analysis of asparagine deamidation and aspartate isomerization in polypeptides. *Electrophoresis*, 31, 1764-1772 (2010).
110. Ni W, Dai S, Karger BL, Zhou ZS. Analysis of Isoaspartic Acid by Selective Proteolysis with Asp-N and Electron Transfer Dissociation Mass Spectrometry. *Analytical Chemistry*, 82, 7485-7491 (2010).
111. Vlasak J, Bussat MC, Wang S *et al.* Identification and characterization of asparagine deamidation in the light chain CDR1 of a humanized IgG1 antibody. *Analytical Biochemistry*, 392, 145-154 (2009).
112. Sharma KK, Santhoshkumar P. Lens aging: effects of crystallins. *Biochimica Biophysica Acta*, 1790, 1095-1108 (2009).

113. Liu YD, van Enk JZ, Flynn GC. Human antibody Fc deamidation in vivo. *Biologicals: Journal of the International Association of Biological Standardization*, 37, 313-322 (2009).
114. Dasari S, Wilmarth PA, Reddy AP, Robertson LJG, Nagalla SR, David LL. Quantification of Isotopically Overlapping Deamidated and 18O-Labeled Peptides Using Isotopic Envelope Mixture Modeling. *Journal of Proteome Research*, 8, 1263-1270 (2009).
115. Liu H, Gaza-Bulseco G, Faldu D, Chumsae C, Sun J. Heterogeneity of monoclonal antibodies. *Journal of Pharmaceutical Science*, 97, 2426-2447 (2008).
116. Jenkins N, Murphy L, Tyther R. Post-translational modifications of recombinant proteins: significance for biopharmaceuticals. *Molecular Biotechnology*, 39, 113-118 (2008).
117. Gaza-Bulseco G, Li B, Bulseco A, Liu H. Method to Differentiate Asn Deamidation That Occurred Prior to and during Sample Preparation of a Monoclonal Antibody. *Analytical Chemistry*, 80, 9491-9498 (2008).
118. Krokhin OV, Antonovici M, Ens W, Wilkins JA, Standing KG. Deamidation of -Asn-Gly- sequences during sample preparation for proteomics: Consequences for MALDI and HPLC-MALDI analysis. *Analytical Chemistry*, 78, 6645-6650 (2006).
119. Hipkiss AR. Accumulation of altered proteins and ageing: causes and effects. *Experimental Gerontology*, 41, 464-473 (2006).
120. Gupta R, Srivastava OP. Deamidation Affects Structural and Functional Properties of Human {alpha}A-Crystallin and Its Oligomerization with {alpha}B-Crystallin. *Journal of Biological Chemistry*, 279, 44258-44269 (2004).
121. Robinson NE. Protein deamidation. *Proceedings of the National Academy of Sciences*, 99, 5283-5288 (2002).
122. Robinson NE, Robinson AB. Prediction of protein deamidation rates from primary and three-dimensional structure. *Proceedings of the National Academy of Sciences*, 98, 4367-4372 (2001).
123. Harris RJ, Kabakoff B, Macchi FD *et al.* Identification of multiple sources of charge heterogeneity in a recombinant antibody. *Journal of Chromatography B*, 752, 233-245 (2001).
124. Carlson AD, Riggin RM. Development of improved high-performance liquid chromatography conditions for nonisotopic detection of isoaspartic acid to determine the extent of protein deamidation. *Analytical Biochemistry*, 278, 150-155 (2000).
125. Hsu YR, Chang WC, Mendiaz EA *et al.* Selective deamidation of recombinant human stem cell factor during in vitro aging: Isolation and characterization of the aspartyl and isoaspartyl homodimers and heterodimers. *Biochemistry*, 37, 2251-2262 (1998).
126. Bischoff R, Kolbe HV. Deamidation of asparagine and glutamine residues in proteins and peptides: structural determinants and analytical methodology. *Journal of Chromatography B*, 662, 261-278 (1994).
127. Bischoff R, Lepage P, Jaquinod M *et al.* Sequence-specific deamidation: isolation and biochemical characterization of succinimide intermediates of recombinant hirudin. *Biochemistry*, 32, 725-734 (1993).
128. Martinez-Morillo E, Nielsen HM, Batruch I *et al.* Assessment of Peptide Chemical Modifications on the Development of an Accurate and Precise Multiplex Selected Reaction Monitoring Assay for Apolipoprotein E Isoforms. *Journal of Proteome Research*, 13, 1077-1087 (2014).
129. Liu H, Ponniah G, Neill A, Patel R, Andrien B. Accurate Determination of Protein Methionine Oxidation by Stable Isotope Labeling and LC-MS Analysis. *Analytical Chemistry*, 85, 11705-11709 (2013).
130. Spickett CM, Pitt AR. Protein oxidation: role in signalling and detection by mass spectrometry. *Amino Acids*, 42, 5-21 (2012).
131. Ghesquiere B, Jonckheere V, Colaert N *et al.* Redox Proteomics of Protein-bound Methionine Oxidation. *Molecular & Cellular Proteomics*, 10, 10.1074/mcp.M110.006866 (2011).

132. Lancellotti S, De F, V, Pozzi N *et al.* Formation of methionine sulfoxide by peroxynitrite at position 1606 of von Willebrand factor inhibits its cleavage by ADAMTS-13: A new prothrombotic mechanism in diseases associated with oxidative stress. *Free Radical Biology Medicine*, 48, 446-456 (2010).
133. Zhang H, Zielonka J, Sikora A, Joseph J, Xu Y, Kalyanaraman B. The effect of neighboring methionine residue on tyrosine nitration and oxidation in peptides treated with MPO, H₂O₂, and NO₂⁻ or peroxynitrite and bicarbonate: Role of intramolecular electron transfer mechanism? *Archives of Biochemistry and Biophysics*, 484, 134-145 (2009).
134. Rebrin I, Bregere C, Gallaher TK, Sohal RS. Detection and characterization of peroxynitrite-induced modifications of tyrosine, tryptophan, and methionine residues by tandem mass spectrometry. *Methods Enzymology*, 441, 283-294 (2008).
135. Shao B, Belaaouaj A, Verlinde CLMJ, Fu X, Heinecke JW. Methionine Sulfoxide and Proteolytic Cleavage Contribute to the Inactivation of Cathepsin G by Hypochlorous Acid: an oxidative mechanism for regulation of erine proteinases by myeloperoxidase. *Journal of Biological Chemistry*, 280, 29311-29321 (2005).
136. Harris RJ. Heterogeneity of recombinant antibodies: linking structure to function. *Developments in Biologicals*, 122, 117-127 (2005).
137. Leichert LI, Jakob U. Protein Thiol Modifications Visualized In Vivo. *PLoS Biology*, 2, e333 (2004).
138. Guan Z, Yates NA, Bakhtiar R. Detection and characterization of methionine oxidation in peptides by collision-induced dissociation and electron capture dissociation. *Journal of the American Society for Mass Spectrometry*, 14, 605-613 (2003).
139. Kanayama A, Inoue Ji, Sugita-Konishi Y, Shimizu M, Miyamoto Y. Oxidation of Ikappa Balpha at Methionine 45 Is One Cause of Taurine Chloramine-induced Inhibition of NF-kappa B Activation. *Journal of Biological Chemistry*, 277, 24049-24056 (2002).
140. Griffiths SW, King J, Cooney CL. The Reactivity and Oxidation Pathway of Cysteine 232 in Recombinant Human alpha 1-Antitrypsin. *Journal of Biological Chemistry*, 277, 25486-25492 (2002).
141. Griffiths SW, Cooney CL. Development of a peptide mapping procedure to identify and quantify methionine oxidation in recombinant human [alpha]1-antitrypsin. *Journal of Chromatography A*, 942, 133-143 (2002).
142. Stadtman ER. Protein oxidation in aging and age-related diseases. *Annals of the New York Academy of Sciences*, 928, 22-38 (2001).
143. Davis DA, Newcomb FM, Moskovitz J *et al.* HIV-2 protease is inactivated after oxidation at the dimer interface and activity can be partly restored with methionine sulphoxide reductase. *Biochemical Journal*, 2, 305-311 (2000).
144. Jiang XSJBAEC. Identification of a MS-MS fragment diagnostic for methionine sulfoxide. *Journal of Mass Spectrometry*, 31, 1309-1310 (1996).
145. Vogt W. Oxidation of methionyl residues in proteins: tools, targets, and reversal. *Free Radical Biology and Medicine*, 18, 93-105 (1995).
146. Li Y, Polozova A, Gruia F, Feng J. Characterization of the Degradation Products of a Color-Changed Monoclonal Antibody: Tryptophan-Derived Chromophores. *Analytical Chemistry*, 86, 6850-6857 (2014).
147. Amano M, Kobayashi N, Yabuta M, Uchiyama S, Fukui K. Detection of Histidine Oxidation in a Monoclonal Immunoglobulin Gamma (IgG) 1 Antibody. *Analytical Chemistry*, 86, 7536-7543 (2014).
148. Roeser J, Bischoff R, Bruins AP, Permentier HP. Oxidative protein labeling in mass spectrometry-based proteomics. *Analytical and Bioanalytical Chemistry*, 397, 3441-3455 (2010).

149. Perdivara I, Deterding LJ, Przybylski M, Tomer KB. Mass Spectrometric Identification of Oxidative Modifications of Tryptophan Residues in Proteins: Chemical Artifact or Post-Translational Modification? *Journal of the American Society for Mass Spectrometry*, 21, 1114-1117 (2010).
150. Bregere C, Rebrin I, Sohal RS. Detection and characterization of in vivo nitration and oxidation of tryptophan residues in proteins. *Methods Enzymology*, 441, 339-349 (2008).
151. Yamakura F, Ikeda K. Modification of tryptophan and tryptophan residues in proteins by reactive nitrogen species. *Nitric Oxide*, 14, 152-161 (2006).
152. Yamakura F, Matsumoto T, Ikeda K *et al.* Nitrated and oxidized products of a single tryptophan residue in human Cu,Zn-superoxide dismutase treated with either peroxynitrite-carbon dioxide or myeloperoxidase-hydrogen peroxide-nitrite. *Journal of Biochemistry*, 138, 57-69 (2005).
153. Fu X, Kao JLF, Bergt C *et al.* Oxidative Cross-linking of Tryptophan to Glycine Restrains Matrix Metalloproteinase Activity: specific structural motifs control protein oxidation. *Journal of Biological Chemistry*, 279, 6209-6212 (2004).
154. Taylor SW, Fahy E, Murray J, Capaldi RA, Ghosh SS. Oxidative Post-translational Modification of Tryptophan Residues in Cardiac Mitochondrial Proteins. *Journal of Biological Chemistry*, 278, 19587-19590 (2003).
155. Hambly DM, Gross ML. Cold Chemical Oxidation of Proteins. *Analytical Chemistry*, 81, 7235-7242 (2009).
156. Zhan X, Wang X, Desiderio DM. Mass spectrometry analysis of nitrotyrosine-containing proteins. *Mass Spectrometry Reviews*, 10.1002/mas.2141 (2013).
157. Radi R. Protein tyrosine nitration: Biochemical mechanisms and structural basis of functional effects. *Accounts of Chemical Research*, 46, 550-559 (2013).
158. Evans AR, Robinson RAS. Proteomics quantification of protein nitration. *Reviews in Analytical Chemistry*, 32, 173-187 (2013).
159. Diaz-Moreno I, Garcia-Heredia JM, Gonzalez-Arzola K, Diaz-Quintana A, De La Rosa MA. Recent methodological advances in the analysis of protein tyrosine nitration. *ChemPhysChem*, 14, 3095-3102 (2013).
160. Allan Butterfield D, Dalle-Donne I. Redox proteomics. *Antioxidants and Redox Signaling*, 17, 1487-1489 (2012).
161. Nuriel T, Hansler A, Gross SS. Protein nitrotryptophan: Formation, significance and identification. *Journal of Proteomics*, 74, 2300-2312 (2011).
162. Aslan M, Dogan S. Proteomic detection of nitroproteins as potential biomarkers for cardiovascular disease. *Journal of Proteomics*, 74, 2274-2288 (2011).
163. Abello N, Kerstjens HA, Postma DS, Bischoff R. Protein Tyrosine Nitration: Selectivity, physicochemical and biological consequences, denitration and proteomics methods for the identification of tyrosine-nitrated proteins. *Journal of Proteome Research*, 8, 3222-3238 (2009).
164. Yeo WS, Lee SJ, Lee JR, Kim KP. Nitrosative protein tyrosine modifications: biochemistry and functional significance. *BMB Reports*, 41, 194-203 (2008).
165. Souza JM, Peluffo G, Radi R. Protein tyrosine nitration-Functional alteration or just a biomarker? *Free Radical Biology and Medicine*, 45, 357-366 (2008).
166. Salzano AM, D'Ambrosio C, Scaloni A. Mass spectrometric characterization of proteins modified by nitric oxide-derived species. *Methods Enzymology*, 440, 3-15 (2008).
167. Nuriel T, Deeb RS, Hajjar DP, Gross SS. Protein 3-nitrotyrosine in complex biological samples: quantification by high-pressure liquid chromatography/electrochemical detection and emergence of proteomic approaches for unbiased identification of modification sites. *Methods Enzymology*, 441, 1-17 (2008).
168. Monteiro HP, Arai RJ, Travassos LR. Protein tyrosine phosphorylation and protein tyrosine nitration in redox signaling. *Antioxidants and Redox Signaling*, 10, 843-889 (2008).

169. Ischiropoulos H. Protein tyrosine nitration--An update. *Archives of Biochemistry and Biophysics*, 484, 117-121 (2008).
170. Butterfield DA, Sultana R. Identification of 3-nitrotyrosine-modified brain proteins by redox proteomics. *Methods Enzymology*, 440, 295-308 (2008).
171. Butt YK, Lo SC. Detecting nitrated proteins by proteomic technologies. *Methods Enzymology*, 440, 17-31 (2008).
172. Peluffo G, Radi R. Biochemistry of protein tyrosine nitration in cardiovascular pathology. *Cardiovascular Research*, 75, 291-302 (2007).
173. Bartesaghi S, Ferrer-Sueta G, Peluffo G *et al.* Protein tyrosine nitration in hydrophilic and hydrophobic environments. *Amino Acids*, 32, 501-515 (2007).
174. Ohmori H, Kanayama N. Immunogenicity of an inflammation-associated product, tyrosine nitrated self-proteins. *Autoimmunity Reviews*, 4, 224-229 (2005).
175. Ischiropoulos H. Biological selectivity and functional aspects of protein tyrosine nitration. *Biochemical and Biophysical Research Communications*, 305, 776-783 (2003).
176. Ghezzi P, Bonetto V. Redox proteomics: identification of oxidatively modified proteins. *Proteomics*, 3, 1145-1153 (2003).
177. Alvarez B, Radi R. Peroxynitrite reactivity with amino acids and proteins. *Amino Acids*, 25, 295-311 (2003).
178. Turko IV, Murad F. Protein nitration in cardiovascular diseases. *Pharmacological Reviews*, 54(4) (2002).
179. Sabetkar M, Low SY, Naseem KM, Bruckdorfer KR. The nitration of proteins in platelets: significance in platelet function. *Free Radical Biology and Medicine*, 33, 728-734 (2002).
180. Radi R, Cassina A, Hodara R, Quijano C, Castro L. Peroxynitrite reactions and formation in mitochondria. *Free Radical Biology and Medicine*, 33, 1451-1464 (2002).
181. Monteiro HP. Signal transduction by protein tyrosine nitration: competition or cooperation with tyrosine phosphorylation-dependent signaling events? *Free Radical Biology and Medicine*, 33, 765-773 (2002).
182. Greenacre SA, Ischiropoulos H. Tyrosine nitration: localisation, quantification, consequences for protein function and signal transduction. *Free Radical Research*, 34, 541-581 (2001).
183. Ischiropoulos H. Biological tyrosine nitration: a pathophysiological function of nitric oxide and reactive oxygen species. *Archives in Biochemistry and Biophysics*, 356, 1-11 (1998).
184. Beckman JS. Oxidative damage and tyrosine nitration from peroxynitrite. *Chemical Research in Toxicology*, 9, 836-844 (1996).
185. Beck A, Bussat MC, Zorn N *et al.* Characterization by liquid chromatography combined with mass spectrometry of monoclonal anti-IGF-1 receptor antibodies produced in CHO and NS0 cells. *Journal of Chromatography B*, 819, 203-218 (2005).
186. Wiegandt A, Meyer B. Unambiguous Characterization of N-Glycans of Monoclonal Antibody Cetuximab by Integration of LC-MS/MS and 1H NMR Spectroscopy. *Analytical Chemistry*, 86, 4807-4814 (2014).
187. Váradi C, Lew C, Guttman A. Rapid Magnetic Bead Based Sample Preparation for Automated and High Throughput N-Glycan Analysis of Therapeutic Antibodies. *Analytical Chemistry*, 86(12), 5682-5687 (2014).
188. Song T, Ozcan S, Becker A, Lebrilla CB. In-Depth Method for the Characterization of Glycosylation in Manufactured Recombinant Monoclonal Antibody Drugs. *Analytical Chemistry*, 86, 5661-5666 (2014).
189. Houel S, Hilliard M, Yu YQ *et al.* N- and O-Glycosylation Analysis of Etanercept Using Liquid Chromatography and Quadrupole Time-of-Flight Mass Spectrometry Equipped with Electron-Transfer Dissociation Functionality. *Analytical Chemistry*, 86, 576-584 (2014).

190. Gahoual R, Busnel J-M, Beck A, François Y-N, Leize-Wagner E. Full Antibody Primary Structure and Microvariant Characterization in a Single Injection Using Transient Isotachopheresis and Sheathless Capillary Electrophoresis–Tandem Mass Spectrometry. *Analytical Chemistry*, 86, 9074-9081 (2014).
191. Zauner G, Selman MHJ, Bondt A *et al.* Glycoproteomic Analysis of Antibodies. *Molecular & Cellular Proteomics*, 12, 856-865 (2013).
192. Patrie SM, Roth MJ, Kohler JJ. Introduction to glycosylation and mass spectrometry. *Methods in Molecular Biology*, 951, 1-17 (2013).
193. Mao Y, Valeja SG, Rouse JC, Hendrickson CL, Marshall AG. Top-Down Structural Analysis of an Intact Monoclonal Antibody by Electron Capture Dissociation-Fourier Transform Ion Cyclotron Resonance-Mass Spectrometry. *Analytical Chemistry*, 85, 4239-4246 (2013).
194. Leymarie N, Griffin PJ, Jonscher K *et al.* Interlaboratory Study on Differential Analysis of Protein Glycosylation by Mass Spectrometry: The ABRF Glycoprotein Research Multi-Institutional Study 2012. *Molecular & Cellular Proteomics*, 12, 2935-2951 (2013).
195. Tsybin YO, Fornelli L, Stoermer C *et al.* Structural Analysis of Intact Monoclonal Antibodies by Electron Transfer Dissociation Mass Spectrometry. *Analytical Chemistry*, 83, 8919-8927 (2011).
196. Szabo Z, Guttman As, Bones J, Karger BL. Rapid High-Resolution Characterization of Functionally Important Monoclonal Antibody N-Glycans by Capillary Electrophoresis. *Analytical Chemistry*, 83, 5329-5336 (2011).
197. Melmer M, Stangler T, Schiefermeier M *et al.* HILIC analysis of fluorescence-labeled N-glycans from recombinant biopharmaceuticals. *Analytical and Bioanalytical Chemistry*, 398, 905-914 (2010).
198. Jiang H, Wu SL, Karger BL, Hancock WS. Characterization of the Glycosylation Occupancy and the Active Site in the Follow-on Protein Therapeutic: TNK-Tissue Plasminogen Activator. *Analytical Chemistry*, 82, 6154-6162 (2010).
199. Gil GC, Velander WH, Van Cott KE. N-glycosylation microheterogeneity and site occupancy of an Asn-X-Cys sequon in plasma-derived and recombinant protein C. *Proteomics*, 9, 2555-2567 (2009).
200. Borisov OV, Field M, Ling VT, Harris RJ. Characterization of oligosaccharides in recombinant tissue plasminogen activator produced in Chinese hamster ovary cells: Two decades of analytical technology development. *Analytical Chemistry*, 81, 9744-9754 (2009).
201. Srebalus Barnes CA, Lim A. Applications of mass spectrometry for the structural characterization of recombinant protein pharmaceuticals. *Mass Spectrometry Reviews*, 26, 370-388 (2007).
202. Fernandez LEM, Kalume DE, Calvo L, Fernandez Mallo M, Vallin A, Roepstorff P. Characterization of a recombinant monoclonal antibody by mass spectrometry combined with liquid chromatography. *Journal of Chromatography B*, 752, 247-261 (2001).
203. Werner RG, Noe W, Kopp K, Schluter M. Appropriate mammalian expression systems for biopharmaceuticals. *Arzneimittel Forschung Drug Research*, 48, 870-880 (1998).
204. Fournier T, Guibourdenche J, Evain-Brion D. Review: hCGs: Different sources of production, different glycoforms and functions. *Placenta*, 10.1016/j.placenta (2015).
205. Wagner-Rousset E, Bednarczyk A, Bussat MC *et al.* The way forward, enhanced characterization of therapeutic antibody glycosylation: comparison of three level mass spectrometry-based strategies. *Journal of Chromatography B*, 872, 23-37 (2008).
206. Beck A, Wagner-Rousset E, Bussat MC *et al.* Trends in glycosylation, glycoanalysis and glycoengineering of therapeutic antibodies and Fc-fusion proteins. *Current Pharmaceutical Biotechnology*, 9, 482-501 (2008).
207. Fares F. The role of O-linked and N-linked oligosaccharides on the structure-function of glycoprotein hormones: development of agonists and antagonists. *Biochimica and Biophysica Acta*, 1760, 560-567 (2006).

208. Sinclair AM, Elliott S. Glycoengineering: the effect of glycosylation on the properties of therapeutic proteins. *Journal of Pharmaceutical Sciences*, 94, 1626-1635 (2005).
209. Gervais A, Hammel YA, Pelloux S *et al.* Glycosylation of human recombinant gonadotrophins: characterization and batch-to-batch consistency. *Glycobiology*, 13, 179-189 (2003).
210. Ulloa-Aguirre A, Timossi C, Damian-Matsumura P, Dias JA. Role of glycosylation in function of follicle-stimulating hormone. *Endocrine*, 11, 205-215 (1999).
211. Storrer PL. Assaying glycoprotein hormones--the influence of glycosylation on immunoreactivity. *Trends in Biotechnology*, 10, 427-432 (1992).
212. Takeuchi M, Kobata A. Structures and functional roles of the sugar chains of human erythropoietins. *Glycobiology*, 1, 337-346 (1991).
213. Cao Q, Zhao X, Zhao Q *et al.* Strategy Integrating Stepped Fragmentation and Glycan Diagnostic Ion-Based Spectrum Refinement for the Identification of Core Fucosylated Glycoproteome Using Mass Spectrometry. *Analytical Chemistry*, 86, 6804-6811 (2014).
214. McCarthy C, Saldova R, Wormald MR, Rudd PM, McElvaney NG, Reeves EP. The Role and Importance of Glycosylation of Acute Phase Proteins with Focus on Alpha-1 Antitrypsin in Acute and Chronic Inflammatory Conditions. *Journal of Proteome Research*, 13, 3131-3143 (2014).
215. Ahn JM, Sung HJ, Yoon YH *et al.* Integrated Glycoproteomics Demonstrates Fucosylated Serum Paraoxonase 1 Alterations in Small Cell Lung Cancer. *Molecular & Cellular Proteomics*, 13, 30-48 (2014).
216. Ruhaak LR, Miyamoto S, Lebrilla CB. Developments in the Identification of Glycan Biomarkers for the Detection of Cancer. *Molecular & Cellular Proteomics*, 12, 846-855 (2013).
217. Chen K, Gentry-Maharaj A, Burnell M *et al.* Microarray Glycoprofiling of CA125 Improves Differential Diagnosis of Ovarian Cancer. *Journal of Proteome Research*, 12, 1408-1418 (2013).
218. Wu J, Xie X, Liu Y *et al.* Identification and Confirmation of Differentially Expressed Fucosylated Glycoproteins in the Serum of Ovarian Cancer Patients Using a Lectin Array and LC-MS/MS. *Journal of Proteome Research*, 11, 4541-4552 (2012).
219. Balog CIA, Stavenhagen K, Fung WLJ *et al.* N-glycosylation of Colorectal Cancer Tissues. *Molecular & Cellular Proteomics*, 11, 571-585 (2012).
220. Alley WR, Vasseur JA, Goetz JA *et al.* N-linked Glycan Structures and Their Expressions Change in the Blood Sera of Ovarian Cancer Patients. *Journal of Proteome Research*, 11, 2282-2300 (2012).
221. Wagner KW, Punnoose EA, Januario T *et al.* Death-receptor O-glycosylation controls tumor-cell sensitivity to the proapoptotic ligand Apo2L/TRAIL. *Nature Medicine*, 13, 1070-1077 (2007).
222. Heo SH, Lee SJ, Ryoo HM, Park JY, Cho JY. Identification of putative serum glycoprotein biomarkers for human lung adenocarcinoma by multilectin affinity chromatography and LC-MS/MS. *Proteomics*, 7, 4292-4302 (2007).
223. Li Y, Tian Y, Rezai T *et al.* Simultaneous Analysis of Glycosylated and Sialylated Prostate-Specific Antigen Revealing Differential Distribution of Glycosylated Prostate-Specific Antigen Isoforms in Prostate Cancer Tissues. *Analytical Chemistry*, 83, 240-245 (2010).
224. Bones J, Mittermayr S, O'Donoghue N, Guttman As, Rudd PM. Ultra Performance Liquid Chromatographic Profiling of Serum N-Glycans for Fast and Efficient Identification of Cancer Associated Alterations in Glycosylation. *Analytical Chemistry*, 82, 10208-10215 (2010).
225. Arnold JN, Saldova R, Galligan MC *et al.* Novel Glycan Biomarkers for the Detection of Lung Cancer. *Journal of Proteome Research*, 10, 1755-1764 (2011).
226. Stanta JL, Saldova R, Struwe WB *et al.* Identification of N-Glycosylation Changes in the CSF and Serum in Patients with Schizophrenia. *Journal of Proteome Research*, 9, 4476-4489 (2010).
227. de Leoz ML, Young LJ, An HJ *et al.* High-Mannose Glycans are Elevated during Breast Cancer Progression. *Molecular & Cellular Proteomics*, 10, 10.1074/mcp.M110.002717 (2011).

228. Abbott KL, Lim JM, Wells L, Benigno BB, McDonald JF, Pierce M. Identification of candidate biomarkers with cancer-specific glycosylation in the tissue and serum of endometrioid ovarian cancer patients by glycoproteomic analysis. *Proteomics*, 10, 470-481 (2010).
229. Liu Y, He J, Li C *et al.* Identification and Confirmation of Biomarkers Using an Integrated Platform for Quantitative Analysis of Glycoproteins and Their Glycosylations. *Journal of Proteome Research*, 9, 798-805 (2009).
230. Tang Z, Varghese RS, Bekesova S *et al.* Identification of N-Glycan Serum Markers Associated with Hepatocellular Carcinoma from Mass Spectrometry Data. *Journal of Proteome Research*, 9, 104-112 (2009).
231. Ahn YH, Lee JY, Lee JY, Kim YS, Ko JH, Yoo JS. Quantitative Analysis of an Aberrant Glycoform of TIMP1 from Colon Cancer Serum by L-PHA-Enrichment and SISCAPA with MRM Mass Spectrometry. *Journal of Proteome Research*, 8, 4216-4224 (2009).
232. Mechref Y, Hussein A, Bekesova S *et al.* Quantitative serum glycomics of esophageal adenocarcinoma and other esophageal disease onsets. *Journal of Proteome Research*, 8, 2656-2666 (2009).
233. Ueda K, Fukase Y, Katagiri T *et al.* Targeted serum glycoproteomics for the discovery of lung cancer-associated glycosylation disorders using lectin-coupled ProteinChip arrays. *Proteomics*, 9, 2182-2192 (2009).
234. Kuzmanov U, Jiang N, Smith CR, Soosaipillai A, Diamandis EP. Differential N-glycosylation of Kallikrein 6 Derived from Ovarian Cancer Cells or the Central Nervous System. *Molecular & Cellular Proteomics*, 8, 791-798 (2009).
235. Matsumoto K, Shimizu C, Arao T *et al.* Identification of Predictive Biomarkers for Response to Trastuzumab Using Plasma FUCA Activity and N-Glycan Identified by MALDI-TOF-MS. *Journal of Proteome Research*, 8, 457-462 (2009).
236. Qiu Y, Patwa TH, Xu L *et al.* Plasma glycoprotein profiling for colorectal cancer biomarker identification by lectin glycoarray and lectin blot. *Journal of Proteome Research*, 7, 1693-1703 (2008).
237. Kaji H, Isobe T. Liquid Chromatography/Mass Spectrometry (LC/MS)-Based Glycoproteomics Technologies for Cancer Biomarker Discovery. *Clinical Proteomics*, 4, 14-24 (2008).
238. Kreunin P, Zhao J, Rosser C, Urquidí V, Lubman DM, Goodison S. Bladder Cancer Associated Glycoprotein Signatures Revealed by Urinary Proteomic Profiling. *Journal of Proteome Research*, 6, 2631-2639 (2007).
239. Abbott KL, Aoki K, Lim JM *et al.* Targeted Glycoproteomic Identification of Biomarkers for Human Breast Carcinoma. *Journal of Proteome Research*, 7, 1470-1480 (2008).
240. Norton PA, Comunale MA, Krakover J *et al.* N-linked glycosylation of the liver cancer biomarker GP73. *Journal of Cellular Biochemistry*, 104, 136-149 (2008).
241. Saldova R, Royle L, Radcliffe CM *et al.* Ovarian Cancer is Associated With Changes in Glycosylation in Both Acute-Phase Proteins and IgG. *Glycobiology*, 17, 1344-1356 (2007).
242. An HJ, Miyamoto S, Lancaster KS *et al.* Profiling of glycans in serum for the discovery of potential biomarkers for ovarian cancer. *Journal of Proteome Research*, 5, 1626-1635 (2006).
243. Yang Z, Harris LE, Palmer-Toy DE, Hancock WS. Multilectin Affinity Chromatography for Characterization of Multiple Glycoprotein Biomarker Candidates in Serum from Breast Cancer Patients. *Clinical Chemistry*, 52, 1897-1905 (2006).
244. Comunale MA, Lowman M, Long RE *et al.* Proteomic analysis of serum associated fucosylated glycoproteins in the development of primary hepatocellular carcinoma. *Journal of Proteome Research*, 5, 308-315 (2006).
245. Troyer DA, Mubiru J, Leach RJ, Naylor SL. Promise and challenge: Markers of prostate cancer detection, diagnosis and prognosis. *Disease Markers*, 20, 117-128 (2004).

246. Marian M, Seghezzi W. Novel Biopharmaceuticals: Pharmacokinetics, Pharmacodynamics, and Bioanalytics. Chapter 4 in: Nonclinical Development of Novel Biologics, Biosimilars, Vaccines and Specialty Biologics. Plitnick, LM, Herzyk, DJ (Eds.) (Academic Press, San Diego), 97-137 (2013).
247. Bults PB, R.; Bakker, H.; van de Merbel, N.C. In vitro and in vivo deamidation of the biopharmaceutical antibody Trastuzumab. *in preparation*, (2015).
248. Bischoff R, Clesse D, Whitechurch O, Lepage P, Roitsch C. Isolation of recombinant hirudin by preparative high-performance liquid chromatography. *Journal of Chromatography B*, 476, 245-255 (1989).
249. Beck A, Sanglier-Cianferani S, Van Dorsselaer A. Biosimilar, Biobetter, and Next Generation Antibody Characterization by Mass Spectrometry. *Analytical Chemistry*, 84, 4637-4646 (2012).
250. Leary BA, Lawrence-Henderson R, Mallozzi C *et al.* Bioanalytical platform comparison using a generic human IgG PK assay format. *Journal of Immunological Methods*, 397, 28-36 (2013).
251. Prudom C, Liu J, Patrie J *et al.* Comparison of competitive radioimmunoassays and two-site sandwich assays for the measurement and interpretation of plasma ghrelin levels. *The Journal of Clinical Endocrinology and Metabolism*, 95, 2351-2358 (2010).
252. Fischer SK, Yang J, Anand B *et al.* The assay design used for measurement of therapeutic antibody concentrations can affect pharmacokinetic parameters: Case studies. *mAbs*, 4, 623-631 (2012).
253. Sukovaty RL, Lee JW, Fox J *et al.* Quantification of recombinant human parathyroid hormone (rhPTH(1-84)) in human plasma by immunoassay: commercial kit evaluation and validation to support pharmacokinetic studies. *Journal of Pharmaceutical and Biomedical Analysis*, 42, 261-271 (2006).
254. Ouyang Z, Furlong MT, Wu S *et al.* Pellet digestion: a simple and efficient sample preparation technique for LC-MS/MS quantification of large therapeutic proteins in plasma. *Bioanalysis*, 4, 17-28 (2012).
255. Li H, Ortiz R, Tran L *et al.* General LC-MS/MS method approach to quantify therapeutic monoclonal antibodies using a common whole antibody internal standard with application to preclinical studies. *Analytical Chemistry*, 84, 1267-1273 (2012).
256. Bronsema KJB, R.; Schlaman, J.; Schalk, F.; Kema, I.P.; van de Merbel, N.C. Development, validation and application of a quantitative LC-MS/MS method for insulin like growth factor-1 in human plasma. *in preparation*, (2015).
257. Wang SJ, Wu ST, Gokemeijer J *et al.* Attribution of the discrepancy between ELISA and LC-MS/MS assay results of a PEGylated scaffold protein in post-dose monkey plasma samples due to the presence of anti-drug antibodies. *Analytical and Bioanalytical Chemistry*, 402, 1229-1239 (2012).
258. Cabaleiro DR, Stöckl D, Kaufman JM, Fiers T, Thienpont LM. Feasibility of standardization of serum C-peptide immunoassays with isotope-dilution liquid chromatography-tandem mass spectrometry. *Clinical Chemistry*, 52, 1193-1196 (2006).
259. Kroot JJ, Laarakkers CM, Geurts-Moespot AJ *et al.* Immunochemical and mass-spectrometry-based serum hepcidin assays for iron metabolism disorders. *Clinical Chemistry*, 56, 1570-1579 (2010).
260. Liu Y, Buil A, Collins BC *et al.* Quantitative variability of 342 plasma proteins in a human twin population. *Molecular Systems Biology*, 11, 1-18 (2015).
261. Carr SA, Abbatiello SE, Ackermann BL *et al.* Targeted Peptide Measurements in Biology and Medicine: Best Practices for Mass Spectrometry-based Assay Development Using a Fit-for-Purpose Approach. *Molecular & Cellular Proteomics*, 13, 907-917 (2014).
262. Surinova S, Huttenhain R, Chang CY, Espona L, Vitek O, Aebersold R. Automated selected reaction monitoring data analysis workflow for large-scale targeted proteomic studies. *Nature Protocols*, 8, 1602-1619 (2013).
263. Picotti P, Aebersold R. Selected reaction monitoring-based proteomics: workflows, potential, pitfalls and future directions. *Nature Methods*, 9, 555-566 (2012).

264. Malmstrom L, Malmstrom J, Selevsek N, Rosenberger G, Aebersold R. Automated Workflow for Large-Scale Selected Reaction Monitoring Experiments. *Journal of Proteome Research*, 11, 1644-1653 (2012).
265. Gillet LC, Navarro P, Tate S *et al.* Targeted Data Extraction of the MS/MS Spectra Generated by Data-independent Acquisition: A New Concept for Consistent and Accurate Proteome Analysis. *Molecular & Cellular Proteomics*, 11, 10.1074/mcp.O11111.016717 (2012).
266. Siegel D, Meinema AC, Permentier HP, Hopfgartner G, Bischoff R. Integrated quantification and identification of aldehydes and ketones in biological samples. *Analytical Chemistry*, 86, 5089-5100 (2014).
267. Lesur A, Domon B. Advances in high-resolution accurate mass spectrometry application to targeted proteomics. *Proteomics*, 10.1002/pmic.201400450 (2014).
268. Tarasow TM, Penny L, Patwardhan A, Hamren S, McKenna MP, Urdea MS. Microfluidic strategies applied to biomarker discovery and validation for multivariate diagnostics. *Bioanalysis*, 3, 2233-2251 (2011).

CHAPTER III

LC-MS/MS based monitoring of *in vivo* protein biotransformation: quantitative determination of trastuzumab and its deamidation products in human plasma

Peter Bults^{1,2}, Rainer Bischoff², Hilde Bakker¹, Jourik A. Gietema³, Nico C. van de Merbel^{1,2}.

¹ Bioanalytical Laboratory, PRA Health Sciences, Early Development Services, Amerikaweg 18, 9407 TK, Assen, The Netherlands.

² Analytical Biochemistry, Department of Pharmacy, University of Groningen, A. Deusinglaan 1, 9700 AV Groningen, The Netherlands.

³ Faculty of Medical Sciences, Department of Medical Oncology, University Medical Centre Groningen, Hanzeplein 1, 9713 GZ Groningen, The Netherlands.

Anal. Chem., 2016, 88(3), 1871-1877

ABSTRACT

An LC-MS/MS-based method is described for quantitatively monitoring the *in vivo* deamidation of the biopharmaceutical monoclonal antibody trastuzumab at a crucial position in its complementarity determining region (CDR). The multiplexed LC-MS/MS assay allows simultaneous quantitation of five molecular species derived from trastuzumab after tryptic digestion: a stable signature peptide (FTISADTSK), a deamidation-sensitive signature peptide (IYPTNGYTR), its deamidated products (IYPTDGYTR and IYPTisoDGYTR) and a succinimide intermediate (IYPTsuccGYTR). Digestion of a 50- μ L plasma sample is performed at pH 7 for three hours at 37°C, which combines a reasonable (>80%) digestion efficiency with a minimal (<1%) formation of deamidation products during digestion. Rapid *in vitro* deamidation was observed at higher pH, leading to a (large) overestimation of the concentrations of deamidation products in the original plasma sample. The LC-MS/MS method was validated in accordance with international bioanalytical guidelines over the clinically relevant range of 0.5 to 500 μ g/mL. Deamidation of trastuzumab was observed in plasma both in a 56-day *in vitro* forced degradation study (up to 37% of the total drug concentration) and in samples obtained from breast cancer patients after treatment with the drug for several months (up to 25%). Comparison with a validated ELISA method for trastuzumab showed that deamidation of the drug at the CDR leads to a loss of recognition by the antibodies used in the ELISA assay.

3.1 INTRODUCTION

In recent years, there has been a considerable increase in the development and marketing of protein-based pharmaceuticals (or: biopharmaceuticals) and, consequently, in the interest for reliable analytical techniques for their quantification in samples of biological origin, to support e.g. pharmacokinetic studies or therapeutic drug monitoring. Traditionally, protein quantification is performed by ligand-binding assays (LBAs), but over the past decade liquid chromatography-tandem mass spectrometry (LC-MS/MS) has been gaining popularity as an alternative analytical platform^{1,2}. LC-MS/MS is well-established for the quantitative determination of small-molecule drugs and, because of its potential to provide structural information, it is also widely used to elucidate and monitor *in vivo* drug metabolism. On the other hand, monitoring the *in vivo* fate of biopharmaceuticals is a relatively unexplored area³, even though proteins are also susceptible to various (bio)chemical modifications which may induce changes in their structure and biological activity. LBAs give a single readout and very often it is unknown if and to what extent a structurally modified form of a protein responds in an assay. No separate concentration results are therefore obtained for the different protein forms and, probably for that reason, protein biotransformation has been traditionally somewhat neglected.

LC-MS/MS is extensively used to study structural modifications of proteins in pharmaceutical formulations, e.g. for quality control purposes. Important spontaneously occurring reactions are the deamidation of asparagine (Asn) and glutamine (Gln) as well as oxidation reactions, particularly of methionine (Met) or tryptophan (Trp) residues⁴. These may cause biologically relevant changes in the protein structure if the modified amino acids are present in the active part of the protein molecule, such as in one of the several complementarity determining regions (CDRs) of an antibody^{5,6,7}. Deamidation and oxidation can potentially also occur *in vivo* and their monitoring could give important information about the inactivation of the protein drug during its residence in the body. This is especially relevant for monoclonal antibodies (mAbs), a major class of biopharmaceuticals⁸, because of their relatively long half-life and consequently their long exposure to conditions that might induce deamidation and/or oxidation. Monitoring these reactions *in vivo*, however, is less straightforward than in pharmaceutical preparations *in vitro*, because of the lower analyte concentrations and the much more complicated sample matrix, which contains a significant number and amount of endogenous proteins that may interfere in the LC-MS/MS assay.

One of the most widely prescribed therapeutic monoclonal antibodies is trastuzumab (Herceptin®). It consists of two heavy and two light chains, is comprised of a total of 1330 amino acids and has an average molecular weight of approximately 145.5 kDa (Supplemental Fig. S-1). Trastuzumab is a humanized monoclonal immuno-globulin gamma 1 (IgG1) antibody directed against the human epidermal growth factor receptor-2 (HER2/neu). This receptor is overexpressed in approximately 25% of all breast cancer patients and trastuzumab inhibits proliferation and induces cell death via extracellular and intracellular mechanisms^{9,10,11}.

Trastuzumab can be deamidated in several places along its peptide chain. Most *in vitro* studies have focused on the deamidation of Asn30 in the light chain, which is known to take place under the slightly acidic conditions of a typical pharmaceutical formulation. The conversion of this amino acid to the corresponding aspartate (Asp) does, however, not lead to any significant decrease in pharmacological activity^{6,12}. Asn55, located in the CDR2 region of the heavy chain, is another deamidation site. This amino acid occurs in several mAbs of the IgG1 subclass and is therefore considered to play a key role in the biological functioning of these proteins¹³. Since Asn55 deamidation does not appear to occur to a large extent in pharmaceutical preparations, it has not been studied as closely as other reactions. The conversion to aspartic acid (Asp55) and the concomitant isomerization to iso-aspartic acid (isoAsp55) for another, not specified, mAB has been described to lead to a substantial (>70%) decrease in activity, because of a reduction in receptor binding affinity¹⁵, so the reaction is potentially relevant for trastuzumab as well.

So far, the *in vivo* deamidation of trastuzumab has not been studied. The Asn55 residue is potentially susceptible to deamidation under physiological conditions as it is followed by glycine, which is known to favor the formation of a succinimide (Asu) intermediate that can be subsequently hydrolyzed to either Asp or isoAsp¹⁴. Huang et al¹⁵ reported the *in vivo* deamidation of Asn55 in an unspecified therapeutic mAB in a study with cynomolgus monkeys, but digested the samples at pH 8 for several hours before LC-MS/MS analysis. This may have induced *in vitro* deamidation during the sample treatment step and thus compromised the accuracy of their results. In this paper, we describe the development, validation and use of an LC-MS/MS methodology for the simultaneous quantification of the non-deamidated (Asn55) and the deamidated (Asp55 and isoAsp55) forms of trastuzumab as well as the succinimide intermediate (Asu55) in plasma of breast cancer patients on long-term treatment with trastuzumab. This analysis is based on enzymatic digestion of plasma and subsequent LC-MS/MS analysis of the resulting peptide containing Asn55 or

its modified forms. In addition, a second peptide from a metabolically stable part of the molecule is quantified for comparative reasons. The digestion conditions were carefully optimized to avoid additional *in vitro* deamidation and to ensure sufficient accuracy. The results are compared to those obtained with a standard enzyme-linked immunosorbent assay (ELISA) to investigate the suitability of this technique to quantify trastuzumab in the presence of its deamidation products.

3.2 MATERIALS AND METHODS

3.2.1 Chemicals and biological materials

Trastuzumab, supplied in a vial containing 150 mg as a lyophilized sterile powder, was obtained from Roche (Basel, Switzerland). For the LC-MS/MS method, custom synthesized peptides (IYPTNGYTR, IYPTDGYTR, IYPTiso-DGYTR and their C-terminal arginine $^{13}\text{C}_6$ - $^{15}\text{N}_4$ -labeled internal standards, FTISADTSK and its C-terminal lysine $^{13}\text{C}_6$ - $^{15}\text{N}_2$ -labeled internal standard were obtained from JPT Peptide Technologies (Berlin, Germany). Acetonitrile, methanol, formic acid, acetic acid, ammonium hydroxide solution (25%), ammonium acetate and hydrochloric acid (37%) were obtained from Merck (Darmstadt, Germany). Tween-20, Trizma® base and Trypsin from porcine pancreas (Type IX-S, lyophilized powder, 13,000-20,000 BAEE units/mg protein) were obtained from Sigma Aldrich (St. Louis, MO, USA).

For the ELISA method, human anti-trastuzumab HCA169 and human anti-trastuzumab HCA177 were obtained from AbD Serotec® (Puchheim, Germany). A biotin protein labeling kit was obtained from Roche Diagnostics (Almere, The Netherlands). Phosphate buffered saline 10x (PBS), 3,3',5,5'-tetramethylbenzidine (TMB) Liquid Substrate System for ELISA and stop reagent for TMB substrate were obtained from Sigma Aldrich. Superblock® T20 (PBS) blocking buffer and Streptavidin-HRP were obtained from Thermo Fisher Scientific (Etten-Leur, The Netherlands). PBS-Tween® tablets (Calbiochem) were obtained from Merck. HPLC grade water was prepared using a water purification system from Merck. Human K_2EDTA plasma from healthy volunteers (hereafter referred to as blank human plasma) was obtained from Seralabs (Haywards Heath, UK).

3.2.2 Preparation of calibration, validation and quality control samples

A trastuzumab stock solution at 20.8 mg/mL was prepared by dissolving the contents of a vial of lyophilized protein (label claim: 150 mg) in 7.20 mL of water according to the

manufacturer's instructions for use. The stock solution was divided into 0.5 mL aliquots in Eppendorf Protein Lo-bind tubes (obtained from VWR International, Amsterdam, The Netherlands) and stored at -80°C. Aqueous standard solutions at 500 and 50.0 µg/mL were prepared freshly from this stock solution, and from these solutions calibration samples were prepared in blank human K₂EDTA plasma at 0.500, 1.00, 2.50, 10.0, 25.0, 100, 250, 400 and 500 µg/mL. Similarly, validation and quality control (QC) samples were prepared at 0.500, 1.50, 25.0 and 400 µg/mL. For the ELISA method, a plasma stock was prepared at 100 µg/mL, from which calibration samples were prepared by serial dilution with blank human K₂EDTA plasma to 60.1, 102, 172, 290, 490, 829, 1400, 2370 and 4000 ng/mL. Similarly, validation and quality control (QC) samples were prepared at 102, 250, 1000, 3000 and 4000 ng/mL. All calibration, validation and QC samples were stored in Eppendorf Protein Lo-bind tubes at -80°C (or -20°C for stability assessment).

3.2.3 LC-MS/MS sample pretreatment

For the LC-MS/MS determination of trastuzumab in human K₂EDTA plasma, 50.0 µL aliquots of sample were pipetted into the 1.2-mL wells of an Eppendorf Protein Lo-bind 96-well plate (obtained from VWR International, Amsterdam, The Netherlands) and 200 µL of methanol was added. After vortex-mixing for 2 minutes, the proteins were pelleted by centrifugation for 10 minutes at 1500g. The supernatant was discarded by inverting the plate above a waste receptacle and placing it upside down on a tissue for 15 minutes. The protein pellet was reconstituted by vortex-mixing in 400 µL of a solution consisting of 50 mM Trizma buffer at a pH of 7.0, 0.02% Tween-20, 3% (v/v) acetonitrile and 200 µg/mL trypsin. Next, 50.0 µL of a solution was added containing 2.00 µg/mL of the SIL-peptide internal standards. The sample was digested at 37°C and 1250 rpm for 3 hours using an Eppendorf Thermomixer® comfort, after which the digestion was stopped by the addition of 50.0 µL of 10% formic acid in water. Finally, the plate was sealed, vortex-mixed and placed in an autosampler at 10°C for analysis.

3.2.4 LC and MS conditions and settings

Experiments were conducted using an Acquity UPLC system (Waters, Milford, MA, USA) coupled to an AB Sciex API 6500 triple quadrupole mass spectrometer equipped with a TurboIonSpray™ source (Concord, Canada). Chromatographic separation was performed at 40°C on a 2.1 × 50 mm, 1.8 µm particle-size, Acquity UPLC HSS T3 column (Waters). Mobile phase A consisted of 10 mM ammonium acetate in water (pH=5) and mobile phase B

was acetonitrile. Samples were separated by gradient elution using the following settings: 0.0-5.0 min: 5-10% B; 5.0-5.1 min: 10-50% B; 5.1-5.6 min: 50% B; 5.6-5.7 min: 50-70% B; 5.7-6.2 min: 70% B; 6.2-6.3 min: 70-90% B; 6.3-6.8 min: 90% B; 6.8-6.9 min: 90-5% B; 6.9-8.0 min: 5% B. The flow rate was 0.600 mL/min and the sample injection volume was 7 μ L. Mass spectrometric settings were optimized by infusion of the peptides into the mass spectrometer. Optimal conditions for all compounds were as follows: ionspray voltage (IS) +5500 V, temperature 750°C, nebulizer gas (GS1) 70, TurbolonSpray gas (GS2) 45, collision-activated dissociation gas (CAD) 10, curtain gas (Cur) 40, dwell time 40 ms, declustering potential (DP) 35 V, collision exit potential (CXP) 14 V and entrance potential (EP) 10 V. Analyte-specific mass spectrometer parameters are represented in Table S-1 (supporting information), as well as the SRM transitions used to monitor the peptides and the corresponding SIL internal standards.

3.2.5 ELISA method

An ELISA Maxisorp plate (Thermo Fisher Scientific) was coated overnight with 100 μ L of a solution containing 1.00 μ g/mL of human anti-trastuzumab HCA169, after which the plate was washed three times with 300 μ L wash buffer (one PBS-Tween® tablet per liter water). After thawing, 15.0 μ L of plasma was pre-diluted with 285 μ L of Superblock T20 and subsequently 100 μ L of diluted sample was transferred in duplicate to the plate and incubated for 1 h at 22 °C and 500 rpm. Next, the plate was washed three times with 300 μ L wash buffer; 100 μ L of detection solution (biotin labeled human anti-trastuzumab HCA177 (at 0.500 μ g/mL) was added and the plate was incubated for 1 h at 22 °C and 500 rpm). Then the plate was washed three times with 300 μ L wash buffer and 100 μ L of conjugate solution (10,000 fold diluted Streptavidin HRP) was added followed by incubation for 0.5 h at 22 °C and 300 rpm. Subsequently, the plate was washed three times with 300 μ L wash buffer and 100 μ L of TMB was added and the plate was incubated for 9 minutes at 22 °C and 300 rpm. Next, 100 μ L of stop solution was added and the plate was analyzed within 10 minutes of stopping the reaction by measuring the absorbance at a wavelength of 450 nm on a SpectraMax M5e plate reader (Molecular Devices, California, USA).

3.2.6 LC-MS/MS and ELISA method validation

Trastuzumab concentrations in the validation and control samples were determined by applying the methods for trastuzumab (LC-MS/MS for peptides IYPTNGYTR and FTISADTSK, and ELISA) and comparing the results to a calibration curve spiked with

trastuzumab in blank plasma, which was analyzed with the same method in the same run. All methods for trastuzumab determination were validated according to international guidelines for bioanalytical method validation^{16,17} by assessing precision, accuracy, selectivity and stability using calibrators and validation samples in plasma (detailed experimental description in supplementary document).

3.2.7 *In vitro* deamidation of trastuzumab

Plasma was set at pH 8 and spiked with trastuzumab at 400 µg/mL, after which the sample was aliquoted into 1 mL portions in Eppendorf protein lo-bind tubes. The samples were prepared and stored under sterile conditions, to avoid external influences during the experiment. They were stored at 37°C for 56 days and at several time points a 1 mL portion was taken out and stored at -70°C until analysis. All samples were subsequently analyzed with the described ELISA and LC-MS/MS methods.

3.2.8 Patient samples

Blood samples were collected from patients with HER2-positive breast cancer, who were receiving trastuzumab intravenously every three weeks (8 mg/kg as initial dose, followed by 6 mg/kg, every three weeks) for a period of one year, as part of their adjuvant treatment for early breast cancer. Samples were withdrawn prior to the first dose and after a minimum of three administrations immediately before the administration of a next dose of trastuzumab. Patient samples were collected under appropriate ethical approval and after written informed patient consent. Plasma was prepared immediately after blood collection and stored at -20°C. All samples were subsequently analyzed with the described ELISA and LC-MS/MS methods.

3.3 RESULTS AND DISCUSSION

3.3.1 Selection of signature peptides

To follow *in vivo* deamidation of Asn55, two signature peptides were selected for trastuzumab: one containing the Asn55 residue and another one from a chemically stable part of the protein. An *in silico* tryptic digestion of the trastuzumab sequence was used to generate a list of candidate peptides using mMass¹⁸ resulting in 62 theoretical peptides that are expected after digestion with trypsin. To avoid interferences from the human plasma proteome, both signature peptides had to be unique for trastuzumab, which was

checked by submitting the preliminary peptide list to the basic local alignment search tool (BLAST) version 2.2.29¹⁹. In addition, to facilitate LC-MS/MS quantification, peptides containing unstable amino acids (other than Asn55), such as methionine and tryptophan as well as glycosylated peptides and peptides forming disulfide bonds were excluded as well as peptides outside the 500-2000 mass range.

The Asn55-containing peptide IYPT**N**GYTR (heavy chain amino acids 51-59, see Fig. S-1 supporting information) fulfilled all criteria, whence digestion with trypsin was concluded to be a suitable approach. A potentially useful second tryptic peptide was FTISADTSK (heavy chain amino acids 68-76), which falls outside the CDRs of trastuzumab. To confirm the suitability for LC-MS/MS analysis, peptide mapping experiments were conducted using trypsin digestion of trastuzumab after protein precipitation with methanol. Both peptides showed appropriate LC-MS/MS characteristics such as good chromatographic retention, efficient ionization and fragmentation and were thus used for further work. Reference standards were obtained for the signature peptides as well as for the deamidated products IYPT**D**GYTR and IYPT**isoD**GYTR and their corresponding stable-isotope labeled (SIL) forms. For all compounds, the parent ion was the doubly charged protonated molecule and the product ion the singly charged y7 fragment. Since the unstable succinimide intermediate could not be obtained in pure form, the same general MS settings were used for this compound, while the SRM transitions were based on a theoretical prediction of the m/z values of its molecular and fragment ions. The suitability of these settings was confirmed by the analysis of a solution of the non-deamidated peptide, which had been stored under conditions that induced succinimide formation and in which the succinimide form was present at relatively high levels.

3.3.2 Separation and identification of the peptides

The Asp55- and isoAsp55-containing peptides have the same mass, which differs only 1 Da from that of the Asn55-containing peptide. This means that the difference in their m/z values is just 0.5 for the doubly charged molecules (Table S-1 in the supporting information). With the triple quadrupole MS having unit mass resolution, the Asp55- and isoAsp55- containing forms cannot be distinguished mass spectrometrically, while the Asn-containing peptide will give a response in the mass transition of the deamidated forms. Hence, all three peptides need to be chromatographically separated.

The best separation (nearly baseline) while keeping sensitivity, was achieved by applying a relatively shallow gradient from 5 to 10% acetonitrile in 5 minutes. All

relevant peptides could thus be individually determined with a still reasonable sample throughput at 10 minutes from injection to injection (see **Figures 1A-D** for representative chromatograms).

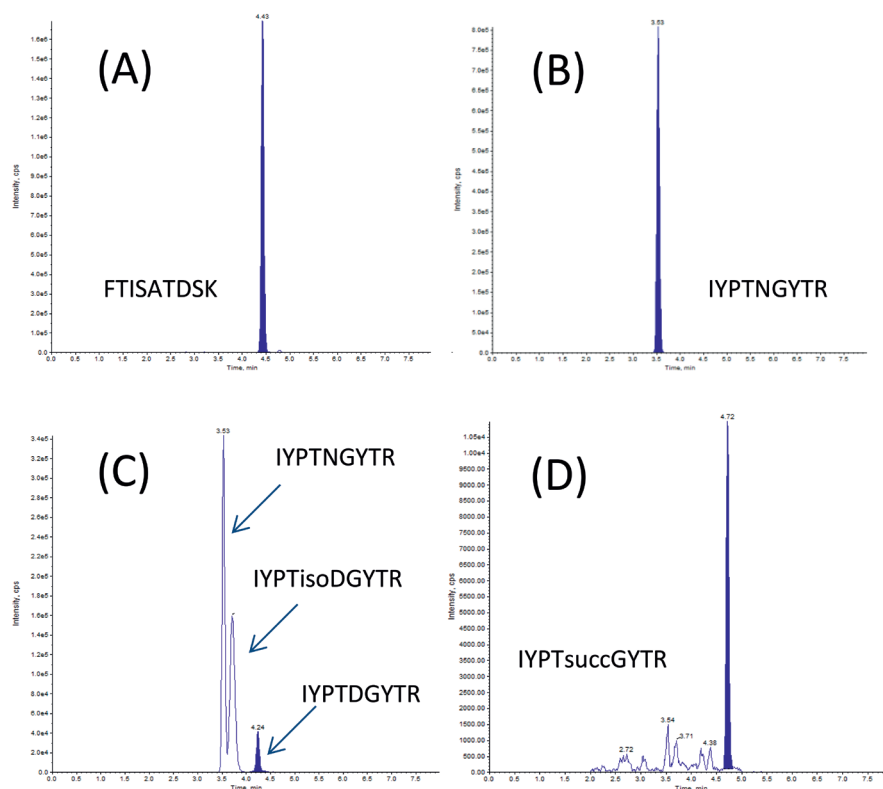


Figure 1: LC-MS/MS chromatograms for the two signature peptides and three degradation products of trastuzumab, recorded for a processed patient plasma sample. (A): FTISATDSK; (B): IYPTNGYTR; (C): IYPTDGYTR and IYPTisoDGYTR; (D): IYPTsuccGYTR.

3.3.3 Sample digestion and deamidation

It has been reported that the rate of asparagine deamidation increases at alkaline pH because of the deprotonation of the peptide bond nitrogen atom, which is the first step in the formation of a succinimide intermediate²⁰. Since tryptic digestion is typically performed at slightly alkaline pH, it is essential to investigate the pH dependence of the kinetics of Asn deamidation for trastuzumab under the digestion conditions. This is especially important since the deamidation rate for small peptides can be considerably higher than for intact proteins²¹ and, once formed after digestion of trastuzumab, the Asn55-containing signature

peptide will be subjected to the deamidation-inducing digestion conditions for a relatively long time.

Tryptic digestion was performed under four different conditions in which the pH of the digestion buffer was varied between pH 7.0 and 8.5. Aliquots of a plasma sample spiked with trastuzumab at 400 µg/mL were digested for up to 20 hours and digests were analyzed at several time points. **Fig. 2** shows a clear pH effect on the stability of IYPTNGYTR while FTISADTSK is stable at all values between 7.0 and 8.5. IYPTNGYTR is deamidated at pH 7.5 and above, with a higher deamidation rate when the pH increases.

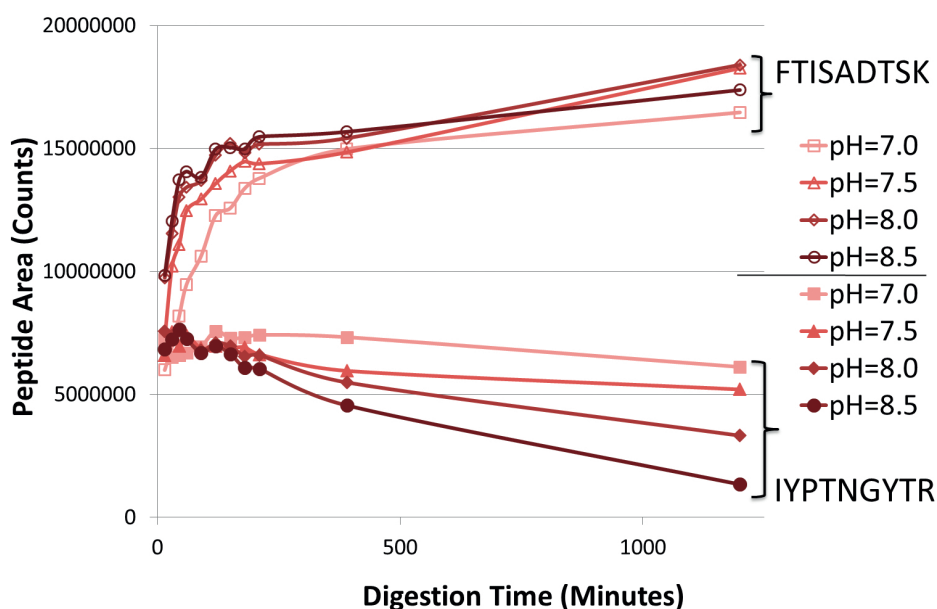


Figure 2: Release of the FTISADTSK signature peptide, and release and degradation of the IYPTNGYTR signature peptide during trypsin digestion of trastuzumab at four different pH values.

This is most apparent after around three hours when trastuzumab has been completely digested, but the effect will also play a role during the first three hours, when the peptide is being liberated from the protein. It was found that the deamidated forms of IYPTNGYTR and the succinimide intermediate were all formed under the various digestion conditions with an increase in concentration at higher pH values (Fig. S-2 in the supporting information). The isoAsp-containing peptide is formed to an approximately four-fold larger extent than the Asp-containing form and has an abundance of about 8% of that of the non-deamidated peptide after three hours of digestion at pH 8.5, which increases to 150% after 20 hours.

To avoid deamidation during digestion and to enable reliable monitoring of the actual deamidation products *in vivo*, it is clear that a pH of 7 is suitable. It combines a reasonable digestion efficiency (>80%) with minimal formation (<1%) of deamidation products during the first 3 hours of digestion.

3.3.4 LC-MS/MS method validation

The described LC-MS/MS method for trastuzumab was validated by quantitation of both signature peptides. All obtained results are included in the supplemental tables S-2 through S-10. For the peptide IYPTNGYTR, all results meet the criteria set for small-molecule bioanalytical method validations, which shows that trastuzumab can be determined with high accuracy and precision and that it can be kept sufficiently stable for a reliable determination in patient samples, despite the presence of a deamidation site in its sequence. For the peptide FTISADTSK, there is interference in the SRM transition, corresponding to approximately 100% to 200% of the response at the lower limit of quantitation (LLOQ), which affects the quantitation of this peptide at low levels of trastuzumab. This interference may be caused by the release of a peptide with a very similar amino acid sequence from an endogenous plasma protein or matrix compound. All other validation results are well within internationally accepted criteria. Monitoring of this signature peptide is therefore reliable at concentrations of trastuzumab above approximately 10 µg/mL.

3.3.5 ELISA method validation

All obtained results from the validation of the trastuzumab ELISA method are included in the supplemental tables S-11 through S-15. For trastuzumab, all results meet the criteria set for large molecule bioanalytical method validations and thus show that trastuzumab can be determined with high accuracy and precision and that it is sufficiently stable during storage and analysis for a reliable determination in patient samples.

3.3.6 Forced *in vitro* degradation

With the deamidation and isomerization of the Asn55-containing peptide under control during LC-MS/MS sample preparation, and the LC-MS/MS and ELISA methods validated, the methods were applied to investigate the deamidation and isomerization process in an *in vitro* forced degradation experiment. Trastuzumab was stored in plasma at 37°C for 56 days, which mimics its residence in the body after intravenous administration (the half-life of trastuzumab in humans ranges up to 32 days). The LC-MS/MS results for all forms

of the protein are shown in Fig. S-3 (supporting information). There is a 37% decrease in concentration of the non-deamidated form over a storage time of 56 days, which can be attributed to the formation of IYPTisoDGYTR (~31% increase), IYPTDGYTR (~4% increase) and IYPTsuccGYTR (~2% increase) with the area ratio between the isoAsp55 and Asp55 peptides remaining constant between 7 and 8 during the entire experiment. Thus, the formation of isoAsp is favored over the formation of Asp. Comparison of Figures S-2 and S-3 shows that the rate of trastuzumab deamidation is much lower in plasma than in digestion buffer at the same pH (8) and temperature (37°C). In digestion buffer, 37% degradation was observed after 4 to 6 hours, while this took 56 days in plasma. This confirms earlier findings²¹ that deamidation of peptides occurs much more rapidly than of intact proteins, probably because of conformational constraints that prevent the formation of the succinimide intermediate²².

Application of the LC-MS/MS method to quantify trastuzumab using the stable and unstable signature peptides and of the ELISA method gave three different concentration profiles (**Fig. 3**). The FTISADTSK concentrations remain stable at the initial level of 400 µg/mL, while the IYPTNGYTR concentrations decrease to 250 µg/mL after 56 days (37.5% decrease compared to t=0). In the same period, the ELISA concentrations decrease to 100 µg/mL (75% decrease).

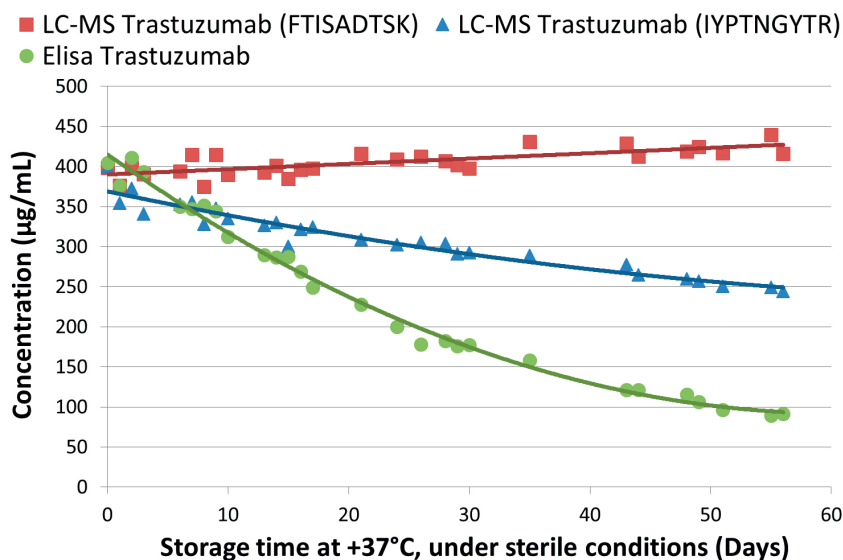


Figure 3: LC-MS/MS (for the signature peptides FTISADTSK and IYPTNGYTR) and ELISA results for trastuzumab in an *in vitro* forced degradation test over a period of 56 days at 37°C and pH 8.

Although all results are expressed as “the” concentration of trastuzumab, it should be realized that each analytical technique measures a different feature of trastuzumab. The signature peptide FTISADTSK represents the total amount of trastuzumab and does not discriminate between non-deamidated and deamidated forms at Asn55, or any other modification outside this peptide, for that matter. The signature peptide IYPTNGYTR specifically represents the concentration of trastuzumab which has not been deamidated at Asn55. Finally, the ELISA result, which decreases exactly two-fold faster than the LC-MS/MS results for IYPTNGYTR, corresponds to the immunoreactive concentration of trastuzumab. Trastuzumab contains two identical light and heavy chains and therefore two IYPTNGYTR sequences. Since the sandwich ELISA format uses two anti-idiotypic antibodies, it is very likely that both IYPTNGYTR sequences need to remain intact to form a detectable immune complex with trastuzumab. Therefore, when one of the two IYPTNGYTR sequences in a trastuzumab molecule is deamidated, LC-MS/MS still gives 50% of the original response, whereas with ELISA the complete signal is lost which explains the two-fold faster decrease of the measured concentration.

3.3.7 Analysis of patient samples

The validated LC-MS/MS and ELISA methods were used to quantify concentrations in plasma samples collected from breast cancer patients, who were treated with trastuzumab. **Fig. 4** presents LC-MS/MS results for a representative patient showing that there is deamidation and isomerization in all post-dose samples with an increase in abundance of the deamidation products over time. Because of the absence of pure reference standards of the intact protein containing Asp55, isoAsp55 and Asu55, the concentrations of the deamidated forms of trastuzumab were calculated by reference to the LC-MS/MS response factors for the peptides. For all deamidated peptides, this was found to be equal to that of the non-deamidated peptide IYPTNGYTR and, therefore, the peak area ratios found for the deamidated forms of trastuzumab could be directly substituted into the calibration curve equation for trastuzumab, quantified through its signature peptide IYPTNGYTR. After 365 days of treatment of this particular patient, a total trastuzumab plasma concentration (as represented by peptide FTISADTSK) of 117 µg/mL was found, while Asn55 non-deamidated trastuzumab (peptide IYPTNGYTR) circulated at 89.2 µg/mL.

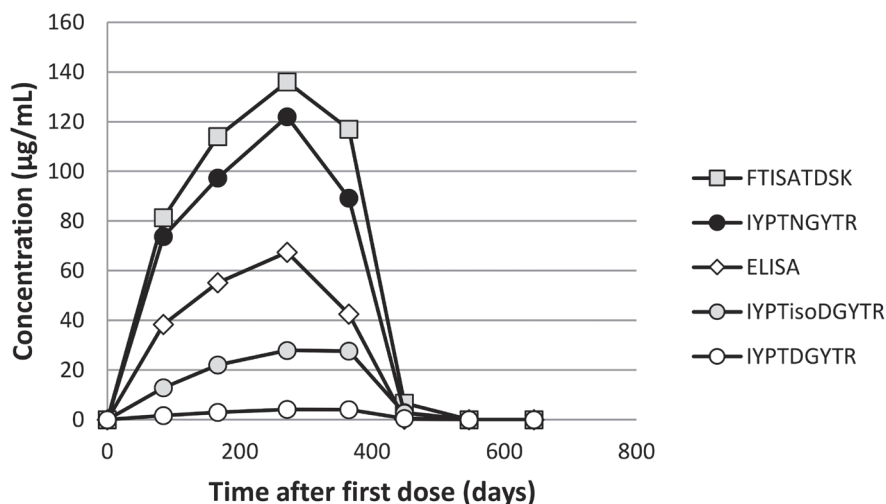


Figure 4: LC-MS/MS and ELISA results in plasma obtained from a breast cancer patient on long-term treatment with trastuzumab. LC-MS/MS concentrations obtained for peptides FTISADTSK, IYPTNGYTR, IYPTDGYTR and IYPTisoDGYTR.

A total of 24% of the drug was thus deamidated and this was mainly to isoAsp55-trastuzumab and much less to Asp55-trastuzumab. The ELISA concentration data are lower than the IYPTNGYTR results measured by LC-MS/MS, but in fact considerably lower than the factor two that was expected based on the *in vitro* experiments. This might be explained by other (e.g. enzymatic) protein degradation processes which further decrease the ELISA response by affecting the binding epitope(s). Alternatively there could be anti-drug antibodies in the circulation, formed as a response to long-term exposure to trastuzumab, competing with the ELISA antibodies for binding and reducing the signal^{23,24}. Although this was not further investigated in the present study, the results do show that an ELISA is potentially hampered by multiple effects and that it is difficult to ascertain which fraction of the drug in plasma is actually measured. Results from the other patients are summarized in the supplemental table S-16. They show that the degree of deamidation varies considerably between patients, which may have an effect on the efficacy of the therapy.

3.4 CONCLUSION

We have developed and validated an LC-MS/MS-based method for quantitatively monitoring the *in vitro* and *in vivo* deamidation of trastuzumab at a potentially crucial position in one of its complementarity determining regions^{15,25}. The Asn55 residue is located at the top of the CDR2 loop, which is involved in the binding of trastuzumab to the HER2/neu receptor. It is, therefore, not unlikely that a modification of Asn55 may result in a conformational change in the CDR2, thus leading to changes in binding affinity of trastuzumab to its receptor and, potentially, to an altered pharmacological effect.

Application of the method to samples of *in vitro* and *in vivo* studies showed deamidation and isomerization with an increase in abundance of the deamidation products over time (weeks to months). Comparison of the LC-MS/MS results for the two signature peptides with ELISA data from the same *in vitro* samples indicated that three different concentrations were found, each of which represented a different entity: total trastuzumab (FTISADTSK), trastuzumab which has not been deamidated at Asn55 (IYPTNGYTR) and immunoreactive trastuzumab (ELISA). This highlights a general aspect of protein quantitation: it is not meaningful to refer to “the” concentration of a protein, since this value depends on the actual part(s) of the protein molecule which are the basis for analysis as well as on the underlying principle of the analytical technique, be it LC-MS/MS or ELISA⁴. LC-MS/MS results from patient plasma samples revealed deamidation and isomerization of Asn55 but these translated into much lower values for the corresponding ELISA results than the factor that was expected based on *in vitro* experiments. This may indicate the effect of trastuzumab binding to anti-drug antibodies or other specific proteins in the sample in addition to deamidation and further emphasizes the complex nature of protein quantification.

Notes

The authors declare no competing financial interest.

Acknowledgments

The authors are thankful to prof. Daan Touw (University Medical Center Groningen) for providing the reference standard for intact trastuzumab. Samenwerkingsverband Noord-Nederland (SNN) is gratefully acknowledged for financial support (grant T3041).

REFERENCES

1. Wilffert, D.; Bischoff, R. & van de Merbel, N.C. *Bioanalysis*, 2015, vol 7, no. 6, 763-779.
2. Zhang, Y. J.; Olah, T. V. & Zeng, J. *Bioanalysis*, 2014, vol 6, no. 13, 1827-1841.
3. Hall, M. P. *Drug Metabolism and Disposition*. 2014, vol 42, no. 11, 1873-1880.
4. Bults, P.; van de Merbel, N. C. & Bischoff, R. *Expert Reviews of Proteomics* 2015, vol 12, no. 4, 1-19.
5. Habberger, M.; Bomans, K.; Diepold, K.; Hook, M.; Gassner, J.; Schlothauer, T.; Zwick, A.; Spick, C.; Kepert, J. F.; Hienz, B.; Wiedmann, M.; Beck, H.; Metzger, P.; Mølhøj, M.; Knoblich, C.; Grauschopf, U.; Reusch, D. & Bulau, P. *MAbs* 2014, vol 6, no. 2, 327-339.
6. Harris, R. J.; Kabakoff, B.; Macchi, F. D.; Shen, F. J.; Kwong, M.; Andya, J. D.; Shire, S. J.; Bjork, N.; Totpal, K. & Chen, A. B. J. *Chromatogr. B. Biomed. Sci. Appl.* 2001, vol 752, no. 2, 233-245.
7. Sydow, J. F.; Lipsmeier, F.; Larrailet, V.; Hilger, M.; Mautz, B.; Mølhøj, M.; Kuentzer, J.; Klostermann, S.; Schoch, J.; Voelger, H. R.; Regula, J. T.; Cramer, P.; Papadimitriou, A. & Kettenberger, H. *PLoS One* 2014.
8. Brekke, O. H. & Sandlie, I. *Nat. Rev. Drug Discov.* 2003, vol 2, 52-62.
9. Hudis, C. A. *N Engl J Med* 2007, vol 357, 39-51.
10. Bange, J.; Zwick, E. & Ullrich, A. *Nat. Med.* 2001, vol 7, 548-552.
11. Damen, C. W. N.; de Groot, E. R.; Heij, M.; Boss, D. S.; Schellens, J. H. M.; Rosing, H.; Beijnen, J. os H. & Aarden, L. Lucien A. *Anal. Biochem.* 2009, vol 391, no. 2, 114-120.
12. Diepold, K.; Bomans, K.; Wiedmann, M.; Zimmermann, B.; Petzold, A.; Schlothauer, T.; Mueller, R.; Moritz, B.; Stracke, J. O.; Mølhøj, M.; Reusch, D & Bulau, P. *PLoS One* 2012.
13. Yan B.; Steen S.; Hambly D.; Valliere-Douglass J.; van den Bos T.; Smallwood S.; Yates Z.; Arroll T.; Han Y.; Gadgil H.; Latypov R. F.; Wallace A.; Lim A.; Kleemann G. R.; Wang W. & Balland A. *Journal of Pharmaceutical Sciences* 2009, vol 98, no. 10, 3509-3521
14. Robinson, N. E.; Robinson, Z. W.; Robinson, B. R.; Robinson, A. L.; Robinson, J. A.; Robinson, M. L. & Robinson, A. B. J. *Pept. Res.* 2004, vol 63, no. 5, 426-436.
15. Huang, L.; Lu, J.; Wroblewski, V. J.; Beals, J. M. & Rigglin, R. M. *Anal. Chem.* 2005, vol 77, no. 5, 1432-1439.
16. Food and Drug Administration. *Guidance for Industry: Bioanalytical Method Validation*. U.S. Department of Health and Human Services 2001.
17. EMA. *Guideline on bioanalytical method validation*. EMA Guideline 2012.
18. Niedermeyer, T. H. J. & Strohm, M. *PLoS One* 2012.
19. Altschul, S. F.; Madden, T. L.; Schaffer, A. A.; Zhang, J.; Zhang, Z.; Miller, W. & Lipmann D. J. *Nucleic acids Res* 1997, vol 25, no. 17, 3389-3402.
20. Peters, B. & Trout, B. L. *Biochemistry* 2006, vol 45, no. 16, 5384-5392.
21. Robinson, N. E. & Robinson, A. B. *Proc. Natl. Acad. Sci. U. S. A.* 2001, vol 98, no. 22, 12409-12413.
22. Ouellette, D.; Chumsae, C.; Clabbers, A.; Radziejewski, C. & Correia, I. *mAbs* 2013, vol 5, no. 3, 432-444.
23. Heudi, O.; Barteau, S.; Zimmer, D.; Schmidt, J.; Bill, K.; Lehmann, N.; Bauer, C. & Kretz, O. *Anal. Chem.* 2008, vol 80, no. 11, 4200-4207.
24. Kushnir, M. M.; Rockwood, A. L.; Roberts, W. L.; Abraham, D.; Hoofnagle, A. N. & Meikle, A. W. *Clin. Chem.* 2013, vol 59, no. 6, 982-990.
25. Magdelaine-Beuzelin, C.; Kaas, Q.; Wehbi, V.; Ohresser, M.; Jefferis, R.; Lefranc, M. P. & Watier, H. *Crit. Rev. Oncol. Hematol.* 2007, vol 64, no. 3, 210-225.

SUPPORTING INFORMATION FOR:

LC-MS/MS based monitoring of *in vivo* protein biotransformation: quantitative determination of trastuzumab and its deamidation products in human plasma

Content

- Graphical representation of trastuzumab, Figure S-1.
- Formation of the deamidation products during digestion, Figure S-2.
- Formation of the deamidation products in an *in vitro* stress test, Figure S-3.
- Amino acid sequences, SRM transitions and charge states for the peptides and their SIL internal standards (Table S-1)
- A short description of the validation experiments for the LC-MS/MS determination of trastuzumab (IYPTNGYTR and FTISADTSK signature peptides).
- Results of the validation experiments for the LC-MS/MS determination of trastuzumab (IYPTNGYTR signature peptide), Table S-2 / S-7.
- Results of the validation experiments for the LC-MS/MS determination of trastuzumab (FTISADTSK signature peptide), Table S-8 / S-10.
- A short description of the validation experiments for the ELISA method for determination of trastuzumab.
- Results of the validation experiments for the ELISA method for determination of trastuzumab, Table S-11 / S-15.
- Individual results from the analyzed patient samples, Table S-16

Trastuzumab heavy chain

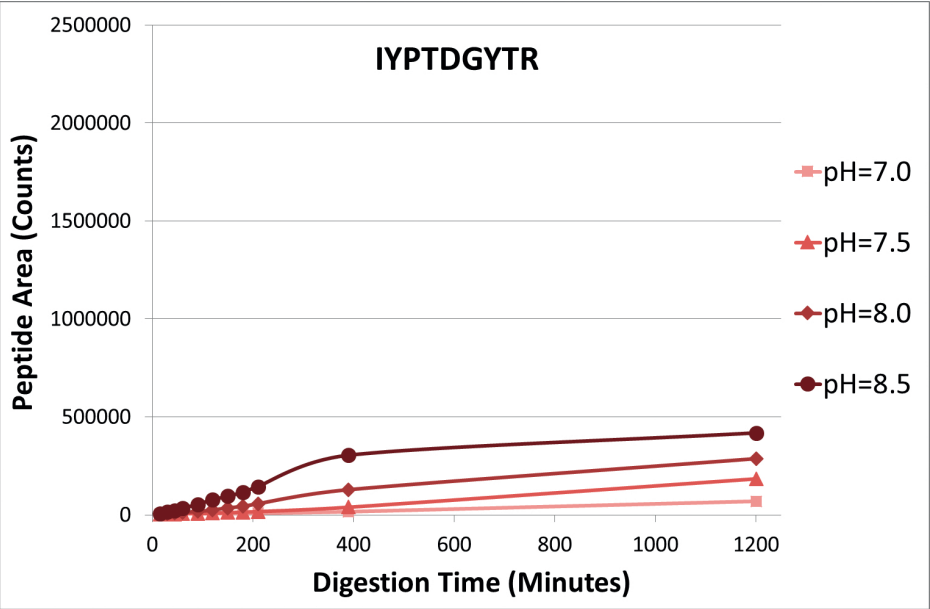
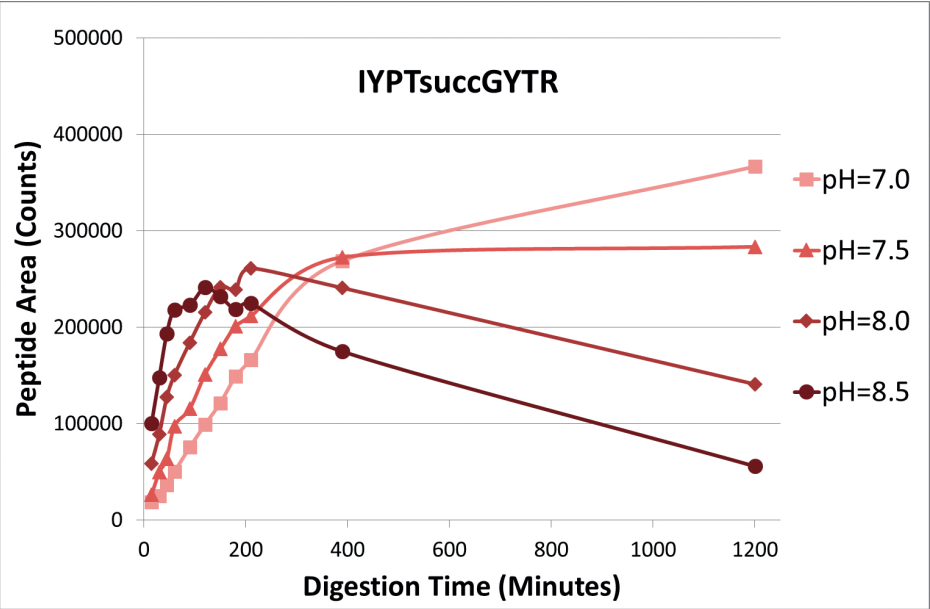
1	EVQLVESGGG	LVQPGGSLRL	SCAASGFNIK	DTYIHWVRQA	PGKGLEWVAR	<u>IYPT</u> NGYTRY
61	ADSVKGR <u>FTI</u>	<u>SADTSK</u> NTAY	LQMNSLRAED	TAVYYCSRWG	GDGFYAMDYW	GQGTLVTVSS
121	ASTKGPSVF	LAPSSKSTSG	GTAALGCLVK	DYFPEPTVS	WNSGALTSGV	HTFPAVLQSS
181	GLYSLSSVVT	VPSSSLGTQT	YICNVNHKPS	NTKVDKKVEP	PKSCDKTHTC	PPCPAPELLG
241	GPSVFLFPPK	PKDTLMISRT	PEVTCVVVDV	SHEDPEVKFN	WYVDGVEVHN	AKTKPREEQY
301	NSTYRVVSVL	TVLHQDWLNG	KEYKCKVSNK	ALPAPIEKTI	SKAKGQPREP	QVYTLPPSRD
361	ELTKNQVSLT	CLVKGFYPSD	IAVEWESNGQ	PENNYKTPP	VLDSDGSFFL	YSKLTVDKSR
421	WQQGNVFSCS	VMHEALHNHY	TQKSLSLSPG	K		

Asn55

Trastuzumab light chain

1	DIQMTQSPSS	LSASVGDRV	ITCRASQDVN	TAVAWYQQK	GKAPKLLIYS	ASFLYSGVPS
61	RFGSRSRGT	FTLTISLQ	EDFATYYCQ	HYTTPPTFG	GTKVEIKRTV	AAPSVFIFPP
121	SDEQLKSGTA	SVVCLLN	FNFPREAKVQ	WKVDNALQSG	NSQESVTEQD	SKDSTYSL
181	LSKADYEKHK	VYACEVTHQ	G	LSSPVTKSFN	RGEC	

Figure S-1: Amino acid sequence of the heavy and light chain of trastuzumab with underlined and in red, both signature peptides.



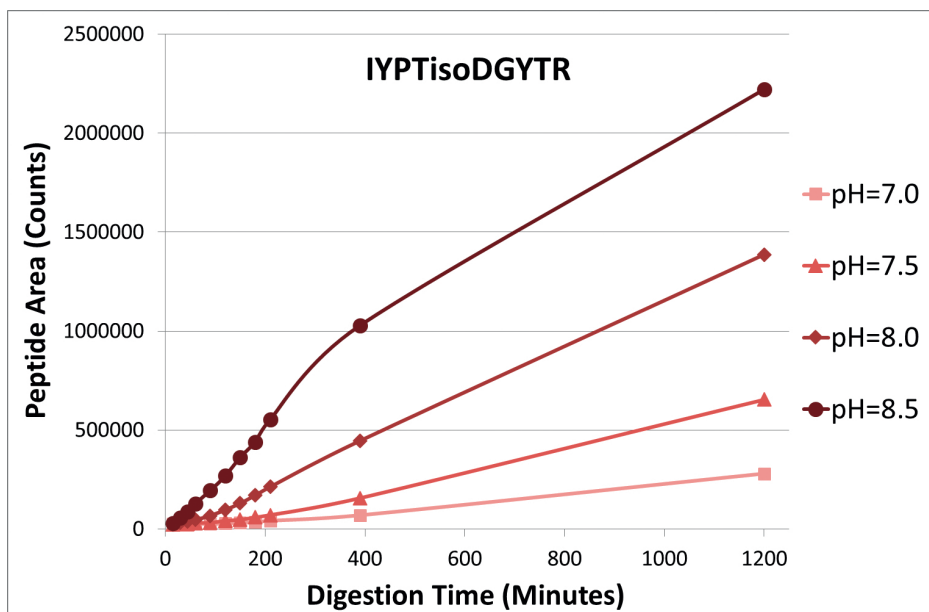


Figure S-2: Formation and degradation of the intermediate IYPTsuccGYTR (A) and the formation of the deamidation products IYPTDGYTR (B) and IYPTisoDGYTR (C) during trypsin digestion of trastuzumab at four different pH values (pH 7.0; 7.5; 8.0; 8.5).

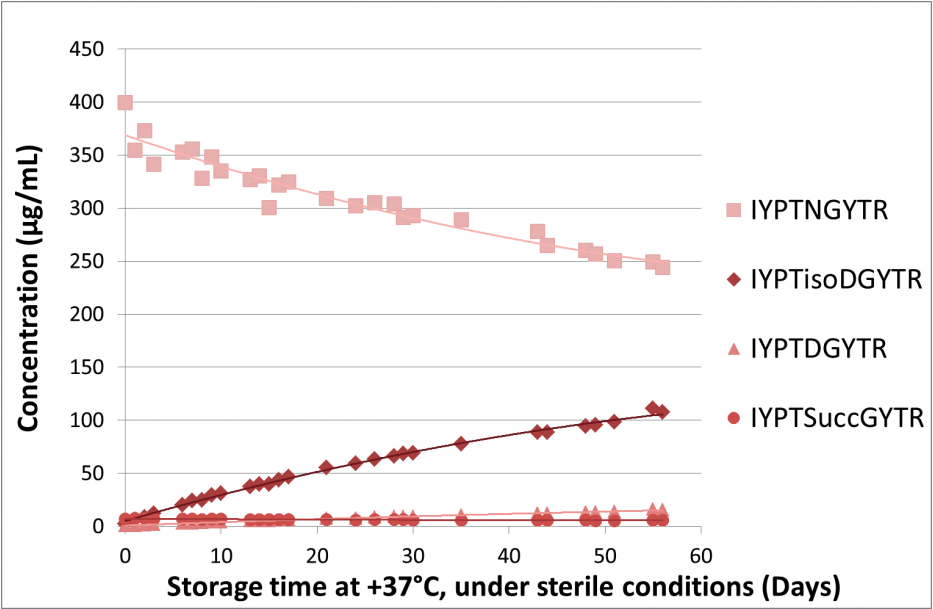


Figure S-3: LC-MS/MS results for four peptides of trastuzumab (in plasma) in an *in vitro* forced degradation test over a period of 56 days at 37°C and pH 8. Degradation of IYPTNGYTR and the formation of the intermediate IYPTSuccGYTR and the deamidation products IYPTDGYTR and IYPTisoDGYTR.

Table S-1: Amino acid sequences, SRM transitions and charge states for the peptides and their SIL internal standards.

Peptide Sequence	Q1 / Precursor ion mass (m/z) and charge state	Q3 / Product ion mass (m/z) and charge state	Collision Energy (V)
FTISADTSK	485.3 / [M+2H] ²⁺	721.4 / Y7 ¹⁺	22
FTISADTSK	489.3 / [M+2H] ²⁺	729.4 / Y7 ¹⁺	22
IYPTNGYTR	542.8 / [M+2H] ²⁺	808.4 / Y7 ¹⁺	23
IYPTNGYTR*	547.8 / [M+2H] ²⁺	818.4 / Y7 ¹⁺	23
IYPTDGYTR	543.3 / [M+2H] ²⁺	809.4 / Y7 ¹⁺	23
IYPTDGYTR*	548.3 / [M+2H] ²⁺	819.4 / Y7 ¹⁺	23
IYPTisoDGYTR	543.3 / [M+2H] ²⁺	809.4 / Y7 ¹⁺	23
IYPTisoDGYTR*	548.3 / [M+2H] ²⁺	819.4 / Y7 ¹⁺	23
IYPTSuccGYTR	534.3 / [M+2H] ²⁺	791.4 / Y7 ¹⁺	23

- C-terminal lysine ¹³C₆-¹⁵N₂-labeled internal standard

* C-terminal arginine ¹³C₆-¹⁵N₄-labeled internal standard

Description of the validation experiments for the LC-MS/MS determination of trastuzumab (IYPTNGYTR and FTISADTSK signature peptides)

All calculations were done in Analyst (version 1.6.2, AB Sciex, Concord, Canada) and/or Microsoft Excel 2003/2010 using validated spreadsheets.

Acceptance criteria. As per international guidelines, all Bias and CV acceptance criteria were set at 15% (20% at the LLOQ), except for the stock-stability assessments, for which 10% limits were used.

Linearity. Each validation run contained a calibration curve prepared in human plasma with the following levels: 0.500, 1.00, 2.50, 10.0, 25.0, 100, 250, 400 and 500 µg/mL. The ratio of the measured peak area of the signature peptide over that of the internal standard was used in calculations. Weighted linear regression was applied with $1/x^2$ as weighting factor.

Accuracy and precision. The accuracy and precision of the method were determined by six-fold analysis in three separate runs analyzed on three different days. The validation samples were prepared in plasma at four concentration levels: 0.500, 1.50, 25.0 and 400 µg/mL. Statistical analysis was performed using analysis of variance (ANOVA).

Matrix variability/selectivity. The influence of the matrix was assessed by preparing samples in six independent human plasma lots at the LLOQ of 0.500 µg/mL. Additionally, from all six plasma lots, blank samples were analyzed and checked for interferences with an area greater than 20% of the area of the same selectivity LLOQ sample. The samples were analyzed in one run.

Freeze-thaw stability. Human plasma samples at 1.50 and 400 µg/mL were stored at -20°C and subjected to five freeze-thaw cycles, in which thawing was performed on the bench-top for a minimum of two hours, followed by frozen storage for at least 12 hours. The samples were analyzed against a freshly spiked and prepared calibration curve.

Frozen stability. Human plasma samples at 1.50 and 400 µg/mL were stored at -20°C for 98 days. The samples were analyzed against a freshly spiked and prepared calibration curve.

Extract stability in the autosampler. Human plasma samples at 1.50 and 400 µg/mL were extracted and analyzed in the first validation run as a part of the accuracy and precision assessment. Subsequently, the extracts were kept in the autosampler at +10°C for 123 hours, after which they were re-analyzed and the concentrations determined against the original calibration curve.

Frozen stability of the stock solution. A 20.8 mg/mL stock solution of trastuzumab was prepared from the reference material, and stored at -80°C. 323 days later a second stock solution was prepared freshly. Aliquots from both stock solutions were diluted with plasma to 400 µg/mL. These samples were analyzed in six-fold using the LC-MS/MS methodology for plasma. Stability evaluation was performed by comparing the analyte area ratios over internal standard found in the samples.

Bench-top stability of the stock solution. An aliquot of the 20.8 mg/mL stock solution of trastuzumab was stored on the bench-top, exposed to normal daylight, while another aliquot of the same stock solution was stored at -80°C. After approximately 25 hours both stock solutions were diluted with plasma to 400 µg/mL. These samples were analyzed in six-fold using the LC- MS/MS methodology for plasma. Stability evaluation was performed by comparing the analyte area ratios over internal standard found in the samples.

Carry-over. For each of the three validation runs which contained accuracy and precision samples, the peak areas for the three blank plasma samples which directly followed the highest calibrator of the calibration curve were compared to the peak areas of the six validation samples prepared at the LLOQ (0.500 µg/mL) from the same run.

Results of the validation experiments for the LC-MS/MS determination of trastuzumab (IYPTNGYTR signature peptide).
Table S-2: Individual calibration curve results from the LC-MS/MS validation of the IYPTNGYTR signature peptide (nominal concentration).

Run #	Measured concentration (µg/mL)									Correlation	slope	intercept
	0.500*	1.00*	2.50*	10.0*	25.0*	100*	250*	400*	500*			
01	0.523	0.918	2.42	10.3	25.7	99.4	242	405	518	0.9989	0.0241	0.000437
02	0.497	1.04	2.32	10.0	26.6	99.8	241	400	508	0.9991	0.0228	-0.000766
03	0.497	1.01	2.53	10.2	25.4	98.1	239	395	517	0.9997	0.0255	0.000793
04	0.490	1.05	2.43	9.88	24.5	101	245	397	524	0.9994	0.0231	-0.000856
Average (µg/mL)	0.502	1.00	2.43	10.1	25.6	99.5	241	399	517	-	-	-
Total bias (%)	0.3	0.4	-3.0	0.9	2.2	-0.5	-3.4	-0.2	3.3	-	-	-
Total CV (%)	2.9	6.0	3.6	1.8	3.3	1.0	1.1	1.1	1.3	-	-	-

Table S-3: Individual accuracy and precision results from the LC-MS/MS validation of the IYPTNGYTR signature peptide.

Run #	Nominal concentration 0.500 (µg/mL)						Average	Bias	CV
	Measured concentration (µg/mL)						(µg/mL)	(%)	(%)
01	0.447	0.406	0.486	0.472	0.446	0.468	0.454	-9.2	6.2
02	0.500	0.554	0.517	0.390	0.543	0.547	0.509	1.7	12.1
03	0.414	0.406	0.479	0.429	0.418	0.420	0.428	-14.5	6.1
	Total						0.463	-7.3	11.2

Run #	Nominal concentration 1.50 (µg/mL)						Average	Bias	CV
	Measured concentration (µg/mL)						(µg/mL)	(%)	(%)
01	1.38	1.44	1.45	1.54	1.45	1.46	1.45	-3.2	3.5
02	1.72	1.62	1.59	1.48	1.56	1.57	1.59	5.8	5.0
03	1.40	1.34	1.49	1.50	1.38	1.48	1.43	-4.6	4.5
	Total						1.49	-0.7	6.0

Run #	Nominal concentration 25.0 (µg/mL)						Average	Bias	CV
	Measured concentration (µg/mL)						(µg/mL)	(%)	(%)
01	24.5	24.7	24.9	25.3	24.3	24.5	24.7	-1.2	1.4
02	25.3	26.5	26.3	25.3	26.8	25.4	25.9	3.7	2.5
03	24.3	23.2	23.1	23.2	24.6	23.7	23.7	-5.3	2.6
	Total						24.8	-1.0	4.4

Run #	Nominal concentration 400 (µg/mL)						Average	Bias	CV
	Measured concentration (µg/mL)						(µg/mL)	(%)	(%)
01	391	383	378	387	381	381	383	-4.1	1.3
02	403	407	418	404	390	403	404	1.0	2.2
03	372	377	391	370	373	388	378	-5.4	2.3
	Total						389	-2.8	3.6

Table S-4: Individual results from the matrix variability experiments of the IYPTNGYTR signature peptide LC-MS/MS validation.

Plasma lot #	Nominal concentration 0.500 (µg/mL) Measured concentration (µg/mL)
01	0.422
02	0.410
03	0.401
04	0.564
05	0.423
06	0.429
Average (µg/mL)	0.442
Bias (%)	-11.7
CV (%)	13.8

Table S-5: Results (n=3) from the stability experiments of the IYPTNGYTR signature peptide LC-MS/MS validation, analyzed against a freshly prepared calibration curve.

Stability item	Nominal concentration 1.50 (µg/mL)		
	Average concentration (µg/mL)	Bias (%)	CV (%)
Freeze-thaw: 5 cycles	1.61	7.5	4.6
Frozen plasma sample: 98 days at -20°C	1.61	7.2	3.9
Autosampler: 123 hours at +10°C	1.55	3.5	6.1

Stability item	Nominal concentration 400 (µg/mL)		
	Average concentration (µg/mL)	Bias (%)	CV (%)
Freeze-thaw: 5 cycles	448	12.1	6.3
Frozen plasma sample: 98 days at -20°C	402	0.5	2.2
Autosampler: 123 hours at +10°C	402	0.5	1.6

Table S-6 : Individual results from the stock stability experiments of the IYPTNGYTR signature peptide LC-MS/MS validation.

Nominal concentration: 20.8 mg/mL								
Storage period at RT (hours)	Peak area signature peptide over internal standard peak area							Bias (%)
	x1	x2	x3	x4	x5	x6	Mean	
0	0.37329	0.37193	0.37338	0.37830	0.37164	0.37518	0.37395	reference
25	0.38760	0.38717	0.38772	0.39046	0.38700	0.38579	0.38762	0.4 3.7

Nominal concentration: 20.8 mg/mL								
Storage period at -80 °C (days)	Peak area signature peptide over internal standard peak area							Bias (%)
	x1	x2	x3	x4	x5	x6	Mean	
0	0.34671	0.34723	0.34742	0.34366	0.34610	0.34710	0.34637	reference
323	0.37329	0.37193	0.37338	0.37830	0.37164	0.37518	0.37395	0.7 8.0

Table S-7: Results from the carry-over experiments of the IYPTNGYTR signature peptide LC-MS/MS validation.

Validation sample	Measured analyte peak area (counts)		
	Run #	Run #	Run #
	01	02	03
LLOQ validation sample	7103.5	6682.2	8176.8
LLOQ validation sample	6518.5	7180.6	7871.1
LLOQ validation sample	7640.5	6878.6	9067.4
LLOQ validation sample	7351.9	5110.9	8121.7
LLOQ validation sample	6959.2	7355.5	7799.8
LLOQ validation sample	7226.8	7224.6	8007.9
Mean analyte peak area	7133.4	6738.7	8174.1
Blank 1	0.0	205.5	0.0
Blank 2	0.0	0.0	0.0
Blank 3	0.0	68.8	0.0
Blank area against mean LLOQ area (%)			
Blank 1	0.0	3.0	0.0
Blank 2	0.0	0.0	0.0
Blank 3	0.0	1.0	0.0

Results of the validation experiments for the LC-MS/MS determination of trastuzumab (FTISADTSK signature peptide).

Table S-8: Individual calibration curve results from the LC-MS/MS validation of the FTISADTSK signature peptide (nominal concentration).

Run #	Measured concentration (µg/mL)									Correlation	slope	intercept
	0.500*	1.00*	2.50*	10.0*	25.0*	100*	250*	400*	500*			
01	-	-	-	10.0	25.0	98.1	239	413	514	0.9994	0.114	0.160
02	-	-	-	9.88	25.7	102	239	386	519	0.9992	0.109	0.143
03	-	-	-	9.86	26.0	99.2	242	390	519	0.9994	0.105	0.197
04	-	-	-	9.88	25.9	98.3	244	395	514	0.9996	0.0889	0.140
Average (µg/mL)	-	-	-	9.91	25.6	99.4	241	396	517	-	-	-
Total bias (%)	-	-	-	-0.9	2.6	-0.6	-3.5	-0.9	3.3	-	-	-
Total CV (%)	-	-	-	0.8	1.8	1.9	1.1	3.0	0.6	-	-	-

Table S-9: Individual accuracy and precision results from the LC-MS/MS validation of the FTISADTSK signature peptide.

Run #	Nominal concentration 25.0 (µg/mL)						Average (µg/mL)	Bias (%)	CV (%)
	Measured concentration (µg/mL)								
01	25.6	25.1	25.4	24.7	24.7	25.0	25.1	0.4	1.4
02	25.7	27.1	27.3	25.5	26.5	25.2	26.2	4.9	3.3
03	24.3	24.2	23.3	23.3	23.9	23.6	23.8	5.0	1.9
Total							25.0	0.1	4.7

Run #	Nominal concentration 400 (µg/mL)						Average (µg/mL)	Bias (%)	CV (%)
	Measured concentration (µg/mL)								
01	382	390	380	395	395	385	388	-3.0	1.7
02	393	411	410	395	401	394	401	0.2	2.1
03	395	388	416	386	400	398	397	-0.7	2.7
Total							395	-1.2	2.5

Table S-10: Results (n=3) from the stability experiments of the FTISADTSK signature peptide LC-MS/MS validation, analyzed against a freshly prepared calibration curve.

Stability item	Nominal concentration 400 (µg/mL)		
	Average concentration (µg/mL)		
Freeze-thaw: 5 cycles	437		
Frozen plasma sample: 98 days at -20°C	411		
Autosampler: 123 hours at +10°C	380		

Description of the validation experiments for the ELISA method for determination of trastuzumab

All calculations were done in Microsoft Excel 2003/2010 using validated spreadsheets

Acceptance criteria. As per international guidelines, all Bias and CV acceptance criteria were set at 20%, (25% at the LLOQ and ULOQ).

Linearity. Each validation run contained a calibration curve prepared in human plasma with the following levels: 60.1, 102, 172, 290, 490, 829, 1400, 2370 and 4000 ng/mL. The optical density (OD) was used in calculations. 4 parameter logistic fit (4PL) was applied.

Accuracy and precision. The accuracy and precision of the method were determined by triplicate analysis in four separate runs analyzed on four different days. The validation samples were prepared in plasma at five concentration levels: 102, 250, 1000, 3000 and 4000 ng/mL. Statistical analysis was performed using analysis of variance (ANOVA).

Integrity of dilution. The integrity of dilution was assessed on two levels, by triplicate analysis on two separate days. Samples were prepared at concentrations of 50.0 and 600 µg/mL and diluted, separately, 200 times with blank plasma.

Dilution linearity / Hook effect. Dilution linearity was assessed by multiple dilutions of a sample containing 600 µg/mL trastuzumab. Dilutions assessed were: undiluted, 20, 200, 500, 1250, 3125 and 7812,5 times diluted.

Matrix variability/selectivity. The influence of the matrix was assessed by preparing samples in 10 independent human plasma lots at a concentration of 150 and 3000 ng/mL. Additionally, from all 10 plasma lots, blank samples were analyzed and checked for interferences. The samples were analyzed in one run.

Results of the validation experiments for the ELISA determination of trastuzumab.

Table S-11: Individual calibration curve results from the ELISA validation.

Run #	Measured concentration (ng/mL)										Curve parameters				Blank OD	Min. OD	Max. OD
	60.1	102	172	290	490	829	1400	2370	4000		A	B	C	D			
01	60.1	101	174	289	495	822	1390	2430	3940		0.0824	1.20	1470	3.85	0.058	0.227	2.967
02	60.8	100	170	294	496	822	1350	2510	3890		0.0508	1.06	1680	4.02	0.057	0.239	2.868
03	55.7	103	179	293	480	823	1400	2460	3880		0.0993	1.32	1460	3.53	0.055	0.200	2.788
04	60.5	99.3	174	293	489	854	1290	2590	3880		0.0530	1.01	2940	4.53	0.052	0.193	2.601
05	57.1	103	179	291	486	807	1420	2470	3830		0.0965	1.28	1250	3.69	0.054	0.238	2.997
06	58.4	105	175	277	509	820	1380	2420	3960		0.0891	1.29	1310	3.46	0.056	0.214	2.812
07	51.3	113	175	296	475	817	1420	2440	3880		0.0993	1.28	1560	3.64	0.054	0.218	2.798
Average (ng/mL)	57.7	104	175	290	490	824	1380	2470	3890		-	-	-	-	0.055	0.218	2.833
Total bias (%)	-4.0	1.5	1.8	0.2	0.0	-0.6	-1.5	4.4	-2.7		-	-	-	-	-	-	-
Total CV (%)	5.9	4.4	1.7	2.2	2.3	1.8	3.4	2.5	1.1		-	-	-	-	3.6	8.3	4.6

Table S-12: Individual accuracy and precision results from the ELISA validation.

Run #	Nominal concentration 102 (ng/mL)			Average	Bias	CV
	Measured concentration (ng/mL)			(ng/mL)	(%)	(%)
01	100	100	99.3	100	-1.9	0.7
02	101	101	97.6	99.9	-2.1	2.0
03	112	112	105	110	7.5	3.8
04	97.7	99.8	97.5	98.3	-3.6	1.3
Total				102	0.0	5.0

Run #	Nominal concentration 250 (ng/mL)			Average	Bias	CV
	Measured concentration (ng/mL)			(ng/mL)	(%)	(%)
01	251	238	252	247	-1.3	3.2
02	246	250	244	247	-1.4	1.2
03	262	282	285	276	10.5	4.6
04	243	249	242	245	-2.1	1.6
Total				254	1.5	6.0

Run #	Nominal concentration 1000 (ng/mL)			Average	Bias	CV
	Measured concentration (ng/mL)			(ng/mL)	(%)	(%)
01	977	961	941	960	-4.0	1.9
02	969	998	992	986	-1.4	1.6
03	982	1050	1000	1010	1.0	3.2
04	925	922	895	914	-8.6	1.8
Total				967	-3.3	4.3

Run #	Nominal concentration 3000 (ng/mL)			Average	Bias	CV
	Measured concentration (ng/mL)			(ng/mL)	(%)	(%)
01	2800	2860	2480	2710	-9.5	7.6
02	2670	2730	2720	2710	-9.7	1.1
03	3120	3210	3010	3110	3.8	3.2
04	2840	3030	2740	2870	-4.3	5.0
Total				2850	-4.9	7.3

Run #	Nominal concentration 4000 (ng/mL)			Average	Bias	CV
	Measured concentration (ng/mL)			(ng/mL)	(%)	(%)
01	3360	3330	3200	3300	-17.6	2.6
02	3060	3190	3360	3200	-19.9	4.6
03	3830	3910	3750	3830	-4.2	2.1
04	3830	3640	3480	3650	-8.7	4.7
Total				3500	-12.6	8.3

Table S-13: Individual results from the matrix variability experiments of the ELISA validation.

Plasma lot #	Nominal concentration Endogenous
	Measured concentration (ng/mL)
01	<LLOQ
02	<LLOQ
03	<LLOQ
04	<LLOQ
05	<LLOQ
06	<LLOQ
07	<LLOQ
08	<LLOQ
09	<LLOQ
10	<LLOQ
Average (ng/mL)	-
Bias (%)	-
CV (%)	-

Plasma lot #	Nominal concentration 150 (ng/mL)
	Measured concentration (ng/mL)
01	173
02	144
03	141
04	147
05	157
06	152
07	144
08	127
09	147
10	139
Average (ng/mL)	147
Bias (%)	-2.0
CV (%)	8.2

Plasma lot #	Nominal concentration 3000 (ng/mL)
	Measured concentration (ng/mL)
01	2960
02	3140
03	3020
04	3140
05	3120
06	2830
07	2520
08	2820
09	3070
10	2940
Average (ng/mL)	2960
Bias (%)	-1.4
CV (%)	6.5

Table S-14: Individual results from the integrity of dilution experiments of the ELISA validation.

Dilution factor 200						
Run #	Nominal concentration 250 (ng/mL)*			Average	Bias	CV
	Measured concentration (ng/mL)			(ng/mL)	(%)	(%)
01	246	253	243	247	-1.0	2.1
02	258	265	248	257	2.7	3.4
Total				252	0.8	3.3

*Concentration after 200 times dilution

Dilution factor 200						
Run #	Nominal concentration 3000 (ng/mL)*			Average	Bias	CV
	Measured concentration (ng/mL)			(ng/mL)	(%)	(%)
01	2970	2410	2750	2710	-9.6	10.6
02	2980	3000	3010	3000	-0.1	0.5
Total				2850	-4.8	8.4

*Concentration after 200 times dilution

Table S-15: Individual results from the dilution linearity experiments of the ELISA validation.

Dilution factor	Diluted concentration	Measured concentration	Bias	Undiluted Concentration
	(ng/mL)	(ng/mL)	(%)	(ng/mL)
-	600000	9130	-	>ULOQ
20	30000	5830	-	>ULOQ
200	3000	3460	15.3	692000
500	1200	1280	6.8	641000
1250	480	528	9.9	660000
3125	192	219	14.3	686000
7812.5	76.8	87.7	-	<LLOQ
Average				670000
Total CV (%)				3.5

Table S-16: Individual results from the analyzed patient samples.

Subject	Sample Collection Days after start of treatment	Sample Collection Days after previous dosage	ELISA (µg/mL)	LC-MS (FTISADTSK) (µg/mL)	LC-MS (IYPTNGYTR) (µg/mL)	LC-MS (IYPTDGYTR) (µg/mL)	LC-MS (IYPTIsoDGYTR) (µg/mL)	LC-MS (IYPTSuccGYTR) (µg/mL)
01	0	0	0	0	0	0	0	0
	86	21	20,1	43,9	34,5	0,628	4,50	0,343
	191	21	29,3	52,0	47,6	0,947	6,86	0,526
	296	22	202	221	233	1,06	8,17	2,443
	338	17	28,9	53,3	51,4	0,891	6,47	0,528
	505	167	0	0	0	0	0	0
	581	243	0	0	0	0	0	0
02	0	0	0	0	0	0	0	0
	28	28	23,4	41,4	33,9	0,382	2,75	0,329
	91	21	36,8	64,6	57,7	1,13	8,43	0,742
	113	43	8,04	23,0	17,7	0,612	4,91	0,271
	175	105	0	0	0	0	0	0
03	0	0	0	0	0	0	0	0
	21	21	35,1	58,3	59,6	0,621	4,94	0,604
	63	21	46,5	86,4	80,2	1,54	12,8	0,826
	168	20	54,3	113	93,8	2,93	22,6	1,24
04	0	0	0	0	0	0	0	0
	77	14	36,9	105	85,2	3,06	24,0	1,04
	83	20	71,2	150	135	3,00	24,7	1,54
	146	21	60,6	152	126	4,30	31,4	1,46
	209	14	210	371	353	6,15	45,1	3,83
	357	22	79,6	263	197	11,0	67,0	2,44
	544	187	0,100	9,30	2,69	0,872	4,46	0,104
	678	321	0	0	0	0	0	0
	0	0	0	0	0	0	0	0
	21	21	24,8	36,5	36,9	0,431	3,21	0,436
06	85	22	28,5	61,7	52,7	1,08	8,42	0,570
	169	21	35,0	75,6	68,5	1,69	12,6	0,823
	232	21	31,9	68,8	63,2	1,58	11,9	0,712

Table S-16: Continued.

Subject	Sample Collection Days after start of treatment	Sample Collection Days after previous dosage	ELISA (µg/mL)	LC-MS (FTISADTSK) (µg/mL)	LC-MS (IYPTNGYTR) (µg/mL)	LC-MS (IYPTDGYTR) (µg/mL)	LC-MS (IYPTIsoDGYTR) (µg/mL)	LC-MS (IYPTSuccGYTR) (µg/mL)
08	337	21	137	215	210	1,75	13,2	2,36
	450	113	0	0	0	0	0	0
	646	309	0	0	0	0	0	0
	0	0	0	0	0	0	0	0
	63	21	36,3	61,0	62,8	1,08	8,47	0,651
09	127	22	49,9	100	86,1	2,22	17,0	0,894
	358	21	51,3	138	112	3,66	27,1	1,34
	616	279	0	0	0	0	0	0
	0	0	0	0	0	0	0	0
	85	21	38,8	81,3	73,7	1,61	12,8	0,879
10	167	19	55,1	114	97,3	2,93	22,0	1,14
	272	19	67,4	136	122	4,09	27,9	1,41
	365	30	42,5	117	89,2	3,98	27,6	1,27
	449	114	0,226	6,65	2,83	0,442	2,58	0,0
	547	212	0	0	0	0	0	0
11	645	310	0	0	0	0	0	0
	0	0	0	0	0	0	0	0
	84	20	30,2	60,6	56,0	1,17	9,66	0,611
	168	20	36,9	74,1	64,5	1,41	11,9	0,829
	253	22	148	199	209	1,78	12,6	2,46
11	365	20	28,9	62,0	52,7	1,40	10,4	0,575
	370	25	38,9	86,0	75,7	2,30	16,8	0,866
	491	146	0	0	0	0	0	0
	552	207	0	0	0	0	0	0
	651	306	0	0	0	0	0	0
11	0	0	0	0	0	0	0	0
	77	14	50,6	85,0	78,9	1,40	10,3	0,99
	280	21	40,6	82,5	78,2	1,62	14,1	0,92
	385	21	44,2	99,6	87,6	2,42	18,2	1,07
	644	238	0	0	0	0	0	0

CHAPTER IV

Analytical and pharmacological consequences of the *in vivo* deamidation of trastuzumab and pertuzumab

Peter Bults^{1,2}, Anna van der Voort³, Coby Meijer⁴, Gabe S. Sonke³, Rainer Bischoff² and Nico C. van de Merbel^{1,2}

¹ Bioanalytical Laboratory, ICON, Early Development Services, Amerikaweg 18, 9407 TK Assen, The Netherlands

² Analytical Biochemistry, Department of Pharmacy, University of Groningen, A. Deusinglaan 1, 9700 AV Groningen, The Netherlands

³ Netherlands Cancer Institute, Division of Medical Oncology, Plesmanlaan 121, 1066 CX Amsterdam, the Netherlands

⁴ Faculty of Medical Sciences, Department of Medical Oncology, University Medical Centre Groningen, Hanzeplein 1, 9713 GZ Groningen, The Netherlands

Anal. Bioanal. Chem. (2022)

ABSTRACT

A liquid chromatography-tandem mass spectrometry method is presented for the quantitative determination of the *in vivo* deamidation of the biopharmaceutical proteins trastuzumab and pertuzumab at a specific amino acid (asparagine) in their complementarity determining regions (CDRs). For each analyte, two surrogate peptides are quantified after tryptic digestion of the entire plasma protein content: one from a stable part of the molecule, representing the total concentration, and one containing the deamidation-sensitive asparagine, corresponding to the remaining non-deamidated concentration. Using a plasma volume of just 10 μL and a 2-hour digestion at pH 7, concentrations between 2 and 1000 $\mu\text{g/mL}$ can be determined for the various protein forms with values for bias and CV below 15% and without unacceptable deamidation taking place during sample storage or analysis. A considerable difference between the total and non-deamidated concentrations, and thus a substantial degree of deamidation, was observed in plasma for both trastuzumab and pertuzumab *in vitro* and *in vivo*. After a 56-day forced deamidation test 40% of trastuzumab and 68% of pertuzumab was deamidated, while trastuzumab and pertuzumab showed up to 47% and 35% of deamidation, respectively, in samples collected from breast cancer patients during treatment with a combination of both drugs. A good correlation between the non-deamidated concentration results and those of a receptor binding assay indicate a loss of receptor binding for both trastuzumab and pertuzumab along with the deamidation in their CDRs. Deamidated trastuzumab also lost its capability to inhibit the growth of breast cancer cells in a cell-based viability assay, suggesting a relation between the degree of deamidation and pharmacological activity.

4.1 INTRODUCTION

The investigation of drug metabolism and disposition is an essential part of the development programs of small-molecule pharmaceuticals and, where relevant for safety and efficacy, concentrations of the formed metabolites are routinely measured during clinical trials. In contrast, the *in vivo* fate of therapeutic proteins has received relatively little attention. This is partly because proteins are typically cleared from the body via catabolism, i.e. degradation to generally inactive peptides and amino acids, which poses only limited safety concerns [1]. Another reason for the apparent lack of interest in protein biotransformation lies in the fact that pharmacokinetic measurements are usually carried out with ligand-binding assays, with which it is technically challenging to separately quantify low levels of closely related protein forms in complex biological matrices [2].

Still, with the rapidly growing number of therapeutic proteins on the market and in development, and with the increasing use of liquid chromatography-mass spectrometry (LC-MS) for protein quantification, it is becoming more and more evident that small changes in the molecular structure of protein drugs due to chemical reactions within the body are very common [3]. Antibody-drug conjugates, for example, consist of multiple toxin molecules conjugated to an antibody and the biotransformation of this class of compounds is relatively well established, especially when it comes to the *in vivo* toxin release because of its potential safety implications [4]. Reports of other biotransformation reactions of therapeutic proteins are relatively scarce. The conversion of N-terminal glutamate to pyroglutamate was described for three unspecified human IgG2 monoclonal antibody (mAb) drugs both *in vitro* and *in vivo* at a similar rate, but no impact on safety or efficacy was reported [5]. The rapid removal of C-terminal lysine from the heavy chain of a human mAb was described and concluded to be due to carboxypeptidase activity, which is also responsible for C-terminal lysine removal of endogenous IgG [6]. The spontaneous *in vivo* reaction of glucose with lysine moieties on both endogenous and therapeutics antibodies was also reported with a broad distribution across the protein structure but with no observable effect on the binding of the modified antibodies to Fc receptors or protein A [7].

A protein modification which is frequently studied *in vitro*, such as during storage of pharmaceutical protein formulations, is deamidation: the conversion of a neutral asparagine or glutamine into an acidic aspartate or glutamate [8,9]. This spontaneous reaction can also occur at the physiological conditions *in vivo*, especially for asparagine when it is followed in the protein chain by a small amino acid such as glycine or serine.

The first step in the reaction is the formation of a succinimide intermediate, which can subsequently be hydrolyzed to either aspartate or isoaspartate. This changes the charge and potentially also the three-dimensional structure of the protein and may impact its binding to endogenous receptors and consequently reduce its pharmacological activity. Previously, we reported a method for quantification of the therapeutic mAb trastuzumab and three deamidated variants (containing succinimide, aspartate or isoaspartate instead of asparagine at amino acid position 55 on the heavy chain) in human plasma [10]. Samples were digested with trypsin and four peptides containing the different amino acids at position 55 were quantified by LC-MS/MS along with a peptide from a stable part of the protein. After a one-year treatment cycle of breast cancer patients with trastuzumab, up to 25% of the circulating protein was found to be deamidated at this position and all three variants were observed in plasma. Similar effects were later described for a few other, unspecified mAbs, in shorter preclinical studies in monkeys [11] and mice [12], with up to 90% deamidation observed on the heavy chains. For trastuzumab, deamidation of asparagine at position 30 on the light chain (LC-Asn30) and isomerization of aspartate at position 102 on the heavy chain (HC-Asp102) were seen next to deamidation of heavy chain asparagine at position 55 (HC-Asn55), in both preclinical and clinical samples [13].

An important question to answer is whether these *in vivo* deamidation reactions have any consequence for the binding of the protein drug to its target receptor and, ultimately, for its pharmacological activity. The asparagine at position 55 in the heavy chain of trastuzumab is located in one of the complementarity determining regions (CDR's), which are involved in the binding of trastuzumab to its target receptor, the human epidermal growth factor receptor type 2 (HER2). Several other therapeutic mAbs of the IgG1 subclass also contain an HC-Asn55, so this amino acid is considered to play a key role in the biological functioning of these proteins [14] and a modification in this part of their molecular structure may very well affect their activity. So far, however, only a few papers on this topic have been published. In an *in vitro* study with a non-trastuzumab monoclonal antibody, the formation of a succinimide at position 55 in the heavy chain was observed. This protein form was isolated and showed 50% reduced receptor binding by surface plasmon resonance (SPR) and 70% reduced biological activity in a cell-based assay [14]. For trastuzumab, a comparable study revealed deamidation of LC-Asn30 and HC-Asn55 and isomerization of HC-Asp102 after a single intravenous dose to mice [15] and a 20% reduced binding to the HER2 receptor by SPR for a sample collected 15 days post-dose, as compared to a reference sample collected 1 day after trastuzumab dosing.

In this paper, we describe the results of a further investigation into the occurrence and pharmacological consequences of *in vivo* deamidation of trastuzumab. Treatment of HER2-positive breast cancer is currently often performed by dosing of trastuzumab and another monoclonal antibody, pertuzumab [16,17], in combination with chemotherapy. Since pertuzumab also contains an asparagine at a crucial position in its CDR, the deamidation of this biopharmaceutical protein is addressed as well. We report the development, validation and application of an LC-MS/MS method for the simultaneous quantification of trastuzumab and pertuzumab in plasma. It provides two concentrations for each antibody: one representing the total concentration via a tryptic peptide from a metabolically stable part of the molecule and one representing the non-deamidated concentration via the peptide containing the deamidation-sensitive asparagine in the heavy chain. Pharmacokinetic results are presented from a clinical trial in HER2-positive breast cancer patients. The relevance of the *in vivo* deamidation of trastuzumab and pertuzumab during treatment of patients is addressed by correlating the LC-MS/MS results to a receptor assay for measuring the binding to HER2 and a cell-based viability assay for activity assessment.

4.2 MATERIALS AND METHODS

4.2.1 Chemicals and biological materials

General. Trastuzumab (Herceptin) was obtained as lyophilized, sterile powder and pertuzumab (Perjeta) as a sterile solution from Roche (Basel, Switzerland). Biotransformed trastuzumab, including deamidation at HC-Asn55, was prepared by incubating a PBS solution containing 1500 µg/mL trastuzumab at 37°C for up to 200 days. The remaining percentage of non-deamidated HC-Asn55 was determined by LC-MS/MS in several samples during this period using the approach described in the next paragraph. Samples containing trastuzumab with 0%, 46% and with 100% non-deamidated HC-Asn55 were used for selected experiments. Human K₂EDTA plasma from healthy volunteers (hereafter referred to as blank human plasma) was obtained from BioIVT (West Sussex, UK).

LC-MS/MS. The following custom-synthesized peptides were purchased from JPT Peptide Technologies (Berlin, Germany): IYPTNGYTR and FTISADTSK (for trastuzumab) and FTLSVDR and GLEWVADVNPNSGGSIYNQR (for pertuzumab) plus the C-terminally labeled arginine-13C6-15N4 or lysine-13C6-15N2 forms of all peptides for use as internal standards. Purity was assessed by the manufacturer using amino acid analysis and was also corrected for the salt forms. Acetonitrile, methanol, dimethyl sulfoxide (DMSO),

formic acid, acetic acid, hydrochloric acid (37%), ammonium hydroxide solution (25%) and ammonium acetate came from Merck (Darmstadt, Germany). Sigma Aldrich (St. Louis, MO, USA) supplied Tween-20, Trizma® base and trypsin from porcine pancreas (Type IX-S, lyophilized powder, 13,000-20,000 BAEE units/mg protein). HPLC grade water was prepared using a water purification system from Merck.

Receptor binding assay. Sodium carbonate, sodium hydrogen carbonate, sodium hydroxide, sulfuric acid, Tween-20 and PBS 10x were obtained from Merck. 1-Step Ultra TMB (3,3',5,5'-tetramethylbenzidine) liquid substrate for ELISA as well as the recombinant extracellular domain (Met 1-Thr 652) of the human HER2- ErbB2- receptor, carrying a human IgG1 Fc tag at the C-terminus (rhHER2), were purchased from Thermo Fisher Scientific (#10004H02H50). Human serum albumin (HSA) 20% was supplied by Sanquin (Amsterdam, The Netherlands) and the HRP-conjugated rabbit anti-human IgG1 (Fab'₂ fragment) antibody was supplied by Jackson ImmunoResearch Europe (Ely, UK).

Cell-based viability assay. The human breast cancer cell line BT474 was obtained from the American Type Culture Collection (Manassas, VA, USA), cultured in RPMI 1640 culture medium supplemented with 10% fetal calf serum (both from Thermo Fisher Scientific, Bleiswijk, the Netherlands) and routinely tested for absence of mycoplasma. Short tandem repeat profiling (BaseClear, Leiden, the Netherlands) was used to authenticate the origin of the cell line. For the cell-based viability assay, the cells were grown in enriched culture medium, consisting of Dulbecco's Modified Eagle's Medium/Ham's Nutrient Mixture F-12 (DME/F12), obtained from Thermo Fisher Scientific, containing 20% fetal calf serum.

4.2.2 Trastuzumab and pertuzumab quantification by LC-MS/MS

For the combined LC-MS/MS determination of trastuzumab and pertuzumab in human plasma, 10.0 µL aliquots of sample were pipetted into the 0.5-mL wells of an Eppendorf Protein Lo-bind 96-well plate (VWR International, Amsterdam, The Netherlands) and 100 µL of methanol : water (70 : 30 (v/v)) was added. After vortex-mixing for 5 minutes at room temperature and 1250 rpm, the proteins were pelleted by centrifugation for 15 minutes at 1500g. The supernatant was discarded by inverting the plate above a waste receptacle and placing it upside down on a tissue for 15-20 minutes. The remaining protein pellet was reconstituted by vortex-mixing in 75.0 µL of a 200 µg/mL trypsin solution in digestion buffer: 50 mM Trizma buffer (pH 7.0) containing 0.05% Tween-20 and 2.5% (v/v) DMSO. Next, 25.0 µL of an internal-standard working solution was added containing the four internal standards in digestion buffer at 1000 ng/mL (labeled IYPTNGYTR), 4000

ng/mL (labeled FTISADTSK), 250 ng/mL (labeled FTLSVDR) and 3000 ng/mL (labeled GLEWVADVNPNSGGSIYNQR). The sample was digested at 37°C and 1250 rpm for 2 hours using an Eppendorf Thermomixer® comfort, after which the digestion was stopped by the addition of 10.0 µL of 10% formic acid in water. Finally, the plate was sealed, vortex-mixed, centrifuged and placed in the autosampler at 10°C for analysis.

Analysis was performed using a Model 1290 Infinity II UHPLC system (Agilent, Santa Clara, CA, USA) coupled to a Sciex (Concord, Canada) Model 6500 triple quadrupole mass spectrometer equipped with a Turbolonspray™ source. Chromatographic separation was achieved at 60°C on a 2.1 × 100 mm, 1.7 µm particle-size, Acquity UPLC CSH C18 column (Waters). Mobile phase A consisted of 0.1% formic acid in water and mobile phase B was acetonitrile. Samples were separated by linear gradient elution using the following settings: 0.0-8.0 min: 2.5-20% B; 8.0-8.1 min: 20-95% B; 8.1-8.9 min: 95% B; 8.9-9.0 min: 95-2.5% B; 9.0-11.0 min: 2.5% B. The flow rate was 0.6 mL/min and the sample injection volume was 15 µL. Detection was performed in positive electrospray ionization mode with an acquisition method consisting of three periods (0-3.3 min, 3.3-6.0 min and 6.0-11.0 min after injection). General and analyte-specific mass spectrometric parameters, as well as the multiple reaction monitoring (MRM) transitions used to monitor the four peptides and their corresponding internal standards, are presented in **Table 1**.

Table 1: mass spectrometric settings for the surrogate peptides and their internal standards

Peptide sequence	Protein	Precursor ion mass (m/z) and charge state	Product ion mass (m/z) and charge state	Collision energy (V)
FTISADTSK	Trastuzumab	485.3 / [M+2H] ²⁺	721.4 / Y ₇ ⁺	22
FTISADTSK*	Trastuzumab	489.3 / [M+2H] ²⁺	729.4 / Y ₇ ⁺	22
IYPTNGYTR	Trastuzumab	542.8 / [M+2H] ²⁺	808.4 / Y ₇ ⁺	24
IYPTNGYTR*	Trastuzumab	547.8 / [M+2H] ²⁺	818.4 / Y ₇ ⁺	24
FTLSVDR	Pertuzumab	419.2 / [M+2H] ²⁺	589.4 / Y ₅ ⁺	21
FTLSVDR*	Pertuzumab	424.2 / [M+2H] ²⁺	599.4 / Y ₅ ⁺	21
GLEWVADVNPNSGGSIYNQR	Pertuzumab	726.1 / [M+3H] ³⁺	580.3 / Y ₄ ⁺	40
GLEWVADVNPNSGGSIYNQR	Pertuzumab	726.1 / [M+3H] ³⁺	894.5 / Y ₈ ⁺	40
GLEWVADVNPNSGGSIYNQR	Pertuzumab	726.1 / [M+3H] ³⁺	981.5 / Y ₉ ⁺	40
GLEWVADVNPNSGGSIYNQR	Pertuzumab	726.1 / [M+3H] ³⁺	1192.6 / Y ₁₁ ⁺	40
GLEWVADVNPNSGGSIYNQR*	Pertuzumab	729.4 / [M+3H] ³⁺	1202.6 / Y ₁₁ ⁺	40

*stable-isotope labeled amino acid: ¹³C₆-¹⁵N₂-lysine (K) or ¹³C₆-¹⁵N₄-arginine (R)

4.2.3 Trastuzumab or pertuzumab quantification by receptor binding assay

A 96-well NUNC Maxisorp immune plate was coated with 100 μL of a 1.00- $\mu\text{g}/\text{mL}$ solution of the capture reagent, the extracellular domain of the rhHER2 receptor, in 0.1M carbonate buffer solution (pH 9.6) per well, by overnight incubation at 4°C. The plate was washed three times with 300 μL of wash buffer solution (PBS pH 7.4 containing 0.1% (v/v) Tween 20), blocked with 150 μL /well of the blocking buffer (PBS pH 7.4 containing 1.0% (w/v) HSA) for 1 hour at 21°C and 500 rpm and washed another three times with 300 μL of wash buffer solution. Plasma was 20-fold diluted by adding 15.0 μL sample to 285 μL blocking buffer solution and 100 μL of each diluted sample was transferred to the plate in duplicate. After incubating for 1 hour at 500 rpm and 21°C, the plate was washed again three times as mentioned above. A solution of 0.032 $\mu\text{g}/\text{mL}$ of HRP-labeled rabbit anti-human IgG (Fab'₂ fragment) antibody in blocking buffer) was then added (100 μL /well) and the plate was incubated for 1 hour at 500 rpm and 21°C in the dark. After washing three times with the washing buffer, 100 μL of the substrate solution was added to each well and incubated for five minutes in darkness at 500 rpm and 21°C. The reaction was stopped by adding 50 μL of 2M sulfuric acid to each well and the absorbance at 450 nm was determined within 15 minutes on a SpectraMax M5e plate reader.

4.2.4 Cell-based viability assay

The HER2 positive breast cancer cell line BT474 was cultured at 37°C in a humidified atmosphere containing 5% carbon dioxide. To test the effect of trastuzumab or pertuzumab and the deamidated forms of trastuzumab on cell viability, the cells were seeded in duplicate in 96-well plates at a density of 8×10^3 cells per well in enriched culture medium and incubated at 37°C/5% carbon dioxide for 96 hours with varying concentrations (0, 0.01, 0.1, 0.5, 1, 5, 10, 50 and 100 $\mu\text{g}/\text{mL}$) of either unmodified trastuzumab, trastuzumab with 54% or 100% deamidation at Asn55, as confirmed by the LC-MS/MS method described above, or unmodified pertuzumab. After this treatment, the samples were further incubated for 4 hours at 37°C/5% carbon dioxide with 3-(4,5-dimethylthiazol-2-yl)-5-(3-carboxymethoxyphenyl)-2-(4-sulphophenyl)-2H-tetrazolium (MTS) solution according to the manufacturer's instructions (Promega Corporation, Leiden, the Netherlands). Cell viability was determined as the remaining cellular metabolic activity, capable of converting MTS to a formazan product, whose absorbance was colorimetrically measured at 490 nm on a microplate reader (BioRad, Veenendaal, the Netherlands). Cell viability was defined as the measured absorbance at 490 nm after treatment with trastuzumab and pertuzumab at

varying percentages of deamidation, as a percentage of the absorbance found for untreated cells. Three independent experiments were performed at 0, 0.01, 0.1, 1 and 10 $\mu\text{g/mL}$, two experiments at 5, 50 and 100 $\mu\text{g/mL}$ and a single experiment at 0.5 $\mu\text{g/mL}$. Before the assays were performed, the linear relationship of cell number to formazan crystal formation was checked and cell growth studies were performed. The cell line was seeded at optimum density in order to test survival after at least two or three cell divisions had taken place in the control cells.

4.2.5 Preparation of calibration, validation and quality control samples

For trastuzumab a stock solution at 21.0 mg/mL was prepared by dissolving the contents of a vial of lyophilized protein (label claim: 150 mg) in 7.2 mL of water according to the manufacturer's instructions for use. For pertuzumab, a stock solution was supplied at 30.0 mg/mL (label claim). To minimize freeze/thaw effects, the stock solutions were divided into 0.5 mL aliquots in Eppendorf Protein Lo-bind tubes (VWR International, Amsterdam, The Netherlands) and stored at -70°C . For both analytes, two separate sets of standard solutions were prepared by diluting the stock solution with water, the standard solutions varied in concentration, depending on which type of assay was used. One set of standard solutions was used to prepare calibration samples and the other to prepare quality control samples, both in blank human EDTA plasma. All samples were stored in Eppendorf Protein Lo-bind tubes at -70°C . For the LC-MS/MS method, both trastuzumab and pertuzumab were present in the calibration samples (range 2.00 – 1000 $\mu\text{g/mL}$) and in the quality control samples at 2.00, 6.00, 200 and 750 $\mu\text{g/mL}$. The samples for the receptor binding assay contained either trastuzumab or pertuzumab, both across the calibration range of 60.1 – 2370 ng/mL with quality control samples at 60.1, 150, 600, 2000 and 2370 ng/mL.

4.2.6 Sample collection

Blood samples were collected from patients with stage II-III HER2-positive breast cancer, treated at the Netherlands Cancer Institute (NKI), who were participating in a nationwide clinical trial (NCT03820063 / BOOG 2018-01). All patients received three to nine cycles trastuzumab and pertuzumab combined with chemotherapy as neoadjuvant treatment and completed one year of HER2 blockade post-operatively. Both hormone-receptor negative (ER and PR expression $< 10\%$) and positive (ER and/or PR expression $\geq 10\%$) patients were eligible. Trastuzumab (6 mg/kg, with a loading dose of 8 mg/kg at the first treatment cycle only) and pertuzumab (420 mg, with a 840-mg loading dose at the first treatment cycle

only) were administered intravenously every three weeks for a period of up to one year. Blood withdrawal took place pre-dose on the first day of each three-weekly cycle. Plasma was harvested by centrifugation immediately after blood collection in EDTA containing blood collection tubes and stored at -70°C until analysis.

4.3 RESULTS AND DISCUSSION

4.3.1 LC-MS/MS method optimization and validation

The main objective of this study was to assess the degree of *in vivo* deamidation of trastuzumab and pertuzumab at a position in their structure, which is assumed to be important for receptor binding [14,15]: HC-Asn55 for trastuzumab and HC-Asn54 for pertuzumab (see the amino acid sequences shown in supplementary Figures S-1 and S-2). Because of the small difference in molecular mass between the non-deamidated and deamidated forms (just 1 atomic mass unit on a total mass of about 150,000), mass spectrometric discrimination at the intact protein level is technically impossible, nor does such an approach allow the exact localization of the deamidation site. Therefore, we adopted a *bottom-up* approach: both protein analytes were enzymatically digested into a series of peptides and several of these were subsequently quantified as a surrogate for the intact forms. By quantifying a peptide comprising HC-Asn55, a measure is obtained for the (remaining) amount of trastuzumab which is non-deamidated at that position. Likewise, the concentration of non-deamidated pertuzumab can be derived from a surrogate peptide containing its HC-Asn54. In addition, the total concentration of the protein analytes can be estimated by reference to peptides from a part of the protein which does not undergo any known *in vivo* modification.

The digestive enzyme trypsin cleaves protein chains at the C-terminal side of a lysine or arginine, except when this amino acid is followed by a proline. It is a preferred reagent for LC-MS analysis, because it generates positively charged peptides of a suitable size and is widely available for a reasonable price. By the action of this enzyme, trastuzumab and pertuzumab are digested into 62 and 67 theoretical peptides, respectively. To ensure selection of analyte-specific surrogate peptides, these candidates were checked for uniqueness against the human plasma proteome by submitting to the basic local alignment search tool (BLAST) [18]. For trastuzumab, the peptides IYPTNGYTR (HC amino acids 51-59) and FTISADTSK (HC 68-76) had already proven to be suitable for quantifying the HC-Asn55 non-deamidated and total concentrations, respectively [10], and they were also

selected for this method. FTLSVDR (HC 68-74) was chosen to represent total pertuzumab, as this sequence does not occur in any endogenous human protein, does not contain unstable amino acids and was found to have excellent LC-MS/MS properties, such as good chromatographic behavior and efficient ionization and fragmentation. The HC-Asn54 containing tryptic peptide for pertuzumab was GLEWVADVNPNSGGSIYNQR (HC 44-63). Although, compared to the other three surrogate peptides, it is more hydrophobic and showed a somewhat higher retention on a standard reversed-phase LC column, by applying a linear gradient from 2.5 to 20% acetonitrile, the four peptides could be well separated from each other and from endogenous interferences in an 11-min chromatographic run. The latter peptide also has a considerably lower mass spectrometric response than the others, because of less efficient ionization and a poor fragmentation behavior, but by applying a high collision energy and summing the signals of four mass transitions (Table 1), detection sensitivity was sufficient to allow quantification down to the relevant, low $\mu\text{g/mL}$ plasma levels. **Figure 1** shows LC-MS/MS chromatograms of the four surrogate peptides, generated after tryptic digestion of trastuzumab and pertuzumab in plasma at 6 $\mu\text{g/mL}$.

In order to reliably assess the degree of *in vivo* deamidation of trastuzumab and pertuzumab, it is essential that no further deamidation should occur at HC-Asn55 and HC-Asn54 of the two protein analytes after sampling, i.e. during storage or analysis. Intramolecular disulfide bonds are often reduced and alkylated to improve subsequent sample digestion, but in our workflow these steps were not necessary for a reproducible and high digestion yield and therefore omitted, to reduce the possibility of analytical artefacts. In particular, digestion by trypsin bears a risk of *in vitro* deamidation, because it is usually performed at slightly alkaline pH, where the enzyme shows its optimum activity, but which also has been reported to increase asparagine deamidation, especially for smaller peptides [19]. Previously [10], a reasonable compromise was found between good digestion efficiency (>80%) and negligible (<1%) *in vitro* formation of deamidated forms of the peptides for trastuzumab, when performing digestion at pH 7.0 (rather than at the usual pH 8.0-8.5) for three hours. At these conditions, pertuzumab was also found to be sufficiently stable, with a slight concentration decrease (<1%) of the formed HC-Asn54 containing peptide only observed after 6 hours. We deliberately digested the entire protein content of a 10- μL plasma sample and did not use any protein extraction prior to digestion, by immunocapture or otherwise. In that way, a potential difference in extraction recovery between the non-deamidated and the deamidated forms of the proteins was avoided and the most accurate estimate of both forms could be obtained.

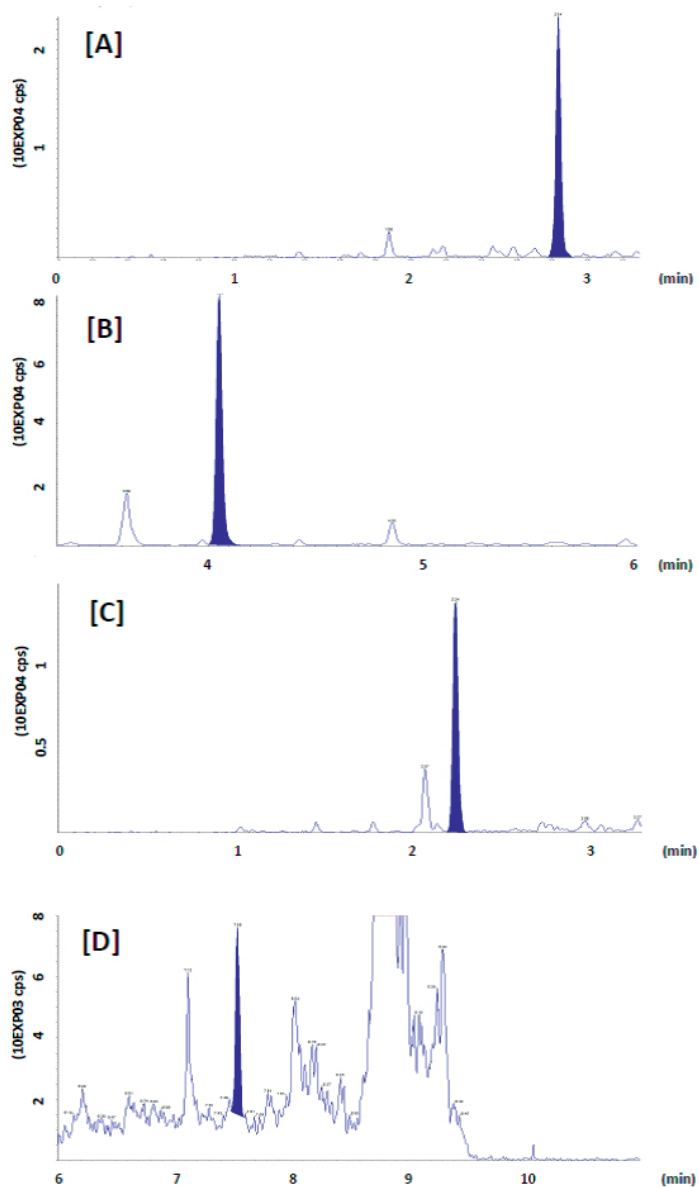


Figure 1: LC-MS/MS chromatograms of the peptides FTISADTSK (A), IYPTNGYTR (B), FTLSDVR (C) and GLEWVADVNPNSGGSIYNQR (D) from a plasma sample spiked at $6 \mu\text{g/mL}$ with both trastuzumab and pertuzumab.

The suitability of the LC-MS/MS method for simultaneous quantification of trastuzumab and pertuzumab was demonstrated by a validation based on international guidelines [20,21]. Results are presented in the supplementary tables S1 to S15. Briefly, precision and accuracy (n=18) across the range of 6-1000 µg/mL for pertuzumab through GLEWVADVNPNSGGSIYNQR and 2-1000 µg/mL for trastuzumab and pertuzumab via the other three surrogate peptides, were better than 12% (coefficient of variation) and 14% (bias from nominal), respectively. Selectivity was acceptable, as judged by the absence of interfering peaks in six individual lots of blank plasma at the retention times of the peptides and their internal standards. Sufficient stability (<15% deviation from the nominal concentration) was observed for all peptides during storage of plasma at ambient temperature for 24 hours, at -70°C for 301 days and over five complete freeze-thaw cycles, which demonstrates the absence of unacceptable *in vitro* deamidation at HC-Asn55 and HC-Asn54 for trastuzumab and pertuzumab, respectively, during normal sample storage conditions.

4.3.2 Receptor binding assay optimization and validation

To investigate the effect of deamidation of the protein analytes on their binding to the target receptor, a binding assay was set up. A recombinant form of the extracellular domain (ECD) of the human HER2 receptor was coated onto an ELISA plate and used as capturing agent for all molecules with binding affinity to this receptor. For subsequent detection of receptor-bound trastuzumab and pertuzumab, a generic detection antibody was added, that binds to the constant part of all forms of human IgG. It generates a response because it is coupled to the enzyme horse-radish peroxidase, which converts the substrate TMB into a colored product. With these capturing and detection reagents, in combination with all necessary blocking and washing steps to avoid or remove non-specifically bound proteins originating from the plasma matrix, a colorimetric read-out is obtained for all forms of trastuzumab or pertuzumab that show binding to the HER2 receptor and also are sufficiently intact to be recognized by the anti-human IgG detection antibody.

The receptor binding assay was first optimized with (non-deamidated) trastuzumab, which is known to bind to sub-domain IV of the HER2 receptor. Acceptable quantitative performance was demonstrated. Details are presented in supplementary tables S-16 to S-21, but in summary precision (%CV) and accuracy (%bias) were below 15% across the concentration range of 60 to 2370 ng/mL, also after 300-fold dilution of the relevant *in vivo* concentrations 50 and 600 µg/mL to levels within the calibration curve. Since pertuzumab

binds to sub-domain II of the HER2 receptor, it was tested if the receptor binding assay could also be used for the quantitation of pertuzumab in plasma. Indeed, also for this mAb acceptable results for precision and accuracy were found across the same concentration range (supplementary table S-22). Altogether, this shows that the binding assay is capable of quantitatively determining trastuzumab as well as pertuzumab in plasma. It should be noted that, in contrast to the LC-MS/MS method, it does not provide separate read-outs for the two analytes, since both are captured by the HER2 receptor and both are also recognized by the detection antibody. Therefore, while the assay can be readily used for analysis of samples containing only trastuzumab or only pertuzumab, it is unsuitable for samples that contain both analytes, such as plasma collected from patients after combined dosing with these biopharmaceuticals.

4.3.3 Analytical consequences of the deamidation of trastuzumab and pertuzumab

Deamidated forms of the analytes were prepared by incubating human plasma (pH 8.0) containing 400 µg/mL of either trastuzumab or pertuzumab at 37°C for a period of 56 or 54 days, respectively, in the dark. Spiked plasma was divided into different tubes at $t=0$, and at specific time-points during the incubation a sample tube was removed from the 37°C storage condition and further kept at -70°C. Analysis took place in one batch at the end of the incubation period against calibration samples containing unmodified trastuzumab and pertuzumab. **Figure 2** shows the effect of this treatment on the analytical outcome of the LC-MS/MS and receptor binding assays.

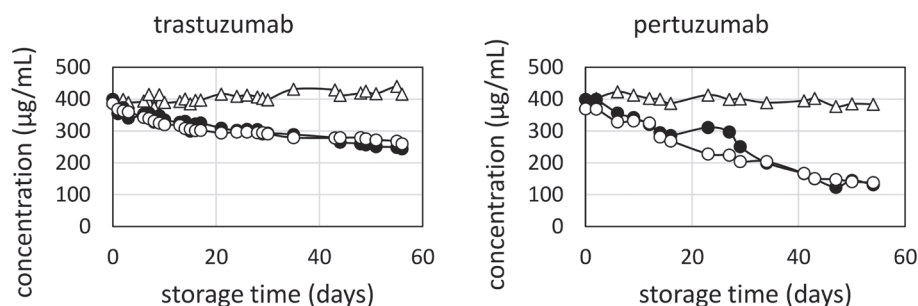


Figure 2: concentrations of trastuzumab and pertuzumab during 56 days and 54 days of storage in human plasma at 37°C, respectively; quantified by LC-MS/MS - stable peptide (Δ), LC-MS/MS - deamidation-sensitive peptide (●) or receptor binding assay (○).

The concentrations of trastuzumab found by measurement of the stable peptide FTISADTSK remained essentially constant over the incubation period and a similar result was obtained for pertuzumab via its stable peptide FTLSDVR. This shows that, regardless of what happened to the rest of the protein structure, these amino acid sequences were unaffected by prolonged storage at 37°C. However, the concentration of trastuzumab measured by the deamidation-sensitive peptide IYPTNGYTR, decreased by about 40%, from 400 to 250 µg/mL in the course of 56 days. For pertuzumab, the concentration decrease represented by peptide GLEWVADVNPNSGGSIYNQR was even more pronounced: from 400 to 130 µg/mL, or 68%, over 54 days. Apparently, the original structure of this part of the proteins was modified to a large extent upon incubation at 37°C.

In an earlier study [10], we found that the storage-induced decrease of IYPTNGYTR in trastuzumab was completely accounted for by the formation of the corresponding sequences containing aspartate, iso-aspartate or succinimide instead of asparagine at position 55. Although we did not specifically look for the formation of deamidated forms of the pertuzumab peptide GLEWVADVNPNSGGSIYNQR in this study, the gradual disappearance of the original sequence is probably also caused by modification of one of the asparagine residues. Since Asn-54 is followed by a serine, it is susceptible to spontaneous deamidation and, as a consequence, it is the most likely residue to be modified *in vitro*. Theoretically, the tryptophan residue (W) in the sequence could be oxidized and thereby contribute to the concentration decrease, but this reaction needs reactive oxygen species to proceed at an appreciable rate [22] and its contribution is probably limited at physiological conditions. It remains unclear why the rate of deamidation is higher for pertuzumab (1.3% per day) than for trastuzumab (0.7% per day) at the same incubation pH and temperature. Although deamidation of asparagine within a protein structure is typically fastest when it is followed by a glycine (such as in trastuzumab), other factors also determine the deamidation rate, such as the solvent accessibility of the asparagine residue itself and its flanking regions, which depend on the actual location within the protein structure and on whether this position is in a conformationally flexible part of the molecule [23].

Interestingly, the trastuzumab and pertuzumab concentrations obtained by the receptor binding assay correlate quite well with the concentrations found with LC-MS for the deamidation-sensitive peptides: the correlation coefficients are 0.94 for trastuzumab and 0.96 for pertuzumab, respectively. This implies that once trastuzumab is deamidated at HC-Asn55 and pertuzumab at HC-Asn54, the mAbs no longer give a response in the receptor binding assay and therefore, very probably, do not bind to the recombinant extracellular

domain of the HER2 receptor anymore. Of course, a correlation between these two sets of results does not necessarily mean causality. It should be realized that more spontaneous modifications, e.g. deamidation at other positions, isomerization and oxidation, will occur along the protein chain, which this specific LC-MS/MS method does not pick up but which may also influence receptor binding. In a study by Liu et al [13], the HER2 receptor was immobilized on magnetic beads and used to extract trastuzumab from plasma prior to LC-MS/MS analysis. Since deamidated forms of trastuzumab at HC-Asn55 and LC-Asn30 were also found in the extract, the receptor apparently also bound these deamidated forms in that setup. This may have been caused by the much higher surface area and, therefore, the higher binding capacity of magnetic beads compared to a microtiter plate, which may have resulted in the binding of low-affinity forms of trastuzumab, such as the deamidated forms, to the beads. Anyhow, the correlation does demonstrate that our LC-MS/MS result for the deamidation-sensitive peptides is likely to represent the fraction of trastuzumab or pertuzumab that is still capable of binding to the receptor in a plate-based setup, regardless of whether deamidation in the surrogate peptide sequence is actually responsible for the loss of receptor binding.

Since trastuzumab and pertuzumab, like all IgG-based antibodies, have two light and two heavy chains, the surrogate peptides occur twice in each analyte molecule. In previous work [10], we applied a bridging ELISA, using the same anti-idiotypic antibody for capture and detection, to analyze plasma spiked with trastuzumab that was subjected to a similar forced deamidation experiment. In that investigation, the concentrations found for trastuzumab with this ELISA decreased roughly two-fold more rapidly than those obtained for the IYPTNGYTR peptide with LC-MS/MS. This was explained by the need for trastuzumab to have two unmodified CDRs to form the capture antibody-trastuzumab-detection antibody complex that is needed for an ELISA detection response. Thus, deamidation in only one of the CDRs leads to a complete loss of signal in the ELISA, while the LC-MS/MS method still gives half of the original concentration. Arguing along the same lines, the good correlation of receptor binding assay and LC-MS/MS results supports the assumption that only one unmodified CDR in the trastuzumab structure is sufficient for binding to the receptor and generating a response. Because of the lack of commercially available anti-pertuzumab antibodies at the time of the study, no experimental comparison between an anti-idiotypic ELISA and the receptor binding assay could be made for pertuzumab.

4.3.4 *In vivo* deamidation of trastuzumab and pertuzumab during cancer treatment

To investigate the extent of *in vivo* deamidation of HC-Asn55 in trastuzumab and HC-Asn54 in pertuzumab after their administration to humans, plasma samples were collected during a clinical research trial with HER2-positive breast cancer patients and analyzed with the described LC-MS/MS method. **Figure 3** shows an example of pharmacokinetic curves for a patient undergoing combined treatment with trastuzumab and pertuzumab. Clearly, for both mAbs the difference between the total concentration and the non-deamidated concentration increases over time, which indicates substantial *in vivo* deamidation over the treatment period. In this case, both trastuzumab and pertuzumab showed up to 25% deamidation of their respective asparagine residues in the CDR. Similar results were found for most of the 43 patients (supplementary table S-23). In **Figure 4**, correlation plots are shown of the total and the non-deamidated concentrations for all samples analyzed.

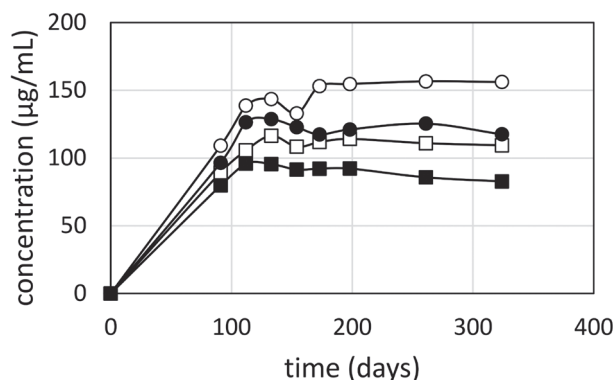


Figure 3: plasma concentration-time curves for trastuzumab, total concentration (○) and HC-Asn55 non-deamidated concentration (●) and pertuzumab, total concentration (□) and HC-Asn54 non-deamidated concentration (■) after i.v. dosing every three weeks of the drugs to a breast cancer patient.

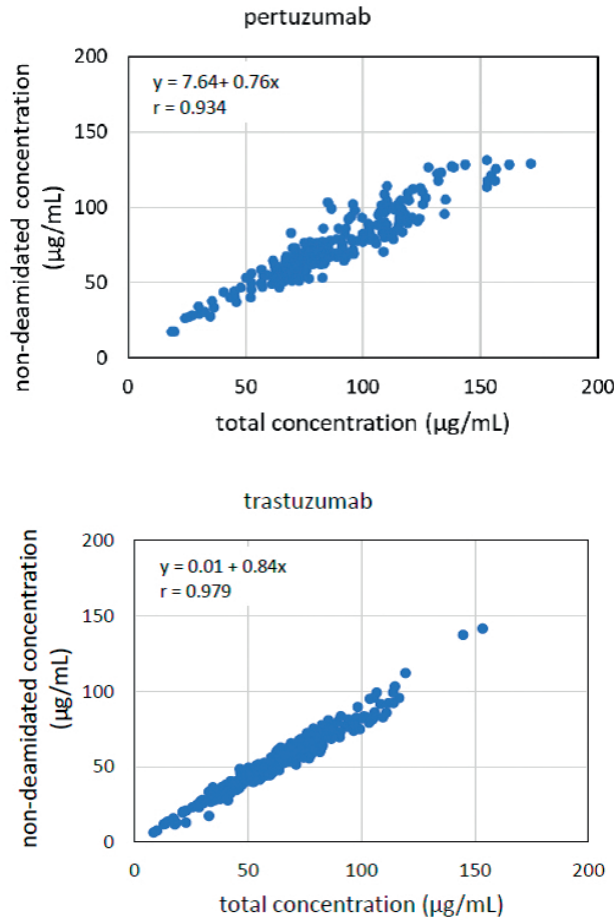


Figure 4: correlation plots of non-deamidated versus total concentration of trastuzumab and pertuzumab, generated from 261 plasma samples of 43 patients.

On average, trastuzumab showed 16% deamidation at HC-Asn55 (0 to 47% lower concentrations for the deamidation-sensitive than for the stable peptide) and pertuzumab 14% deamidation at HC-Asn54 (range: -22% to 35%). These results indicate that, in contrast to the *in vitro* stress test, trastuzumab and pertuzumab have an about equal average degree of deamidation *in vivo*. In general, the largest differences between total and non-deamidated results were found at the higher concentrations for both mAbs. Samples with these higher concentrations were typically obtained at the later time-points, and thus after a longer period of presence of trastuzumab and pertuzumab in the body.

4.3.5 Pharmacological consequences of the deamidation of trastuzumab and pertuzumab

To investigate the potential pharmacological consequences of the deamidation of trastuzumab and pertuzumab, a cell viability assay was performed with the human HER2-positive breast cancer cell line BT474. Cells were cultivated in the presence of different concentrations of (unmodified) trastuzumab and, as shown in **Figure 5**, cell survival decreased by 50% at concentrations higher than 1 $\mu\text{g/mL}$ trastuzumab. However, when cells were grown in the presence of trastuzumab which was completely deamidated at HC-Asn55, cell survival was not affected in the presence of up to 100 $\mu\text{g/mL}$ of deamidated trastuzumab.

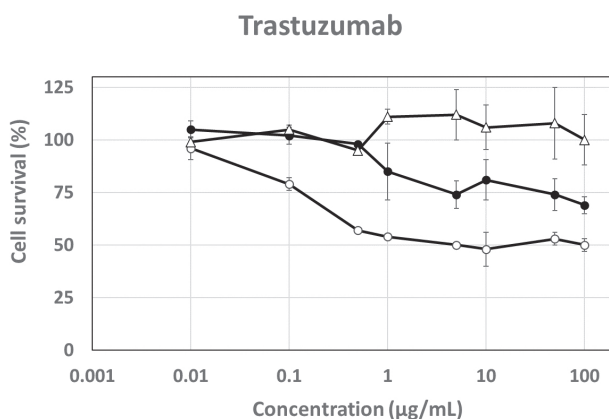


Figure 5: survival of breast cancer cell line BT474 in the presence of increasing concentrations of trastuzumab, either unmodified (o), 100% deamidated at HC-Asn55 (Δ) or 54% deamidated at HC-Asn55 (\bullet).

This demonstrates that the structural modifications that trastuzumab undergoes during prolonged incubation, among which HC-Asn55 deamidation, lead to a loss of its tumor growth reducing effect. Incubation of the breast cancer cells with trastuzumab that was deamidated at HC-Asn55 for 54% also reduced cell survival, but to a lesser degree (a decrease of 30%) and it needed higher concentrations (above 0.5 $\mu\text{g/mL}$) to reduce cell survival. The highest tested level at 100 $\mu\text{g/mL}$ of this deamidated form of trastuzumab still corresponds to 46 $\mu\text{g/mL}$ of the HC-Asn55 non-deamidated form, which should be able to increase cell death to 50% if it were completely unmodified. This finding suggests that other protein modifications than HC-Asn55 deamidation are also involved in the reduction of the pharmacological activity of trastuzumab. One possible modification could

be HC-Asp102 isomerization. In a previous report, this modified form of trastuzumab was isolated from a pharmaceutical formulation and showed reduced potency in a similar BT474 antiproliferation assay [24]. In contrast, cultivation of the breast cancer cells in the presence of unmodified pertuzumab did not result in any decrease of cell survival in our hands, even up to 500 $\mu\text{g/mL}$ (results not shown). Apparently, although pertuzumab does bind to the HER2 receptor, this fact alone is not enough to induce cell death. Pertuzumab preferentially binds to HER2 heterodimers at the cell surface, i.e. to a combination of one HER2 and one other HER receptor [25]. These may not have been sufficiently present, and the membranes of the BT474 breast cancer cells may have mainly contained HER2 homodimers, which are sensitive to trastuzumab but not pertuzumab [26]. Because of this observation, further testing of the deamidated forms of pertuzumab with this cell line was not considered relevant.

Altogether, these results indicate that HC-Asn55 deamidation in trastuzumab is not the single cause of its lost ability to induce cell death, since more modifications will have occurred in the protein structure. It does, however, demonstrate that deamidation in the CDR of trastuzumab, its reduced binding to HER2 and its loss of pharmacological activity happen at the same time.

4.4 CONCLUSION

Liquid chromatography coupled to tandem mass spectrometry allows the quantitative determination of the degree of *in vitro* and *in vivo* deamidation of trastuzumab and pertuzumab at an important position in their complementarity determining regions, HC-Asn55 and HC-Asn54, respectively. The approach involves isolating and subsequently digesting the total protein fraction of plasma, and quantifying two surrogate peptides per analyte in the digest by multiple reaction monitoring of eight mass transitions (four for the peptides and four for the added internal standards: stable-isotope labeled forms of all peptides). Analysis of plasma samples obtained from *in vitro* forced degradation tests and collected from breast cancer patients during treatment with trastuzumab and pertuzumab revealed considerable deamidation with an increasing percentage over time (up to 54 weeks). The concentrations obtained by LC-MS/MS for the peptides from the deamidation-sensitive part of the CDR correlated well with the concentrations obtained by a receptor binding assay, which suggests that the modified forms of the protein analytes lose their ability to bind to (a recombinant form of) their target receptor,

HER2. Moreover, trastuzumab which was incubated for a prolonged period of time, and as a result was fully deamidated at HC-Asn55, showed a complete loss of its capability to induce cell death in a HER2 positive breast cancer cell line. Although it is difficult to demonstrate causality, these results do show that trastuzumab and pertuzumab undergo significant *in vivo* biotransformation, which is likely to reduce their pharmacological effect. For monitoring purposes, LC-MS/MS measurement of the remaining non-deamidated concentration at HC-Asn55 and HC-Asn54 of trastuzumab and pertuzumab is likely to give the best representation of the pharmacologically active drug fraction. As other structural modifications very probably also occur, future studies should address those as well to obtain more detailed picture of the *in vivo* biotransformation of these biopharmaceutical proteins and LC-MS/MS with proper surrogate peptides is a straightforward and reliable way of doing this in a multiplexed assay.

Acknowledgment

We thank all patients for their participation, the staff of the NKI trial laboratory, in particular dr. T. Korse, who assisted in collecting the samples, and the Dutch Breast Cancer Research Group (BOOG) as the sponsor of the clinical trial.

Declarations

Samples were collected after ethical approval by the medical ethics committee of the Netherlands Cancer Institute and all patients provided written informed consent prior to study inclusion. All procedures performed in this study involving human participants were in accordance with the ICH Harmonized Tripartite Guideline for Good Clinical Practice and with the 1964 Helsinki Declaration and its later amendments.

REFERENCES

1. S. Schadt, S. Hauri, F. Lopes, M.R. Edelmann, R.F. Staack, R. Villasenor, H. Kettenberger, A.B. Roth, F. Schuler, W.F. Richter, C. Funk. Are biotransformation studies of therapeutic proteins needed? Scientific considerations and technical challenges. *Drug Metab. Disp.* 47 (2019) 1443-1456.
2. Y. Li, M. Monine, Y. Huang, P. Swann, I. Nestorov, Y. Lyubarskaya. Quantitation and pharmacokinetic modeling of therapeutic antibody quality attributes in human studies. *mAbs* 8 (2015) 1079-1087.
3. J.F. Kellie, M.Z. Karlinsey. Review of approaches and examples for monitoring biotransformation in protein and peptide therapeutics by MS. *Bioanalysis* 10 (2018) 1877-1890.
4. L.N. Tumey, B. Rago, X. Han. In vivo biotransformations of antibody-drug conjugates. *Bioanalysis* 7 (2015) 1649-1664.
5. Y.D. Liu, A.M. Goetze, R.B. Bass, G.C. Flynn. N-terminal glutamate to pyroglutamate conversion in vivo for human IgG2 antibodies. *J. Biol. Chem.* 286 (2011) 11211-11217.
6. B. Cai, H. Pan, G.C. Flynn. C-terminal lysine processing of human immunoglobulin G2 heavy chain in vivo. *Biotechnol. Bioengin.* 108 (2010) 404-412.
7. A.M. Goetze, Y.D. Liu, T. Arroll, L. Chu, G.C. Flynn. Rates and impact of human antibody glycation in vivo. *Glycobiology* 22 (2012) 221-234.
8. K. Diepold, K. Bomans, M. Wiedmann, B. Zimmerman, A. Petzold, T. Schlothauer, R. Mueller, B. Moritz, J.O. Stracke, M. Mølhøj, D. Reusch, P. Bulau. Simultaneous assessment of Asp isomerization and Asn deamidation in recombinant antibodies by LC-MS following incubation at elevated temperature. *Plos One* 7 (2012) e30295.
9. M. Habegger, K. Bomans, K. Diepold, M. Hook, J. Gassner, T. Schlothauer, A. Zwick, C. Spick, J.F. Kepert, B. Hientz, M. Wiedmann, H. Beck, P. Metzger, M. Mølhøj, C. Knoblich, U. Grauschopf, D. Reusch, P. Bulau. Assessment of chemical modifications of sites in the CDRs of recombinant antibodies. *mAbs* 6 (2014) 327-339.
10. P. Bults, R. Bischoff, H. Bakker, J.A. Gietema, N.C. van de Merbel. LC-MS/MS-based monitoring of in vivo protein biotransformation: quantitative determination of trastuzumab and its deamidation products in human plasma. *Anal. Chem.* 88 (2016) 1871-1877.
11. J.T. Mehl, B.G. Slecka, E.F. Ciccimaro, A.T. Kozhich, D.G. Gilbertson, R. Vuppugalla, C.S. Huang, B. Stevens, J. Mo, E.G. Deyanova, Y. Wang, R.Y.C. Huang, G. Chen, T.V. Olah. Quantification of in vivo site-specific Asp isomerization and Asn deamidation of mAbs in animal serum using IP-LC-MS. *Bioanalysis* 8 (2016) 1611-1622.
12. J.C. Tran, D. Tran, A. Hildebrand, N. Andersen, T. Huang, K. Reif, I. Hotzel, E.G. Stefanich, Y. Liu, J. Wang. Automated affinity capture and on-tip digestion to accurately quantitate in vivo deamidation of therapeutic antibodies. *Anal. Chem.* 88 (2016) 11521-11526.
13. L. Liu, K. Xu, J. Li, M. Maia, M. Mathieu, R. Elliot, J. Yang, I. Nijem, S. Kaur. Optimizing hybrid LC-MS/MS binding conditions is critical: impact of biotransformation on quantification of trastuzumab. *Bioanalysis* 10 (2018) 1819-1831.
14. B. Yan, S. Steen, D. Hambly, J. Valliere-Douglass, T. vanden Bos, S. Smallwood, Z. Yates, T. Arroll, Y. Han, H. Gadgil, R.F. Latypov, A. Wallace, A. Lim, G.R. Kleemann, W. Wang, A. Balland. Succinimide formation at Asn55 in the complementarity determining region of a recombinant monoclonal antibody IgG1 heavy chain. *J. Pharmac. Sci.* 98 (2009) 3509-3521.
15. I. Schmid, L. Bonnington, M. Gerl, K. Bomans, A.L. Thaller, K. Wagner, T. Schlothauer, R. Falkenstein, B. Zimmermann, J. Kopitz, M. Hasmann, F. Bauss, M. Habegger, D. Reusch, P. Bulau. Assessment of susceptible chemical modification sites of trastuzumab and endogenous human immunoglobulins at physiological conditions. *Commun. Biol.* 1:28 (2018) 1-10.

16. S. Schokker, F. Fusetti, F. Bonardi, R.J. Molenaar, R.A.A. Mathôt, H.W.M. van Laarhoven. Development and validation of an LC-MS/MS method for simultaneous quantification of co-administered trastuzumab and pertuzumab. *mAbs* 12(1) (2020) DOI: 10.1080/19420862.2020.1795492.
17. L.-L. Gui, L. Li, L.-H. Dong, S.-S. Xiang, J.-P. Zhai, Z.-Q. Ge, H.-F. Song. Method development and validation of LC-MS/MS-based assay for the simultaneous quantitation of trastuzumab and pertuzumab in cynomolgus monkey serum and its application in pharmacokinetic study. *Biomed. Chromatogr.* 34(12) (2020) doi: 10.1002/bmc.4903.
18. <https://blast.ncbi.nlm.nih.gov/>
19. N.E. Robinson, A.B Robinson. Deamidation of human proteins. *Proc. Natl. Acad. USA* 98 (2001) 12409-12413.
20. European Medicines Agency. Guideline on bioanalytical method validation; EMA: London, UK, 2012
21. Food and Drug Administration. Bioanalytical Method Validation - Guidance for Industry; U.S. Department of Health and Human Services: Washington, DC, USA, 2018.
22. M. Ehrenshaft, L. J. Deterding, R. P. Mason. Tripping up Trp: modification of protein tryptophan residues by reactive oxygen species, modes of detection, and biological consequences. *Free Radic. Biol. Med.* 89 (2015) 220–228.
23. H.A. Schiffter. Pharmaceutical proteins – structure, stability and formulation, in: *Comprehensive Biotechnology*, second edition, volume 5, M. Moo-Young (Ed), Elsevier, 2011, pp 521-541.
24. R. J. Harris, B. Kabakoff, F.D. Macchi, F.J. Shen, M. Kwong, J.D. Andya, S.J. Shire, N. Bjork, K. Totpal, A.B. Chen. Identification of multiple sources of charge heterogeneity in a recombinant antibody. *J. Chromatogr. B* 752 (2001) 233-245.
25. B. Nami, H. Maadi, Z. Wang. Mechanisms underlying the action and synergism of trastuzumab and pertuzumab in targeting HER2-positive breast cancer. *Cancers* 10 (2018) 342.
26. C.A. Hudis, Trastuzumab – mechanism of action and use in clinical practice. *N. Engl. J. Med.* 357 (2007) 39-51.

SUPPORTING INFORMATION FOR:

Analytical and pharmacological consequences of the *in vivo* deamidation of trastuzumab and pertuzumab

Content

- Figure S-1: amino acid sequence of trastuzumab
- Figure S-2: amino acid sequence of pertuzumab
- A short description of the validation experiments for the LC-MS/MS method for determination of trastuzumab and pertuzumab
- Tables S-1 to S-4: validation results of the LC-MS/MS method for peptide FTISADTSK
- Tables S-5 to S-8: validation results of the LC-MS/MS method for peptide IYPTNGYTR
- Tables S-9 to S-12: validation results of the LC-MS/MS method for peptide FTLSVDR
- Tables S-13 to S-15: validation results of the LC-MS/MS method for peptide GLEWVADVNPNSGGSIYNQR
- A short description of the validation experiments for the receptor binding assay for determination of trastuzumab or pertuzumab
- Tables S-16 to S-22: Results of the validation experiments for the receptor binding ELISA method for determination of trastuzumab or pertuzumab
- Table S-23: results of patient sample analysis using the LC-MS method for determination of trastuzumab and pertuzumab

Trastuzumab heavy chain

1 EVQLVESGGG LVQPGGSLRL SCAASGFNIK DTYIHWVRQA PGKGLEWVAR IYPT**NG**YTRY
 61 ADSVKGR**FTI SADTSK**NTAY LQMNSLRAED TAVYYCSRWG GDGFYAMDYV GQGTLVTVSS
 121 ASTKGPSVFP LAPSSKSTSG GTAALGCLVK DYFPEPVTVS WNSGALTSGV HTFPAVLQSS
 181 GLYSLSSVVT VPSSSLGTQT YICNVNHKPS NTKVDKKEVP PKSCDKTHTC PPCPAPELLG
 241 GPSVFLFPPK PKDTLMISRT PEVTCVVVDV SHEDPEVKFN WYVDGVEVHN AKTKPREEQY
 301 NSTYRVVSVL TVLHQDWLNG KEYKCKVSNK ALPAPIEKTI SKAKGQPREP QVYTLPPSRD
 361 ELTKNQVSLT CLVKGFYPSD IAVEWESNGQ PENNYKTTPP VLDSGDSFFL YSKLTVDKSR
 421 WQQGNVFSCS VMHEALHNHY TQKSLSLSPG K

Trastuzumab light chain

1 DIQMTQSPSS LSASVGDRVT ITCRASQDVN TAVAWYQQKP GKAPKLLIYS ASFLYSGVPS
 61 RFSGSRSGTD FTLTISSLQP EDFATYYCQQ HYTTPPTFGQ GTKVEIKRTV AAPSVFIFPP
 121 SDEQLKSGTA SVVCLLNNFY PREAKVQWKV DNALQSGNSQ ESVTEQDSKD STYLSSTLT
 181 LSKADYEKHK VYACEVTHQG LSSPVTKSFN RGEK

Figure S-1: Amino acid sequence of the heavy and light chain of trastuzumab with both signature peptides underlined in red and the deamidation-sensitive Asn-55 in bold.

Pertuzumab heavy chain

1 EVQLVESGGG LVQPGGSLRL SCAASGFTFT DYTMDWVRQA PGKGLEWVAD VNP**N**SGGSIY
 61 NQRFKGRFTL SVDRSKNTLY LQMNSLRAED TAVYYCARNL GPSFYFDYWG QGTLVTVSSA
 121 STKGPSVFPL APSSKSTSGG TAALGCLVKD YFPEPVTVSW NSGALTSGVH TFPAVLQSSG
 181 LYSLSVVTV PSSSLGTQTY ICNVNHNKPSN TKVDKKVEPK SCDKTHTCPP CPAPELLGGP
 241 SVFLFPPKPK DTLMISRTPE VTCVVVDVSH EDPEVKFNWY VDGVEVHNAK TKPREEQYNS
 301 TYRVVSVLTV LHQDWLNGKE YKCKVSNKAL PAPIEKTISK AKGQPREPQV YTLPPSREEM
 361 TKNQVSLTCL VKGFYPSDIA VEWESNGQPE NNYKTTPPVL DSDGSFFLYS KLTVDKSRWQ
 421 QGNVFSCSVM HEALHNHYTQ KSLSLSPG

Pertuzumab light chain

1 DIQMTQSPSS LSASVGDRVT ITCKASQDVS IGVAWYQQKPK GKAPKLLIYS ASYRYTGVPSS
 61 RFSGSGSGTD FTLTISSLQP EDFATYYCQQ YYIYPYTFGQ GTKVEIKRTV AAPSVFIFPP
 121 SDEQLKSGTA SVVCLLNIFY PREAKVQWKV DNALQSGNSQ ESVTEQDSKD STYLSSTLT
 181 LSKADYEKHK VYACEVTHQG LSSPVTKSFN RGEK

Figure S-2: Amino acid sequence of the heavy and light chain of pertuzumab with both signature peptides underlined in red and the deamidation-sensitive Asn-54 in bold.

Description of the validation experiments for the LC-MS/MS determination of trastuzumab and pertuzumab

Acceptance criteria. As per international guidelines, all bias and CV acceptance criteria were set at 15% (20% at the LLOQ).

Linearity. Each validation run contained a calibration curve prepared in human plasma with the following levels: 2.00, 4.00, 10.0, 50.0, 200, 500, 800 and 1000 µg/mL. Due to a preparation error, for pertuzumab, the standard at 800 µg/mL was actually prepared at 400 µg/mL. The ratio of the measured peak area of the signature peptide over that of the internal standard was used in calculations. Weighted linear regression was applied with $1/x^2$ as weighting factor.

Accuracy and precision. The accuracy and precision of the method were determined by six-fold analysis in three separate runs analyzed on three different days. The validation samples were prepared in plasma at four concentration levels: 2.00, 6.00, 75.0 and 750 µg/mL. Statistical analysis was performed using analysis of variance (ANOVA).

Matrix variability/selectivity. The influence of the matrix was assessed by preparing samples at 2.00 µg/mL in six independent human plasma lots plus one lot of hemolytic plasma (fortified with 2% v/v lysed blood) and one lot of lipemic plasma (triglyceride level >300 mg/dL). Additionally, from all six plasma lots, blank samples were analyzed and checked for interferences with responses exceeding 20% of the response at 2 µg/mL.

Freeze-thaw stability. Human plasma samples at 6.00 and 750 µg/mL were stored at -70°C and subjected to three and five freeze-thaw cycles, in which thawing was performed on the bench-top for a minimum of two hours, followed by frozen storage for at least 12 hours. The samples were analyzed against a freshly spiked and prepared calibration curve.

Frozen stability. Human plasma samples at 6.00 and 750 µg/mL were stored at -70°C for 301 days and analyzed against a freshly spiked and prepared calibration curve.

Carry-over. For each of the three validation runs which contained accuracy and precision samples, the peak areas for the three blank plasma samples which directly followed the highest calibrator of the calibration curve were compared to the peak areas of the six validation samples prepared at the LLOQ (0.500 µg/mL) from the same run.

Results of the validation experiments for the LC-MS/MS determination of trastuzumab (FTISADTSK signature peptide)

Table S-1: Individual calibration curve results from the LC-MS/MS validation of the FTISADTSK signature peptide (nominal concentration).

Run #	Measured concentration (µg/mL)								Correlation	Slope	Intercept
	2.00*	4.00*	10.0*	50.0*	200*	500*	800*	1000*			
01	1.99	3.99	10.3	51.7	188	490	818	1010	0.9994	0.00752	0.00314
02	2.02	3.89	10.2	51.4	191	504	798	1010	0.9996	0.00772	0.00232
03	1.97	3.97	10.7	54.1	198	500	759	928	0.9983	0.00726	0.00355
04	1.95	4.16	10.2	51.1	181	522	779	1020	0.9987	0.00536	0.000676
Average (µg/mL)	1.98	4.00	10.4	52.1	190	504	789	992	-	-	-
Total bias (%)	-1.0	0.0	4.0	4.2	-5.0	0.8	-1.4	-0.8	-	-	-
Total CV (%)	1.5	2.8	2.3	2.6	3.7	2.7	3.2	4.3	-	-	-

Table S-2: Individual accuracy and precision results from the LC-MS/MS validation of the FTISADTSK signature peptide.

Run #	Nominal concentration 2.00 (µg/mL)						Average	Bias	CV
	Measured concentration (µg/mL)						(µg/mL)	(%)	(%)
01	2.01	1.98	2.02	2.12	2.07	1.99	2.04	1.8	2.6
02	1.69	1.78	1.75	1.80	1.92	2.02	1.83	-8.7	6.5
03	1.84	1.94	2.07	1.84	1.96	2.06	1.95	-2.5	5.1
Total							1.94	-3.1	6.5

Run #	Nominal concentration 6.00 (µg/mL)						Average	Bias	CV
	Measured concentration (µg/mL)						(µg/mL)	(%)	(%)
01	5.58	5.87	5.73	6.09	5.97	6.36	5.93	-1.1	4.6
02	5.89	5.46	6.22	5.91	5.74	6.19	5.90	-1.6	4.8
03	6.08	6.29	6.09	5.96	6.71	6.71	6.31	5.1	5.3
Total							6.05	0.8	5.6

Run #	Nominal concentration 75.0 (µg/mL)						Average	Bias	CV
	Measured concentration (µg/mL)						(µg/mL)	(%)	(%)
01	69.2	71.4	70.3	73.4	70.9	73.7	71.5	-4.7	2.5
02	75.3	69.1	65.7	64.1	69.8	80.7	70.8	-5.6	8.8
03	72.7	79.0	71.2	67.3	71.4	83.1	74.1	-1.2	7.9
Total							72.1	-3.8	6.9

Run #	Nominal concentration 750 (µg/mL)						Average	Bias	CV
	Measured concentration (µg/mL)						(µg/mL)	(%)	(%)
01	706	707	732	740	754	745	731	-2.6	2.7
02	762	763	664	724	787	765	744	-0.8	5.9
03	742	745	633	738	767	786	735	-2.0	7.3
Total							737	-1.8	5.4

Table S-3: Individual results from the matrix variability experiments of the FTISADTSK signature peptide LC-MS/MS validation.

Plasma lot #	Nominal concentration 2.00 (µg/mL)
	Measured concentration (µg/mL)
01	1.92
02	1.85
03	1.98
04	1.88
05	1.92
06	1.92
Hemolytic	2.00
Lipemic	2.08
Average (µg/mL)	1.94
Bias (%)	-2.8
CV (%)	3.8

Table S-4: Results (n=3) from the stability experiments of the FTISADTSK signature peptide LC-MS/MS validation, analyzed against a freshly prepared calibration curve.

Stability item	Nominal concentration 6.00 (µg/mL)	Bias (%)	CV (%)
	Average concentration (µg/mL)		
Freeze-thaw: 5 cycles	5.74	-4.4	8.2
Frozen plasma sample: 301 days at -70°C	5.33	-11.2	1.5
Bench top: 24 hours	6.17	2.9	3.4

Stability item	Nominal concentration 750 (µg/mL)	Bias (%)	CV (%)
	Average concentration (µg/mL)		
Freeze-thaw: 5 cycles	716	-4.5	2.6
Frozen plasma sample: 301 days at -70°C	645	-14.0	2.2
Bench top: 24 hours	647	-13.7	2.2

Results of the validation experiments for the LC-MS/MS determination of trastuzumab (IYPTNGYTR signature peptide)
Table S-5: Individual calibration curve results from the LC-MS/MS validation of the IYPTNGYTR signature peptide (nominal concentration).

Run #	Measured concentration (µg/mL)								Correlation	Slope	Intercept
	2.00*	4.00*	10.0*	50.0*	200*	500*	800*	1000*			
01	1.99	3.98	10.3	51.5	187	500	805	1010	0.9994	0.00274	0.000190
02	2.02	3.88	10.2	50.6	207	467	756	1080	0.9989	0.00284	0.000132
03	1.98	3.96	10.7	53.4	214	466	723	982	0.9975	0.00267	0.000597
04	2.00	3.96	10.1	52.7	186	508	794	1010	0.9992	0.00214	0.000592
Average (µg/mL)	2.00	3.95	10.3	52.1	199	485	770	1020	-	-	-
Total bias (%)	0.0	-1.3	3.0	4.2	-0.5	-3.0	-3.8	2.0	-	-	-
Total CV (%)	0.9	1.1	2.5	2.4	7.1	4.5	4.9	4.1	-	-	-

Table S-6: Individual accuracy and precision results from the LC-MS/MS validation of the IYPTNGYTR signature peptide.

Run #	Nominal concentration 2.00 (µg/mL)						Average	Bias	CV
	Measured concentration (µg/mL)						(µg/mL)	(%)	(%)
01	1.81	1.68	1.91	1.74	1.89	1.87	1.82	-9.1	5.0
02	1.71	1.86	1.86	1.80	2.07	1.89	1.86	-6.8	6.4
03	1.89	1.76	2.11	2.26	2.00	2.33	2.06	2.8	10.6
Total							1.91	-4.4	9.3

Run #	Nominal concentration 6.00 (µg/mL)						Average	Bias	CV
	Measured concentration (µg/mL)						(µg/mL)	(%)	(%)
01	5.65	5.98	5.71	5.90	6.24	6.04	5.92	-1.3	3.7
02	5.58	6.63	6.43	6.37	7.46	6.74	6.54	8.9	9.3
03	6.97	5.91	6.18	6.85	7.16	7.83	6.82	13.6	10.1
Total							6.42	7.1	10.0

Run #	Nominal concentration 75.0 (µg/mL)						Average	Bias	CV
	Measured concentration (µg/mL)						(µg/mL)	(%)	(%)
01	68.9	71.8	71.4	75.8	71.4	71.5	71.8	-4.3	3.1
02	73.9	79.1	71.5	72.1	74.8	83.2	75.8	1.0	6.0
03	73.9	81.6	76.3	69.0	78.4	93.6	78.8	5.1	10.6
Total							75.5	0.6	8.0

Run #	Nominal concentration 750 (µg/mL)						Average	Bias	CV
	Measured concentration (µg/mL)						(µg/mL)	(%)	(%)
01	712	720	713	711	750	711	719	-4.1	2.1
02	697	799	783	777	889	812	793	1.0	6.0
03	815	865	744	768	836	909	823	9.7	7.4
Total							778	3.8	8.4

Table S-7: Individual results from the matrix variability experiments of the IYPTNGYTR signature peptide LC-MS/MS validation.

Plasma lot #	Nominal concentration 2.00 (µg/mL)
	Measured concentration (µg/mL)
01	1.77
02	1.86
03	1.97
04	1.81
05	1.97
06	1.83
2% Hemolytic	2.02
Lipemic	1.95
Average (µg/mL)	1.90
Bias (%)	-5.1
CV (%)	4.8

Table S-8: Results (n=3) from the stability experiments of the IYPTNGYTR signature peptide LC-MS/MS validation, analyzed against a freshly prepared calibration curve.

Stability item	Nominal concentration 6.00 (µg/mL)		
	Average concentration (µg/mL)	Bias (%)	CV (%)
Freeze-thaw: 5 cycles	5.83	-2.9	9.0
Frozen plasma sample: 301 days at -70°C	5.58	-7.0	1.5
Bench top: 24 hours	6.34	5.6	3.5

Stability item	Nominal concentration 750 (µg/mL)		
	Average concentration (µg/mL)	Bias (%)	CV (%)
Freeze-thaw: 5 cycles	690	-8.0	2.0
Frozen plasma sample: 301 days at -70°C	660	-12.0	1.5
Bench top: 24 hours	653	-12.9	4.7

Results of the validation experiments for the LC-MS/MS determination of pertuzumab (FTLSVDR signature peptide)

Table S-9: Individual calibration curve results from the LC-MS/MS validation of the FTLSVDR signature peptide (nominal concentration).

Run #	Measured concentration (µg/mL)								Correlation	Slope	Intercept
	2.00*	4.00*	10.0*	50.0*	200*	400*	500*	1000*			
01	1.98	3.98	10.5	51.7	191	394	474	1050	0.9991	0.0139	0.00223
02	1.98	3.96	10.7	49.2	196	403	475	1030	0.9996	0.00772	0.00232
03	1.96	4.02	11.0	50.8	199	403	470	961	0.9986	0.0135	0.00180
04	2.01	3.87	10.6	51.5	191	374	505	1040	0.9988	0.0125	0.000375
Average (µg/mL)	1.98	3.96	10.7	50.8	194	394	481	1020	-	-	-
Total bias (%)	-1.0	-1.0	7.0	1.6	-3.0	-1.5	-3.8	2.0	-	-	-
Total CV (%)	1.0	1.6	2.0	2.2	2.0	3.5	3.4	4.0	-	-	-

Table S-10: Individual accuracy and precision results from the LC-MS/MS validation of the FTLSDVR signature peptide.

Run #	Nominal concentration 2.00 (µg/mL)						Average	Bias	CV
	Measured concentration (µg/mL)						(µg/mL)	(%)	(%)
01	1.86	1.91	1.91	1.88	1.88	1.83	1.88	-6.0	1.4
02	1.71	1.69	1.80	1.71	1.72	1.75	1.73	-13.5	2.4
03	2.03	2.08	2.08	2.01	2.17	2.17	2.09	4.6	3.2
Total							1.90	-4.9	8.4

Run #	Nominal concentration 6.00 (µg/mL)						Average	Bias	CV
	Measured concentration (µg/mL)						(µg/mL)	(%)	(%)
01	6.00	6.27	6.15	6.48	6.59	6.98	6.41	6.9	5.5
02	5.72	5.76	5.73	6.08	5.75	6.18	5.87	-2.2	3.5
03	5.71	5.25	5.77	5.85	5.93	6.64	5.86	-2.3	7.7
Total							6.05	0.8	7.0

Run #	Nominal concentration 75.0 (µg/mL)						Average	Bias	CV
	Measured concentration (µg/mL)						(µg/mL)	(%)	(%)
01	73.8	75.2	74.0	75.4	74.3	73.8	74.4	-0.8	1.0
02	65.6	66.9	65.5	72.0	68.2	68.3	67.7	-9.7	3.6
03	68.0	67.2	65.6	64.2	68.2	66.2	66.6	-11.2	2.3
Total							69.6	-7.2	5.6

Run #	Nominal concentration 750 (µg/mL)						Average	Bias	CV
	Measured concentration (µg/mL)						(µg/mL)	(%)	(%)
01	704	723	724	738	762	810	743	-0.9	5.1
02	698	737	734	683	731	774	726	-3.2	4.4
03	692	690	682	692	709	796	710	-5.3	6.0
Total							727	-3.1	5.3

Table S-11: Individual results from the matrix variability experiments of the FTLSVDR signature peptide LC-MS/MS validation.

Plasma lot #	Nominal concentration 2.00 (µg/mL)
	Measured concentration (µg/mL)
01	1.86
02	1.91
03	1.91
04	1.88
05	1.88
06	1.83
2% Hemolytic	1.91
Lipemic	1.97
Average (µg/mL)	1.89
Bias (%)	-5.1
CV (%)	2.2

Table S-12: Results (n=3) from the stability experiments of the FTLSVDR signature peptide LC-MS/MS validation, analyzed against a freshly prepared calibration curve.

Stability item	Nominal concentration 6.00 (µg/mL)		
	Average concentration (µg/mL)	Bias (%)	CV (%)
Freeze-thaw: 5 cycles	6.00	0.1	1.6
Frozen plasma sample: 301 days at -70°C	5.52	-8.0	4.1
Bench top: 24 hours	6.02	0.4	3.7

Stability item	Nominal concentration 750 (µg/mL)		
	Average concentration (µg/mL)	Bias (%)	CV (%)
Freeze-thaw: 5 cycles	761	1.4	2.0
Frozen plasma sample: 301 days at -70°C	698	-7.0	10.1
Bench top: 24 hours	673	-10.3	4.4

Results of the validation experiments for the LC-MS/MS determination of pertuzumab (GLEWVADVNPNSGGSIYNQR signature peptide)

Table S-13: Individual calibration curve results from the LC-MS/MS validation of the GLEWVADVNPNSGGSIYNQR signature peptide (nominal concentration)

Run #	Measured concentration (µg/mL)								Correlation	Slope	Intercept
	2.00*	4.00*	10.0*	50.0*	200*	400*	500*	1000*			
01	#NR	3.95	10.3	48.0	218	375	478	1040	0.9983	0.124	0.0141
02	#NR	3.81	11.3	48.5	195	389	484	1030	0.9977	0.120	0.0473
03	#NR	3.78	11.4	49.5	198	390	482	998	0.9975	0.117	0.0617
04	#NR	4.69	10.8	49.3	178	356	493	1120	0.9927	0.152	0.0848
Average (µg/mL)	-	4.06	11.0	48.8	197	378	484	1050	-	-	-
Total bias (%)	-	1.5	10.0	-2.4	-1.5	-5.5	-3.2	5.0	-	-	-
Total CV (%)	-	10.6	4.6	1.4	8.3	4.2	1.3	4.9	-	-	-

#NR: No Result (<LLOQ)

Table S-14: Individual accuracy and precision results from the LC-MS/MS validation of the GLEWVADVNPNSGGSIYNQR signature peptide.

Run #	Nominal concentration 6.00 (µg/mL)						Average	Bias	CV
	Measured concentration (µg/mL)						(µg/mL)	(%)	(%)
01	5.84	6.14	6.08	5.97	6.00	6.24	6.05	0.8	2.3
02	6.88	6.40	5.97	5.89	6.77	6.65	6.43	7.1	6.5
03	5.65	6.43	6.31	6.53	6.16	5.89	6.16	2.7	5.5
Total							6.21	3.5	5.5

Run #	Nominal concentration 75.0 (µg/mL)						Average	Bias	CV
	Measured concentration (µg/mL)						(µg/mL)	(%)	(%)
01	71.1	66.2	69.4	69.4	75.5	67.1	69.8	-6.9	4.7
02	66.9	66.0	63.5	64.2	63.0	72.1	65.9	-12.1	5.1
03	76.1	68.9	70.8	64.1	62.6	74.8	69.6	-7.2	7.9
Total							68.4	-8.7	6.3

Run #	Nominal concentration 750 (µg/mL)						Average	Bias	CV
	Measured concentration (µg/mL)						(µg/mL)	(%)	(%)
01	722	756	728	740	711	772	738	-1.6	3.1
02	786	739	670	753	661	893	750	0.0	11.4
03	638	745	672	718	769	798	723	-3.6	8.3
Total							737	-1.7	8.0

Table S-15: Results (n=3) from the stability experiments of the GLEWVADVNPNSGGSIYNQR signature peptide LC-MS/MS validation, analyzed against a freshly prepared calibration curve.

Nominal concentration 6.00 (µg/mL)			
Stability item	Average concentration (µg/mL)	Bias (%)	CV (%)
Freeze-thaw: 5 cycles	5.96	-0.7	10.2
Frozen plasma sample: 301 days at -20°C	6.62	10.4	8.2
Bench top: 24 hours	6.80	13.3	4.3

Nominal concentration 750 (µg/mL)			
Stability item	Average concentration (µg/mL)	Bias (%)	CV (%)
Freeze-thaw: 5 cycles	759	1.2	2.8
Frozen plasma sample: 301 days at -20°C	736	3.7	7.1
Bench top: 24 hours	778	-1.9	11.8

Description of the validation experiments for the receptor binding assay for determination of trastuzumab

Acceptance criteria. As per international guidelines, all Bias and CV acceptance criteria were set at 20% (25% at the LLOQ and ULOQ).

Linearity. Each validation run contained a calibration curve prepared in human plasma with the following levels: 60.1, 102, 172, 290, 490, 829, 1400 and 2370 ng/mL. The optical density (OD) was used in calculations. 4 parameter logistic fit (4PL) was applied.

Accuracy and precision. The accuracy and precision of the method were determined by triplicate analysis in four separate runs analyzed on four different days. The validation samples were prepared in plasma at five concentration levels: 60.1, 150, 600, 2000 and 2370 ng/mL. Statistical analysis was performed using analysis of variance (ANOVA).

Integrity of dilution. The integrity of dilution was assessed on two levels, by six-fold analysis. Samples were prepared at concentrations of 50.0 and 600 µg/mL and separately diluted 300 times with blank plasma.

Dilution linearity / Hook effect. Dilution linearity was assessed by multiple dilutions of a sample containing 600 µg-mL trastuzumab. Dilutions assessed were: 500-, 1250-, 3125- and 7812.5-fold.

Matrix variability/selectivity. The influence of the matrix was assessed by preparing samples in 10 independent human plasma lots at a concentration of 100 and 2000 ng/mL. Additionally, from all 10 plasma lots, blank samples were analyzed and checked for interferences. The samples were analyzed in one run.

Freeze-thaw stability. Human plasma samples at 150, 2000 ng/mL and 50.0 µg/mL were stored at -20°C and subjected to three freeze-thaw cycles, in which thawing was performed on the bench-top for a minimum of two hours, followed by frozen storage for at least 12 hours. The samples were analyzed against a freshly spiked and prepared calibration curve.

Frozen stability. Human plasma samples at 150, 2000 ng/mL and 50.0 µg/mL were stored at RT (20 ±2 °C) for 24 hours. The samples were analyzed against a freshly spiked and prepared calibration curve.

Description of the validation experiments for the receptor binding assay for determination of pertuzumab (cross validation)

Run#: 07

Acceptance criteria. As per international guidelines, all Bias and CV acceptance criteria were set at 20% (25% at the LLOQ and ULOQ).

Linearity. Each validation run contained a calibration curve of trastuzumab prepared in human plasma with the following levels: 60.1, 102, 172, 290, 490, 829, 1400 and 2370 ng/mL. The optical density (OD) was used in calculations. 4 parameter logistic fit (4PL) was applied.

Accuracy and precision. The accuracy and precision of the method towards **pertuzumab** were determined by triplicate analysis in one run. Validation samples were prepared in plasma at five concentration levels: 60.1, 150, 600, 2000 and 2370 ng/mL. Statistical analysis was performed using analysis of variance (ANOVA).

Results of the validation experiments for the receptor binding assay for determination of trastuzumab.

Table S-16: Individual calibration curve results from the receptor binding assay validation.

Run #	Measured concentration (ng/mL)										Curve parameters			
	60.1	102	172	290	490	829	1400	2370			A	B	C	D
01	64.0	106	169	261	507	906	1560	2390			0.067	1.48	1700	1.05
02	56.0	97.7	161	253	499	898	1560	2370			0.068	1.47	1700	1.05
03	56.3	98.0	161	253	500	898	1560	2370			0.067	1.45	1710	1.05
04	56.7	98.3	162	253	500	898	1560	2380			0.067	1.50	1690	1.05
05	66.7	100	150	250	500	900	1550	2380			0.066	1.54	1700	1.05
06	56.7	96.7	157	250	497	897	1550	2360			0.068	1.53	1720	1.05
07	61.3	98.0	158	251	498	898	1550	2370			0.0690	1.54	1700	1.05
Average (ng/mL)	59.7	99.2	160	253	500	899	1560	2370			-	-	-	-
Total bias (%)	7.3	3.0	3.6	1.4	0.7	0.3	0.3	0.4			-	-	-	-
Total CV (%)	-0.7	-2.7	-7.2	-12.8	2.1	8.5	11.1	0.2			-	-	-	-

Table S-17: Individual accuracy and precision results from the receptor binding assay validation.

Run #	Nominal concentration 60.1 (ng/mL)			Average	Bias	CV
	Measured concentration (ng/mL)			(ng/mL)	(%)	(%)
01	59.8	63.2	60.7	61.2	1.9	2.8
02	59.3	59.3	57.7	58.8	-2.2	1.6
03	53.0	54.7	53.0	53.6	-10.9	1.8
04	55.0	56.7	56.7	56.1	-6.6	1.7
Total				57.4	-4.5	6.0

Run #	Nominal concentration 150 (ng/mL)			Average	Bias	CV
	Measured concentration (ng/mL)			(ng/mL)	(%)	(%)
01	130	126	133	130	-13.6	2.9
02	129	133	133	132	-12.3	1.5
03	170	171	166	169	12.7	1.5
04	127	127	128	127	-15.2	0.8
Total				139	-7.1	14.4

Run #	Nominal concentration 600 (ng/mL)			Average	Bias	CV
	Measured concentration (ng/mL)			(ng/mL)	(%)	(%)
01	596	597	603	599	-0.2	0.7
02	602	596	599	599	-0.1	0.5
03	640	636	630	635	5.9	0.8
04	580	587	587	584	-2.6	0.7
Total				604	0.7	3.6

Run #	Nominal concentration 2000 (ng/mL)			Average	Bias	CV
	Measured concentration (ng/mL)			(ng/mL)	(%)	(%)
01	1760	1760	1750	1760	-12.2	0.3
02	1780	1740	1750	1760	-12.2	1.3
03	1820	1820	1820	1820	-9.0	0.2
04	1750	1750	1750	1750	-12.6	0.1
Total				1770	-11.5	2.0

Run #	Nominal concentration 2370 (ng/mL)			Average	Bias	CV
	Measured concentration (ng/mL)			(ng/mL)	(%)	(%)
01	2310	2310	2310	2310	-2.6	0.1
02	2300	2290	2300	2300	-3.1	0.1
03	2360	2360	2360	2360	-0.4	0.1
04	2360	2360	2360	2360	-0.4	0.1
Total				2330	-1.6	1.4

Table S-18: Individual results from the matrix variability experiments of the receptor binding assay validation.

Plasma lot #	Nominal concentration Endogenous
	Measured concentration (ng/mL)
01	<LLOQ
02	<LLOQ
03	<LLOQ
04	<LLOQ
05	<LLOQ
06	<LLOQ
07	<LLOQ
08	<LLOQ
09	<LLOQ
10	<LLOQ
Average (ng/mL)	-
Bias (%)	-
CV (%)	-

Plasma lot #	Nominal concentration 100 (ng/mL)
	Measured concentration (ng/mL)
01	103
02	106
03	105
04	103
05	94.5
06	111
07	87.0
08	99.3
09	106
10	96.3
Average (ng/mL)	101
Bias (%)	1.0
CV (%)	6.9

Plasma lot #	Nominal concentration 2000 (ng/mL)
	Measured concentration (ng/mL)
01	1940
02	1950
03	1940
04	1970
05	1940
06	2050
07	1930
08	1920
09	1960
10	1960
Average (ng/mL)	1960
Bias (%)	-2.0
CV (%)	1.9

Table S-19: Individual results from the integrity of dilution experiments of the receptor binding assay validation.

Dilution factor 300									
Run #	Nominal concentration 50000 (ng/mL)						Average	Bias	CV
	Measured concentration (ng/mL)						(ng/mL)	(%)	(%)
01	46000	43500	48000	47500	46000	43000	45700	-8.7	4.5
	Total						45700	-8.7	4.5

Dilution factor 300									
Run #	Nominal concentration 600000 (ng/mL)						Average	Bias	CV
	Measured concentration (ng/mL)						(ng/mL)	(%)	(%)
01	553000	554000	549000	549000	549000	552000	551000	-8.2	0.4
	Total						551000	-8.2	0.4

Table S-20: Individual results from the dilution linearity experiments of the receptor binding assay validation.

Dilution factor	Diluted concentration (ng/mL)	Measured concentration (ng/mL)	Bias (%)	Undiluted Concentration (ng/mL)
500	1200	1330	10.4	663000
1250	480	423	-11.8	529000
3125	192	168	-12.3	526000
7812.5	76.8	65.0	-15.4	508000
Average				670000
Total CV (%)				12.8

Table S-21: Results (n=3) from the stability experiments of the receptor binding assay validation, analyzed against a freshly prepared calibration curve.

Nominal concentration 150 (ng/mL)			
Stability item	Average concentration (µg/mL)	Bias (%)	CV (%)
Freeze-thaw: 3 cycles	142	-5.0	0.7
Bench Top: 24 hours at RT	143	-4.9	1.2
Nominal concentration 2000 (ng/mL)			
Stability item	Average concentration (µg/mL)	Bias (%)	CV (%)
Freeze-thaw: 3 cycles	1920	-3.8	0.1
Bench Top: 24 hours at RT	1920	-3.9	0.0
Nominal concentration 50000 (ng/mL)			
Stability item	Average concentration (µg/mL)	Bias (%)	CV (%)
Freeze-thaw: 3 cycles	53600	7.3	0.9
Bench Top: 24 hours at RT	54500	9.0	0.0

Table S-22: Individual accuracy and precision results from the receptor binding assay validation for pertuzumab.

Run #	Nominal concentration 60.1 (ng/mL)			Average	Bias	CV
	Measured concentration (ng/mL)			(ng/mL)	(%)	(%)
07	64.8	66.5	64.8	65.4	8.8	1.5

Run #	Nominal concentration 150 (ng/mL)			Average	Bias	CV
	Measured concentration (ng/mL)			(ng/mL)	(%)	(%)
07	146	145	146	145	-3.1	0.4

Run #	Nominal concentration 600 (ng/mL)			Average	Bias	CV
	Measured concentration (ng/mL)			(ng/mL)	(%)	(%)
07	563	647	650	620	3.3	8.0

Run #	Nominal concentration 2000 (ng/mL)			Average	Bias	CV
	Measured concentration (ng/mL)			(ng/mL)	(%)	(%)
07	1830	1830	1830	1830	-8.5	0.1

Run #	Nominal concentration 2370 (ng/mL)			Average	Bias	CV
	Measured concentration (ng/mL)			(ng/mL)	(%)	(%)
07	2280	2280	2280	2280	-3.7	0.1

Table S-23: Results of patient sample analysis, originating from the clinical study TRAIN3, using the LC-MS method for determination of trastuzumab and pertuzumab.

Subject Number	Sample collection after start-up dose (Days)	Trastuzumab concentration			Pertuzumab concentration		
		FTISADTSK (µg/mL)	IYPTNGYTR (µg/mL)	FTLSVDR (µg/mL)	GLEWVADVNPNSGGSIYNQR (µg/mL)		
2	0	74.6	67.0	108		102	
2	20	79.7	70.6	121		113	
2	62	78.9	68.0	110		114	
2	82	81.7	74.0	106		95.0	
2	146	78.8	75.3	106		88.2	
2	188	37.7	28.5	62.5		61.7	
3	0	77.6	57.9	96.5		97.8	
3	20	86.6	68.5	74.0		63.1	
3	37	105	81.4	52.5		45.3	
3	62	103	79.2	35.6		37.7	
3	82	96.5	73.9	19.6		17.7	
3	127	90.2	69.6	3.06		< LLOQ (4.00)	
3	211	32.7	17.4	< LLOQ (2.00)		< LLOQ (4.00)	
4	0	33.5	26.7	64.0		58.1	
4	20	41.3	32.6	80.6		76.7	
4	41	47.2	39.5	81.5		65.3	
4	62	47.5	38.3	83.2		77.2	
4	83	52.5	45.5	92.3		81.7	
4	126	56.2	44.8	107		97.0	
4	176	17.7	11.7	45.3		44.1	
7	0	40.8	36.3	43.3		40.1	
7	7	33.8	29.7	34.9		27.6	
7	41	68.9	65.5	71.0		71.7	
7	70	63.1	61.1	67.0		65.8	
7	102	85.4	80.8	86.4		99.3	
7	154	61.1	56.7	62.7		58.9	
7	213	66.2	58.2	66.5		62.2	
8	0	82.5	77.6	111		101	

Table S-23: Continued.

Subject Number	Sample collection after start-up dose (Days)	Trastuzumab concentration			Pertuzumab concentration		
		FTISADTSK (µg/mL)	IYPTNGYTR (µg/mL)	FTLSVDR (µg/mL)	GLEWVADVPNSGGSIYNQR (µg/mL)		
8	21	92.6	76.9	116		98.0	
8	42	68.3	53.5	94.9		93.7	
8	64	76.1	60.4	109		109	
8	105	82.7	63.5	128		127	
8	168	89.2	70.4	131		122	
8	189	89.9	71.1	138		127	
9	0	65.0	52.1	84.8		103	
9	28	79.2	62.4	95.7		102	
9	49	51.2	41.5	69.2		83.3	
9	71	66.5	58.5	71.3		73.1	
9	133	79.4	62.9	79.8		74.7	
9	160	60.7	46.2	69.9		72.9	
9	182	56.8	45.2	66.7		62.7	
9	202	56.1	46.6	71.0		67.8	
10	0	67.0	62.2	57.4		54.5	
10	42	64.3	62.7	52.4		55.9	
10	63	62.5	59.7	52.5		49.5	
10	84	63.8	55.9	59.4		55.0	
10	105	72.3	67.4	64.3		58.7	
10	141	98.3	89.5	92.6		85.9	
10	189	61.2	51.0	66.1		60.0	
10	231	69.4	60.0	65.7		55.5	
13	0	66.9	57.2	114		102	
13	20	75.1	57.4	119		109	
13	41	78.6	59.7	124		113	
13	62	76.8	55.7	110		98.8	
13	83	71.1	51.4	116		105	
13	104	74.3	56.0	109		90.0	
13	125	75.7	59.5	115		91.6	
13	146	74.0	56.7	116		99.3	

Table S-23: Continued.

Subject Number	Sample collection after start-up dose (Days)	Trastuzumab concentration		Pertuzumab concentration	
		FTISADTSK (µg/mL)	IYPTNGYTR (µg/mL)	FTLSVDR (µg/mL)	GLEWVADVNPNSGGSIYNQR (µg/mL)
13	209	81.7	59.7	119	104
14	0	48.4	45.3	80.1	65.8
14	126	88.0	73.9	116	98.6
14	161	101	83.3	135	105
14	182	97.3	78.9	132	118
14	210	90.4	70.1	125	110
14	271	114	99.2	152	131
19	0	< LLOQ (2.00)	< LLOQ (2.00)	< LLOQ (2.00)	< LLOQ (4.00)
19	99	89.4	79.7	109	96.5
19	120	106	95.9	139	126
19	141	116	95.5	143	129
19	162	108	91.5	133	123
19	181	112	92.1	153	117
19	206	114	92.2	155	121
19	269	111	85.8	157	125
19	332	109	82.7	156	118
21	0	< LLOQ (2.00)	< LLOQ (2.00)	< LLOQ (2.00)	< LLOQ (4.00)
21	22	30.0	27.9	56.5	49.5
21	84	48.2	47.6	64.5	54.7
21	103	54.7	51.7	63.1	59.5
21	126	51.2	44.5	61.2	49.3
21	146	51.2	47.2	62.4	53.9
21	166	57.2	52.6	64.8	55.4
21	188	48.7	43.9	57.0	47.1
21	251	42.2	38.4	51.9	39.9
22	0	< LLOQ (2.00)	< LLOQ (2.00)	< LLOQ (2.00)	< LLOQ (4.00)
22	19	37.8	34.4	71.2	54.1
22	90	104	94.9	153	113
22	106	65.0	54.2	110	84.8
22	125	77.4	63.0	121	93.4

Table S-23: Continued.

Subject Number	Sample collection after start-up dose	Trastuzumab concentration			Pertuzumab concentration		
	(Days)	FTISADTSK (µg/mL)	IYPTNGYTR (µg/mL)	FTLSVDR (µg/mL)	GLEWVADVPNSGGSIYNQR (µg/mL)		
22	146	76.6	63.0	119		89.9	
22	166	93.7	76.5	135		95.7	
22	232	68.7	55.0	94.9		79.2	
22	316	22.6	12.8	45.9		37.0	
30	0	< LLOQ (2.00)	< LLOQ (2.00)	< LLOQ (2.00)		< LLOQ (4.00)	
30	29	32.7	33.3	75.6		59.7	
30	94	54.0	47.8	113		78.7	
30	115	60.1	56.0	115		88.5	
30	122	60.7	49.8	112		80.7	
30	142	66.3	52.9	105		78.8	
30	164	66.3	53.8	108		89.5	
30	172	58.0	46.5	96.1		69.4	
30	196	60.6	46.6	95.0		69.5	
30	204	53.3	42.1	91.9		64.6	
30	214	69.8	59.1	113		81.1	
30	269	85.2	71.7	105		75.9	
30	310	100	82.1	117		91.4	
36	0	< LLOQ (2.00)	< LLOQ (2.00)	< LLOQ (2.00)		< LLOQ (4.00)	
36	21	38.4	36.5	75.0		76.8	
36	77	107	99.1	126		102	
36	91	84.1	74.1	117		91.8	
36	112	82.3	70.5	124		92.4	
36	133	82.5	68.8	117		83.4	
36	155	90.5	72.9	118		95.7	
36	238	106	83.7	123		91.1	
44	0	46.4	39.3	70.4		53.0	
44	20	52.2	46.3	74.2		54.9	
44	42	48.9	42.7	72.7		51.7	
44	62	60.5	52.5	82.3		63.5	
44	104	61.8	51.7	78.0		63.2	

Table S-23: Continued.

Subject Number	Sample collection after start-up dose (Days)	Trastuzumab concentration		Pertuzumab concentration	
		FTISADTSK (µg/mL)	IYPTNGYTR (µg/mL)	FTLSVDR (µg/mL)	GLEWVADVNPNSGGSIYNQR (µg/mL)
44	126	68.0	56.3	92.1	70.1
44	146	75.1	59.7	95.7	71.9
44	167	65.2	54.1	91.5	70.5
52	0	42.9	37.6	78.1	70.9
52	49	42.0	36.5	75.7	67.9
52	71	42.9	36.7	76.7	70.2
52	92	42.6	35.1	77.0	72.2
52	113	42.5	34.3	77.7	65.0
52	195	18.4	12.7	45.4	40.2
56	0	< LLOQ (2.00)	< LLOQ (2.00)	< LLOQ (2.00)	< LLOQ (4.00)
56	28	35.0	31.8	77.9	73.6
56	51	35.2	31.3	78.9	70.5
56	57	30.2	25.9	68.0	59.2
56	78	45.5	39.9	85.8	77.5
56	100	51.3	44.1	93.8	92.2
56	106	38.7	33.4	67.2	67.7
56	112	76.0	72.3	119	107
56	126	44.8	40.1	76.3	73.7
56	133	38.3	32.7	69.3	65.5
56	155	46.2	38.4	78.4	73.4
56	161	38.3	29.9	66.5	55.5
56	183	44.9	35.9	82.2	77.2
56	191	35.4	27.8	67.3	66.0
56	210	49.7	40.4	83.6	74.9
62	0	21.1	19.4	50.1	53.1
62	21	25.4	23.0	47.8	46.7
62	28	17.4	14.7	40.8	43.7
62	35	9.91	7.70	24.3	26.3
62	63	13.5	12.1	27.4	28.3
62	84	17.1	15.8	32.5	30.7

Table S-23: Continued.

Subject Number	Sample collection after start-up dose	Trastuzumab concentration			Pertuzumab concentration		
	(Days)	FTISADTSK (µg/mL)	IYPTNGYTR (µg/mL)	FTLSVDR (µg/mL)	GLEWVADVNPNSGGSIYNQR (µg/mL)		
62	107	16.2	14.2	30.2		29.3	
62	126	21.4	20.2	36.4		33.4	
62	139	8.37	6.40	18.6		17.2	
62	147	34.5	36.3	61.5		64.3	
62	161	12.9	11.9	25.9		27.3	
62	182	14.4	13.6	29.8		34.4	
70	0	< LLOQ (2.00)	< LLOQ (2.00)	< LLOQ (2.00)		< LLOQ (4.00)	
70	31	44.4	38.8	68.1		54.3	
70	52	52.7	44.4	73.7		69.2	
70	73	59.1	51.0	70.7		60.4	
70	94	64.6	55.7	81.2		67.4	
70	136	70.4	58.0	89.4		86.2	
70	144	58.8	46.1	78.7		73.3	
70	171	55.0	41.4	73.6		64.5	
70	195	59.8	44.6	81.2		75.7	
71	0	37.1	32.7	69.9		61.6	
71	21	49.3	43.1	75.1		70.6	
71	57	37.5	28.9	56.8		58.7	
71	96	65.8	54.5	80.7		72.2	
76	0	< LLOQ (2.00)	< LLOQ (2.00)	< LLOQ (2.00)		< LLOQ (4.00)	
76	23	31.6	27.4	78.7		69.1	
76	44	33.9	32.2	67.6		60.3	
76	64	40.3	38.2	72.7		67.0	
76	85	42.3	40.2	78.7		71.5	
76	107	48.7	42.7	83.7		74.3	
76	128	48.2	41.9	81.4		76.0	
76	149	44.7	38.1	77.5		76.9	
76	170	50.3	44.3	91.0		75.8	
76	191	52.5	42.1	86.3		77.4	
90	0	< LLOQ (2.00)	< LLOQ (2.00)	< LLOQ (2.00)		< LLOQ (4.00)	

Table S-23: Continued.

Subject Number	Sample collection after start-up dose (Days)	Trastuzumab concentration		Pertuzumab concentration	
		FTISADTSK (µg/mL)	IYPTNGYTR (µg/mL)	FTLSVDR (µg/mL)	GLEWVADVNPNSGGSIYNQR (µg/mL)
90	21	42.3	40.3	82.2	73.3
90	42	46.3	48.5	92.7	66.5
90	63	73.3	68.4	100	82.2
90	82	84.3	75.4	110	104
90	105	68.4	63.1	94.0	93.0
90	126	74.9	69.1	102	89.1
90	166	44.9	34.6	73.6	64.1
90	187	53.4	48.2	83.1	86.1
95	0	< LLOQ (2.00)	< LLOQ (2.00)	< LLOQ (2.00)	< LLOQ (4.00)
95	10	< LLOQ (2.00)	< LLOQ (2.00)	< LLOQ (2.00)	< LLOQ (4.00)
95	33	46.5	45.9	79.7	70.0
95	55	61.4	56.0	77.6	63.6
95	76	74.4	67.4	74.9	54.8
95	97	75.6	66.1	79.4	66.8
95	118	80.6	70.3	78.5	61.9
95	125	65.4	53.4	69.5	60.2
95	132	119	112	116	92.9
95	146	70.1	60.4	77.0	67.9
95	167	72.0	62.9	83.3	64.5
95	174	58.7	46.0	66.2	52.6
112	0	< LLOQ (2.00)	< LLOQ (2.00)	< LLOQ (2.00)	< LLOQ (4.00)
112	21	22.8	20.9	66.9	59.8
112	41	29.0	27.1	71.4	65.4
112	62	33.5	29.1	72.4	63.4
112	83	33.6	28.3	67.1	60.4
112	104	35.6	30.1	72.9	63.1
112	125	36.1	30.6	64.0	51.6
112	145	37.3	31.0	66.2	50.9
132	0	< LLOQ (2.00)	< LLOQ (2.00)	< LLOQ (2.00)	< LLOQ (4.00)
132	21	34.5	31.7	62.6	53.6

Table S-23: Continued.

Subject Number	Sample collection after start-up dose	Trastuzumab concentration			Pertuzumab concentration		
	(Days)	FTISADTSK (µg/mL)	IYPTNGYTR (µg/mL)	FTLSVDR (µg/mL)	GLEWVADVNPNSGGSIYNQR (µg/mL)		
132	42	44.7	40.4	61.2		48.8	
132	63	47.4	42.4	69.5		56.3	
132	84	53.2	45.4	64.4		46.6	
132	105	51.5	42.0	70.5		62.4	
133	0	< LLOQ (2.00)	< LLOQ (2.00)	< LLOQ (2.00)		< LLOQ (4.00)	
133	18	< LLOQ (2.00)	< LLOQ (2.00)	< LLOQ (2.00)		< LLOQ (4.00)	
133	40	50.2	49.5	69.7		58.1	
133	89	66.2	58.6	72.0		56.3	
133	103	90.9	83.6	99.5		93.5	
133	110	76.7	69.2	83.9		70.2	
133	131	94.1	81.3	95.2		77.6	
135	0	< LLOQ (2.00)	< LLOQ (2.00)	< LLOQ (2.00)		< LLOQ (4.00)	
135	20	53.5	50.7	73.1		56.5	
135	41	68.9	61.7	85.5		67.2	
135	67	145	137	162		128	
135	83	97.6	82.5	110		88.4	
135	103	106	86.1	127		106	
135	111	153	142	171		129	
135	123	102	83.0	108		83.1	
158	0	< LLOQ (2.00)	< LLOQ (2.00)	< LLOQ (2.00)		< LLOQ (4.00)	
158	21	49.6	46.0	68.4		57.2	
158	44	54.2	47.4	72.1		58.1	
158	63	69.1	62.2	76.2		64.6	
158	77	115	103	114		98.5	
158	84	82.1	71.5	81.9		67.3	
158	104	87.7	76.8	88.7		78.7	
159	0	< LLOQ (2.00)	< LLOQ (2.00)	< LLOQ (2.00)		< LLOQ (4.00)	
159	30	40.4	32.1	75.9		57.9	
159	51	59.3	46.4	91.5		69.7	
159	70	74.3	57.4	103		79.6	

Table S-23: Continued.

Subject Number	Sample collection after start-up dose (Days)	Trastuzumab concentration			Pertuzumab concentration		
		FTISADTSK (µg/mL)	IYPTNGYTR (µg/mL)	FTLSVDR (µg/mL)	GLEWVADVNPNSGGSIYNQR (µg/mL)		
159	79	59.6	44.4	77.1		52.9	
159	100	74.9	59.0	109		79.8	
159	121	81.8	61.3	109		70.6	
169	0	45.4	38.5	92.1		67.2	
169	21	61.8	52.2	103		85.4	
169	28	46.6	37.3	85.7		67.2	
169	48	70.2	53.8	103		78.3	
169	90	41.1	27.7	76.5		61.5	
172	0	< LLOQ (2.00)	< LLOQ (2.00)	< LLOQ (2.00)		< LLOQ (4.00)	
172	17	< LLOQ (2.00)	< LLOQ (2.00)	< LLOQ (2.00)		< LLOQ (4.00)	
172	38	39.2	35.6	81.8		62.4	
172	59	51.6	41.9	85.1		73.2	
172	66	37.9	31.6	68.9		60.8	
172	84	67.6	55.9	100		77.1	
172	104	76.1	59.4	105		79.3	
172	111	58.2	44.2	87.9		69.4	
173	0	< LLOQ (2.00)	< LLOQ (2.00)	< LLOQ (2.00)		< LLOQ (4.00)	
173	22	28.4	23.1	63.5		49.5	
173	43	34.5	27.8	70.2		57.5	
173	63	46.1	35.7	82.2		62.2	
173	85	42.4	32.6	71.5		59.1	
173	103	51.9	40.1	83.0		68.3	
173	110	40.9	29.8	69.6		51.4	
180	0	< LLOQ (2.00)	< LLOQ (2.00)	< LLOQ (2.00)		< LLOQ (4.00)	
180	31	34.5	29.4	79.4		63.5	
180	52	52.5	41.3	82.8		53.4	
180	75	55.8	42.7	84.7		66.8	
180	96	63.7	47.7	88.8		66.7	
183	0	< LLOQ (2.00)	< LLOQ (2.00)	< LLOQ (2.00)		< LLOQ (4.00)	
183	24	39.9	32.1	90.9		72.7	

Table S-23: Continued.

Subject Number	Sample collection after start-up dose	Trastuzumab concentration			Pertuzumab concentration		
		FTISADTSK	IYPTNGYTR	FTLSVDR	GLEWVADVNPNSGGSIYNQR		
	(Days)	(µg/mL)	(µg/mL)	(µg/mL)	(µg/mL)		
183	45	51.6	41.7	97.7			77.5
183	66	61.5	47.3	110			80.4
183	86	52.4	40.0	83.3			62.5
190	0	< LLOQ (2.00)	< LLOQ (2.00)	< LLOQ (2.00)			< LLOQ (4.00)
197	0	27.4	24.7	77.1			64.2
197	42	41.1	32.6	70.1			58.8
199	0	< LLOQ (2.00)	< LLOQ (2.00)	< LLOQ (2.00)			< LLOQ (4.00)
199	27	< LLOQ (2.00)	< LLOQ (2.00)	< LLOQ (2.00)			< LLOQ (4.00)
199	57	59.3	46.4	84.4			68.0
199	76	99.1	74.9	117			95.5
208	0	49.9	43.4	100			80.9
208	22	66.1	53.3	107			88.5
208	42	82.8	65.6	116			93.5
215	0	43.1	34.8	102			80.5
215	21	61.8	50.7	103			81.7
215	39	75.0	61.0	114			85.2
222	0	< LLOQ (2.00)	< LLOQ (2.00)	< LLOQ (2.00)			< LLOQ (4.00)
222	21	< LLOQ (2.00)	< LLOQ (2.00)	< LLOQ (2.00)			< LLOQ (4.00)
222	42	45.4	37.1	82.7			64.4
228	0	< LLOQ (2.00)	< LLOQ (2.00)	< LLOQ (2.00)			< LLOQ (4.00)
228	26	44.7	36.0	91.6			72.5
246	0	< LLOQ (2.00)	< LLOQ (2.00)	< LLOQ (2.00)			< LLOQ (4.00)
246	33	43.9	36.6	65.8			53.9
259	0	< LLOQ (2.00)	< LLOQ (2.00)	< LLOQ (2.00)			< LLOQ (4.00)
259	9	< LLOQ (2.00)	< LLOQ (2.00)	< LLOQ (2.00)			< LLOQ (4.00)

CHAPTER V

Intact protein bioanalysis by liquid chromatography – high-resolution mass spectrometry

Peter Bults^{1,2}, Baubek Spanov¹, Oladapo Olaleye¹, Nico C. van de Merbel^{1,2}, Rainer Bischoff^{1*}

¹ *Department of Analytical Biochemistry, Groningen Research Institute of Pharmacy, University of Groningen, Antonius Deusinglaan 1, 9713 AV, Groningen, The Netherlands*

² *Bioanalytical Laboratory, PRA Health Sciences, Amerikaweg 18, 9407 TK, Assen, The Netherlands*

J. Chromatogr. B-Analyt. Technol. Biomed. Life Sci., 2019, 1110-1111, 155-167

5.1 INTRODUCTION

Liquid chromatography coupled online to mass spectrometry (LC-MS) is arguably the most widely used bioanalytical technique due to its sensitivity and selectivity. It is a very versatile analytical approach that can be tuned to address a wide range of molecules with applications from environmental analysis to drug analysis and doping control. LC-MS is increasingly used for the analysis of proteins, typically after a proteolytic digestion step which converts the macromolecular analytes into lower-molecularweight peptides, which can be readily quantified. LC-MS analysis of intact proteins, however, is still in its infancy, being mainly restricted to the detailed characterization of biopharmaceuticals in dose formulations [1–10]. The analysis of intact proteins in complex biological samples, referred to here as protein bioanalysis, has remained the realm of ligand binding assays (LBAs) and notably of enzyme-linked immunosorbent assays (ELISAs) due to their exquisite sensitivity and specificity. A disadvantage of ELISAs is that specificity can often not be assessed due to a lack of alternative analytical techniques and the fact that the binding site is not known (or not provided by the manufacturer). Despite considerable advances in mass spectrometry and liquid chromatography, protein bioanalysis by LC-MS remains challenging due to the fact that a given (set of) protein(s) needs to be detected in a sensitive and selective manner in a matrix of (hundreds of) thousands of other proteins. The task is further complicated by the fact that proteins are not very amenable to LC separation and that they generate complex mass spectra upon electrospray ionization (ESI), the most widely used ionization method for protein analysis by LC-MS, due to multiple charge states (so-called charge-state envelopes). Quantitative protein bioanalysis, notably in the area of biopharmaceuticals, would, however, benefit from analysis at the intact protein rather than at the peptide level, since protein species (also known as proteoforms) [11–18] should be separated from each other to facilitate the assignment of modifications to a given species. Despite these incentives, it is fair to say that protein bioanalysis is currently dominated by the bottom-up approach using so-called signature or proteotypic peptides as surrogates for the proteins of interest, since LC-MS analysis at the protein level is often not sensitive and specific enough.

This review discusses the challenges of quantitative protein bioanalysis by LC-MS at the protein level. We will notably address the possibilities and current limitations of protein sample preparation, separation by LC, the challenge of interpreting protein ESI-MS spectra and the options for protein quantification based on extracted ion chromatograms

or deconvoluted spectra. The possibilities of high-resolution mass spectrometry (HRMS) with respect to improving the signal-to-noise (S/N) ratio and the challenges of analyzing complex mass spectra will be highlighted based on examples.

5.2 SAMPLE PREPARATION: A CRITICAL STEP IN PROTEIN BIOANALYSIS

The bioanalysis, and notably the quantification, of therapeutic proteins (biopharmaceuticals) and macromolecular biomarkers in complex biological samples like serum or plasma requires dedicated sample preparation. Because of the often low concentrations of the protein analyte and the presence of many endogenous proteins that easily interfere in the LC-MS analysis, it is essential that the sample should be cleaned up and the protein(s) of interest enriched [19].

Enrichment strategies for intact proteins are typically based on selectively capturing the protein of interest with an affinity ligand such as an antibody, receptor or another affinity binder. More generic enrichment techniques, such as solid-phase extraction (SPE) using electrostatic or hydrophobic interactions, immobilized metal affinity columns (IMAC) or fractionated protein precipitation can also be applied but they require careful optimization based on the physical-chemical properties of the target protein to obtain sufficient selectivity [20].

Sample preparation for intact protein analysis by LC-MS, and specifically affinity-based enrichment, depends on the specificity of the affinity ligand. Monoclonal-, polyclonal- or engineered recombinant antibodies as well as biological receptors are widely used as capturing agents. For each type of ligand, it is important to know against which part of the protein analyte it is directed and which proteoform of the protein is captured, to allow proper interpretation of the results. For example, when using the biological receptor to capture a protein, it must be considered that only protein species that retain affinity for the receptor will be enriched, indicating that they still have at least some biological activity. Any proteoform of the protein that has undergone enzymatic (e.g. by proteolysis) or chemical modifications (e.g. by oxidation or deamidation) at the site of binding and, as a consequence, has lost its ability to bind to the receptor, will not be captured and thus escape analysis.

There is a growing number of affinity binders that are based on other protein scaffolds. Examples are DARPins, aptamers and affimers. DARPins (Designed Ankyrin Repeat

Proteins) are genetically engineered proteins typically exhibiting highly specific and high-affinity target protein binding [21]. They are derived from natural ankyrin proteins, one of the most common classes of binding proteins in nature. Affimers are affinity binders based on a structurally robust protease inhibitor scaffold (e.g. Cystatin A) [22,23]. Both types of binders are selected by phage display against the target protein and produced in an *E. coli* protein expression system. DARPins and affimers have a defined amino acid sequence with defined binding regions that are amenable to protein engineering (e.g. the insertion of a unique cysteine residue for immobilization in affimers). Multiple affimers may be used in a single assay to capture several proteins and to analyze them by LC-MS [24].

If a broad recognition of the different forms of a protein analyte is desired, it is sometimes advantageous to use polyclonal antibodies that recognize multiple epitopes. However, this may come at the price of more unspecific binding. As often is the case with complex analytical problems, there is no 'one size fits all' solution and complementary strategies may have to be used to get a comprehensive view of the species that are related to a given protein. An important parameter to be optimized during method development is the ratio of the carrier (e.g. the magnetic bead volume) to the amount of capturing affinity binder, which must be related to the estimated maximum protein concentration, to determine at which point all binding sites are saturated. Such 'titration experiments' prevent inaccurately low results at high analyte concentrations due to antibody saturation and competition between protein species for binding. In general, for all types of sample preparation approaches, it is critical to assess and ideally avoid non-specific binding of proteins to carrier materials to arrive at reproducible results with good recovery.

Affinity ligands can be coupled to polymer resins, magnetic beads, immobilized on 96-well enzyme-linked immunosorbent assay (ELISA) microtiter plates or on monolithic micro-columns. The coupling chemistry depends on the reactive groups on the carrier and the functional groups on the affinity ligands. It is beyond the scope of this review to cover this field completely, but a few examples will be described to delineate the principle. An antibody can, for example, be biotinylated using an N-hydroxysuccinimide biotin derivative that reacts with primary amino groups on lysine residues and the N-termini of the heavy and light chains. The biotinylated antibody can then be coupled to a streptavidin-labelled carrier, because of the strong interaction between biotin and streptavidin. When using an ELISA plate, there is a choice between unmodified and a variety of surface-activated microtiter plates. As in the case of setting up a regular sandwich ELISA assay, it is necessary to evaluate different types of ELISA plates for the best recovery and selectivity. There

are many examples where affinity-based sample preparation is used for protein analysis, although enrichment is typically followed by trypsin digestion and LC-MS analysis at the peptide level [25]. Kellie *et al.* described immunocapture to enrich a monoclonal antibody (mAb) from human plasma followed by digestion with IdeS (see later in this section for details about this approach) and reduction of the disulfide bonds [26]. LC-MS analysis on a C₄ reversed-phase column at 65°C allowed separation of the Fc/2, LC and Fd subunits. The LC subunit of the captured antibody was used as internal standard to correct for losses. The method was quantitative across the range of 0.5 – 10 µg/mL based on Extracted Ion Chromatograms (EICs) of the 20⁺ charge state. Other examples of intact protein bioanalysis are scarce, but many of the ‘peptide-based’ methods might serve as the basis for intact protein analysis by analyzing the proteins that are eluted from the capturing agents directly by LC-MS without prior digestion. Immunoaffinity-MS analysis of intact proteins has also been shown successfully in conjunction with matrix-assisted laser desorption ionization (MALDI) albeit for relatively small proteins [27–29].

Since protein A and protein G show affinity towards the constant part of human IgG, carriers can be coated with one or a combination of both proteins in order to immobilize capturing antibodies or to extract therapeutic mAbs. There are positive and negative aspects of this kind of sample preparation. Advantageous is that such methods can be applied to different types of proteins containing IgG-like Fc parts. They are robust, can be used to capture multiple therapeutic antibodies (or their protein species) in one analysis and are easy to transfer to 96-well plate formats. A negative aspect of using protein A and/or G is that they bind all human IgG molecules, of which there are many in blood serum or plasma, at a total concentration of 15 mg/mL, so that analysis at the protein level is generally not possible. In recent years, affinity enrichment has been shifting from manual sample preparation to automated platforms based on well-plate-, magnetic bead-, cartridge- or tip-based immunocapture platforms. Automation leads to improved precision, shorter sample preparation times and more robust methods, because samples can be processed (captured, washed and eluted) according to the same protocol and often simultaneously.

The affinity enrichment method described by Berna *et al.* [30] incorporates a sample preparation step using immunoprecipitation (IP) for quantitative protein analysis by LC-MS. IP was set up in a 96-well plate format using protein A/G to immobilize the capture antibody. The authors refer to this technique as immunoprecipitation in ELISA format or IPE. Proteins were eluted from the antibodies with 5% aqueous acetic acid, which is MS

compatible, so this method could also be used for intact protein analysis. This approach, with some modifications, was applied by Klont *et al.* [31], to enrich the soluble Receptor of Advanced Glycation End-products (sRAGE), a biomarker that is under investigation in Chronic Obstructive Pulmonary Disease (COPD), from serum and to quantify it by LC-MS at the sub-ng/mL level after digestion.

Reversed-phase SPE is commonly used for the enrichment of proteins between 10 and 35 kDa. With relatively small pore sizes of 80 – 130 Å (8 – 13 nm), the separation is not only based on hydrophobic interactions of the proteins with the stationary phase, but also on size-exclusion effects, which helps remove larger, highly abundant proteins like albumin or IgGs from serum or plasma, as they cannot penetrate into the pores. An example of reversed phase SPE for protein enrichment is the quantification of human growth hormone (approx. 22 kDa) in serum by Pritchard *et al.* [32]. These authors used a two-step reversed phase SPE process at high and low pH for enrichment at the intact protein level prior to tryptic digestion directly on the C₁₈-based SPE material. Monolithic SPE phases may be beneficial for protein extraction for several reasons. Monolithic column materials consist of a single piece of a highly porous structure that is silica- or polymer-based [33,34]. Due to the high porosity of the material and the large accessible surface area, binding of high-molecular-weight proteins is improved. Yang *et al.* [35] used monolithic C₁₈ SPE for quantification of PEGylated interferon alpha-2a (approx. 40 kDa) at the low ng/mL level in serum. These levels were achieved with LC-MS analysis at the peptide level, while the monolithic SPE step was performed at the protein level.

The use of IMAC-SPE during sample preparation is rather uncommon for protein enrichment, whereas it is widely used for the enrichment of phosphorylated peptides. Some proteins have a particularly high affinity for metal ions, notably for doubly or triply charged transition metal cations. Surface-exposed histidine residues are known to exhibit affinity for immobilized Ni²⁺, a feature that was used by Wilffert *et al.* [20] for the enrichment of recombinant human TNF-related apoptosis-inducing ligand (rhTRAIL) from serum. In analogy to the enrichment of phosphorylated peptides, IMAC is also used for the enrichment of proteins containing phosphorylated threonine, serine or tyrosine residues, which have a strong affinity for trivalent metal ions like Fe³⁺, Ga³⁺ and Al³⁺.

When it comes to mAbs, the most widely used class of biopharmaceuticals, there is a specific approach for bioanalysis at the protein domain level after digestion with IdeS (immunoglobulin-degrading enzyme from *Streptococcus Pyogenes*) [19-21]. IdeS is a cysteine protease that cleaves at the hinge region of all IgG subclasses. The enzyme is highly

specific and no other substrate besides IgG is known [36,37]. Digestion of IgG with IdeS generates a homogenous pool of $F(ab')_2$ and $Fc/2$ fragments and there is no 'over-digestion' or further degradation of the fragments as is often the case with other proteolytic enzymes.

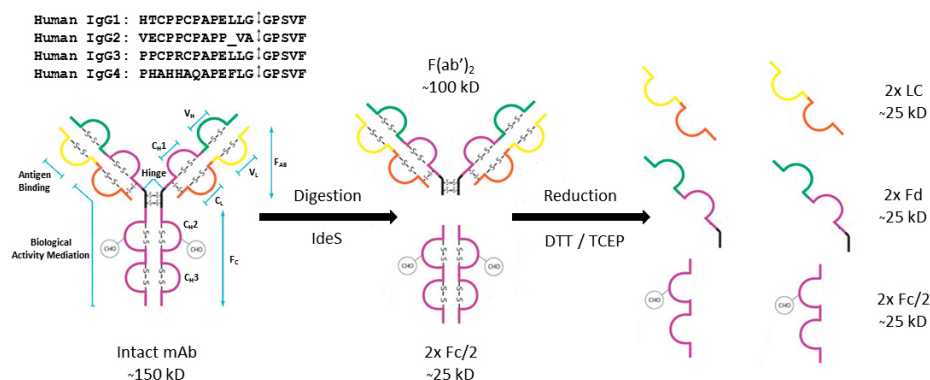


Figure 1: Schematic representation of the digestion of an antibody (IgG) with IdeS followed by reduction of disulfide bonds resulting in Fd' , LC (light chain) and $Fc/2$ fragments of approximately 25 kDa each.

Since the hinge region of IgG molecules is flexible and solvent-exposed, digestion is fast. Digestion of IgG using IdeS produces two identical mAb subunits that correspond to the constant region of the heavy chain and are called $Fc/2$, plus a larger domain that is referred to as $F(ab')_2$. This consists of the two light chains (LC) and the variable parts of the heavy chains that are interconnected via a number of disulfide bonds. Treatment with a reducing agent cleaves the disulfide bonds and converts $F(ab')_2$ into two light chains and two separate variable parts of the heavy chain, Fd (**Figure 1**). All subunits are approximately 25 kDa and thus more amenable to LC-MS analysis than the entire antibody, while still providing most of the molecular context for structural modifications.

The use of IdeS in the analysis and characterization of IgGs and fusion proteins at the protein domain level using liquid chromatography or capillary electrophoresis in combination with high-resolution mass spectrometry has been described in several reports, albeit primarily for pharmaceutical product control in samples of limited complexity [38–41]. An *et al.* [42] developed a method for the identification and routine monitoring of domain-specific modifications. Suitability of the methodology was demonstrated for a number of IgG subclasses (IgG1, IgG2 and IgG4), as well as for an Fc fusion protein. IdeS digestion was followed by reduction of disulfide bonds and subsequent analysis by LC-MS, capillary isoelectric focusing and glycan mapping to enable domain-specific profiling of oxidations, charge heterogeneity, and glycoform distribution. Leblanc *et al.* [43] used IdeS to study long-term storage stability of a proprietary mAb at 5°C. An aged mAb, stored

for nine years at 5°C and presenting a complex charge variant profile, was investigated by cation-exchange (CEX)-LC and high-resolution MS. Mobile phases consisted of 50 mM ammonium formate buffered with formic acid at pH 3.9 (Buffer A) and 500 mM ammonium acetate, pH 7.4 (Buffer B), resulting in both a pH and a salt gradient. Peptide mapping was subsequently used to localize modified sites and provide quantitative information. Results showed a remarkable consistency of the data. IdeS digestion has also been implemented for the comparison of originator mAbs and biosimilars. Pisupati *et al.* [44] demonstrated the utility of a ‘multiple-attribute monitoring’ workflow using Remicade (Infliximab) and its biosimilar Remsima as models. IdeS digestion was used to determine the intact masses of the resulting fragments in their fully glycosylated state, after deglycosylation and/or disulfide bond reduction. They concluded that the workflow effectively proved that the two antibodies were similar, yet not identical. Reported differences, related to the levels of charge variants attributed to C-terminal truncation and dimer formation, were ultimately deemed non-consequential. Wagner-Rousset *et al.* [45] described the development of a rapid analytical platform to assess charge variants of mAbs (acidic and basic species). The workflow was based on comparative analysis by CEX of intact IgGs versus F(ab)₂ and Fc domains generated by IdeS digestion. The analytical procedure was validated according to FDA and EMA guidelines in analogy to already approved mAb-based biopharmaceuticals. Functional assays and peptide mapping were performed to localize the modifications and assess their effect on biological activity. This approach can be used during the early stages of research and development of novel biopharmaceuticals to screen for and select optimized candidates by discriminating between critical and less critical charge variants, according to the CEX charge variant profiles of IdeS digested mAbs. This is an important feature since the identification of ‘hot spots’ is an important part in further (pre)-clinical development.

5.3 PROTEIN SEPARATION BY LIQUID CHROMATOGRAPHY

Liquid chromatography (LC) is one of the most powerful separation techniques and in combination with mass spectrometry is widely used in the field of bioanalysis. Due to their large size, intricate higher order structure and heterogeneity, chromatographic separation of proteins is extremely challenging. While sample preparation is a crucial and indispensable step to achieve sensitivity and selectivity in protein bioanalysis, it would not be possible to address protein heterogeneity to any appreciable extent without efficient LC separation prior to mass spectrometry. In the following, we will highlight some aspects of

column technology as well as operational variables of chromatographic protein separations related to intact protein bioanalysis. Many aspects were developed for the characterization of therapeutic proteins and have only been partially translated to their analysis in complex samples. This is one of the main challenges lying ahead for protein bioanalysis.

Pioneering work of the groups of Regnier, Hearn and others in the 1980s established that efficient protein separation requires chromatographic materials with large enough pores to allow access to the inner pore volume [46–53]. Insufficiently large pores lead to peak broadening due to slow mass transfer and may result in column fouling since not all proteins are eluted. A better theoretical understanding of protein separations by high-performance (HPLC) and later ultra-high-performance LC (UHPLC) led to the development of novel concepts, such as silica or polymer monoliths, with large, μm -sized flow-through pores and mesopores on the order of hundreds of nm allowing for efficient and rapid protein separation [54–59]. More recent developments in separation science based on the design and engineering of micropillar-containing columns instead of packed bed or monolithic materials hold promise that separation media for intact proteins can be designed based on fundamental chromatographic theory and nanoscale engineering [60–64]. While advances in protein separation by LC have been relatively slow over the last decades, we may be entering a new phase with breakthroughs ahead. As the following examples will show, such breakthroughs are sorely needed in order to advance LC separation of proteins to a level that is commensurate with the complexity of individual proteins such as biopharmaceuticals or biomarkers let alone with the complexity of entire proteomes. LC separation of intact proteins currently lags behind in separation power of two-dimensional gel electrophoresis, an approach that was developed in the 1970s, but which is cumbersome and not suitable for robust, quantitative protein bioanalysis.

Reversed-phase LC (RPLC) is one of the major analytical techniques used in the bioanalysis of proteins. RPLC as such is not ideal for protein analysis since the harsh mobile phase conditions and the elevated hydrophobicity of the stationary phase result in denaturation and may even induce protein precipitation or irreversible protein adsorption leading to poor recoveries and the loss of certain protein species. However, the wide range of stationary phases and notably the ease with which RPLC can be coupled to mass spectrometry counterbalance these disadvantages. Damen *et al.* [65] developed one of the first bioanalytical methods for the quantitative determination of intact trastuzumab, a monoclonal antibody for the treatment of metastatic breast cancer, by immunoaffinity enrichment followed by HPLC with fluorescence detection mainly based on Trp residues in

the protein. Gradient elution was applied at a flow rate of 0.5 mL/min through a 150×2.1mm ID column packed with a C₈ material with a particle size of 5µm and an average pore size of 300Å (30nm). The column temperature was 75°C and mobile phase A consisted of 0.1% trifluoroacetic acid (TFA) in water while mobile phase B consisted of 0.1% TFA in a mixture of isopropanol-acetonitrile-water (70:20:10)). Coupling the LC separation to mass spectrometry resulted in insufficient sensitivity, indicating that efficient ionization of intact proteins is challenging. The authors suggested two reasons explaining the loss of sensitivity. Firstly, the high viscosity of the mobile phase as a result of isopropanol presence negatively affected spray performance. Secondly, the presence of TFA as ion pairing agent in the mobile phase led to ionization suppression. Thus, the authors decided to discontinue the use of mass spectrometry and switched to fluorescence detection. To prove the selectivity of the LC separation, trastuzumab was mixed with other therapeutic mAbs like adalimumab, bevacizumab, and rituximab. All components of the mixture were separated well. A number of limitations of this approach are obvious. First, fluorescence detection does not allow to gather chemical information from the analytes, such as molecular mass, or elucidate potential sources of heterogeneity. Second, while more sensitive than mass spectrometry, in this particular case, intrinsic Trp fluorescence is not very strong resulting in a limit of detection on the order of 5 µg/mL. While this is sufficient for highly dosed monoclonal antibodies like trastuzumab, it is insufficient for many other biopharmaceuticals and for most biomarkers. This is also due to the fact that almost every protein contains Trp, which results in a considerable background signal (**Figure 2**). Mass spectrometry and notably high-resolution mass spectrometry allows more specific detection of proteins based on EICs with narrow mass extraction windows (MEWs) (see later in this article). However, the efficient ionization of proteins in their intact form remains a considerable challenge.

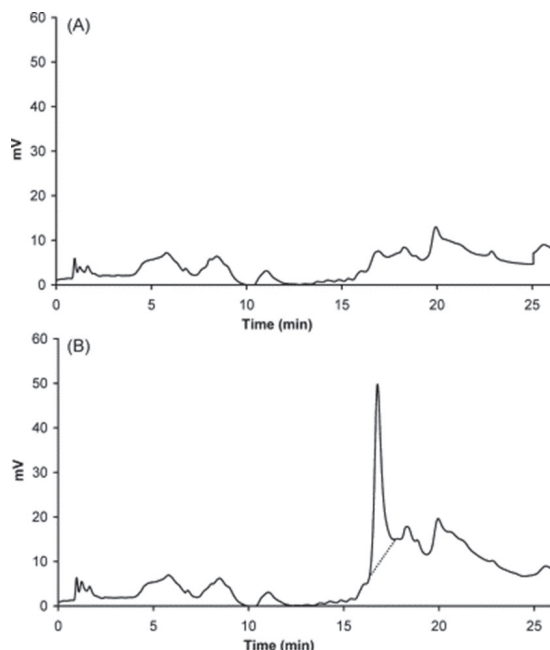


Figure 2: Chromatograms of blank serum (A) and trastuzumab-spiked serum at the LLOQ (5 $\mu\text{g/mL}$) (B) after immunoaffinity enrichment using anti-trastuzumab idiotype antibodies. The retention time of trastuzumab is around 16.8 min (reproduced from Damen *et al.* 2009 with permission, copyright Elsevier).

Another interesting feature of protein RPLC is that elevated temperatures lead to much improved separations. While this is a general phenomenon in LC, since the viscosity of the mobile phase decreases with increasing temperature, it is particularly striking for proteins. In their study of intact protein bioanalysis by high-resolution full scan mass spectrometry, Ruan *et al.* [66] used human lysozyme as a model protein to evaluate the effect of different column temperatures. While chromatography at room temperature resulted in a broad peak with poor peak shape, increasing the column temperature to 70°C gave a narrow, symmetrical peak. The fact that different interchanging protein conformations may result in broad, asymmetric chromatographic peaks was already studied by Cohen *et al.* [67] in the 1980s, who reported that raising the column temperature is important for reducing the number of protein conformers (most likely by denaturing the protein into its unfolded state) and hence reducing peak broadening. Elevated column temperature is thus considered essential for efficient protein separation and notably for the separation and recovery of hydrophobic proteins and peptides. It can be concluded that sharp peaks at high temperatures are due not only to an increase in column efficiency but also due to reducing the number of conformational states of a given protein.

An acidic ion-pairing agent is typically added to the mobile phase of RPLC separations of peptides and proteins to improve chromatographic performance. TFA, at a concentration of 0.05-0.1% is widely used for this purpose since its introduction by Bennett *et al.* in 1977 [68] and further studies by Pearson *et al.* [69] TFA reduces peak broadening and tailing since it binds to and neutralizes positively-charged amino acids thereby reducing interactions with silanol groups on the stationary phase. TFA and its less widely used longer chain analogue heptafluorobutyric acid (HFBA), further improve solubility and strengthen the interaction with the hydrophobic stationary phase. While less effective in improving chromatographic separation efficiency, formic acid (FA) has gained in popularity for LC-MS separations of proteins and peptides, since TFA suppresses ion formation in the electrospray source. Jian *et al.* [70] established a workflow for the absolute quantitation of large therapeutic proteins in biological samples at the intact level by LC-HRMS. The authors used FA as a mobile phase additive rather than TFA, despite the fact that FA gave broader peaks, in favour of maximizing signal intensity. Somsen *et al.* [71] showed recently that the ionization suppression effect of TFA may be counterbalanced by adding a dopant gas to the electrospray interface. While this option is not available in all mass spectrometers, it is of interest to note that LC separation efficiency, which is better with TFA as ion pairing agent, may not have to be compromised in favour of a strong ESI-MS signal.

In the recent past, wide pore (>300 Å) core-shell particles have been developed for the separation of proteins [72,73]. Core-shell particles, also called superficially porous particles, have a porous shell on top of a non-porous core resulting in a material with an efficiency that is comparable to particles of smaller diameter due to the shorter diffusion path length, resulting in fast mass transfer while producing less backpressure than UHPLC-type particles (1.7-1.8 µm diameter). Todoroki *et al.* [74] used a wide-pore core-shell RPLC column at 70°C for the separation of purified mAbs as sharp peaks within 20 min. This approach was developed into a bioanalytical method for the quantification of bevacizumab and infliximab in human plasma by a combination of immunoaffinity enrichment, high-temperature RPLC and fluorescence detection.

Organic polymer-based monolithic columns emerged as an alternative to silica-based stationary phases for rapid and efficient biomolecule separation. A monolith is a cylindrically shaped polymer that contains a continuous and interconnected network of pores (channels). The first monolithic stationary phases were based on polymethacrylate

or polystyrene-divinylbenzene in large inner diameter columns [75]. Nowadays, a wide variety of monomers is available for the preparation of polymer-based monoliths [75–77]. Polymer monoliths are stable at elevated column temperatures and across a broad pH range.

The porosity of polymers is a macromolecular characteristic that can be controlled by varying the composition of the polymerization mixture and the reaction conditions, such as polymerization temperature and time [77]. Most monolithic columns developed so far feature hydrophobic reversed-phase functionalities, because RPLC is generally regarded as the most effective separation mode. However, the wide variety of functional and cross-linking monomers allows the creation of monoliths carrying the desired surface chemistry to achieve LC separations in different modes. An example is an ion-exchange column based on a polymer monolith [78].

Monolithic materials are well-suited for the design of miniaturized columns [75]. The robustness of such columns can be increased via covalent linkage of the monolith to the inner capillary wall. Lanshoeft *et al.* used a 1 mm × 250 mm polymer-based monolithic column to develop an immunoaffinity enrichment, LC-HRMS workflow for quantification of a hlgG1 at the intact protein level in rat serum [79]. The column was based on an ethylvinylbenzene-divinylbenzene copolymer and the column temperature was raised to 70°C for better separation and peak resolution.

Recently, Jin *et al.* reported a method for the quantitation of an intact antibody-drug conjugate (ADC), trastuzumab emtansine, in rat plasma [80]. Both trastuzumab and trastuzumab emtansine eluted at very similar (almost identical) retention times. The broader chromatographic peak for trastuzumab emtansine as compared to trastuzumab indicated some separation of species with different drug-to-antibody ratios (DARs). According to mass spectrometric analysis, the authors observed that lower DAR species eluted first and higher DAR species later when a shallow gradient was used. Since the attached drug (maytansinoid) is hydrophobic, the hydrophobicity of trastuzumab emtansine increases with the number of attached drug molecules resulting in the observed elution order. Determining the average DAR is a critical quality attribute (CQA) for ADCs and elucidating the distribution of species with different DARs is important to ensure consistent quality and notably efficacy of the conjugates. However, for LC-MS quantitation and DAR distribution studies, chromatographic separation of different DAR species was not sufficient, so the authors had to rely on the resolving power of HRMS and the spectral deconvolution software to distinguish different DAR species.

Size exclusion chromatography (SEC), ion exchange chromatography (IXC), hydrophobic interaction chromatography (HIC) as well as hydrophilic interaction chromatography (HILIC) are all used in the quality control of therapeutic proteins during manufacturing. It would go beyond the scope of this review to discuss each of them in detail, so we will only present a few examples. The reader is referred to the cited literature for further details.

Size exclusion chromatography (SEC) is particularly suitable to address the question of protein aggregation during manufacturing and storage [81,82]. While there have been reports that SEC can be coupled to MS, this is not routine because, unless non-volatile buffer components are used, SEC is not compatible with online coupling to MS. It is, however, possible to collect fractions, desalt the proteins and analyze them by MS. Both anion- and cation-exchange chromatography (IEX) are widely used for the purification as well as for the analysis of proteins. IEX is particularly suitable for charge-variants, notably due to deamidation [83,84] and has been coupled online to MS for the characterization of therapeutic proteins [85]. Hydrophilic interaction chromatography (HILIC) operates on the basis of hydrophilic interactions between the analytes and the stationary phase, which is more hydrophilic than the mobile phase. An inverse gradient of organic solvent is used for elution, which makes HILIC highly complementary to RPLC. Recent work by Somsen *et al.* [71] showed that HILIC can be coupled online to MS and that different glycoforms of intact proteins can be efficiently separated in this way. Hydrophobic interaction chromatography (HIC) is primarily used as a preparative chromatographic method to purify proteins under native conditions [86]. However, HIC in conjunction with volatile buffer and salt components has recently also been coupled to MS [87]. Whether this will develop into a widely used, robust approach remains to be seen.

The field of high-resolution protein separation by chromatography has not advanced as much as that of high-resolution mass spectrometry, since its inception in the 1980s. This has greatly hampered our current understanding of protein heterogeneity and its implications for protein function. While the challenges are immense and possibly bigger than in the field of MS, it is good to see that the growing field of biopharmaceuticals has revived this area of research and that fundamentally new approaches, such as nanoengineered chromatographic columns, are being developed to advance the field [88].

5.4 PROTEIN MASS SPECTROMETRY

Mass spectrometers, especially the widely used triple quadrupole instruments, initially focused on the analysis of small molecules. More recent developments and advances in the field of HRMS have opened new possibilities in the field of protein analysis. Most commonly used HRMS-systems are based on quadrupole time-of-flight (QTOF) and Orbitrap mass analyzers combined with ‘soft ionization’ modes like electrospray ionization (ESI) and matrix-assisted laser desorption ionization (MALDI). While ionizing large macromolecules is a challenge in itself, it is further difficult to steer heavy ions through the mass analyzers and the ion optics to the detector resulting in low ion transmission when compared to small molecules and peptides. Advances in hardware and operating conditions (e.g. residual pressures in different sections of the instrument) have improved the capability of QTOF and Orbitrap MS systems to handle higher masses enabling the analysis of intact antibodies and even viruses. The coupling of ion mobility with mass spectrometry has allowed the separation of ions on the basis of charge and shape inside the mass spectrometer adding another dimension to HRMS systems.

ESI and MALDI can generate intact gas-phase molecular ions from hundreds to millions of Daltons. MALDI relies on ion generation upon irradiation of a light-absorbing matrix in which the proteins are embedded. While the mechanism for ion formation is still not fully understood, the process entails evaporation and activation of the matrix by a laser, generating a plume of hot gas containing ionized matrix ions, which in turn ionize the proteins. MALDI mass spectra of proteins predominantly show singly-charged ions and, to a lesser extent, doubly and triply charged ions. This low degree of charge distribution has the advantage of producing less complicated mass spectra compared to ESI, which makes interpretation easier. MALDI is, however, prone to ion suppression and cannot be easily coupled to LC. It is also difficult to combine MALDI of high-molecular weight molecules with commonly used mass analyzers like ion traps, triple quadrupoles or orbitraps, since ions of increasing mass carrying only a single charge are very difficult to trap efficiently in the quadrupole or orbitrap field regions.

ESI is based on an electrical potential that is applied to the ESI-needle in the source of the MS. This causes a build-up of positive or negative ions, depending on the ionization mode (positive or negative), at the tip of the needle [89–91] leading to the production of charged droplets carrying the proteins. While the droplets evaporate under elevated temperature, the ions inside the decreasing volume of the droplet cause electrostatic

repulsion leading to droplet fission, ultimately yielding gas-phase ions. ESI produces mass spectra with multiple charge states, varying from a few to tens of charges per ion, giving a so-called charge state envelope. The width of the envelope is influenced by the state (unfolded / partially folded or folded) of the protein in the liquid phase as well as by the energy the ions receive in the interface of the ESI source. Folded proteins are more compact and the interior amino acids are less prone to be charged than amino acids at the surface of the protein. Thus unfolded proteins tend to have broader charge state envelopes with a higher average number of charges [92]. A wide envelope has the disadvantage that the intensity of the signal is dispersed over many charge states, leading to a loss of sensitivity. In addition, each molecular ion in the envelope is divided into species with a different mass due to the occurrence of natural heavy isotopes such as ^{13}C , the so-called isotopologues. The signal for large proteins with many isotopologues is thus spread out over even more ions, leading to a further loss in sensitivity. With increasing number of charges, the isotopologue peaks within one charge state will be spaced ever more closely ultimately merging into a single peak whose width is determined by the isotopologue cluster. The charge state envelope can be modified by adding chemicals [93], so-called superchargers, to the LC-flow (e.g. post-column) [94] or to the gas-phase of the ESI source [95]. While these chemicals were first used in the field of peptide analysis [96], they have also been applied for intact protein analysis [93–95,97,98]. Super-charging shifts the charge state envelope to higher charge values, thus lowering the m/z ratios. This improves ion transmission and brings the m/z values within the range of most commonly used mass analyzers (notably quadrupoles). Reducing the width of the charge state envelope may also increase sensitivity by collecting more ions per charge state resulting in an increase in peak intensity. **Figure 3** shows the shift in the charge state envelope of recombinant human growth hormone (rhGH) upon addition of meta-nitrobenzylalcohol (m-NBA), a supercharging agent, to the mobile phase after the chromatographic separation. In the lower trace (magenta) of **figure 3** it is noticeable that the sensitivity of rhGH is increased besides shifts in the charge state envelope. However, this is also the case for the background and signals arising from possible co-eluting adducts (Na^+ and K^+). There should thus be a thorough investigation of the effect of supercharging on the S/N ratio, especially near the lower limit of quantification.

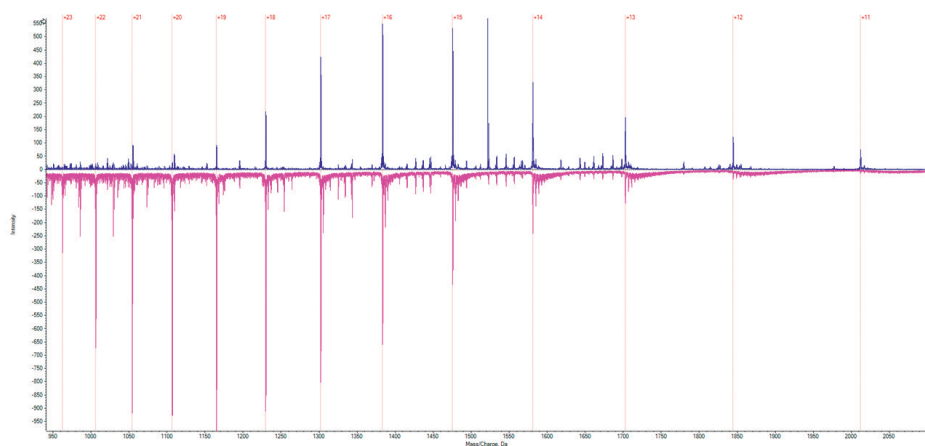


Figure 3: Shift of the charge state envelope for recombinant human growth hormone (rhGH) to higher z values upon addition of metanitrobenzylalcohol (NBA) to the mobile phase after the chromatographic separation. Upper trace (blue); no addition of NBA; Lower trace (magenta); with post-column addition of 0.16% (v/v) of NBA.

The field of super-charging is still in its infancy and it remains to be seen whether other additives or other means of doping the electrospray to increase the average charge state and to reduce the width of the charge state envelope will lead to more sensitive and possibly more selective detection of intact proteins upon LC-MS. An attractive option was recently shown by Somsen *et al.* [71], who doped the gas phase in the ion source rather than the mobile phase of the LC separation. While the main goal of these authors was to reduce the ionization suppressive effect of TFA, they also observed that adding 1% propanoic acid to the drying gas increased the charge state and reduced the number of TFA adducts. This approach merits further study, since it allows to affect the charge state envelope without interfering with the chromatographic separation.

Another way of reducing the width of the charge state envelope is to use so-called ‘native mass spectrometry’, meaning mass spectrometry under conditions that do not denature proteins or that denature them only partially [99–101]. As the protein maintains (part of) its 3-dimensional structure, it acquires fewer charges through protonation or the association with other cations. This facilitates the resolution of proteoforms in the m/z domain in contrast to supercharging, which puts more demands on the resolution of the mass analyzer. However, native mass spectrometry places considerable constraints on the mobile phase conditions for the LC separation, the instrumental set-up and the conditions for effective ion transmission (e.g. potentials and residual pressures). LC-MS under ‘native’ conditions is thus currently not as sensitive as LC-MS under denaturing conditions.

Considering that efficient protein separation by LC requires elevated temperatures, complicates the application of native MS to the bioanalysis of proteins and notably protein species. Native mass spectrometry is thus mainly used for product characterization when a large amount of purified therapeutic protein is available for analysis [43,102–107]. Since most proteins (e.g. mAbs) acquire their specificity due to a well-defined 3-dimensional structure [108], it is conceivable that native LC-MS may also be used to distinguish biologically active forms of a protein from inactive forms (e.g. when combined with the results of activity assays). This makes native LC-MS a subject that is worth exploring further for the bioanalysis of protein species and more generally to investigate protein-protein and protein-small molecule interactions.

Recently the use of ion mobility spectrometry (IMS) has entered the field of protein analysis [104,106,109–111]. IMS may be described as ‘gas-phase electrophoresis’ and introduces an extra separation dimension after the LC separation and ahead of the actual mass analyzer. Separation is based on the physical characteristics of proteins such as lipophilicity, shape and charge [112]. The mobility of ions along the IMS cell is based on the number of interactions with the neutral gas under the influence of a potential gradient, which slows the ions down. Within a single charge state, folded proteins drift faster than unfolded proteins because they experience fewer interactions with the buffer gas, and thus have a smaller collisional cross-section. Within a single charge state, folded proteins drift faster than unfolded proteins because they experience fewer interactions with the buffer gas, and thus have a smaller collisional cross-section. The most widely used types of IMS cells are drift tubes, the field asymmetric wave ion mobility cell [113] and the traveling wave IMS (T-Wave). In the first technique, the proteins move in the drift tube under the influence of a constant electrical field, while the second technique uses electric fields modulated by radio frequencies that are produced by coils. T-Wave IMS utilizes non-uniform, moving electric fields / voltage pulses to push ions through a neutral buffer gas. Species with high mobility (lower collisional cross-section) surf more on the wave front and are overtaken by the wave less often than species of low mobility (higher collisional cross-section). At present, IMS is predominantly used for biopharmaceutical product characterization and to evaluate disulfide bond heterogeneity, conjugation heterogeneity (e.g. in ADCs), analysis of protein aggregation and global conformational changes [114–120]. It must be noted that gas phase conformations (evaluated by IMS) may be related, but are not identical to solution-phase conformations. A topic that requires further investigation and which is of utmost interest for the field of ‘native’ mass spectrometry. Another caveat

of IMS is currently that it decreases ion transmission and thus sensitivity considerably, which may be one reason why it is not commonly used.

5.5 PROCESSING AND ANALYSIS OF INTACT PROTEIN LC-MS DATA

LC-MS analyses of intact proteins produce complex raw data consisting of retention times, peak heights or areas and m/z ratios. Since most proteins do not exist as single molecular entities, each protein species gives rise to a slightly different charge state envelope. The fact that many protein species are not chromatographically resolved results in overlapping charge state envelopes, each with their isotopologues distribution. To complicate matters further, proteins often form non-covalent adducts with cations such as Na^+ or K^+ , which adds to the complexity of the resulting ESI-MS spectra. Together, this makes conversion of the information provided in the ESI-MS raw data into simple readouts, such as the amount or concentration of a given protein species or its molecular mass, rather difficult. Examples of the mass spectrometric output for proteins of increasing molecular mass are shown in **Figure 4**.

For a relatively small protein such as IGF-1 (molecular mass of 7.5 kDa, **Figure 4A**), the number of charge states is limited to just a few. As mass increases, proteins acquire more and more charges (**Figures 4B and C**) so that for a complete mAb such as trastuzumab (mass of around 150 kDa, **Figure 4D**), more than 40 different charge states can be formed during ESI, with the number of charges varying from around 30 to over 70. **Figure 4** also shows that for smaller proteins the isotopologues of a given charge state can be resolved in a TOF mass analyzer with a resolution of 30,000. For proteins with masses of more than 25 kDa, the resolution of this mass analyzer is insufficient to resolve the isotopologues and a mass spectrometer with a considerably higher resolution would be needed for a complete separation of their signals.

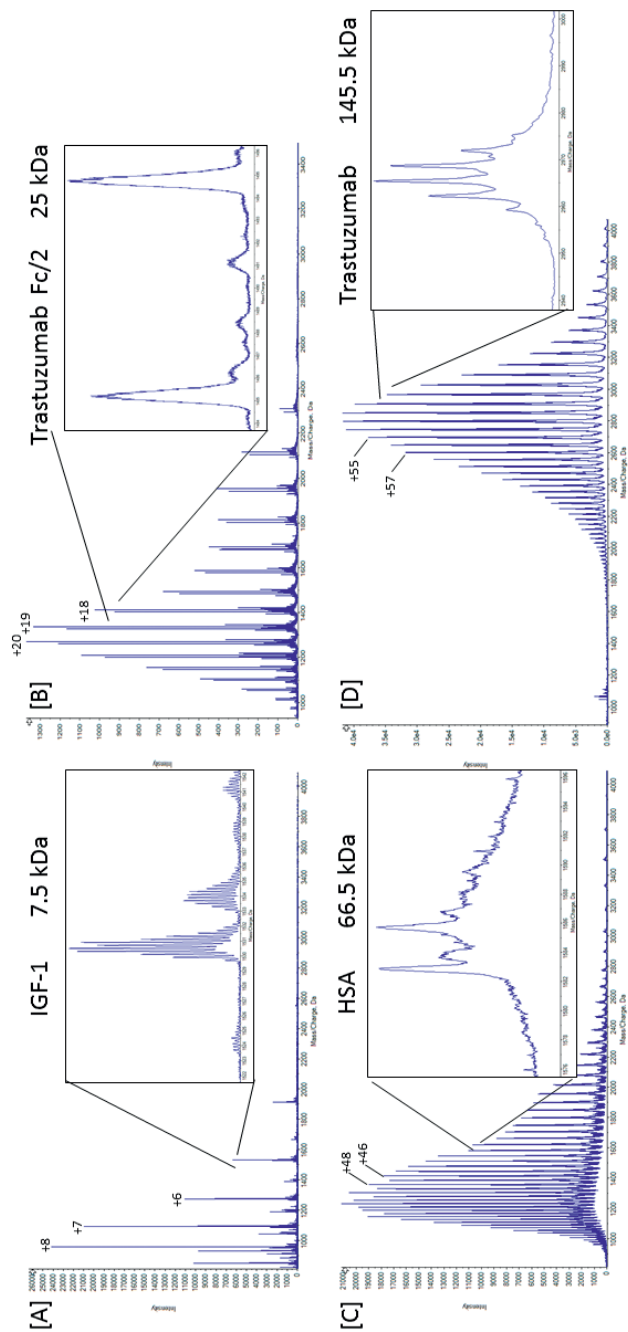


Figure 4: Charge state envelope of IGF-1 (A), the Fc/2 part of trastuzumab (B), human serum albumin (C) and trastuzumab (D) with a zoom into one charge state, as indicated in the figure (data acquired with a QTOF mass spectrometer at a resolution of 30,000). While the isotopologue cluster of IGF-1 is still resolved, this is no longer the case for the larger proteins. The zoom spectra indicate the presence of different protein species.

Typically, for each data point in a chromatogram a full mass spectrum is acquired, containing the response of all ions corresponding to the various charge states of a protein that elutes at the particular retention time. An EIC is then constructed by defining a small MEW around the m/z value that corresponds to the ion of interest. As an example, **Figure 5** shows an EIC of the 20^+ charge state of the Fc/2 fragment and the 44^+ charge state of the $F(ab')_2$ of 1 $\mu\text{g/mL}$ of trastuzumab, after immunoaffinity enrichment from human plasma and IdeS digestion. Increasing the width of the MEW may be beneficial, as a larger number of analyte ions will be detected, and the sensitivity therefore improved. At the same time, it may also result in the co-extraction of ions from interfering matrix proteins that elute at the same time and have an m/z value close to the protein of interest [121]. Alternatively, it is possible to select only one of the most abundant charge state ions for quantification and to optimize the width of the EIC extraction window in order to reach an optimal S/N ratio. Ruan *et al.* [66] showed that by selecting the most abundant charge state of lysozyme, it is possible to improve the S/N ratio from 12 to 40 upon reducing the MEW from 0.5 m/z to 10 ppm.

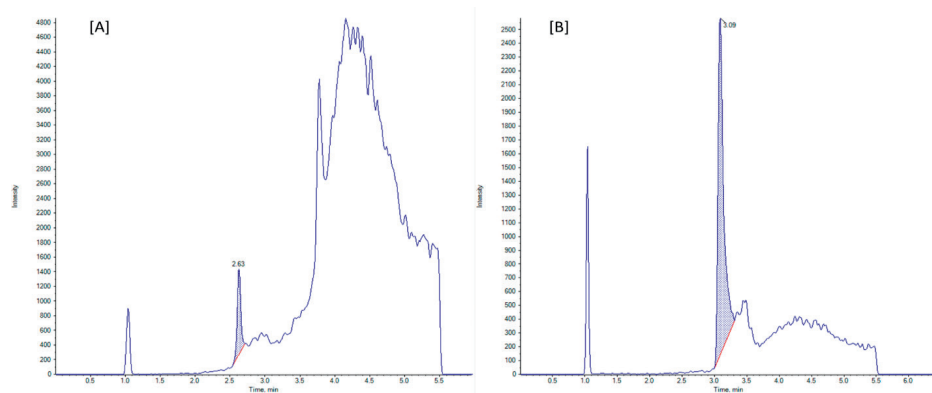


Figure 5: LC-MS chromatograms (EICs) of 1 $\mu\text{g/mL}$ trastuzumab in rat plasma, after immunoaffinity enrichment using the HER2-receptor as capturing agent and IdeS digestion. (A) the 20^+ charge state of the Fc/2 fragment (2.63 min) and (B) the 44^+ charge state of the $F(ab')_2$ fragment (3.09 min). Separation was by reversed-phase LC on a C_4 column at 80°C and detection on a QTOF mass spectrometer at resolution 30,000. The MEW used was 0.5 m/z units.

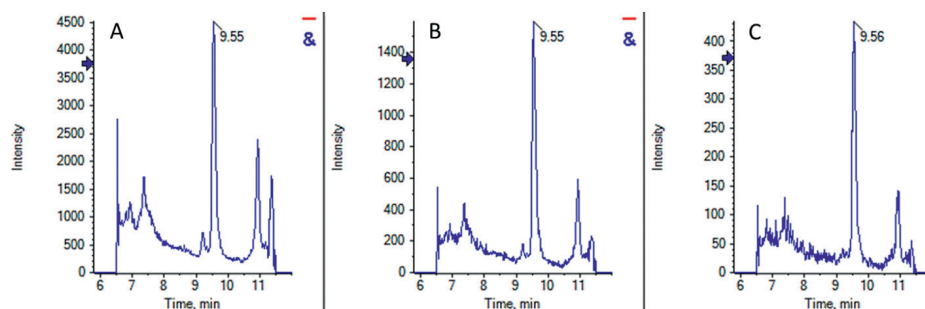


Figure 6: LC-MS chromatograms (HRMS) of 10.0 ng/mL of recombinant human growth hormone after immunoaffinity enrichment from rat plasma. EICs for the 15⁺ charge state were recorded with an MEW of 1.0 Da (A), 0.25 Da (B) or 0.0625 Da (C).

Figure 6 shows the effect of decreasing the MEW from 1.0 Da (entire 15⁺ charge state) to 0.25 Da and ultimately to 0.0625 Da (1 isotope of the 15⁺ charge state isotope cluster) for the 15⁺ charge state of recombinant human growth hormone (rhGH) after enrichment from rat plasma. The results show that decreasing the EIC extraction window does not lead to significant improvements in S/N ratio in this case and while the absolute signal intensity decreases, the selectivity increases due to less interference. It has to be noted, that adjusting the EIC extraction window may improve the S/N ratio in other cases depending on the nature of the background.

Simplifying protein ESI-MS spectra based on the deconvolution of each charge state envelope into a single peak giving the average molecular mass of the protein (or protein species) is an attractive approach. The mathematical process of converting the measured m/z values into molecular masses starts with assigning a charge state to a given ion. This can be achieved based on the knowledge (assumption) that two neighbouring peaks from the same protein molecule are separated by a single charge and that this charge is due to the attachment of a hydrogen cation (also called a ‘proton’ or simply an H^+ ion). If this assumption is correct, one can use simple algebra to define the charge state of a given protein ion in a charge state envelope (see **Box 1**).

Box 1: Example of a calculation to derive the molecular mass of the Fc/2 fragment of trastuzumab (after IdeS digestion).

Figure 4 shows the ESI spectrum of the Fc/2 part of trastuzumab. To determine the charge state of the ion at 1262.5632 (P_1), we consider that the following peak at 1328.9577 (P_2) has one H^+ less and that $z_1 - z_2 = 1$. The mass difference between the two protein ions is thus 1,00794 amu (atomic mass units), the mass of an H^+ ion. This knowledge allows us to calculate the charge state of P_1 and from thereon to derive all other charge states based on the assumption that each consecutive peak towards increasing m/z values in the spectrum is due to the loss of one H^+ ion. From the measured data we derive:

$$P_1 = m/z_1 = 1262.5632 \text{ and } P_2 = m/z_2 = 1328.9577$$

From the assumption that each charge state is due to a difference in one H^+ ion, we derive:

$$z_1 - z_2 = 1 \quad \text{or} \quad z_1 = z_2 + 1$$

Thus: $m = M - z \cdot H^+$; with m being the molecular mass of the protein and M the molecular mass of the respective molecular ion of charge state z .

Referring back to the measured values P_1 and P_2 results in:

$$P_1 = M - z_1 \cdot H^+ / z_1 \quad \text{or}$$

$$P_1 = M - (z_2 + 1) \cdot H^+ / z_2 + 1 \quad \text{and}$$

$$P_2 = M - z_2 \cdot H^+ / z_2$$

Resolving these equations with respect to M gives:

$$P_1 \cdot z_1 + z_1 \cdot H^+ = M \quad \text{and}$$

$$P_2 \cdot z_2 + z_2 \cdot H^+ = M$$

Which can be rearranged to:

$$P_1 \cdot z_1 + z_1 \cdot H^+ = P_2 \cdot z_2 + z_2 \cdot H^+ \quad \text{or} \quad P_1 \cdot z_1 + z_1 \cdot H^+ = P_2 \cdot (z_1 - 1) + (z_1 - 1) \cdot H^+$$

Resolving the equation on the right with respect to z_1 gives:

$$z_1 = - (H^+ + P_2) / P_1 - P_2$$

This allows to calculate the number of charges z_1 based on the measured values of P_1 and P_2 .

Inserting the measured values and using the known mass of the H^+ ion of 1.00794 gives:

$$z_1 = - (1.00794 + 1328.9577) / 1262.5632 - 1328.9577 = 20.03, \text{ which is close to } z_1 = 20, \text{ as charge states can only acquire integer values.}$$

With $z_1 = 20$, we can now calculate the approximate molecular mass of the Fc/2 fragment of trastuzumab as:

$$M + 20 \cdot H^+ / 20 = 1262.5632 \text{ or } M = 1262.5632 \cdot 20 - 20 \text{ or } \mathbf{M = 25231.26 Da}$$

The same calculation for $z_2 = 19$ gives:

$$M + 19 \cdot H^+ / 19 = 1328.9577$$

$$\text{or} \quad M = 1328.9577 \cdot 19 - 19 \quad \text{or} \quad \mathbf{M = 25231.20 Da}$$

Both values are quite consistent and correspond closely to the expected mass of 25232.0 Da. By going through the entire charge state envelope in this manner (using a computer algorithm), we get a list of calculated molecular masses that differ slightly from each other giving an average value with an estimate of the measurement error.

To calculate molecular masses from charge state envelopes, algorithms based on different principles have been developed. The so-called 'Maximum Entropy (MaxEnt)'-based approach, which forms the basis of most commercially available software packages, tries to take peak broadening effects, due to unresolved isotopes and limited resolution of the mass analyzer, into account thereby improving the original quality of the spectrum

(higher resolution and reduction in noise). The MaxEnt program, as developed by Skilling *et al.* [122] processes different *in silico* generated trial spectra and compares them to the observed spectrum. Once a predefined level of convergence has been reached, trial spectra that agree with the original data compose the final probability distribution of spectra in m/z scale. The spectrum with the highest entropy, the MaxEnt spectrum, is chosen as the most probable representation of the original data. The width of the probability distribution reflects the uncertainty of the MaxEnt result, which is presented in form of error bars. Since peaks in an ESI-MS charge state envelope are intrinsically connected (see Box 1), this criterion is used to qualify the MaxEnt spectrum, as it must explain the entire charge state envelope above a pre-defined threshold across the selected m/z range. However, the MaxEnt algorithm does not need to assign a specific charge state to a given peak to start with. It rather uses all of the information to connect 'peaks that belong together'. It is noteworthy to mention that considerable improvements in mass accuracy and resolution of modern mass analyzers facilitate accurate deconvolution of ESI-MS spectra even for large biopharmaceuticals, such as monoclonal antibodies [70]. However, they do not take all of the caveats away. That is why further developments in both mass spectrometry (e.g. reducing the number of charges per protein ion by 'native' mass spectrometry) and algorithms are ongoing [99].

Figure 7 shows the results of deconvoluting the charge state envelope of the Fc/2 subunit of trastuzumab using a maximum-entropy-based algorithm. While the deconvoluted mass (25231.6) of the left major peak corresponds closely to the expected mass of 25232.0 Da of one glycoform of trastuzumab (Fc/2 G0F) with the loss of a Lys residue from the C-terminus, there are other smaller signals that indicate additional protein species or non-covalent adducts (see insert). It is currently still under investigation whether this kind of transformation results in valid quantitative data [70].

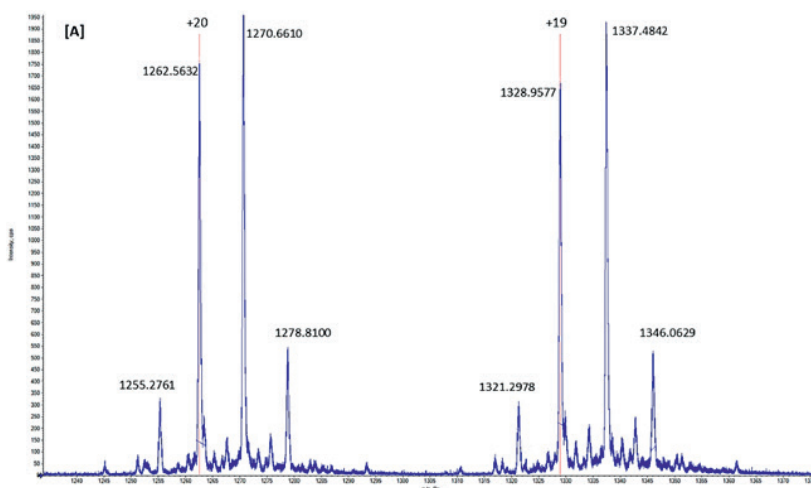


Figure 7: Deconvolution of the charge states 20⁺ and 19⁺ of the Fc/2 fragments [A] of trastuzumab after IdeS digestion using a maximum entropy-based algorithm [B] integrated into proprietary software (SCIEX).

While deconvolution makes subsequent data analysis and quantification considerably easier, it is prone to artefacts. Mathematical deconvolution algorithms may introduce bias and errors and may not give an accurate reflection of the intensity of the original signals. The result of such a deconvolution process depends further on the chosen parameters such as peak width, signal threshold and the chosen m/z range. Deconvolution of charge state envelopes from ESI-MS spectra of different protein species requires their chromatographic separation or, if this cannot be achieved, sufficient resolution of the mass analyzer to resolve the charge state envelopes in order for the algorithm to assign different deconvoluted signals to each form. The occurrence of non-covalent adducts (e.g. Na⁺ or K⁺), which is quite common in protein ESI-MS spectra, as well as modifications resulting in small mass differences (e.g. due to deamidations) may confound the deconvolution algorithm leading to artefacts with incorrect mass and peak heights or areas. The use of deconvolution algorithms in regulated, quantitative bioanalysis thus represents a considerable challenge.

5.6 CONCLUSIONS AND FUTURE OUTLOOK

The analysis of intact proteins by LC-MS receives considerable interest from industry and academia alike. After initial breakthroughs in the 1980s due to improved chromatography materials (e.g. wide-pore silica beads) and due to a better understanding of the

chromatographic separation of macromolecules from a theoretical point of view, there were many years of little progress in this field. The emergence of recombinant proteins as therapeutic drugs and their increasing relevance from a medical as well as from a commercial point of view, has created renewed interest and led to improvements of protein separations by LC (e.g. based on core-shell particles and monoliths) in conjunction with tailor-made surface chemistries in combination with high-resolution mass spectrometry. Ongoing development of HRMS-systems and new affinity agents will aid in studying *in vivo* protein biotransformation in greater detail possibly leading to a better understanding of how this affects therapeutic efficacy.

Efficient separation of proteins by (U)HPLC has turned out to be a much more difficult task than initially anticipated. The low diffusion coefficient of proteins results in slow mass transfer kinetics and the possibility to assume multiple interchanging conformations has rendered efficient chromatographic separations more challenging than for peptides. New developments in the field, for example, the emergence of columns containing nanoengineered micropillars, hold promise of improving analytical protein separations, but we must remember that the fundamental physical properties of proteins cannot be changed. They will define the limits of protein separations by liquid chromatography.

In this review, we have given an overview of the area of intact protein (bio)analysis by LC-MS starting with the challenges of sample preparation and ending with the deconvolution of highly complex mass spectra after electrospray ionization. We notably focused on the LC-MS analysis of intact proteins in biological matrices, an area that is in its infancy but that is instrumental for the further development of therapeutic proteins, for the detailed characterization of biomarkers and for biological and biomedical research in general. While there is still a long way to go until LC can rival two-dimensional gel electrophoresis with respect to intact protein separation, the payback for advances in this area will be large, since protein heterogeneity, for example due to post-translational modifications, is inherent to the way how nature modulates the biological activity of proteins and of biological systems in general. We will not be able to understand this in sufficient detail unless we develop the necessary bioanalytical tools.

Acknowledgements

O.O. and B.S. are funded by a grant of the European Commission (H2020 MSCA-ITN 2017 “Analytics for Biologics”).

REFERENCES

1. M. Tassi, J. De Vos, S. Chatterjee, F. Sobott, J. Bones, S. Eeltink, Advances in native high-performance liquid chromatography and intact mass spectrometry for the characterization of biopharmaceutical products, *J. Sep. Sci.* 41 (2018) 125–144.
2. D. Stoll, J. Danforth, K. Zhang, A. Beck, Characterization of therapeutic antibodies and related products by two-dimensional liquid chromatography coupled with UV absorbance and mass spectrometric detection, *J. Chromatogr. B Anal. Technol. Biomed. Life Sci.* 1032 (2016) 51–60.
3. S. Fekete, J.L. Veuthey, A. Beck, D. Guilleme, Hydrophobic interaction chromatography for the characterization of monoclonal antibodies and related products, *J. Pharm. Biomed. Anal.* 130 (2016) 3–18.
4. P. Bults, N.C. Van De Merbel, R. Bischoff, Quantification of biopharmaceuticals and biomarkers in complex biological matrices: A comparison of liquid chromatography coupled to tandem mass spectrometry and ligand binding assays, *Expert Rev. Proteomics.* 12 (2015) 355–374.
5. J. Zheng, J. Mehl, Y. Zhu, B. Xin, T. Olah, Application and challenges in using LC-MS assays for absolute quantitative analysis of therapeutic proteins in drug discovery, *Bioanalysis.* 6 (2014) 859–879.
6. K. Sandra, I. Vandenheede, P. Sandra, Modern chromatographic and mass spectrometric techniques for protein biopharmaceutical characterization, *J. Chromatogr. A.* 1335 (2014) 81–103.
7. S. Fekete, D. Guilleme, Ultra-high-performance liquid chromatography for the characterization of therapeutic proteins, *TrAC - Trends Anal. Chem.* 63 (2014) 76–84.
8. I. van den Broek, W.M.A. Niessen, W.D. van Dongen, Bioanalytical LC-MS/MS of protein-based biopharmaceuticals, *J. Chromatogr. B Anal. Technol. Biomed. Life Sci.* 929 (2013) 161–179.
9. G. Hopfgartner, A. Lesur, E. Varesio, Analysis of biopharmaceutical proteins in biological matrices by LC-MS/MS II. LC-MS/MS analysis, *TrAC - Trends Anal. Chem.* 48 (2013) 52–61.
10. A. Staub, D. Guilleme, J. Schappler, J.L. Veuthey, S. Rudaz, Intact protein analysis in the biopharmaceutical field, *J. Pharm. Biomed. Anal.* 55 (2011) 810–822.
11. P. Steffen, M. Kwiatkowski, W.D. Robertson, A. Zarrine-Afsar, D. Deterra, V. Richter, H. Schlüter, Protein species as diagnostic markers, *J. Proteomics.* 134 (2016) 5–18.
12. F.E. Regnier, J. Kim, Proteins and Proteoforms: New Separation Challenges, *Anal. Chem.* 90 (2018) 361–373.
13. R. Bischoff, H. Permentier, V. Guryev, P. Horvatovich, Genomic variability and protein species - Improving sequence coverage for proteogenomics, *J. Proteomics.* 134 (2016) 25–36.
14. A. Lisitsa, S. Moshkovskii, A. Chernobrovkin, E. Ponomarenko, A. Archakov, Profiling proteoforms: Promising follow-up of proteomics for biomarker discovery, *Expert Rev. Proteomics.* 11 (2014) 121–129.
15. H. Schlüter, R. Apweiler, H.G. Holzhütter, P.R. Jungblut, Finding one's way in proteomics: A protein species nomenclature, *Chem. Cent. J.* 3 (2009) 11.
16. H. Schlüter, H.G. Holzhütter, R. Apweiler, P.R. Jungblut, Suggestions for a Protein Species Identifier System, *Beilstein-Institut.De.* (2009) 79–86.
17. P.R. Jungblut, H.G. Holzhütter, R. Apweiler, H. Schlüter, The speciation of the proteome, *Chem. Cent. J.* 2 (2008) 16.

18. R. Aebersold, J.N. Agar, I.J. Amster, M.S. Baker, C.R. Bertozzi, E.S. Boja, C.E. Costello, B.F. Cravatt, C. Fenselau, B.A. Garcia, Y. Ge, J. Gunawardena, R.C. Hendrickson, P.J. Hergenrother, C.G. Huber, A.R. Ivanov, O.N. Jensen, M.C. Jewett, N.L. Kelleher, L.L. Kiessling, N.J. Krogan, M.R. Larsen, J.A. Loo, R.R. Ogorzalek Loo, E. Lundberg, M.J. MacCoss, P. Mallick, V.K. Mootha, M. Mrksich, T.W. Muir, S.M. Patrie, J.J. Pesavento, S.J. Pitteri, H. Rodriguez, A. Saghatelian, W. Sandoval, H. Schlüter, S. Sechi, S.A. Slavoff, L.M. Smith, M.P. Snyder, P.M. Thomas, M. Uhlén, J.E. Van Eyk, M. Vidal, D.R. Walt, F.M. White, E.R. Williams, T. Wohlschläger, V.H. Wysocki, N.A. Yates, N.L. Young, B. Zhang, How many human proteoforms are there?, *Nat. Chem. Biol.* 14 (2018) 206–214.
19. N.C. van de Merbel, Sample preparation for quantitative bioanalysis of proteins. In: *Sample Preparation in LC-MS Bioanalysis*, W. Li, J. Zhang and F.L.S. Tse (Eds), John Wiley and Sons, in press.
20. D. Wilffert, A. Asselman, R. Donzelli, J. Hermans, N. Govorukhina, W.J. Quax, N.C. Van De Merbel, R. Bischoff, Highly sensitive antibody-free μ C-MS/MS quantification of rhTRAIL in serum, *Bioanalysis*. 8 (2016) 881–890.
21. Y.L. Boersma, A. Plückthun, DARPs and other repeat protein scaffolds: Advances in engineering and applications, *Curr. Opin. Biotechnol.* 22 (2011) 849–857.
22. C. Tiede, R. Bedford, S.J. Heseltine, G. Smith, I. Wijetunga, R. Ross, D. Alqallaf, A.P. Roberts, A. Balls, A. Curd, R.E. Hughes, H. Martin, S.R. Needham, L.C. Zanetti-Domingues, Y. Sadigh, T.P. Peacock, A.A. Tang, N. Gibson, H. Kyle, G.W. Platt, N. Ingram, T. Taylor, L.P. Coletta, I. Manfield, M. Knowles, S. Bell, F. Esteves, A. Maqbool, R.K. Prasad, M. Drinkhill, R.S. Bon, V. Patel, S.A. Goodchild, M. Martin-Fernandez, R.J. Owens, J.E. Nettleship, M.E. Webb, M. Harrison, J.D. Lippiat, S. Ponnambalam, M. Peckham, A. Smith, P.K. Ferrigno, M. Johnson, M.J. McPherson, D.C. Tomlinson, Affimer proteins are versatile and renewable affinity reagents, *Elife*. 6 (2017).
23. C. Tiede, A.A.S. Tang, S.E. Deacon, U. Mandal, J.E. Nettleship, R.L. Owen, S.E. George, D.J. Harrison, R.J. Owens, D.C. Tomlinson, M.J. McPherson, Adhiron: A stable and versatile peptide display scaffold for molecular recognition applications, *Protein Eng. Des. Sel.* 27 (2014) 145–155.
24. F. Klont, M. Hadderingh, P. Horvatovich, N.H.T. Ten Hacken, R. Bischoff, Affimers as an Alternative to Antibodies in an Affinity LC-MS Assay for Quantification of the Soluble Receptor of Advanced Glycation End-Products (sRAGE) in Human Serum, *J. Proteome Res.* 17 (2018) 2892–2899.
25. M.T. Furlong, S. Zhao, W. Mylott, R. Jenkins, M. Gao, V. Hegde, J. Tamura, A. Tymiak, M. Jemal, Dual universal peptide approach to bioanalysis of human monoclonal antibody protein drug candidates in animal studies, *Bioanalysis*. 5 (2013) 1363–1376.
26. J.F. Kellie, J.R. Kehler, T.J. Mencken, R.J. Snell, C.S. Hottenstein, A whole-molecule immunocapture LC-MS approach for the in vivo quantitation of biotherapeutics, *Bioanalysis*. 8 (2016) 2103–2114.
27. R. Popp, H. Li, A. LeBlanc, Y. Mohammed, A. Aguilar-Mahecha, A.G. Chambers, C. Lan, O. Poetz, M. Basik, G. Batist, C.H. Borchers, Immuno-Matrix-Assisted Laser Desorption/Ionization Assays for Quantifying AKT1 and AKT2 in Breast and Colorectal Cancer Cell Lines and Tumors, *Anal. Chem.* 89 (2017) 10592–10600.
28. B. Shah, J.D. Reid, M.A. Kuzyk, C.E. Parker, C.H. Borchers, Developing an iMALDI method, *Methods Mol. Biol.* 1023 (2013) 97–120.
29. F. Klont, N.H.T. Ten Hacken, P. Horvatovich, S.J.L. Bakker, R. Bischoff, Assuring Consistent Performance of an Insulin-Like Growth Factor 1 MALDIImmunoassay by Monitoring Measurement Quality Indicators, *Anal. Chem.* 89 (2017) 6188–6195.
30. M. Berna, B. Ackermann, Increased throughput for low-abundance protein biomarker verification by liquid chromatography/tandem mass spectrometry, *Anal. Chem.* 81 (2009) 3950–3956.
31. F. Klont, S.D. Pouwels, J. Hermans, N.C. van de Merbel, P. Horvatovich, N.H.T. ten Hacken, R. Bischoff, A fully validated liquid chromatography-mass spectrometry method for the quantification of the soluble receptor of advanced glycation end-products (sRAGE) in serum using immunopurification in a 96-well plate format, *Talanta*. 182 (2018) 414–421.

32. C. Pritchard, K.J. Groves, S. Biesenbruch, G. Oconnor, A.E. Ashcroft, C. Arsene, D. Schulze, M. Quaglia, Quantification of human growth hormone in serum with a labeled protein as an internal standard: Essential considerations, *Anal. Chem.* 86 (2014) 6525–6532.
33. J.C. Masini, F. Svec, Porous monoliths for on-line sample preparation: A review, *Anal. Chim. Acta.* 964 (2017) 24–44.
34. L. Rieux, H. Niederländer, E. Verpoorte, R. Bischoff, Silica monolithic columns: Synthesis, characterisation and applications to the analysis of biological molecules, *J. Sep. Sci.* 28 (2005) 1628–1641.
35. Z. Yang, J. Ke, M. Hayes, M. Bryant, F.L.S. Tse, A sensitive and high-throughput LC-MS/MS method for the quantification of pegylated-interferon- α 2a in human serum using monolithic C18 solid phase extraction for enrichment, *J. Chromatogr. B Anal. Technol. Biomed. Life Sci.* 877 (2009) 1737–1742.
36. U. Von Pawel-Rammingen, B.P. Johansson, L. Björck, IdeS, a novel streptococcal cysteine proteinase with unique specificity for immunoglobulin G, *EMBO J.* 21 (2002) 1607–1615.
37. K. Wenig, L. Chatwell, U. von Pawel-Rammingen, L. Björck, R. Huber, P. Sonderrmann, Structure of the streptococcal endopeptidase IdeS, a cysteine proteinase with strict specificity for IgG., *Proc. Natl. Acad. Sci. U. S. A.* 101 (2004) 17371–6.
38. J. Strand, C.T. Huang, J. Xu, Characterization of Fc-fusion protein aggregates derived from extracellular domain disulfide bond rearrangements, *J. Pharm. Sci.* 102 (2013) 441–453.
39. H. Lynaugh, H. Li, B. Gong, Rapid Fc glycosylation analysis of Fc fusions with IdeS and liquid chromatography mass spectrometry, *MAbs.* 5 (2013) 641–645.
40. S. Zhou, O. Mozziconacci, B.A. Kerwin, C. Schöneich, Fluorogenic tagging methodology applied to characterize oxidized tyrosine and phenylalanine in an immunoglobulin monoclonal antibody, *Pharm. Res.* 30 (2013) 1311–1327.
41. G. Chevreux, N. Tilly, N. Bihoreau, Fast analysis of recombinant monoclonal antibodies using IdeS proteolytic digestion and electrospray mass spectrometry, *Anal. Biochem.* 415 (2011) 212–214.
42. Y. An, Y. Zhang, H.M. Mueller, M. Shameem, X. Chen, A new tool for monoclonal antibody analysis Application of IdeS proteolysis in IgG domain-specific characterization, *MAbs.* 6 (2014) 879–893.
43. Y. Leblanc, C. Ramon, N. Bihoreau, G. Chevreux, Charge variants characterization of a monoclonal antibody by ion exchange chromatography coupled on-line to native mass spectrometry: Case study after a long-term storage at +5 °C, *J. Chromatogr. B Anal. Technol. Biomed. Life Sci.* 1048 (2017) 130–139.
44. K. Pisupati, Y. Tian, S. Okbazghi, A. Benet, R. Ackermann, M. Ford, S. Saveliev, C.M. Hosfield, M. Urh, E. Carlson, C. Becker, T.J. Tolbert, S.P. Schwendeman, B.T. Ruotolo, A. Schwendeman, A Multidimensional Analytical Comparison of Remicade and the Biosimilar Remsima, *Anal. Chem.* 89 (2017) 4838–4846.
45. E. Wagner-Rousset, S. Fekete, L. Morel-Chevillet, O. Colas, N. Corvaia, S. Cianférani, D. Guillarme, A. Beck, Development of a fast workflow to screen the charge variants of therapeutic antibodies, *J. Chromatogr. A.* 1498 (2017) 147–154.
46. F.E. Regnier, K.M. Gooding, High-performance liquid chromatography of proteins, *Anal. Biochem.* 103 (1980) 1–25.
47. M.T. Hearn, High-performance liquid chromatography and its application to protein chemistry., *Adv. Chromatogr.* 20 (1982) 1–82.
48. F.E. Regnier, High-performance liquid chromatography of biopolymers, *Science* (80-.). 222 (1983) 245–252.
49. M.T.W. Hearn, General strategies in the separation of proteins by high-performance liquid chromatographic methods, *J. Chromatogr. B Biomed. Sci. Appl.* 418 (1987) 3–26.
50. F.E. Regnier, Chromatography of complex protein mixtures, *J. Chromatogr. B Biomed. Sci. Appl.* 418 (1987) 115–143.

51. F.E. Regnier, The role of protein structure in chromatographic behavior, *Science* (80-.). 238 (1987) 319–323.
52. M.T.W. Hearn, B. Anspach, Chemical, physical, and biochemical concepts in isolation and purification of proteins, *Sep. Purif. Methods*. 30 (2001) 221–263.
53. K.K. Unger, A.I. Liapis, Adsorbents and columns in analytical high-performance liquid chromatography: A perspective with regard to development and understanding, *J. Sep. Sci.* 35 (2012) 1201–1212.
54. K. Cabrera, G. Wieland, D. Lubda, K. Nakanishi, N. Soga, H. Minakuchi, K.K. Unger, SilicaROD™ — A new challenge in fast high-performance liquid chromatography separations, *TrAC Trends Anal. Chem.* 17 (1998) 50–53.
55. S. Xie, R.W. Allington, F. Svec, J.M.J. Fréchet, Rapid reversed-phase separation of proteins and peptides using optimized “moulded” monolithic poly(styrene-co-divinylbenzene) columns, in: *J. Chromatogr. A*, 1999: pp. 169–174.
56. F.C. Leinweber, D. Lubda, K. Cabrera, U. Tallarek, Characterization of silica-based monoliths with bimodal pore size distribution, *Anal. Chem.* 74 (2002) 2470–2477.
57. S. Xie, R.W. Allington, J.M.J. Fréchet, F. Svec, Porous polymer monoliths: an alternative to classical beads., *Adv. Biochem. Eng. Biotechnol.* 76 (2002) 87–125.
58. B. Barroso, D. Lubda, R. Bischoff, Applications of Monolithic Silica Capillary Columns in Proteomics, *J. Proteome Res.* 2 (2003) 633–642. doi:10.1021/pr0340532.
59. F. Svec, Preparation and HPLC applications of rigid macroporous organic polymer monoliths., *J. Sep. Sci.* 27 (2004) 747–66.
60. W. De Malsche, D. Clicq, V. Verdoold, P. Gzil, G. Desmet, H. Gardeniers, Integration of porous layers in ordered pillar arrays for liquid chromatography, *Lab Chip.* 7 (2007) 1705–1711.
61. W. De Malsche, H. Eghbali, D. Clicq, J. Vangelooen, H. Gardeniers, G. Desmet, Pressure-driven reverse-phase liquid chromatography separations in ordered nonporous pillar array columns, *Anal. Chem.* 79 (2007) 5915–5926.
62. W. De Malsche, H. Gardeniers, G. Desmet, Experimental study of porous silicon shell pillars under retentive conditions, *Anal. Chem.* 80 (2008) 5391–5400.
63. X. Illa, W. De Malsche, J. Bomer, H. Gardeniers, J. Eijkel, J.R. Morante, A. Romano-Rodríguez, G. Desmet, An array of ordered pillars with retentive properties for pressure-driven liquid chromatography fabricated directly from an unmodified cyclo olefin polymer, *Lab Chip.* 9 (2009) 1511–1516.
64. G. Desmet, S. Eeltink, Fundamentals for LC miniaturization, *Anal. Chem.* 85 (2013) 543–556.
65. C.W.N. Damen, E.J.B. Derissen, J.H.M. Schellens, H. Rosing, J.H. Beijnen, The bioanalysis of the monoclonal antibody trastuzumab by high-performance liquid chromatography with fluorescence detection after immuno-affinity purification from human serum, *J. Pharm. Biomed. Anal.* 50 (2009) 861–866.
66. Q. Ruan, Q.C. Ji, M.E. Arnold, W.G. Humphreys, M. Zhu, Strategy and its implications of protein bioanalysis utilizing high-resolution mass spectrometric detection of intact protein, *Anal. Chem.* 83 (2011) 8937–8944.
67. K.A. Cohen, K. Schellenberg, K. Benedek, B.L. Karger, B. Grego, M.T.W. Hearn, Mobile-phase and temperature effects in the reversed phase chromatographic separation of proteins, *Anal. Biochem.* 140 (1984) 223–235.
68. H.P. Bennett, A.M. Hudson, C. McMartin, G.E. Purdon, Use of octadecasilyl-silica for the extraction and purification of peptides in biological samples. Application to the identification of circulating metabolites of corticotropin-(1-24)-tetracosapeptide and somatostatin in vivo., *Biochem. J.* 168 (1977) 9–13.
69. M.C. McCroskey, V.E. Groppi, J.D. Pearson, Separation and purification of S49 mouse lymphoma histones by reversed-phase high-performance liquid chromatography, *Anal. Biochem.* 163 (1987) 427–432.

70. W. Jian, L. Kang, L. Burton, N. Weng, A workflow for absolute quantitation of large therapeutic proteins in biological samples at intact level using LC-HRMS, *Bioanalysis*. 8 (2016) 1679–1691.
71. A.F.G. Gargano, L.S. Roca, R.T. Fellers, M. Bocxe, E. Domínguez-Vega, G.W. Somsen, Capillary HILIC-MS: A New Tool for Sensitive Top-Down Proteomics, *Anal. Chem.* 90 (2018) 6601–6609.
72. S.A. Schuster, B.M. Wagner, B.E. Boyes, J.J. Kirkland, Optimized superficially porous particles for protein separations, *J. Chromatogr. A*. 1315 (2013) 118–126.
73. J.J. Kirkland, S.A. Schuster, W.L. Johnson, B.E. Boyes, Fused-core particle technology in high-performance liquid chromatography: An overview, *J. Pharm. Anal.* 3 (2013) 303–312.
74. K. Todoroki, T. Nakano, Y. Eda, K. Ohyama, H. Hayashi, D. Tsuji, J.Z. Min, K. Inoue, N. Iwamoto, A. Kawakami, Y. Ueki, K. Itoh, T. Toyooka, Bioanalysis of bevacizumab and infliximab by high-temperature reversed-phase liquid chromatography with fluorescence detection after immunoaffinity magnetic purification, *Anal. Chim. Acta*. 916 (2016) 112–119.
75. S. Eeltink, S. Wouters, J.L. Does-Sousa, F. Svec, Advances in organic polymer-based monolithic column technology for high-resolution liquid chromatography-mass spectrometry profiling of antibodies, intact proteins, oligonucleotides, and peptides, *J. Chromatogr. A*. 1498 (2017) 8–21.
76. F. Detobel, K. Broeckhoven, J. Wellens, B. Wouters, R. Swart, M. Ursem, G. Desmet, S. Eeltink, Parameters affecting the separation of intact proteins in gradient-elution reversed-phase chromatography using poly(styrene-co-divinylbenzene) monolithic capillary columns, *J. Chromatogr. A*. 1217 (2010) 3085–3090.
77. S. Eeltink, S. Dolman, F. Detobel, G. Desmet, R. Swart, M. Ursem, 1 mm ID poly(styrene-co-divinylbenzene) monolithic columns for high-peak capacity one- and two-dimensional liquid chromatographic separations of intact proteins, *J. Sep. Sci.* 32 (2009) 2504–2509.
78. A. Nordborg, E.F. Hilder, Recent advances in polymer monoliths for ion-exchange chromatography, *Anal. Bioanal. Chem.* 394 (2009) 71–84.
79. C. Lanshoeft, S. Cianféroni, O. Heudi, Generic Hybrid Ligand Binding Assay Liquid Chromatography High-Resolution Mass Spectrometry-Based Workflow for Multiplexed Human Immunoglobulin G1 Quantification at the Intact Protein Level: Application to Preclinical Pharmacokinetic Studies, *Anal. Chem.* 89 (2017) 2628–2635.
80. W. Jin, L. Burton, I. Moore, LC-HRMS quantitation of intact antibody drug conjugate trastuzumab emtansine from rat plasma, *Bioanalysis*. 10 (2018) 851–862. doi:10.4155/bio-2018-0003.
81. K. Muneeruddin, J.J. Thomas, P.A. Salinas, I.A. Kaltashov, Characterization of small protein aggregates and oligomers using size exclusion chromatography with online detection by native electrospray ionization mass spectrometry, *Anal. Chem.* 86 (2014) 10692–10699.
82. J. Woodard, H. Lau, R.F. Latypov, Nondenaturing size-exclusion chromatography-mass spectrometry to measure stress-induced aggregation in a complex mixture of monoclonal antibodies, *Anal. Chem.* 85 (2013) 6429–6436.
83. R.J. Harris, B. Kabakoff, F.D. Macchi, F.J. Shen, M. Kwong, J.D. Andya, S.J. Shire, N. Bjork, K. Totpal, A.B. Chen, Identification of multiple sources of charge heterogeneity in a recombinant antibody, *J. Chromatogr. B Biomed. Sci. Appl.* 752 (2001) 233–245.
84. R. Bischoff, D. Speck, P. Lepage, L. Delatre, C. Ledoux, T.W. Brown, C. Roitsch, Purification and Biochemical Characterization of Recombinant α 1-Antitrypsin Variants Expressed in *Escherichia coli*, *Biochemistry*. 30 (1991) 3464–3472.
85. K. Muneeruddin, M. Nazzaro, I.A. Kaltashov, Characterization of Intact Protein Conjugates and Biopharmaceuticals Using Ion-Exchange Chromatography with Online Detection by Native Electrospray Ionization Mass Spectrometry and Top-Down Tandem Mass Spectrometry, *Anal. Chem.* 87 (2015) 10138–10145.
86. M. Belew, E.A. Peterson, J. Porath, A high-capacity hydrophobic adsorbent for human serum albumin, *Anal. Biochem.* 151 (1985) 438–441.

87. B. Chen, Z. Lin, A.J. Alpert, C. Fu, Q. Zhang, W.A. Pritts, Y. Ge, Online Hydrophobic Interaction Chromatography-Mass Spectrometry for the Analysis of Intact Monoclonal Antibodies, *Anal. Chem.* 90 (2018) 7135–7138.
88. S. Jespers, S. Schlautmann, H. Gardeniers, W. De Malsche, F. Lynen, G. Desmet, Chip-Based Multicapillary Column with Maximal Interconnectivity to Combine Maximum Efficiency and Maximum Loadability, *Anal. Chem.* 89 (2017) 11605–11613.
89. C.M. Whitehouse, R.N. Dreyer, M. Yamashita, J.B. Fenn, Electrospray Interface for Liquid Chromatographs and Mass Spectrometers, *Anal. Chem.* 57 (1985) 675–679.
90. J.B. Fenn, M. Mann, C.K. Meng, S.F. Wong, C.M. Whitehouse, Electrospray ionization for mass spectrometry of large biomolecules., *Science.* 246 (1989) 64–71.
91. J. Hermans, S. Ongay, V. Markov, R. Bischoff, Physicochemical Parameters Affecting the Electrospray Ionization Efficiency of Amino Acids after Acylation, *Anal. Chem.* 89 (2017) 9159–9166.
92. R.R. Ogorzalek Loo, R. Lakshmanan, J.A. Loo, What protein charging (and Supercharging) reveal about the mechanism of electrospray ionization, *J. Am. Soc. Mass Spectrom.* 25 (2014) 1675–1693.
93. A.T. Iavarone, E.R. Williams, Mechanism of charging and supercharging molecules in electrospray ionization, *J. Am. Chem. Soc.* 125 (2003) 2319–2327.
94. M. Nshanian, R. Lakshmanan, H. Chen, R.R.O. Loo, J.A. Loo, Enhancing sensitivity of liquid chromatography–mass spectrometry of peptides and proteins using supercharging agents, *Int. J. Mass Spectrom.* 427 (2018) 157–164.
95. S.M. Miladinović, L. Fornelli, Y. Lu, K.M. Piech, H.H. Girault, Y.O. Tsybin, In-spray supercharging of peptides and proteins in electrospray ionization mass spectrometry, *Anal. Chem.* 84 (2012) 4647–4651.
96. R.G. Kay, J. Howard, S. Stensson, A current perspective of supercharging reagents and peptide bioanalysis, *Bioanalysis.* 8 (2016) 157–161.
97. X. Zhao, J. Sun, L. Sun, J. Chen, Y. Cheng, X. Duan, Targeted LC-MS quantification of intact TAT-fusion therapeutics: A case study, *Bioanalysis.* 7 (2015) 981–990.
98. M.A. Zenaidee, W.A. Donald, Electron capture dissociation of extremely supercharged protein ions formed by electrospray ionisation, *Anal. Methods.* 7 (2015) 7132–7139.
99. M. Bern, T. Caval, Y.J. Kil, W. Tang, C. Becker, E. Carlson, D. Kletter, K.I. Sen, N. Galy, D. Hagemans, V. Franc, A.J.R. Heck, Parsimonious Charge Deconvolution for Native Mass Spectrometry, *J. Proteome Res.* 17 (2018) 1216–1226.
100. B.T. Ruotolo, C. V Robinson, Aspects of native proteins are retained in vacuum, *Curr. Opin. Chem. Biol.* 10 (2006) 402–408.
101. J. Marcoux, C. V Robinson, Twenty years of gas phase structural biology, *Structure.* 21 (2013) 1541–1550.
102. R. Gahoual, A.-K. Heidenreich, G.W. Somsen, P. Bulau, D. Reusch, M. Wuhler, M. Habberger, Detailed Characterization of Monoclonal Antibody Receptor Interaction Using Affinity Liquid Chromatography Hyphenated to Native Mass Spectrometry, *Anal. Chem.* 89 (2017) 5404–5412.
103. R.D. Melani, O.S. Skinner, L. Fornelli, G.B. Domont, P.D. Compton, N.L. Kelleher, Mapping Proteoforms and Protein Complexes From King Cobra Venom Using Both Denaturing and Native Top-down Proteomics, *Mol. Cell. Proteomics.* 15 (2016) 2423–2434.
104. G. Terral, A. Beck, S. Cianférani, Insights from native mass spectrometry and ion mobility-mass spectrometry for antibody and antibody-based product characterization, *J. Chromatogr. B Anal. Technol. Biomed. Life Sci.* 1032 (2016) 79–90.
105. I.D.G. Campuzano, C. Netirojjanakul, M. Nshanian, J.L. Lippens, D.P.A. Kilgour, S. Van Orden, J.A. Loo, Native-MS Analysis of Monoclonal Antibody Conjugates by Fourier Transform Ion Cyclotron Resonance Mass Spectrometry, *Anal. Chem.* 90 (2018) 745–751.

106. A. Ekhkirch, O. Hernandez-Alba, O. Colas, A. Beck, D. Guilleme, S. Cianféroni, Hyphenation of size exclusion chromatography to native ion mobility mass spectrometry for the analytical characterization of therapeutic antibodies and related products, *J. Chromatogr. B Anal. Technol. Biomed. Life Sci.* 1086 (2018) 176–183.
107. N.J. Thompson, S. Rosati, A.J.R. Heck, Performing native mass spectrometry analysis on therapeutic antibodies, *Methods*. 65 (2014) 11–17.
108. Y. Liang, M. Guttman, T.M. Davenport, S.L. Hu, K.K. Lee, Probing the Impact of Local Structural Dynamics of Conformational Epitopes on Antibody Recognition, *Biochemistry*. 55 (2016) 2197–2213.
109. C.E. Doneanu, M. Anderson, B.J. Williams, M.A. Lauber, A. Chakraborty, W. Chen, Enhanced Detection of Low-Abundance Host Cell Protein Impurities in High-Purity Monoclonal Antibodies Down to 1 ppm Using Ion Mobility Mass Spectrometry Coupled with Multidimensional Liquid Chromatography, *Anal. Chem.* 87 (2015) 10283–10291.
110. J. Marcoux, T. Champion, O. Colas, E. Wagner-Rousset, N. Corvaia, A. Van Dorsselaer, A. Beck, S. Cianféroni, Native mass spectrometry and ion mobility characterization of trastuzumab emtansine, a lysine-linked antibody drug conjugate, *Protein Sci.* 24 (2015) 1210–1223.
111. B.C. Bohrer, S.I. Merenbloom, S.L. Koeniger, A.E. Hilderbrand, D.E. Clemmer, Biomolecule Analysis by Ion Mobility Spectrometry, *Annu. Rev. Anal. Chem.* 1 (2008) 293–327.
112. E.S. Baker, K.E. Burnum-Johnson, Y.M. Ibrahim, D.J. Orton, M.E. Monroe, R.T. Kelly, R.J. Moore, X. Zhang, R. Théberge, C.E. Costello, R.D. Smith, Enhancing bottom-up and top-down proteomic measurements with ion mobility separations, *Proteomics*. 15 (2015) 2766–2776.
113. V. D'Atri, T. Causon, O. Hernandez-Alba, A. Mutabazi, J.L. Veuthey, S. Cianferani, D. Guilleme, Adding a new separation dimension to MS and LC-MS: What is the utility of ion mobility spectrometry?, *J. Sep. Sci.* 41 (2018) 20–67.
114. U. Distler, J. Kuharev, P. Navarro, S. Tenzer, Label-free quantification in ion mobility-enhanced data-independent acquisition proteomics, *Nat. Protoc.* 11 (2016) 795–812.
115. F.C. Liu, S.R. Kirk, C. Bleiholder, On the structural denaturation of biological analytes in trapped ion mobility spectrometry-mass spectrometry, *Analyst*. 141 (2016) 3722–3730.
116. X. Zhang, K. Quinn, C. Cruickshank-Quinn, R. Reisdorph, N. Reisdorph, The application of ion mobility mass spectrometry to metabolomics, *Curr. Opin. Chem. Biol.* 42 (2018) 60–66.
117. S. Mehmood, J. Marcoux, J.T.S. Hopper, T.M. Allison, I. Liko, A.J. Borysik, C. V Robinson, Charge reduction stabilizes intact membrane protein complexes for mass spectrometry, *J. Am. Chem. Soc.* 136 (2014) 17010–17012.
118. R.Y.-C. Huang, E.G. Deyanova, D. Passmore, V. Rangan, S. Deshpande, A.A. Tymiak, G. Chen, Utility of Ion Mobility Mass Spectrometry for Drug-to-Antibody Ratio Measurements in Antibody-Drug Conjugates, *J. Am. Soc. Mass Spectrom.* 26 (2015) 1791–1794.
119. C.E. Daly, L.L. Ng, A. Hakimi, R. Willingale, D.J.L. Jones, Qualitative and quantitative characterization of plasma proteins when incorporating traveling wave ion mobility into a liquid chromatography-mass spectrometry workflow for biomarker discovery: Use of product ion quantitation as an alternative data analysis, *Anal. Chem.* 86 (2014) 1972–1979.
120. A.A. Shvartsburg, K. Tang, R.D. Smith, Two-dimensional ion mobility analyses of proteins and peptides, *Methods Mol. Biol.* 492 (2009) 417–445.
121. P. Bults, M. Meints, A. Sonesson, M. Knutsson, R. Bischoff, N.C. Van De Merbel, Improving selectivity and sensitivity of protein quantitation by LC-HR-MS/MS: Determination of somatropin in rat plasma, *Bioanalysis*. 10 (2018) 1009–1021.
122. A.G. Ferrige, M.J. Seddon, B.N. Green, S.A. Jarvis, J. Skilling, J. Staunton, Disentangling electrospray spectra with maximum entropy, *Rapid Commun. Mass Spectrom.* 6 (1992) 707–711.

CHAPTER VI

Improving selectivity and sensitivity of protein quantitation by LC-HR-MS/MS: determination of somatropin in rat plasma

Peter Bults^{1,2}, Marcel Meints¹, Anders Sonesson³, Magnus Knutsson³, Rainer Bischoff², Nico C. van de Merbel^{1,2}.

¹ *Bioanalytical Laboratory, PRA Health Sciences, Amerikaweg 18, 9407 TK, Assen, The Netherlands.*

² *University of Groningen, Department of Analytical Biochemistry, A. Deusinglaan 1, 9700 AV Groningen, The Netherlands.*

³ *Ferring Pharmaceuticals, Kay Fiskers Plads 11, DK-2300 Copenhagen, Denmark*

Bioanalysis, 2018, 10(13), 1009-1021

ABSTRACT

Background: Protein quantitation by digestion of a biological sample followed by LC–MS analysis of a signature peptide can be a challenge because of the high complexity of the digested matrix. Results/methodology: The use of LC with high-resolution (Q-TOF) MS detection allowed quantitation of the 22-kDa biopharmaceutical somatropin in 60 μ L of rat plasma down to 25 ng/mL with minimal further sample treatment. Reducing the mass-extraction window to 0.01 Da considerably decreased the interference of tryptic peptides, enhanced sensitivity and improved accuracy and precision. Analysis with LC MS/MS resulted in a less favorable limit of quantitation of 100 ng/mL. Conclusion: High-resolution MS is an interesting option for the quantitation of proteins after digestion and has the potential to improve sensitivity with minimal method development.

6.1 INTRODUCTION

Liquid chromatography (LC) in combination with tandem mass spectrometry (MS/MS), performed on a triple-quadrupole mass spectrometer in the multiple reaction monitoring (MRM) mode, has been the gold standard for over two decades when it comes to the quantification of small molecules and peptides in biological matrices. This technique is known for its robustness, high selectivity, sensitivity and reproducibility, and is used as the bioanalytical workhorse in laboratories across the globe.

An important new development of the past few years is the application of LC-MS/MS for the quantification of proteins, as an alternative for, or an addition to, the traditional ligand-binding assays (LBAs) [1-3]. Although LC-MS/MS for proteins has many technical advantages, such as improved precision and accuracy, a larger linear dynamic range, independence of critical immunological reagents which may suffer from cross-reactivity and batch-to-batch differences, it is typically inferior to LBAs in terms of sensitivity [4]. One of the reasons for this is related to the fact that large proteins need to be digested to peptides of much reduced size to be compatible with the mass range of a triple-quadrupole mass spectrometer. If a protein-rich matrix such as serum or plasma is digested, a highly complex sample is obtained containing a multitude of peptides, which are all composed of the same limited number of natural amino acids and, thus, have masses and properties that are much more similar to one another than those of the original proteins. As a result, many peaks often show up in the MRM chromatograms, which greatly impacts method selectivity and typically limits the obtainable sensitivity for protein analytes to the low $\mu\text{g/mL}$ or high ng/mL range [5-7]. In a recent paper, the magnitude of this effect was studied for salmon calcitonin [8]. The lower limit of quantification (LLOQ) for digested plasma was found to be a factor of 100 higher than that for a digested test solution and this was only due to the presence of interfering matrix peaks in the LC-MS/MS chromatograms. For obtaining better sensitivity, the usual approach is to remove interfering peptides by applying extraction procedures at the protein and/or peptide level, such as immunodepletion, immunocapture and solid-phase extraction [9-11]. Although this can improve sensitivity considerably, even down to the pg/mL range [12,13], the required research will add to method development time and the additional steps may negatively impact accuracy and precision.

The limited selectivity of MS/MS detection for digested biological samples is related to the relatively low mass resolution of a quadrupole mass spectrometer and the corresponding rather wide mass extraction window (MEW) that is used to select analyte

ions for detection. The typical setting in tandem mass spectrometry is unit-mass resolution for both quadrupoles with a MEW corresponding to full width at half maximum (FWHM) of 0.7 Da, which allows distinction between ions with m/z values that are one unit apart. While this generally provides appropriate selectivity for small-molecule analytes, the strong similarity of the peptides in biological sample digests, the frequent occurrence of multiple charges and their comparable fragmentation patterns, makes it highly likely that multiple precursor and product ions will be generated with very close m/z values, which all will be selected in the triple-quadrupole mass spectrometer and, ultimately, will be detected and give a response in the chromatograms. Although many of these peptides can be chromatographically separated from the surrogate peptide released by the analyte, interferences at the same retention time as the surrogate peptide will often be unavoidable, and this will negatively impact the selectivity and sensitivity of the method.

An obvious approach to reduce interferences is to select a narrower MEW for detection, a situation which can be provided by high-resolution mass spectrometry (HRMS). Typically, HRMS is run in full-scan mode, which records all sample ions. Extracted-ion chromatograms are subsequently constructed by setting an MEW around the theoretical mass-to-charge ratio of the analyte ion and recording the response of all ions within the MEW. In contrast to detection on a triple quadrupole, in HRMS the magnitude of the MEW can be easily reduced, and the sensitivity and selectivity of the detection optimized. In recent years, the field of HRMS has seen considerable improvements with regard to sensitivity, linear dynamic range and scan-modes and the technique is increasingly seen as a serious option for quantitative bioanalysis, even though the instrument sensitivity of triple-quadrupole mass spectrometry typically still is superior [14,15]. So far, most published applications of HRMS in quantitative bioanalysis have been for small molecules or peptides [16-19] and although the applicability of HRMS has also been demonstrated for protein quantification after digestion [20-25], this field clearly still is in its infancy and a systematic investigation of the potential of HRMS to improve selectivity is still lacking.

In this paper, we present and evaluate a quantitative LC-HR-MS/MS method for the 22-kDa biopharmaceutical protein somatotropin (recombinant human growth hormone, rhGH) in rat plasma. After trypsin digestion, three signature peptides from different parts of the protein molecule are quantified on LC coupled to a quadrupole-time of flight (Q-TOF) mass spectrometer, which combines unit-mass resolution for selection of the precursor ion (quadrupole) and high resolution for selection of the product ion after fragmentation (TOF). The effect of the MEW and of the summing up of multiple ions on assay performance

(precision, accuracy, selectivity and sensitivity) of all three peptides is described and a comparison to the performance of a triple-quadrupole MS is provided. The applicability of the optimized HR-MS/MS approach is illustrated by analysis of rat plasma samples from a pharmacokinetic study.

6.2 EXPERIMENTAL SECTION

6.2.1 Chemicals & materials

Recombinant human growth hormone (somatropin), supplied as a lyophilized sterile powder, was obtained from Ferring (Copenhagen, Denmark). Information on the amino acid sequence is given in **Figure 1**. Custom synthesized internal standard peptides (SNLELLR and LFDNAMLRL with a $^{13}\text{C}_6$ - $^{15}\text{N}_4$ -labeled C-terminal arginine and FDTNSHNDDALLK with a $^{13}\text{C}_6$ - $^{15}\text{N}_2$ -labeled C-terminal lysine) were obtained from JPT Peptide Technologies (Berlin, Germany). Acetonitrile, methanol, 2-propanol, formic acid, acetic acid, ammonia (25%) and hydrochloric acid (37%) were obtained from Merck (Darmstadt, Germany). Tween-20, Trizma[®] base and trypsin from porcine pancreas (Type IX-S, lyophilized powder, 13,000-20,000 BAEE units/mg protein) were obtained from Sigma Aldrich (St. Louis, MO, USA). HPLC grade water was prepared using a water purification system from Merck. Rat EDTA plasma (hereafter referred to as blank rat plasma) was obtained from Seralabs (Haywards Heath, UK). ESI Positive Calibration Solution for the Q-TOF system was obtained from Sciex (Toronto, Canada).

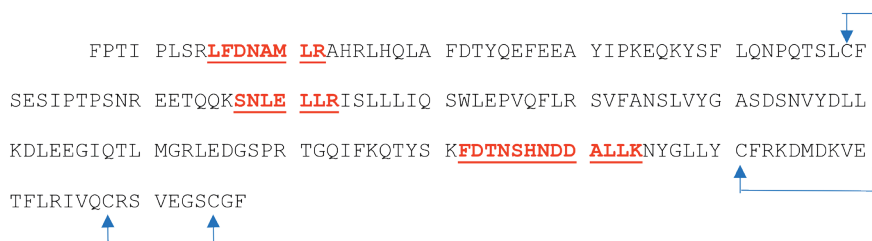


Figure 1: amino acid sequence of somatropin. The three signature peptides are highlighted, and the disulfide bonds shown as arrows.

6.2.2 Preparation of calibration and quality control samples

A somatropin stock solution at 10.0 mg/mL was prepared by dissolving the contents of a vial of lyophilized protein (label claim: 10.0 mg) in 1.00 mL of water according to the manufacturer's instructions for use. The stock solution was divided into 0.2 mL aliquots in Eppendorf Protein Lo-bind tubes (obtained from VWR International, Amsterdam, The Netherlands) and stored at -80°C. Two sets of aqueous standard solutions at 2.50, 25.0 and 200 µg/mL were prepared freshly from this stock solution. One set was used to prepare calibration samples in blank rat plasma at 25.0, 50.0, 100, 125, 250, 500, 1250, 2000, 5000, 8000 and 10000 ng/mL. Similarly, quality control (QC) samples were prepared from the other set at 25.0, 50.0, 75.0, 1250 and 8000 ng/mL. All calibration and QC samples were stored in Eppendorf Protein Lo-bind tubes at -80°C.

6.2.3 Sample pretreatment

Aliquots of 60 µL of rat plasma were pipetted into the 1.2-mL wells of an Eppendorf Protein Lo-bind 96-well plate (VWR International) and 200 µL of an 80:20 (v/v) mixture of acetonitrile and water was added. After vortex-mixing for 2 minutes, the proteins were pelleted by centrifugation for 10 minutes at 1500g. The supernatant was discarded by inverting the plate above a waste receptacle and placing it upside down on a tissue for 15 minutes. The protein pellet was reconstituted by vortex-mixing in 400 µL of a digestion solution consisting of 50 mM Trizma buffer (pH 8.0), 2.5% (v/v) acetonitrile and 200 µg/mL trypsin in water. Next, 60 µL of the digestion solution, excluding trypsin and containing 8000 ng/mL of the internal standards was added. The sample was digested at 37°C and 1250 rpm for 90 minutes using an Eppendorf (Hamburg, Germany) Thermomixer® comfort, after which the digestion was stopped by the addition of 25 µL of 10% formic acid in water. The complete digest was transferred onto an Oasis PRiME HLB 96-well plate with 30 mg sorbent (Waters, Milford, MA, USA). The solid-phase extraction (SPE) columns were washed with 800 µL methanol/water (5:95, v/v) and eluted with 250 µL methanol/water (50:50, v/v), followed by 250 µL 5% ammonia in methanol/water (50:50, v/v) into an Eppendorf Protein Lo-bind 96-well plate. The combined eluate fractions were evaporated to dryness under nitrogen at 60°C (upper) and 80°C (lower) using a Biotage (Uppsala, Sweden) SPE Dry 96 dual sample concentrator system and reconstituted in 60 µL 0.1% formic acid in acetonitrile/water (5:95, v/v). Finally, the plate was sealed, vortex-mixed and placed in an autosampler at 10°C for analysis.

6.2.4 Chromatography

Digested samples were analyzed using a NexeraX2 system (Shimadzu, Tokyo, Japan) coupled to a Sciex TripleTOF 6600 Q-TOF mass spectrometer equipped with a Dual Spray source or using a 1290 Infinity II system (Agilent, Santa Clara, USA) coupled to a Sciex TripleQuad 6500 triple-quadrupole mass spectrometer equipped with a IonDrive TurboV source.

Chromatographic separation was performed at 60°C on a 2.1 × 100 mm (particle size 1.6 µm, pore size 100Å) Luna Omega C18 column (Phenomenex, Torrance, CA, USA). Mobile phase A consisted of 0.1% formic acid in a mixture of water and 2-propanol (95:5, v/v) and mobile phase B was 0.1% formic acid in a mixture of acetonitrile and 2-propanol (95:5, v/v). Gradient elution was performed at 0.6 mL/min using the following profile: 0.0-6.0 min: 0-13% B; 6.0-6.2 min: 13-55% B; 6.2-6.7 min: 55% B; 6.7-6.9 min: 55-95% B; 6.9-7.9 min: 95% B; 7.9-8.1 min: 95-0% B; 8.1-11.5 min: 0% B. The injection volume was 15 µL. The mobile phase was diverted to waste between 0 and 1.5 min and between 8 and 11.5 min using a VICI (Houston, TX, USA) switching valve.

6.2.5 Mass spectrometry

The Q-TOF mass spectrometer was operated in high sensitivity mode at a resolution of approximately 20,000 at m/z 1000 and in ESI positive ion mode. Mass spectrometric settings were optimized by infusion of the labeled peptides into the mass spectrometer. Specific settings are included in **Table 1**. All mass spectra were collected in profile mode with the start and end mass set respectively at 350 and 900 m/z . Analyst TF software 1.7.1 in combination with MultiQuant 2.0.1 and PeakView 3.0.2 (Sciex) were used for data acquisition and processing. The system was calibrated by application of the standard calibration mixture through the calibrant delivery system unit prior to every batch and during analysis after every 6 injections.

The triple-quadrupole mass spectrometer was operated at unit-mass resolution in ESI positive ion mode. Analyst software 1.6.2 was used for data acquisition and processing. For both MS-systems the following settings were used: IS voltage was set at 5500V, source temperature at 700°C and the DP at 60V. Curtain gas value was 35 psi. For the nebulizer and drying gas 50 and 50 psi were used, respectively. Collision-activated dissociation (CAD) gas was set at 9.

Table 1: amino acid sequence, precursor and product ion m/z, charge states and analyte specific MS-settings for the signature peptides and their SIL-internal standards

Peptide Sequence	Triple Quad MS/ MS and HR-MS/ MS Precursor ion mass (m/z) and charge state	Triple Quad MS/MS Product ion mass (m/z) and charge state	HR-MS/MS Extracted product ion mass (m/z), charge state and extraction window (Da)	CE (V)	Triple Quad MS/MS Dwell Time (ms)	HR-MS/MS Accumulation Time (ms)
FDTNSHNDDALLK	497.2 / [M+3H] ³⁺	671.8 / y ₁₂ ²⁺	614.3090 / y ₁₁ ²⁺ / 0.01, 0.07 and 0.5	22	50	40
FDTNSHNDDALLK [§]	500.0 / [M+3H] ³⁺	675.8 / y ₁₂ ²⁺	671.8236 / y ₁₂ ²⁺ / 0.01, 0.07 and 0.5 618.3152 / y ₁₁ ²⁺ / 0.01	22	50	15
SNLELLR	422.8 / [M+2H] ²⁺	643.4 / y ₅ ⁺	675.8308 / y ₁₂ ²⁺ / 0.01 401.2871 / y ₃ ⁺ / 0.01, 0.07 and 0.5	20	50	40
SNLELLR [*]	427.8 / [M+2H] ²⁺	653.4 / y ₅ ⁺	643.4200 / y ₅ ⁺ / 0.01, 0.07 and 0.5 411.2956 / y ₃ ⁺ / 0.01	20	50	15
LFDNAMLRL	490.3 / [M+2H] ²⁺	719.4 / y ₆ ⁺	653.4290 / y ₅ ⁺ / 0.01 604.3271 / y ₅ ⁺ / 0.01, 0.07 and 0.5	25	50	40
LFDNAMLRL [*]	495.3 / [M+2H] ²⁺	729.4 / y ₆ ⁺	719.3563 / y ₆ ⁺ / 0.01, 0.07 and 0.5 866.4330 / y ₇ ⁺ / 0.01, 0.07 and 0.5 614.3369 / y ₅ ⁺ / 0.01	25	50	15
			876.4395 / y ₇ ⁺ / 0.01			

[§] C-terminal lysine ¹³C₆¹⁵N₂-labeled internal standard

^{*} C-terminal arginine ¹³C₆¹⁵N₄-labeled internal standard

6.2.6 Pharmacokinetic study

Sprague Dawley rats were dosed under appropriate ethical approval with a single 2 mg/kg subcutaneous bolus injection of somatropin (Zomacton®). Blood samples were collected in K₃-EDTA tubes prior to dosing and at 0.5, 1, 2, 4, 8 and 24 hours post-dose. Plasma was prepared immediately after blood collection and stored at -80°C until analysis.

6.3 RESULTS & DISCUSSION

6.3.1 Selection of signature peptides and method optimization

An *in silico* tryptic digestion of the somatropin sequence with Skyline [26] was used to generate a list of, in total, 17 candidate signature peptides. To avoid interferences from the rat plasma proteome, all signature peptides had to be unique for somatropin, which was checked by submitting the preliminary peptide list to the basic local alignment search tool (BLAST) version 2.2.29 [27]. In addition, to facilitate LC-MS quantitation and avoid reduction and alkylation steps, peptides forming disulfide bonds were excluded as well as peptides outside the 300-2000 mass range.

For an extensive evaluation of the applicability of HRMS for the analysis of plasma digests, we wanted to include multiple peptides. Since the three peptides LFDNAMLRL (amino acids 9-16), SNLELLR (71-77) and FDTNSHNDDALLK (146-158) fulfilled all criteria, these were evaluated for further use, also because they represent different parts of the protein structure (C-terminal region, center and N-terminal region, respectively) and because the first peptide contains an oxidizable methionine [28]. Together they will therefore provide extended information about the *in vivo* fate of the protein drug. To confirm the suitability for LC-MS analysis, peptide mapping experiments were conducted using a tryptic digest of a test solution of somatropin after protein precipitation with acetonitrile. Since all three peptides showed appropriate LC-MS characteristics such as good chromatographic retention, efficient ionization and fragmentation and peptide LFDNAMLRL also showed negligible *in vitro* oxidation, they were selected for further work. A multi-step chromatographic gradient was optimized to achieve good peak shape, retention and separation of the peptides (retention times 2.0, 4.2 and 5.6 minutes for peptides LFDNAMLRL, SNLELLR and FDTNSHNDDALLK, respectively). Analyte-specific mass spectrometric parameters are presented in Table 1, as well as the mass transitions used to monitor the peptides and the corresponding stable-isotope labeled internal standards.

Sample preparation was kept as basic as possible to maintain digest complexity and allow optimal evaluation of the effect of the mass spectrometric settings on method selectivity. After protein precipitation of spiked plasma with acetonitrile, pellet digestion performed at pH 8.0 and 37°C and in the presence of 2.5% acetonitrile was complete after 90 min when using 200 µg/mL of trypsin. To increase sensitivity, the relatively large digest volume of 425 µL was reduced to 60 µL by using reversed-phase SPE, evaporation and reconstitution. The recovery of all signature peptides was about 75%. Although very polar

and very non-polar matrix peptides may not have been recovered from the digest because of their breakthrough and non-elution, respectively, the generic SPE approach is expected not to introduce a high degree of selectivity. In particular, matrix peptides eluting at or around the retention times of the signature peptides on the reversed-phase LC column, are not likely to have been removed from the digest using the described procedure.

6.3.2 Reduction of mass extraction window and summation of product ions

The effect of the MEW value on method selectivity is exemplified in **Figure 2A** for peptide SNLELLR, after digestion of plasma spiked at the desired LLOQ of 25 ng/mL of somatotropin. The doubly charged precursor ion (m/z 422.8) was selected in the quadrupole and extracted ion chromatograms were constructed around product ion m/z 401.2871, which corresponds to the singly charged y_3 ion. At a mass extraction window of 0.5 Da, which simulates the typical settings of a triple quadrupole, the signature peptide peak is obscured by a wide range of interfering peaks (**Figure 2A-1**). This illustrates the enormous complexity of the plasma digest and the high similarity of the signature peptide to tryptic peptides that are generated from the plasma proteome. Reducing the MEW to 0.07 Da results in a slight decrease of the signature peptide peak intensity, but more importantly causes a much more pronounced reduction of the interferences (**Figure 2A-2**). By further narrowing the MEW to 0.01 Da, an additional decrease of the interfering peaks is obtained and although the signature peptide response is also further reduced, the resulting signal to noise ratio is more favorable than for the wider MEWs (**Figure 2A-3**).

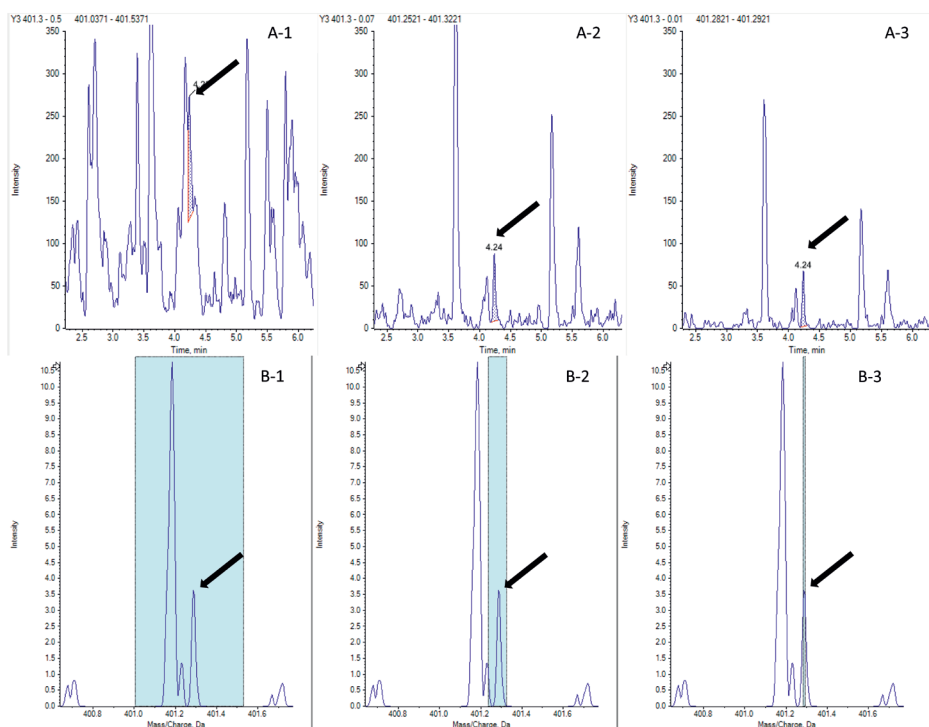


Figure 2: extracted ion chromatograms for signature peptide SNLELLR after digestion of rat plasma spiked with somatropin at 25 ng/mL (A) and corresponding product ion mass spectra (m/z 401.2871 (y_3^{+1}) at the retention time of the analyte (B); MEW of 0.5 Da (A-1, B-1), 0.07 Da (A-2, B-2) and 0.01 Da (A-3, B-3). Arrows indicate retention time (A) or m/z (B) of the analyte. Precursor ion: m/z 422.8.

The cause of this phenomenon is illustrated in **Figure 2B**. The quadrupole, which operates at unit-mass resolution and a MEW of 0.7 Da, selects precursor ions in the m/z range of 422.8 ± 0.35 . After fragmentation of these precursor ions, the TOF mass analyzer, when used at a MEW of 0.5 Da (Figure 2B-1), captures all y_3 ions of the signature peptide, but at the same time also all other matrix product ions in the m/z range of 401.2871 ± 0.25 . At the retention time of the signature peptide alone, at least two other (mass-resolved) peptides contribute to the detection signal and across the entire chromatogram this amounts to more than 30 peptides. The mass resolution of the TOF that was used in this work is approximately 20,000 and at this value a MEW of 0.07 Da extracts the majority of the signature peptide y_3 ions. Within the selected m/z range of 401.2871 ± 0.035 , it appears that one other peptide product ion is partially co-extracted (**Figure 2B-2**). Optimal selectivity is obtained at a MEW of 0.01 Da, or a m/z range of 401.2871 ± 0.005 (**Figure 2B-3**).

An interesting feature of HRMS is the fact that the responses that are obtained for different analyte-related ions can easily be summed post-acquisition to enhance detection sensitivity. Figure 3 illustrates the advantages and disadvantages of this approach. For peptide SNLELLR, three product ions (y_3 , y_4 and y_5) are generated with useful intensities after collision-induced dissociation of the precursor ion, and combining the signals of these product ions leads to an increased analyte response. The summation of y_3 and y_4 causes an approximately 50% increase of the peak area compared to capturing only y_3 (**Figure 3A and 3B**), while after the further inclusion of y_5 the final peak area is about 2-fold higher than for y_3 alone (**Figure 3C**). However, the summation of ion intensities not only causes an increase in analyte peak intensity, but also of the abundance of matrix interferences. Clearly, addition of the response corresponding to the y_4 ion (m/z range: 530.3328 ± 0.005) and of the y_5 ion (m/z range: 643.4200 ± 0.005) introduces a number of additional peaks in the extracted ion chromatograms. Altogether, this demonstrates that summation of the responses of different ions may help improve sensitivity but, depending on the actual m/z values and extraction windows used, the signal to noise ratio may not increase or may even decrease. In addition, accuracy and precision may or may not be affected. Consequently, whether summation of ion intensities is beneficial needs to be determined case by case.

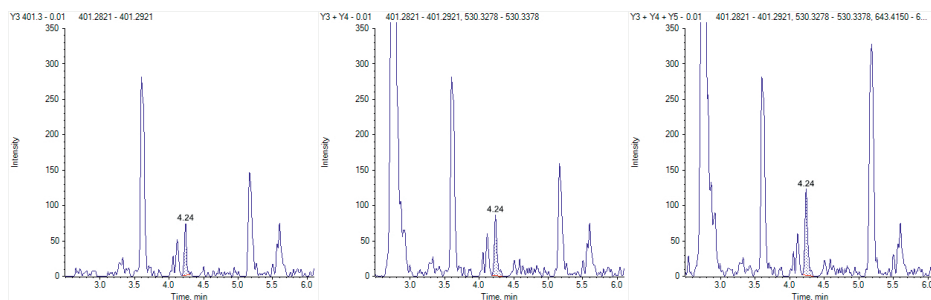


Figure 3: extracted ion chromatograms (MEW 0.01 Da) for signature peptide SNLELLR after digestion of rat plasma spiked with somatropin at 25 ng/mL; precursor ion: m/z 422.8, product ions: y_3 ; m/z 401.2871, y_4 ; m/z 530.3328, y_5 ; m/z 643.4200. (A) response for y_3 only, (B) response for the sum of y_3+y_4 , (C) response for the sum of $y_3+y_4+y_5$. Arrows indicate retention time of the analyte.

Here, two important other remarks have to be made. First, the intensity of the ions to be summated should be approximately equal or at least not be too different. At low analyte levels, ions with insufficient intensity may otherwise be lost, not included in the summation and results may thus be inconsistent with those at higher levels. In the current work, this was no issue for any of the peptides of somatropin. Furthermore, if different charge states of an ionized analyte are to be summated, it should be realized

that the charge state distribution of a peptide or protein can change due to differences in experimental conditions (such as pH or ionic strength of the mobile phase, MS source settings or analyte concentration) [29]. Although for tryptic peptides not many charge states of equal sensitivity typically occur, this effect may also complicate straightforward analyte quantification and should be carefully investigated. For the three tryptic peptides of somatropin only one charge state was encountered for the precursor ion, so this effect did not play a role here.

6.3.3 Accuracy and precision

The gain in selectivity at lower values of the MEW is directly related to method performance in terms of accuracy and precision. **Table 2** shows the results for the different product ions of peptide SNLELLR at different MEW values, for samples spiked with somatropin at the desired LLOQ of 25 ng/mL.

Table 2: summary of precision (CV) and accuracy results for peptide SNLELLR under different HR-MS/MS settings (MEW); somatropin concentration in plasma: 25 ng/mL, n=6.

Product ion	Extraction window (Da)	CV (%)	Accuracy (%)
y_3 (m/z 401.2871)	0.5	61.4	222.0
	0.07	6.0	104.2
	0.01	19.6	94.4
y_4 (m/z 530.3328)	0.5	39.4	106.1
	0.07	18.8	108.1
	0.01	21.8	109.3
y_5 (m/z 643.4200)	0.5	31.0	631.1
	0.07	25.0	135.9
	0.01	19.3	88.5
$y_3 + y_4$	0.5	21.7	209.2
	0.07	9.5	97.6
	0.01	11.9	103.3
$y_3 + y_5$	0.5	19.3	420.8
	0.07	23.1	89.3
	0.01	24.4	84.0
$y_4 + y_5$	0.5	37.8	318.9
	0.07	10.4	97.6
	0.01	7.3	92.7
$y_3 + y_4 + y_5$	0.5	33.2	467.6
	0.07	12.7	91.5
	0.01	8.5	82.6

For y_3 , y_4 as well as y_5 , the presence of the interferences at an MEW of 0.5 Da generally resulted in unfavorable values for accuracy (up to 630%) and precision (CV up to 60%). The responses of the two co-eluting peptides (see **Figure 2**) led to a considerable overestimation of the added analyte concentration, while the high variability in the results was a result of the difficulty in consistently integrating the analyte peak in the presence of an elevated background.

Narrowing the MEW to 0.07 Da and further to 0.01 Da improved the accuracy and precision found for nearly all y-ions or combinations of ions to values that meet international acceptance criteria for small molecules of $\pm 20\%$ at the LLOQ level. Clearly, the decrease of the interfering signals caused by these narrower MEW's resulted in a strongly reduced overestimation of analyte levels and a more reproducible peak integration. For peptide SNLELLR, we selected the sum of the responses for the y_3 and y_4 product ions at a MEW of 0.01 Da as the final approach for quantitation. Although other combinations also resulted in acceptable accuracy and precision, the chromatograms corresponding to this setting allowed the most straightforward integration and this was deemed the most robust compromise between the required selectivity and sensitivity.

For peptides FDTNSHNDDALLK and LFDNAMLRL a comparable situation was found, as shown in the supplementary data (Tables 1 and 2). At a MEW of 0.5 Da, the signature peptide peak in some cases disappeared into the background signal, leading to underestimation of analyte levels (accuracies <75%). The detection sensitivity found for FDTNSHNDDALLK was lower than for the other two peptides and reducing the MEW to 0.01 Da resulted in peaks that were too small to be accurately quantified. Instead, an MEW of 0.07 Da was used as a compromise between sensitivity and selectivity. For this peptide, the combination of the two product ions y_{11} and y_{12} gave the best results. For peptide LFDNAMLRL, summation of three product ions y_5 , y_6 and y_7 was needed at MEW 0.01 Da to obtain optimal results. Because of their higher levels, for all internal standards an MEW of 0.01 Da was sufficient and summation of ions was not necessary. **Table 3** shows the results for accuracy and precision found for all three peptides, obtained using the optimized settings for MEW and summation, for concentrations across the anticipated relevant concentration range. It demonstrates that the usual acceptance criteria for LC-MS as applied to small-molecule quantitation can be met.

Table 3: LLOQ, summary of precision (CV) and accuracy results for the final HR-MS/MS settings for all three peptides; n=6.

Peptide	Precursor ion (m/z)	Product ions (m/z)	MEW (Da)	Concentration (ng/mL)	CV (%)	Accuracy (%)
FDTNSHNDDALLK	497.2	614.3090 (y_{11}) + 671.8236 (y_{12})	0.07	25	15.7	106.6
				50	10.6	103.7
				75	4.4	110.1
				1250	5.4	95.1
				8000	6.4	88.9
SNLELLR	422.8	401.2871 (y_3) + 530.3328 (y_4)	0.01	25	11.9	103.3
				50	10.4	98.7
				75	10.9	99.6
				1250	9.0	97.3
				8000	6.8	91.7
LFDNAMLRL	490.3	604.3271 (y_5) + 719.3563 (y_6) + 866.4330 (y_7)	0.01	25	11.3	88.6
				50	16.3	80.8
				75	7.2	110.2
				1250	12.7	105.4
				8000	1.8	108.3

As shown in **Fig. 2B-3**, at low values for the MEW the mass accuracy of the detector becomes very important, since a slight shift in the mass will easily result in a major difference in the acquired signal or, in the worst case, in completely missing the signal. It is therefore essential that the Q-TOF system is set in a stable climate, because temperature fluctuations can influence the mass calibration due to contraction and expanding of the TOF detector tube. To ensure optimal performance, it is good practice to calibrate the system once every two to three hours, in our situation by infusing a calibrant solution into the source after every six samples. This resulted in an excellent mass accuracy (<2 mDa) as shown in supplementary Figure 1. Depending on the instrument type (e.g. orbitrap) and vendor, the required frequency of recalibration may be different.

6.3.4 Comparison to tandem mass spectrometry

In **Figure 4**, chromatograms are shown for the peptides SNLELLR and FDTNSHNDDALLK, recorded upon triple-quadrupole LC-MS/MS (**Fig. 4A, 4C**) and LC-HR-MS/MS (**Fig. 4B, 4D**) analysis of the same tryptic digest of rat plasma spiked with somatropin at 25 ng/mL.

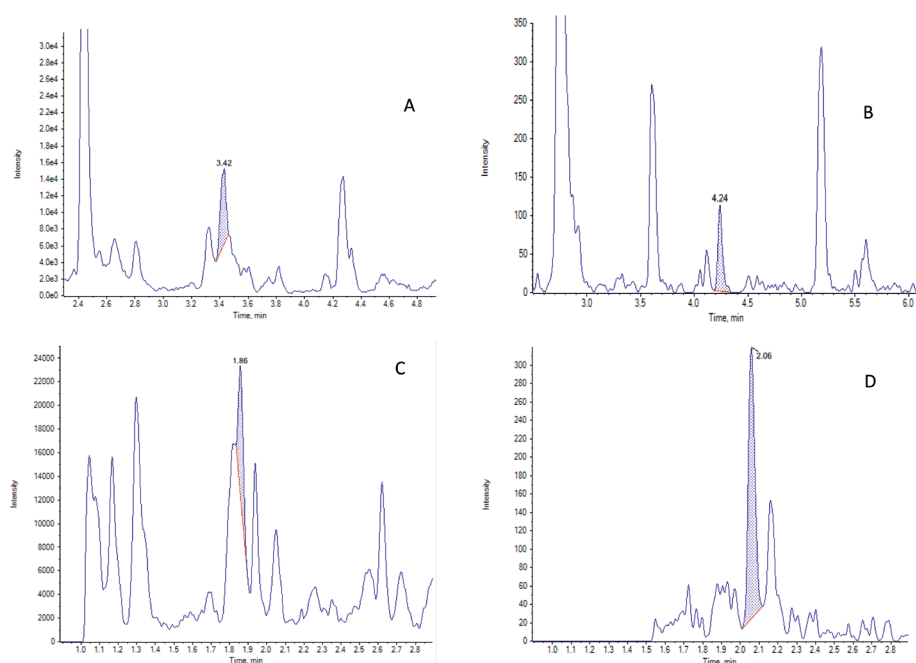


Figure 4: chromatograms for two signature peptides after digestion of rat plasma spiked with somatropin at 25 ng/mL. (A) LC-MS/MS and (B) LC-HR-MS/MS for SNLELLR, (C) LC-MS/MS and (D) LC-HR-MS/MS for FDTNSHNDALLK, recorded using the final settings as summarized in Tables 3 and 4.

For LC-HR-MS/MS, the optimized settings with regard to MEW and summation of ions were used, while for LC-MS/MS the typical approach was followed of quantifying a single product ion (optimized with regard to sensitivity and selectivity) at unit-mass resolution (MEW 0.7 Da). The chromatograms confirm that LC-MS/MS generally gives rise to more interferences in the chromatograms and that a lower LLOQ can be attained using LC-HR-MS/MS, although the absolute instrument sensitivity for LC-MS/MS is better. It is also evident that the degree of improvement varies from peptide to peptide, as FDTNSHNDALLK suffers more from interfering matrix peptides with LC-MS/MS than SNLELLR. The resulting values for accuracy and precision that were obtained for LC-MS/MS are presented in **Table 4**. The interferences are clearly causing poor results for accuracy at lower somatropin concentrations, just as was observed for LC-HR-MS/MS at a MEW of 0.5 Da. Acceptable results for all three peptides were found for somatropin levels at and above 100 ng/mL, which was therefore the practical LLOQ for LC-MS/MS.

Table 4: LLOQ, summary of precision (CV) and accuracy results for the final LC-MS/MS settings for all three peptides; n=6.

Peptide	Precursor ion (m/z)	Product ions (m/z)	Concentration (ng/mL)	CV (%)	Accuracy (%)
FDTNSHNDDALLK	497.2	671.8 (y_{12})	25	4.4	242.2
			50	4.5	143.6
			75	2.2	144.9
			100	2.1	94.7
			1250	0.8	93.7
			8000	0.8	107.1
SNLELLR	422.8	643.4 (y_5)	25	8.1	230.4
			50	7.3	135.8
			75	3.5	125.3
			100	5.3	87.5
			1250	0.4	84.0
			8000	0.9	94.2
LFDNAMLRL	490.3	719.4 (y_6)	25	3.5	226.9
			50	4.5	131.6
			75	2.5	133.4
			100	0.9	93.0
			1250	0.5	86.6
			8000	1.0	100.2

6.3.5 Analysis of preclinical samples

As an example, the pharmacokinetic curves for the three signature peptides, obtained by LC-HR-MS/MS analysis of plasma samples after s.c dosing of somatropin to a rat, are shown in **Figure 5A**. These curves illustrate that the obtained LLOQ of 25 ng/mL for all signature peptides is adequate to monitor the relevant plasma somatropin concentrations. In **Figure 5B**, the corresponding curves after analysis of the same samples by LC-MS/MS are presented. Comparison of the two curves indicates that for some of the later time-points unquantifiable concentrations were found by LC-MS/MS because of its higher LLOQ, and that the use of HR-MS/MS for detection therefore is an advantage. Otherwise, the pharmacokinetic profiles agreed very well. For completeness, the individual plasma concentration results for all animals are shown in the supplementary information (Figure 2).

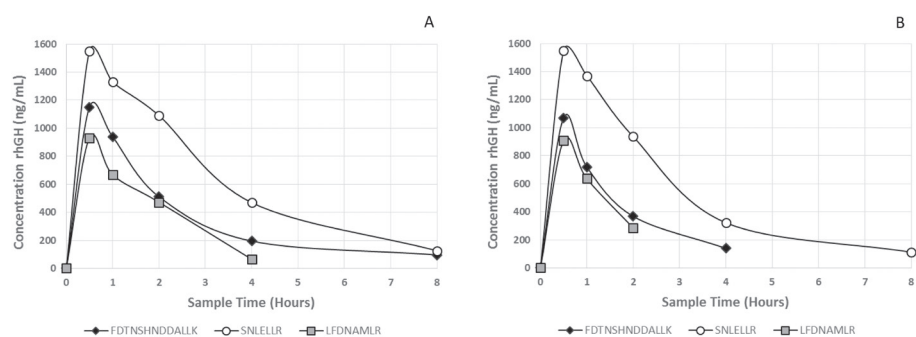


Figure 5: somatropin (rhGH) plasma concentration-time curves obtained for the signature peptides SNLELLR (○), FDTNSHNDALLK (◊) and LFDNAMLRL (□) after 2 mg/kg s.c. dosing to a rat, obtained with LC-HR-MS/MS (A) and LC-MS/MS (B).

The three signature peptides consistently gave dissimilar concentration results in the plasma samples of dosed rats, whereas no differences were seen in spiked samples. Generally, the highest concentrations were found for the mid-protein peptide SNLELLR. The other two peptides, which are located closer to the C- and N-terminus of somatropin, respectively, typically yielded lower and also more comparable concentrations. Altogether, this suggests an *in vivo* effect, in which the central part of the protein is less susceptible to enzymatic and/or chemical modifications than the C- and N-terminal parts. The fact that the concentrations found for FDTNSHNDALLK and for the methionine-containing peptide LFDNAMLRL generally were quite similar suggests that oxidation of the methionine probably plays a negligible role.

6.4 CONCLUSION & DISCUSSION

In this work, we show the potential of LC-HR-MS/MS for the quantitation of proteins after the digestion of a complex biological matrix. The use of a Q-TOF mass spectrometer with a mass resolution of about 20,000 allowed the selection of a relatively large part of the product ions that were formed after collision-induced dissociation in a narrow mass extraction window. In this way, a good analyte detection signal was obtained, while at the same time peptides originating from the digestion of matrix proteins were largely excluded from detection. By reducing the MEW from 0.5 to 0.01 Da, the number of interfering peaks in the extracted ion chromatograms was considerably reduced which facilitated the determination of three different signature peptides. Detection sensitivity

was further enhanced by the summation of the responses of multiple product ions for each of the signature peptides, allowing quantitation with acceptable accuracy and precision down to levels corresponding to 25 ng/mL of the intact protein somatropin in rat plasma. The conditions for optimal selectivity and sensitivity varied from peptide to peptide and, in general, the MEW settings as well as the summation of responses have to be optimized for any given signature peptide and product ion. To avoid missing the detection of part or all of the product ions when a narrow MEW is used, a high mass accuracy of the mass spectrometer is important and frequent calibration of the instrument is advisable. Comparison of LC-HR-MS/MS with LC-MS/MS showed that, while the absolute instrument sensitivity of the latter typically is better, the possibility of removing interfering peaks from the chromatograms by narrowing the MEW on HRMS may finally result in lower LLOQ values. Published LC-MS methods for the quantification of somatropin or endogenous hGH after digestion use elaborate sample preparation strategies such as immunocapture and multi-stage SPE, in combination with nano-LC or two-dimensional LC to achieve LLOQs in the 2.7-10 ng/mL-range with sample volumes of 100 to 800 μ L of plasma/serum [30-32]. The results of the current work demonstrate that LC-HR-MS/MS can be a straightforward alternative to reach the same order of sensitivity. Although HRMS may not always outperform triple quadrupole MS in terms of selectivity and sensitivity, the results in the current paper show that the use of HRMS can be a useful tool to improve the performance of bioanalytical LC-MS methods for proteins.

EXECUTIVE SUMMARY

- In HRMS, the mass extraction window (MEW) can be reduced from 0.5 Da, which is comparable to triple quadrupole MS detection, down to values as low as 0.001 Da.
- Reducing the MEW typically results in an increase of selectivity and although reduction to values below 0.05 Da will result in a loss of absolute sensitivity, there may be a gain in signal to noise ratio.
- With HRMS, it is relatively easy to sum the responses of different ions to enhance sensitivity, although this summation may also increase the response of background interferences.
- LC with HR-MS/MS detection may represent a useful tool for the quantitation of proteins after digestion of biological samples and improve method selectivity and sensitivity without the need for lengthy experimental extraction procedures.

FUTURE PERSPECTIVE

With LC-MS now being an established analytical platform for protein quantitation, mass spectrometric approaches other than MS/MS on a triple quadrupole are beginning to be explored. Because of its potential to improve selectivity and sensitivity of bioanalytical methods, as shown in this paper, we expect that HRMS for protein quantitation will grow in importance in the next few years and that the technique will find its place in research and regulated laboratories, probably next to triple-quadrupole mass spectrometry. If technological advances continue to provide more sensitive, robust and affordable instruments, LC-HR-MS/MS may in the end be expected to become the technique of first choice for protein quantitation in complex biological matrices.

REFERENCES

1. Li F, Fast D, Michael S. Absolute quantitation of protein therapeutics in biological matrices by enzymatic digestion and LC-MS. *Bioanalysis* 3(21), 2459–2480 (2011).
2. Van den Broek I, Niessen WMA, van Dongen WD. Bioanalytical LC-MS/MS of protein-based biopharmaceuticals. *J. Chromatogr. B* (929), 161–179 (2013).
3. Yang Z, Li W, Smith HT, Tse FLS. LC-MS bioanalysis of proteins. In: Li W, Zhang J, Tse FLS (eds) *Handbook of LC-MS bioanalysis*. John Wiley & sons, 601–605 (2013).
4. Cross TG, Hornshaw MP. Can LC and LC-MS ever replace immunoassays?, *Journal of Applied Bioanalysis* 2(4), 108–116 (2016).
5. An B, Zhang M, Johnson RW, Qu J. Surfactant-aided precipitation/on-pellet-digestion (SOD) procedure provides robust and rapid sample preparation for reproducible, accurate and sensitive LC/MS quantification of therapeutic protein in plasma and tissues. *Anal. Chem.* 87(7), 4023–4029 (2015).
6. Bronsema KJ, Bischoff R, Pijnappel WWMP, van der Ploeg AT, van de Merbel NC. Absolute quantification of the total and antidrug antibody-bound concentrations of recombinant human α -glucosidase in human plasma using protein G extraction and LC-MS/MS. *Anal. Chem.* 87(8), 4394–4401(2015).
7. Bults P, Bischoff P, Bakker H, Gietema JA, van de Merbel NC. LC-MS/MS-based monitoring of in vivo protein biotransformation: quantitative determination of trastuzumab and its deamidation products in human plasma. *Anal. Chem.* 88(3), 1871–1977 (2016).
8. Bronsema KJ, Bischoff R, van de Merbel NC. High-sensitivity LC-MS/MS quantification of peptides and proteins in complex biological samples: the impact of enzymatic digestion and internal standard selection on method performance. *Anal. Chem.* 85(20), 9528–9535 (2013).
9. Bischoff R, Bronsema KJ, van de Merbel NC. Analysis of biopharmaceutical proteins in biological matrices by LC-MS/MS – I. Sample preparation. *Trends Anal. Chem.* 48, 41–51 (2013).
10. Wilffert D, Bischoff R, van de Merbel NC. Antibody-free workflows for protein quantification by LC-MS. *Bioanalysis* 7(6), 763–779 (2015).
11. Van de Merbel NC. Sample preparation for quantitative LC-MS bioanalysis of proteins, in: Li W, Jian W, Fu Y (eds) *Sample preparation in quantitative LC-MS bioanalysis*, John Wiley & sons, in press.
12. Wilffert D, Donzelli R, Asselman A et al. Quantitative antibody-free LC-MS/MS analysis of sTRAIL in sputum and saliva at the sub-ng/mL level. *J. Chromatogr. B* 1032, 205–210 (2016).
13. Zhou S, Vazvaei F, Ferrari L, Qu J. Practical considerations in enhancing LC-MS sensitivity for therapeutic protein bioanalysis. *Bioanalysis* 9(18), 1353–1356 (2017).
14. Huang MQ, Lin Z, Weng N. Applications of high-resolution MS in bioanalysis. *Bioanalysis* 5, 1269–1276 (2013).
15. Fung EN, Jemal M, Aubry AF. High-resolution MS in regulated bioanalysis: where are we now and where do we go from here? *Bioanalysis* 5, 1277–1284 (2013).
16. Zhang NR, Yu S, Tiller P, Yeh S, Mahan E, Emary WB. Quantitation of small molecules using high-resolution accurate mass spectrometers – a different approach for analysis of biological samples. *Rapid Commun. Mass Spectrom.* 23, 1085–1094 (2009).
17. Henry H, Sobhi HR, Scheibner O, Bromirski M, Nimkar SB, Roc B. Comparison between a high-resolution single-stage Orbitrap and a triple quadrupole mass spectrometer for quantitative analyses of drugs. *Rapid Commun. Mass Spectrom.* 26, 499–509 (2012).
18. Dillen L, Cools W, Vereyken L et al. Comparison of triple quadrupole and high-resolution TOF-MS for quantification of peptides. *Bioanalysis* 4, 565–579 (2012).
19. Morin LP, Mess JN, Garofolo F. Large-molecule quantification: sensitivity and selectivity head-to-head comparison of triple quadrupole with Q-TOF. *Bioanalysis* 5, 1181–1193 (2013).

20. Plumb RS, Fujimoto G, Mather J *et al.* Comparison of the quantification of a therapeutic protein using nominal and accurate mass MS/MS. *Bioanalysis* 4, 605-615 (2012).
21. Mekhssian K, Mess JN, Garofolo F. Application of high-resolution MS in the quantification of a therapeutic monoclonal antibody in human plasma. *Bioanalysis* 6, 1767-1799 (2014).
22. Kellie JF, Kehler JR, Szapacs ME. Application of high-resolution MS for development of peptide and large-molecule drug candidates. *Bioanalysis* 8, 169-177 (2016).
23. Sundberg M, Strage EM, Bergquist J, Holst BS, Ramström M. Quantitative and selective analysis of feline growth related proteins using parallel reaction monitoring high resolution mass spectrometry. *PLoS One*, 11(12) (2016).
24. Sun H, Zhang Q, Zhang Z, Tong J, Chu D, Gu J. Simultaneous quantitative analysis of polyethylene glycol (PEG), PEGylated paclitaxel and paclitaxel in rats by MS/MSALL technique with hybrid quadrupole time-of-flight mass spectrometry. *J. Pharm. Biomed. Anal.* 145, 255-261 (2017).
25. Zhao Y, Liu G, Yuan X, et al. Shen. Strategy for the quantitation of a protein conjugate via hybrid immunocapture-liquid chromatography with sequential HRMS and SRM-based LC-MS/MS analyses. *Anal. Chem.* 89(9), 5144-5151 (2017).
26. Niedermeyer THJ, Strohal M. mMass as a Software Tool for the Annotation of Cyclic Peptide Tandem Mass Spectra. *PLoS One* 7(9) (2012).
27. Altschul S, Madden T, Schaffer A *et al.* Gapped BLAST and PSI- BLAST: a new generation of protein database search programs. *Nucleic acids Res.* 25(17), 3389-3402 (1997).
28. Bults P, van de Merbel NC, Bischoff R. Quantification of biopharmaceuticals and biomarkers in complex biological matrices: a comparison of liquid chromatography coupled to tandem mass spectrometry and ligand binding assays. *Expert Rev. Proteomics.*, 1-19 (2015).
29. Campbell J, Blanc J Le. Peptide and protein drug analysis by MS: challenges and opportunities for the discovery environment. *Bioanalysis*, 645-657 (2011).
30. Pritchard C, Groves KJ, Biesenbruch S *et al.* Quantification of human growth hormone in serum with a labeled protein as an internal standard: essential consideration. *Anal. Chem.* 86 (13), 6525-6532 (2014).
31. Arsene CG, Henrion A, Diekmann N *et al.* Quantification of growth hormone in serum by isotope dilution mass spectrometry. *Anal. Biochem* 401(2), 228-235 (2010).
32. Such-Sanmartín G, Bache N, Bosch J *et al.* Detection and differentiation of 22kDa and 20kDa growth hormone proteoforms in human plasma by LC-MS/MS. *Biochim. Biophys. Acta - Proteins and Proteomics* 1854(4), 284-290 (2015).

ACKNOWLEDGMENTS

Samenwerkingsverband Noord-Nederland (SNN) is gratefully acknowledged for financial support (grant T3041).

FINANCIAL & COMPETING INTERESTS DISCLOSURE

The authors have no other relevant affiliations or financial involvement with any organization or entity with a financial interest in or financial conflict with the subject matter or materials discussed in the manuscript. This includes employment, consultancies, honoraria, stock ownership or options, expert testimony, grants or patents received or pending, or royalties. No writing assistance was utilized in the production of this manuscript.

ETHICAL CONDUCT OF RESEARCH

The authors state that they have obtained appropriate institutional review board approval or have followed the principles outlined in the Declaration of Helsinki for all human or animal experimental investigations.

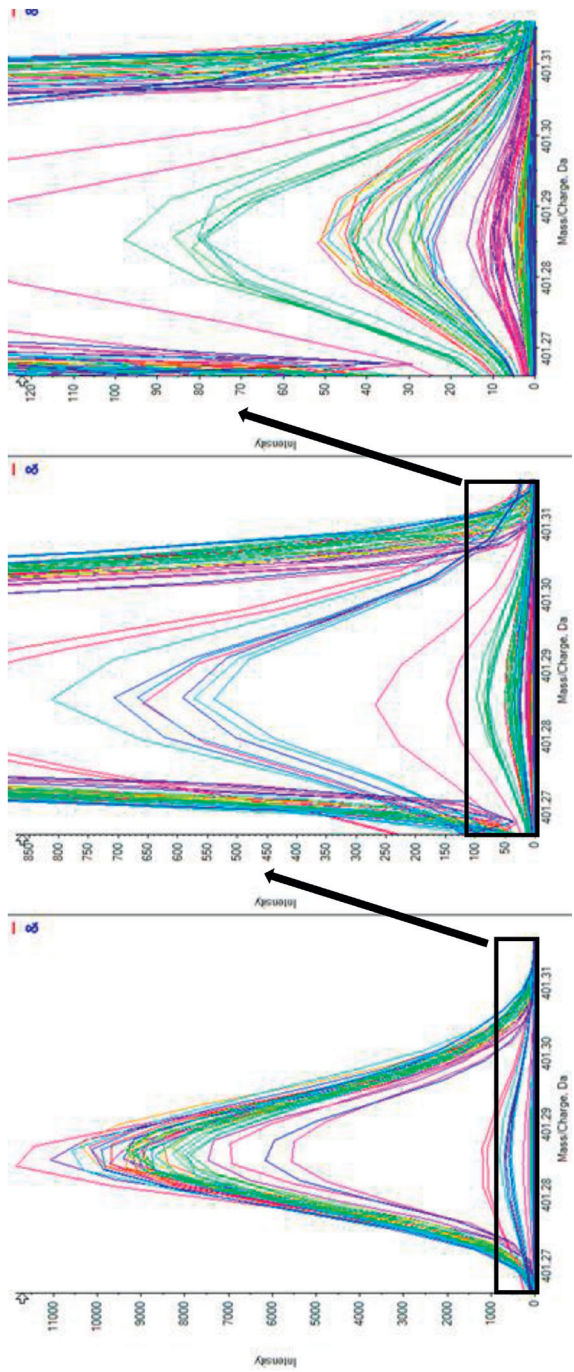
SUPPLEMENTARY DATA

Supplementary Table 1: summary of precision (CV) and accuracy results for peptide FDTNSHNDDALLK under different HR-MS/MS settings (MEW); somatropin concentration in plasma: 25 ng/mL, n=6.

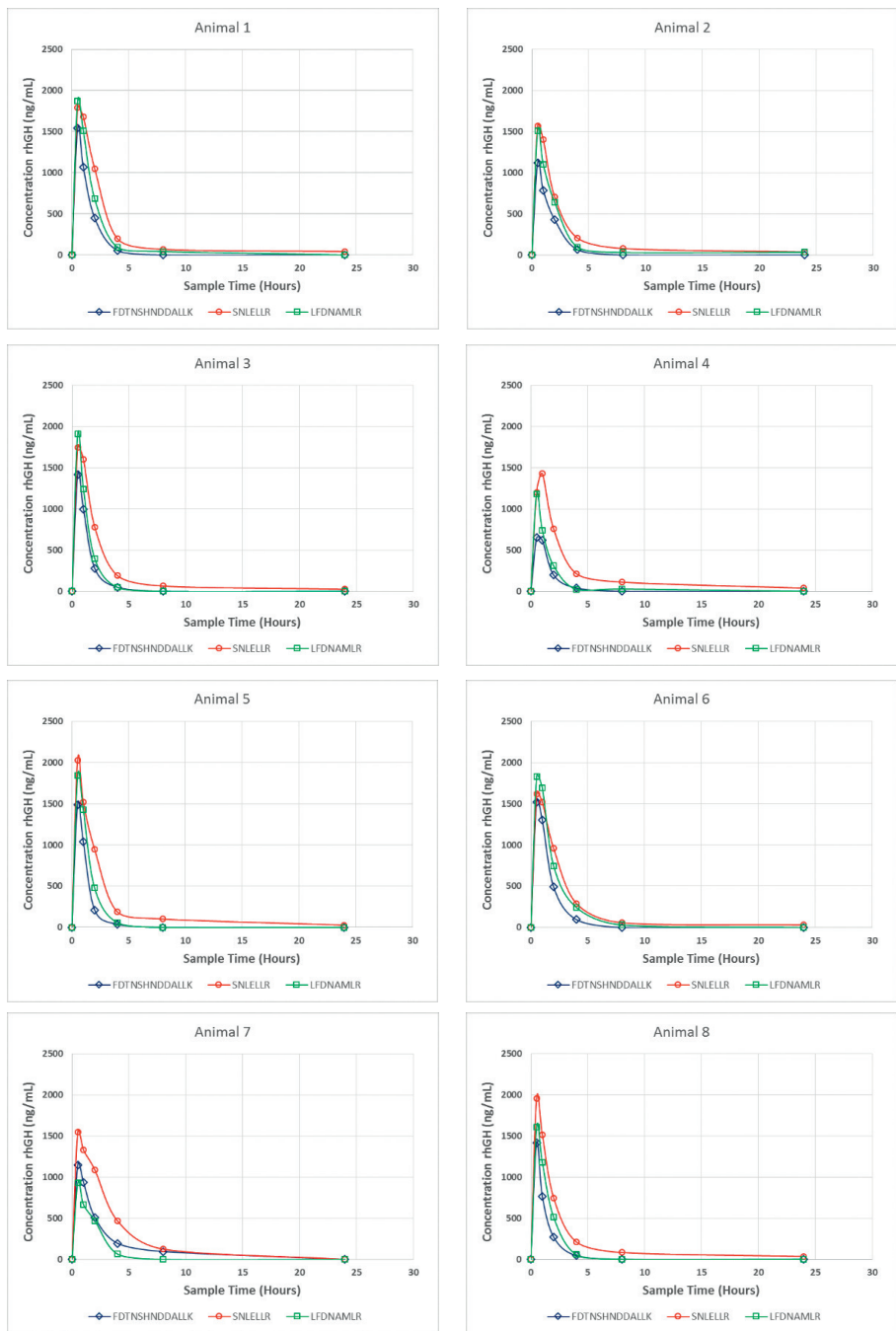
Product ion	Extraction window (Da)	CV (%)	Accuracy (%)
y_{11} (m/z 614.3090)	0.5	9.1	90.1
	0.07	16.8	66.4
	0.01	27.3	67.9
y_{12} (m/z 671.8236)	0.5	12.7	259.4
	0.07	17.4	232.8
	0.01	18.2	139.6
$y_{11} + y_{12}$	0.5	24.2	134.2
	0.07	15.7	106.6
	0.01	21.3	106.8

Supplementary Table 2: summary of precision (CV) and accuracy results for peptide LFDNAMLRL under different HR-MS/MS settings (MEW); somatropin concentration in plasma: 25 ng/mL, n=6.

Product ion	Extraction window (Da)	CV (%)	Accuracy (%)
y_5 (m/z 614.3369)	0.5	14.0	328.8
	0.07	31.7	311.5
	0.01	22.1	265.2
y_6 (m/z 729.3678)	0.5	40.0	22.7
	0.07	21.1	26.0
	0.01	17.2	51.5
y_7 (m/z 876.4395)	0.5	19.8	131.8
	0.07	34.5	72.2
	0.01	17.3	123.3
$y_5 + y_6$	0.5	24.1	45.0
	0.07	23.1	54.8
	0.01	17.4	89.8
$y_5 + y_7$	0.5	10.1	160.9
	0.07	20.4	173.4
	0.01	16.7	201.4
$y_6 + y_7$	0.5	39.3	27.6
	0.07	17.3	43.0
	0.01	16.7	68.7
$y_5 + y_6 + y_7$	0.5	18.7	53.1
	0.07	17.2	54.9
	0.01	11.3	88.6



Supplementary Figure 1: mass accuracy across a batch of 80 samples. Each trace represents a product ion mass spectrum (y_3^+ , m/z 401.2871) of one sample for the signature peptide SNLELLR.



Supplementary Figure 2: somatotropin (rhGH) plasma concentration-time curves obtained for the signature peptides SNLELLR (○), FDTNSHNDALLK (◇) and LFDNAMLR (□) after 2 mg/kg s.c. dosing to different rats (A-H), obtained with LC-HRMS.

CHAPTER VII

Intact Protein Quantification in Biological Samples by Liquid Chromatography – High-Resolution Mass Spectrometry: Somatropin in Rat Plasma

Peter Bults^{1,2}, Anders Sonesson³, Magnus Knutsson³, Rainer Bischoff¹, Nico C. van de Merbel^{1,2}

¹ *Department of Analytical Biochemistry, Groningen Research Institute of Pharmacy, University of Groningen, Antonius Deusinglaan 1, 9713 AV, Groningen, The Netherlands*

² *Bioanalytical Laboratory, PRA Health Sciences, Amerikaweg 18, 9407 TK, Assen, The Netherlands*

³ *Ferring Pharmaceuticals, Kay Fiskers Plads 11, DK-2300 Copenhagen, Denmark.*

J. Chromatogr. B, 2020, 1144, 122079

ABSTRACT

The quantitative determination of intact proteins in biological samples by LC with high-resolution MS detection can be a useful alternative to ligand-binding assays or LC-MS-based quantification of a surrogate peptide after protein digestion. The 22-kDa biopharmaceutical protein somatropin (recombinant human growth hormone) was quantified down to 10 ng/mL (0.45 nM) in 75 μ L of rat plasma by the combination of an immunocapture step using an anti-somatropin antibody and LC-MS on a quadrupole-time of flight instrument. Accuracy and precision of the method as well as its selectivity and sensitivity did not depend on the width of the mass extraction window nor on whether only one or a summation of multiple charge states of the protein analyte were used as the detection response. Quantification based on deconvoluted mass spectra showed equally acceptable method performance but with a less favorable lower limit of quantification of 30 ng/mL. Concentrations in plasma after dosing of somatropin to rats correlated well for the deconvolution approach and the quantification based on the summation of the response of the four most intense charge states (14+ to 17+) of somatropin.

7.1 INTRODUCTION

Over the past decade, there have been many developments in the field of targeted protein quantification by liquid-chromatography-mass spectrometry (LC-MS) and this technique has become a viable alternative to the traditional ligand-binding assays (LBAs). Analytical advantages of LC-MS for protein quantification include superior accuracy and precision, a wider linear dynamic range, the potential to measure multiple analytes simultaneously and no, or at least a lesser, dependence on critical immunochemical reagents that may be difficult to obtain and/or vary in quality. The major drawback of LC-MS compared to LBA is its limited detection sensitivity. Consequently, complicated workflows may be needed to allow protein quantification at trace levels in complex matrices. In particular, an enzymatic digestion step to convert a protein into a series of peptides is part of most LC-MS methods, to reduce the macromolecular analyte to a size that can readily and sensitively be quantified by MS/MS detection on a triple-quadrupole mass spectrometer [1-6].

Although this quantification approach via a so-called signature or surrogate peptide is being applied with much success in the medical and pharmaceutical sciences, it is increasingly recognized that it also has some disadvantages. The selected signature peptide may represent as little as a few percent of the original protein analyte and since the rest of the molecule is disregarded, important information about the *in vivo* fate of a dosed or endogenously occurring protein may be lost. This can be addressed to some extent by including multiple peptides from relevant parts of the protein in an LC-MS assay [7], but quantification of the intact protein would be the most direct and most comprehensive approach.

In recent years, the proof of principle of intact protein quantification by LC-MS has been demonstrated, typically by using high-resolution mass spectrometry (HRMS) on an Orbitrap or quadrupole-time of flight (QTOF) system. Initially, the approach was restricted to relatively small (< 15 kDa) proteins [8], but more recently molecules as large as protein domains [9] and even intact monoclonal antibodies [10,11] were successfully quantified in biological samples at the low- $\mu\text{g/mL}$ to high- ng/mL level. Intact protein quantification requires a quite different analytical approach than analysis after digestion [12]. Next to the need for specific LC stationary phases to separate the intact protein species, selective extraction from the biological matrix by means of immunocapture techniques is indispensable to avoid interference from endogenous matrix proteins. In addition, data handling is more complicated. Electrospray ionization (ESI) leads to complex mass spectra

because the ionized protein analyte occurs in multiple charge states (the so-called charge-state envelope). The number of different charge states depends on the size and shape of the protein as well as on the ionization conditions; for large proteins such as antibodies, it can be as high as 30 [10,11]. Each of the charge states is further subdivided into several ions with different mass-to-charge (m/z) ratios because of the occurrence of different numbers of heavy isotopes, notably ^{13}C -atoms, in the protein structure, and these isotopologue ions may or may not be mass spectrometrically resolved. All this results in a distribution of the MS-signal over a large number of analyte ions with different m/z values, which leads to a limited detection response per ion. Typically, so-called extracted ion chromatograms (EIC's) are created by recording the responses of one or more ions and detection sensitivity can be enhanced by summing up the intensities of multiple ions. Alternatively, dedicated software can be applied to deconvolute the entire mass spectrum into a much-simplified neutral spectrum, which can be used as the basis for quantification. Since all approaches have their theoretical pros and cons, careful optimization is required to arrive at a method that shows acceptable sensitivity, selectivity, precision and accuracy [13].

To support preclinical research with the 22-kDa recombinant protein somatotropin in rats, we previously developed and validated an LC-HRMS method which included a digestion step and quantification of three peptides from different parts of the molecule [14]. In the present report, we describe a complementary method which enables quantification of the intact protein in rat plasma down to 10 ng/mL. The importance of an immunocapture step and the data handling approach (selection of charge states and deconvolution) is described, and a comparison of the pharmacokinetic results for intact somatotropin obtained after quantitation based on extracted ion chromatograms and obtained after deconvolution is provided.

7.2 EXPERIMENTAL

7.2.1 Chemicals and materials

Somatotropin (recombinant human growth hormone, rhGH; UniProtKB ID 'P01241'; Phe27-Phe217), supplied as a lyophilized sterile powder, was obtained from Ferring (Copenhagen, Denmark), its amino acid sequence is given in Figure S-1 (supplementary information). The internal standard, N-terminal His-tag labelled rhGH (Cat. No. ABIN1719793; six histidine moieties) was purchased from Antibodies-online (Aachen, Germany). The capture antibody, mouse anti-human growth hormone monoclonal antibody (Cat. No. ab9821), was

obtained from Abcam (Cambridge, United Kingdom). A protein biotin labelling kit (Cat. No. 11418165001; Roche) was purchased from Sigma Aldrich (St. Louis, MO, USA). Pierce™ streptavidin-coated magnetic beads (Cat No. 88817) were obtained from Thermo Fisher Scientific (Waltham, MA, USA). Rat growth hormone binding protein (Cat. No. CYT-933) was purchased from ProSpec Protein Specialists (Ness-Ziona, Israel) and catalase (2000-5000 units/mg, Cat. No. C9322) from Sigma Aldrich. Acetonitrile, formic acid, ammonia (25%) and hydrochloric acid (37%) were obtained from Merck (Darmstadt, Germany) and Tween-20, citric acid, sodium chloride, hydrogen peroxide (30%) and Tris from Sigma Aldrich. HPLC grade water was prepared using a water purification system from Merck-Millipore. Rat EDTA plasma (Sprague Dawley, hereafter referred to as (blank) rat plasma) was obtained from Seralabs (Haywards Heath, UK). ESI positive calibration solution for the Q-TOF system (Cat No. 4463272) was obtained from Sciex (Toronto, Canada). Oxidized somatropin was prepared in house by incubating a mixture of 475 μ L 1.00- μ g/mL somatropin solution in water and 25 μ L 5% hydrogen peroxide at 20°C for up to 165 min. Excess hydrogen peroxide was subsequently removed from the sample by adding 25 μ L catalase solution (the equivalent of 500 units) and further incubating for 5 min at 20°C.

7.2.2 Preparation of calibration and quality control samples

A somatropin stock solution at 10.0 mg/mL was prepared by dissolving the contents of a vial of lyophilized protein (label claim: 10.0 mg) in 1.00 mL of water according to the manufacturer's instructions for use. The stock solution was divided into 0.2 mL aliquots in Eppendorf Protein Lo-bind tubes (VWR International, Amsterdam, The Netherlands) and stored at -80°C. Two plasma stocks were prepared by diluting the stock solution to 10000 ng/mL with blank rat plasma. One plasma stock was used to prepare calibration samples in rat plasma at 10.0, 20.0, 50.0, 100, 200, 500, 800 and 1000 ng/mL. Similarly, quality control (QC) samples were prepared in rat plasma from the other stock at 30.0, 100 and 500 ng/mL. All samples were stored in Eppendorf Protein Lo-bind tubes at -80°C.

7.2.3 Pharmacokinetic study

After obtaining ethical approval, Sprague Dawley rats were dosed with a single subcutaneous bolus injection of 2 mg/kg somatropin (Zomacton®). Blood samples were collected in K₃-EDTA tubes before and 0.5, 1, 2, 4, 8 and 24 hours after dosing. Plasma was prepared immediately after blood collection and transferred to -80°C until analysis.

7.2.4 Sample pretreatment

The capture antibody was biotinylated according to the instructions provided with the protein biotin labelling kit. Briefly, 300 μL anti-human rhGH antibody (1.00 mg/mL in PBS with 0.1% sodium azide, pH 7.4) was incubated at room temperature and protected from light, at 250 rpm for two hours with 20.0 μL freshly prepared Biotin 7-NHS labelling solution (0.710 mg/mL in DMSO). After incubation, the mixture was purified by running it over a Sephadex G-25 gel filtration column. The concentration of the biotinylated antibody was calculated by measuring the optical density (280 nm) of the purified solution against a corresponding blank solution and found to be 181 $\mu\text{g/mL}$. The biotinylated antibody was stored in 100 μL aliquots in Protein Lo-bind tubes at -80°C .

Sample analysis was performed as follows. Aliquots of 75 μL of rat plasma were pipetted into the 500- μL wells of an Eppendorf Protein Lo-bind 96-well plate (VWR International) and 50 μL of a freshly diluted capture antibody solution, at 10.0 $\mu\text{g/mL}$ in water, was added. Next, 200 μL of immunocapture buffer (75 mM NaCl and 8.4 mM aqueous Tris buffer at pH 7.2), containing 100 ng/mL of internal standard (His-tag labelled rhGH) was added to each of the samples. The samples were incubated at 45°C and 900 rpm for 60 minutes using an Eppendorf (Hamburg, Germany) Thermomixer® comfort, to allow binding of somatropin and internal standard to the biotinylated capture antibody. Simultaneously, 15- μL aliquots of the streptavidin-coated magnetic bead solution were washed twice with 200 μL 0.2% Tween-20 in immunocapture buffer, in a separate Protein Lo-bind 96-well plate. The magnetic beads were isolated by letting the plate stand for 8 minutes on a 96-well magnet plate from Alpaqua Magnum FLX (Beverly, MA, USA) and removing the wash solution. Next, the samples were transferred to the plate containing the washed magnetic beads and subsequently incubated for 90 minutes at 45°C and 900 rpm, using a Thermomixer®, to allow capturing of the antibody-somatropin complex by the magnetic beads. The beads were washed twice with 300 μL immunocapture buffer and once with 300 μL water. Somatropin and internal standard were eluted by mixing the beads for 10 minutes with 60 μL elution buffer (0.1M citric acid in water : acetonitrile (90 : 10, v/v)) at 45°C and 900 rpm, using a Thermomixer®, and subsequent capture of the beads for 5 minutes (total elution time: 15 minutes). The eluates were transferred into 300- μL glass vials and placed in an autosampler or refrigerator at 10°C until analysis.

7.2.5 Chromatography

Processed samples were analyzed using a NexeraX2 (Shimadzu, Tokyo, Japan) LC system. Chromatographic separation was performed at 80°C on a 2.1 × 100 mm (particle size 1.7 µm, pore size 300Å) ACQUITY UPLC Protein BEH C4 column (Waters, Milford, MA, USA, Cat No. 186004496). Mobile phase A consisted of 0.1% formic acid in water and mobile phase B was 0.1% formic acid in acetonitrile. Gradient elution was performed at 0.6 mL/min using the following profile: 0.0-10.0 min: 10-45% B; 10.0-10.5 min: 45-85% B; 10.5-12.5 min: 85% B; 12.5-12.6 min: 85-10% B; 12.6-15.0 min: 10% B. The injection volume was 40 µL. The mobile phase was diverted to waste between 0 and 6.5 min and between 11.5 and 15.0 min, after injection, using a VICI (Houston, TX, USA) switching valve, placed between the column and the mass spectrometer.

7.2.6 Mass spectrometry

Detection took place on a Sciex TripleTOF 6600 Q-TOF mass spectrometer equipped with a Dual Spray source, which was operated in positive-ion TOF MS mode at a resolution of approximately 40,000 at m/z 829. Analyst TF software 1.7.1 in combination with MultiQuant™ 2.1.2 including Research Features Software for charge state deconvolution, PeakView™ 3.0.2 and BioPharmaView™ 3.0 (Sciex) were used for data acquisition and processing. For the MS-system the following optimum settings were used: ionspray voltage at 5500V, source temperature at 600°C, declustering potential at 30V, curtain, nebulizer and drying gas at 35 psi, 50 psi and 50 psi, respectively. All mass spectra were recorded over the range of m/z 550 to m/z 2100. The system was calibrated by application of the ESI positive calibration solution through the calibrant delivery system unit prior to every batch and during analysis after every 6 injections. Extracted ion chromatograms were created by the extraction and subsequent summation of the 14⁺, 15⁺, 16⁺ and 17⁺ charge states of somatropin, each with a mass extraction window (MEW) of ± 0.5 Da around the target mass, details of which are presented in **Table 1**. Deconvolution was performed using the integrated, maximum entropy algorithm within MultiQuant™. The deconvolution parameters used are shown in Supplementary Figure S-2. The resulting main peak in the reconstructed average mass spectrum was subsequently integrated and the ratio of its area over that of the similarly deconvoluted internal standard was used for further quantification.

Table 1: Overview of m/z values and mass extraction windows used for quantification of the different charge states of somatropin and internal standard.

Compound	Charge state	Center extraction mass (m/z)	Mass extraction window (m/z)		
			1.0 Da	0.25 Da	0.0625 Da
Somatropin	14+	1581.3000	1580.8000 - 1581.8000	1581.1750 - 1581.4250	1581.2688 - 1581.3313
Somatropin	15+	1476.1000	1475.6000 - 1476.6000	1475.9750 - 1476.2250	1476.0688 - 1476.1313
Somatropin	16+	1383.9000	1383.4000 - 1384.4000	1383.7750 - 1384.0250	1383.8688 - 1383.9313
Somatropin	17+	1302.5000	1302.0000 - 1303.0000	1302.3750 - 1302.6250	1302.4688 - 1302.5313
Internal Standard	15+	1530.1750	1529.6750 - 1529.9250		
Internal Standard	16+	1434.6250	1434.1250 - 1434.3750		
Internal Standard	17+	1350.2750	1349.7750 - 1350.0250		
Internal Standard	18+	1275.3250	1274.8250 - 1275.0750		

7.3 RESULTS AND DISCUSSION

7.3.1 Immunocapture performance

For the selective LC-MS-based quantification of trace levels of intact proteins in complex biological matrices such as plasma and serum, it is important that samples are sufficiently cleaned up, to avoid interference of endogenous matrix proteins, many of which are present at much higher concentrations than the analytes. Conventional techniques such as solid-phase extraction (SPE), based on reversed-phase or ion-exchange principles, typically do not provide enough discrimination between endogenous proteins and the analyte for detection at the ng/mL level in plasma, which was required for supporting the preclinical study with somatropin in rats. Therefore, a more selective immunocapture (IC) step was optimized using a commercially available anti-somatropin monoclonal antibody. Because of its practical ease of use and high sample throughput, a magnetic-bead-based approach in a 96-well format was selected. The capture antibody was biotinylated and

after incubation with sample, the resulting complex was captured by streptavidin-coated beads, which results in an IC complex that is very strongly bound to the beads, because of the high affinity of the biotin-streptavidin interaction [5]. The extraction was optimized with regard to amount of antibody and magnetic beads, duration and temperature of the capture and elution steps, and the composition of the wash and elution solvents (see Table S-1 in the supplementary materials for details).

Although various other IC approaches exist [15,16], in our hands pre-incubation of 75 μ L of rat plasma with 50 μ L of a capture antibody solution (10 μ g/mL) and an incubation step, followed by subsequent addition of 15 μ L of magnetic beads solution and a second incubation step, resulted in high and reproducible extraction recoveries (>80%) with good linearity. This indicates that the amounts of IC materials used had adequate binding capacity. Endogenous plasma constituents, which could possibly interfere at the retention time of somatotropin, were sufficiently removed, as judged from the chromatograms obtained for blank rat plasma (**Fig. 1**).

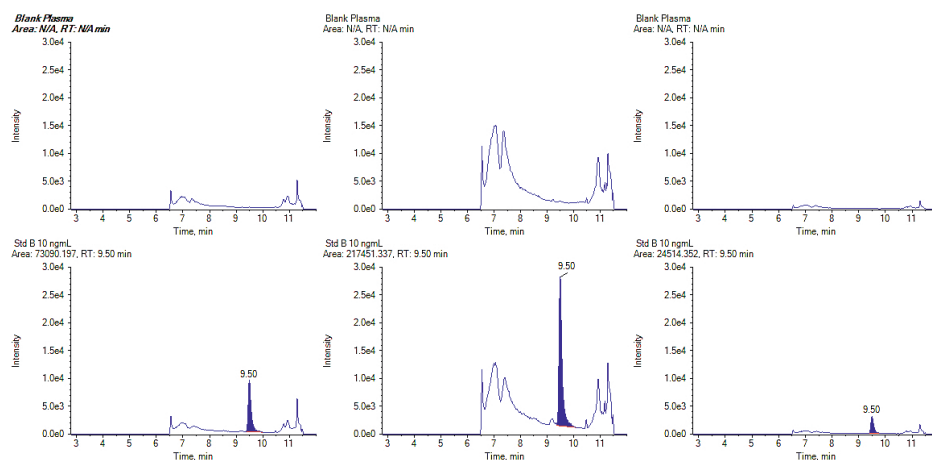


Figure 1: Extracted ion chromatograms for intact somatotropin; upper panels: blank rat plasma, lower panels: 10.0 ng/mL in rat plasma; quantification by: only 16⁺ charge state with MEW 1.0 Da (left panels), 14⁺ to 17⁺ summated with MEW 1.0 Da (middle panels), 14⁺ to 17⁺ summated with MEW 0.0625 Da (right panels).

Of note is the need to include Tween-20 during part of the sample preparation to counter the negative effects of non-specific binding of somatotropin to the sample preparation materials. To avoid interference of Tween-20 in the subsequent LC-MS assay, a final wash step with pure water to eliminate Tween-20 was added after IC, and elution was done with a solution containing 10% acetonitrile to guarantee sufficient solubility of the analyte in the final extract.

7.3.2 Internal standardization

A challenge of using IC for intact protein extraction is the selection of a proper internal standard (IS), which ideally should be added as early as possible in the analytical work-flow and, thus, correct for variability in a maximum number of steps: not only for fluctuations in chromatography and mass spectrometry, but also for differences in capturing efficiency by the antibody. The best choice for an IS in protein quantification is a stable-isotope labelled form of the analyte [11,17], but in practice such a compound is often difficult to obtain for researchers without access to the cell lines used to produce the recombinant protein of interest, or the associated costs may be prohibitive. For somatotropin, a protein analogue containing six additional histidine moieties at the N-terminus is commercially available, and this compound was recognized by the anti-somatotropin antibody and, therefore, extracted together with the analyte. The mass difference between analyte and internal standard was sufficient to distinguish them by mass spectrometry (see **Fig. 2**), so this internal standard could be readily used to correct for losses during sample preparation and other variability in the LC-MS assay.

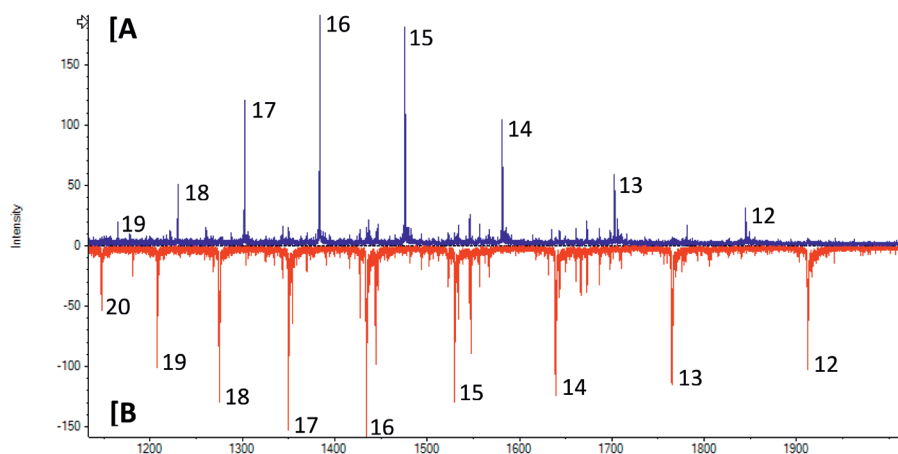


Figure 2: Mass spectra for somatotropin (A) and internal standard (B), showing their different charge states.

7.3.3 Impact of in vivo protein binding

Another important aspect to consider is the potential interaction of a protein analyte with a macromolecular binding partner that occurs in the biological sample, such as the pharmacological target or a specific binding protein. Unbound and bound forms of the

analyte exist in equilibrium *in vivo*, and while only the unbound fraction is initially available for extraction, removal of unbound analyte from the sample by the capture antibody may shift the equilibrium. In the most extreme case, the equilibrium is completely shifted and the total amount of analyte extracted, but, depending on the differences in affinity of the two competing binding reactions, a lower recovery may also be obtained [18]. Since an extraction recovery of >80% was found for spiked samples, the current method appears to extract something close the total concentration of somatropin. Equally importantly, unknown concentrations are calculated by reference to calibration samples which are assumed to display the same degree of *in vivo* protein binding, and thus also have a similar IC recovery. Therefore, concentrations found will always represent the total analyte fraction, even if the IC recovery is incomplete, as long as the matrix of calibrators and study samples is the same. To study the effect of potential differences in protein binding between samples of the same biological matrix, a recombinant form of the endogenous protein possibly involved in somatropin binding (soluble rat growth hormone binding protein) was added in a three-fold molar excess to a spiked rat plasma sample (500 ng/mL of somatropin) and incubated for 2 hours at 37°C. In this way, a study sample with an approximately three-fold higher than average concentration of the binding protein was generated, to represent a worst-case scenario. Quantification of this sample against a calibration curve without additional binding protein resulted in an accurate estimation of the added somatropin (bias: -5.8%, n=3), which leads to the conclusion that sample-to-sample differences in binding protein levels do not impact the accuracy of the method and that total somatropin concentration are indeed obtained.

7.3.4 Selectivity of the immunocapture step

As with most commercial antibodies, the specific antigen-binding sites of the used anti-somatropin capture antibody are not known (or at least not disclosed), and therefore it is unknown which potential isoforms of somatropin the antibody actually recognizes. Very little is known about the *in vivo* fate of somatropin after dosing. In dose formulations, oxidized and deamidated forms of the protein have been identified [19] and these may potentially be formed *in vivo* as well. Since protein deamidation typically is a relatively slow process under physiological conditions, which occurs to a significant degree only after days to weeks [7], it is less likely to be relevant for a protein such as somatropin, with a half-life of just a few hours. We therefore focused on the oxidation of somatropin and prepared an oxidized form of the protein by treatment with hydrogen peroxide. Analysis by HRMS of a

test solution obtained after 165 min of reaction, confirmed the presence of molecules with a mass increased by 16 and 32 amu, corresponding to the insertion of one or two oxygen atoms in the somatropin structure, at a relative abundance of 47% and 20%, respectively, and a low proportion (<3%) of a compound with three oxygen atoms added (mass increase of 48 amu). Since somatropin contains three oxidizable methionines, it is likely that two of these are readily oxidized upon treatment with hydrogen peroxide and the third only to a much lesser extent, because of its location at the inside of the protein molecule making it less susceptible to possible modifications. Interestingly, these oxidized forms of somatropin – when added to plasma (1000 ng/mL) and subjected to the immunocapture step – were not recovered in the eluate at all. This suggests that the used capture antibody does not recognize these potential biotransformation products of somatropin, which would mean that the binding sites on the somatropin molecule, with this specific antibody, include one or more methionine moieties. It could also be that the protein denatures to some extent during the oxidation process and that the conformational epitopes necessary for immunocapture were lost. On the one hand, this finding shows that the IC step is highly selective, which is a positive feature if only concentrations of the dosed drug are required, but on the other hand it also demonstrates that these and other proteoforms may easily be missed upon IC extraction, which means a loss of potentially important information about the *in vivo* fate of a protein drug.

7.3.5 Chromatography and detection

Using an analytical LC column with a C4 stationary phase and a pore size of 300Å, proper selectivity, retention and peak shape were found for intact somatropin and internal standard, provided that the column was kept at 80°C, with lower temperatures resulting in peak broadening. No degradation products were formed at this relatively high chromatographic temperature (data not shown), demonstrating the suitability of the selected LC conditions. Operating at a linear gradient of acetonitrile increasing from 10% to 45% at 3.5% per minute, the protein analyte eluted at 9.5 minutes and the His-tag labelled internal standard eluted at 9.2 minutes. Including a step gradient at 85% acetonitrile and equilibration at the initial mobile phase composition of 10% acetonitrile, the total run time was 15 min per injection.

Upon positive-mode electrospray ionization, the intact somatropin molecule was converted into multiple ions with different m/z values, as shown in Fig. 2. Most abundant were the ions with 14, 15, 16 and 17 positive charges at m/z 1581.376, m/z 1476.008,

m/z 1383.815 and 1302.483, respectively. For the internal standard, these were the ions with 15, 16, 17 and 18 positive charges at m/z 1530.175, m/z 1434.625, m/z 1350.275 and 1275.325, respectively. These ions each showed a further subdivision in about 20 partially resolved ions with different m/z values, which correspond to the masses of ions with increasing numbers of natural heavy isotopes, as exemplified in **Fig. 3** for the 16-fold positively charged form of somatropin.

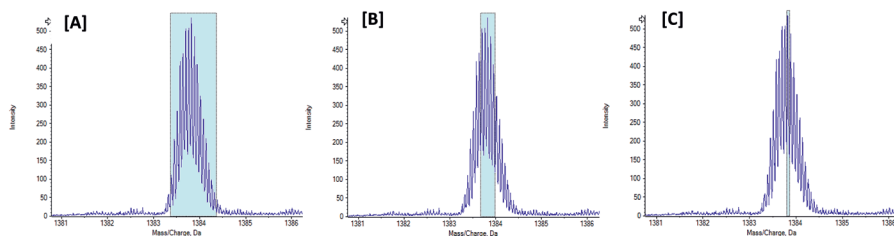


Figure 3: Mass extraction windows of 1.0 Da (A), 0.25 Da (B) and 0.0625 Da (C) for the 16⁺ charge state of somatropin.

Rather than selecting just one m/z value for detection, it is an option to summate the responses of several charge states and increase the total detection intensity. In addition, the so-called mass extraction window (MEW) can be increased around each of the selected m/z values to include more ions per charge state. Using these approaches, the total MS response will increase and, consequently, the detection sensitivity will improve, provided that background noise remains constant. The potential disadvantage is that, because a larger m/z range is included, matrix components with m/z values within this extended range will also generate responses that might interfere in the chromatograms.

To determine the effect of the summation of several charge states and of the width of the MEW on method performance, rat plasma samples spiked with somatropin at four levels (10.0, 30.0, 100 and 500 ng/mL) were analyzed and chromatograms recorded with different detection settings. Responses for somatropin were determined for each of the four most intense charge states (14⁺, 15⁺, 16⁺ and 17⁺) alone and for two, three and four charge states combined. In all cases, a MEW of 1.0 Da was used which corresponds to the inclusion of nearly all different isotopologues per charge state. For the situation in which the four most abundant charge states were summated, chromatograms were also recorded for MEW values reduced to 0.25 Da (corresponding to the four most intense ions of each charge state) and to 0.0625 Da (corresponding to only the most intense single ion per charge state). Example chromatograms recorded for somatropin in plasma at 10.0 ng/

mL are depicted in Fig. 1. Although the absolute detection response increases when more charge states are included and when the MEW is larger, the signal to noise ratio in the chromatograms is essentially unaffected, which indicates that along with more analyte signal more background noise is also extracted. Furthermore, there is no clear indication of the appearance of additional peaks in the chromatograms when the number of charge states or the MEW is increased. This means that no endogenous matrix components are present in the plasma extracts with m/z values falling in the ranges used for the detection of somatropin.

7.3.6 Method performance

All spiked samples were analyzed in six-fold on three separate days. Results were calculated against a spiked calibration curve in rat plasma, which was analyzed using the same settings, and precision and accuracy were determined. An overview of the results is included in Table S-2 in the supplementary material with a summary shown below in **Table 2**.

Table 2: Summary of accuracy and precision results (n=18) obtained for four different detection settings. ND: not detectable

Charge State(s)	MEW (Da)	Nominal Concentration (ng/mL)	Measured Concentration (ng/mL)	CV (%)	Accuracy (%)
16	1.0	10.0	8.54	11.9	85.4
17 - 16 - 15 - 14	1.0	10.0	8.61	10.6	86.1
17 - 16 - 15 - 14	0.0625	10.0	8.70	10.6	87.0
Deconvoluted	N.a.	10.0	ND	-	-
16	1.0	30.0	27.6	13.4	92.1
17 - 16 - 15 - 14	1.0	30.0	26.9	13.1	89.7
17 - 16 - 15 - 14	0.0625	30.0	27.5	13.0	91.7
Deconvoluted	N.a.	30.0	26.9	12.0	89.8
16	1.0	100	103.9	7.0	103.9
17 - 16 - 15 - 14	1.0	100	102.9	7.2	102.9
17 - 16 - 15 - 14	0.0625	100	103.5	6.6	103.5
Deconvoluted	N.a.	100	107.0	11.2	107.0
16	1.0	500	524.2	14.4	104.8
17 - 16 - 15 - 14	1.0	500	529.7	14.0	105.9
17 - 16 - 15 - 14	0.0625	500	505.3	18.7	101.1
Deconvoluted	N.a.	500	531.8	8.1	106.4

For all detection settings, the values for precision (expressed as coefficient of variation) were below 15%, except for the highest concentration that was measured with a reduced MEW, where it was between 15% and 20%. Values for accuracy (average result found relative to the nominal spiked concentration) were between 85% and 115%. These results show that method performance in terms of selectivity, obtainable concentration sensitivity, accuracy and precision is essentially independent of the MEW and the number of charge states used. This is unlike what we found earlier for the signature peptides of digested somatropin [14], where interference in the chromatograms was greatly reduced and accuracy and precision were much improved by narrowing the MEW. Very probably, this is due to the extensive clean-up of the plasma sample by the immunocapture step and the virtual absence of interfering compounds in the extracts in the current method, while the direct analysis of a plasma digest in the digestion-based method leads to generation of a large number of interfering peptides and their subsequent introduction into the LC-MS system. Altogether, the use of a MEW of 1.0 Da gives acceptable results. It could therefore be speculated that analysis of intact somatropin on a low-resolution mass spectrometer, such as a triple quadrupole or ion-trap, may be a possibility, if such a system allows measurement of ions with m/z values up to about 2000 and as long as samples are pretreated by immunocapture.

Deconvolution of mass spectra leads to reconstructed spectra showing the calculated mass of the neutral protein (see **Fig. 4**). The ratio of the area of this deconvoluted neutral mass peak (22124 Da) to that of the corresponding internal standard was used as the analytical response for each of the samples. The results for accuracy and precision are included in Table 2 and show that the performance of the deconvolution approach is comparable to using a limited number of charge states. The detection sensitivity of the deconvolution approach, however, is less favorable than that of using EICs (**Fig. 4**).

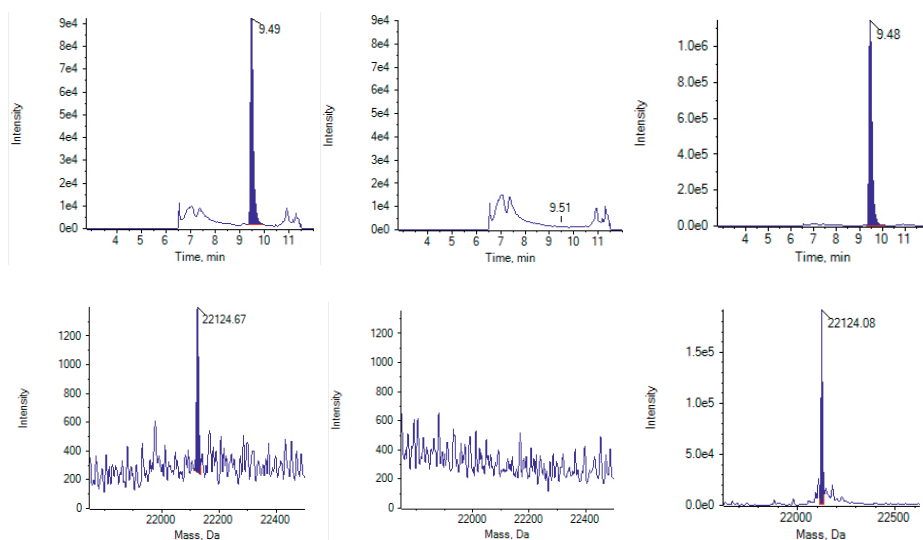


Figure 4: Extracted ion chromatograms, 14⁺ to 17⁺ charge states summated with MEW 1.0 Da (upper panels) and deconvoluted mass spectra (lower panels) for extracted rat plasma samples: spiked plasma standard at 30.0 ng/mL (left panels), pre-dose samples (middle panels) and 0.5 h post-dose samples (right panels).

For the current method, the sample at 10 ng/mL was undetectable but the 30-ng/mL level showed acceptable performance in terms of precision and accuracy (CV and bias <15%) and this level was therefore selected as a workable LLOQ with the deconvolution approach.

7.3.7 Analysis of preclinical samples

Based on the results described above, it was decided to select the summation of the four most intense charge states, extracted with a MEW of 1.0 Da, as the final detection setting for further analysis. Fig. 5 shows an example of a pharmacokinetic curve as obtained for intact somatropin after subcutaneous 2 mg/kg dosing to a rat, by immunocapture and LC–HRMS analysis. The figure demonstrates that the LLOQ of 10 ng/mL is sufficient to monitor the relevant somatropin concentrations in rat plasma after this dose up to 4 hours post-dose. The results obtained in the same samples by deconvolution of the detection signals are included in **Fig. 5**.

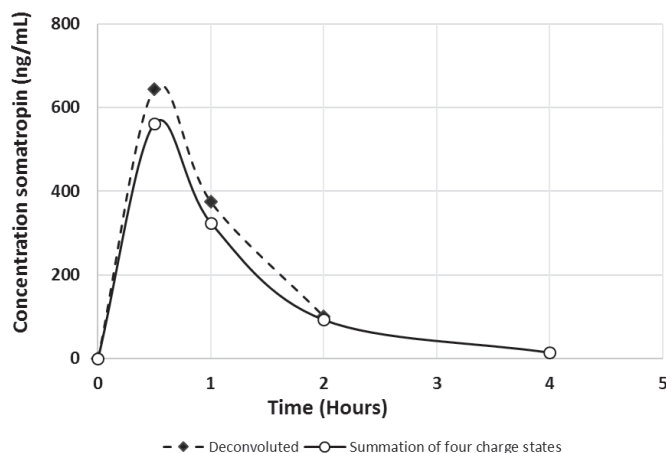


Figure 5: Intact somatropin concentrations in rat plasma after a single 2-mg/kg subcutaneous dose.

The latest time-point is unquantifiable because of the higher LLOQ after deconvolution, but otherwise the data of both quantification approaches agree quite well. When comparing the concentration data (obtained after analysis of all rat plasma samples) of the EIC approach to those of the deconvolution approach, a good correlation ($R^2 > 0.97$) was found. On average, the results after summation of the four most abundant ions were 12% lower than when using deconvolution (**Fig. 6**). This is somewhat surprising, because the concentrations in the preclinical samples were calculated against calibrators whose raw data were processed in the same way. Therefore, it would imply that a systematically higher response is found in the preclinical samples than in the corresponding spiked calibration samples with the deconvolution approach but not with the EIC approach. The spiked validation samples did not show this discrepancy (see: **Table 2**), so the reason for this (slight) deviation remains unclear.

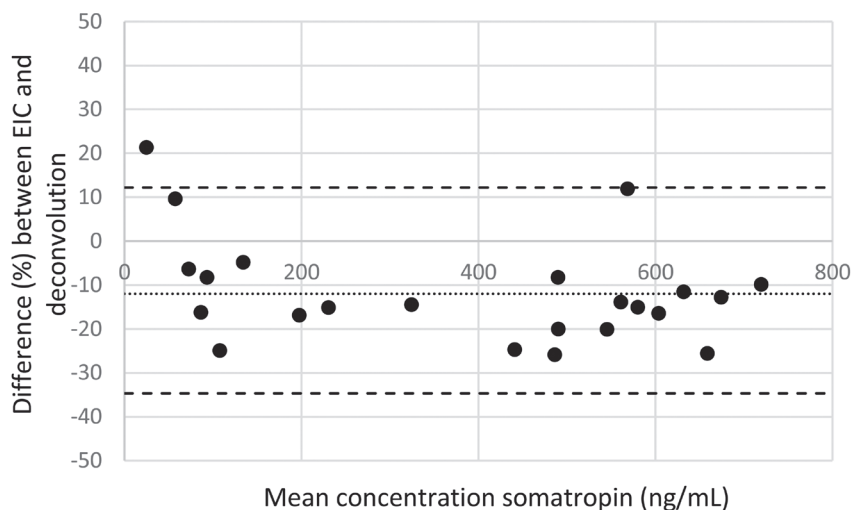


Figure 6: Comparison of somatropin concentrations ($n=23$) found in rat plasma after a single 2-mg/kg subcutaneous dose: Bland-Altman plot with mean and 95% limits of agreement (mean bias (%) \pm 1.96 standard deviation).

7.4 CONCLUSION

LC-HRMS can be successfully used for the quantitation of intact proteins down to the low ng/mL level in a complex, protein-rich biological matrix, when used in combination with immunocapture extraction as a selective sample preparation step. For the 22-kDa protein somatropin, an LLOQ of 10 ng/mL (0.45 nM) was obtained in 75 μ L of rat plasma, using a Q-TOF mass spectrometer with a mass resolution of about 40,000. The summation of the responses of the four most abundant charge states and the use of a relatively large mass-extraction window of 1.0 Da increased the absolute detection sensitivity but did not substantially improve the LLOQ because the signal to noise ratio remained the same. Deconvolution of the mass spectra and using the resulting processed data for quantification gave equally acceptable results, although the obtainable LLOQ was less favorable at 30 ng/mL. A previously published LC-MS/MS method for somatropin, which involved digestion of the plasma sample and quantification of three surrogate peptides, had an LLOQ of 25 ng/mL [12]. This shows that intact protein quantification by LC-HRMS has the potential of better sensitivity, if it is used in combination with a thorough sample clean-up by immunocapture extraction. Here, it should be realized that somatropin is a relatively small protein with rather straightforward chromatographic and mass spectrometric

properties. It is structurally less complex than monoclonal antibodies, the most widely used class of biopharmaceuticals, for which other conclusions have been drawn [13]. The effect of a potentially variable binding of somatropin to endogenous plasma proteins on immunocapture recovery was found to be negligible. Although a good protein internal standard was commercially available for this particular analyte, finding an adequate internal standard remains a potential challenge for intact protein analysis in general.

Acknowledgement

Samenwerkingsverband Noord-Nederland (SNN) is gratefully acknowledged for financial support (grant T3041).

REFERENCES

1. F. Li, D. Fast, S. Michael. Absolute quantitation of protein therapeutics in biological matrices by enzymatic digestion and LC-MS. *Bioanalysis* 3 (2011) 2459–2480.
2. Z. Ouyang, M.T. Furlong, S. Wu, B. Slecicka, J. Tamura, H. Wang, S. Suchard, A. Suri, T. Olah, A. Tymiak, M. Jemal. Pellet digestion: a simple and efficient sample preparation technique for LC-MS/MS quantification of large therapeutic proteins in plasma. *Bioanalysis* 4 (2012) 17–28.
3. K.J. Bronsema, R. Bischoff, N.C. van de Merbel. High-sensitivity LC-MS/MS quantification of peptides and proteins in complex biological samples: the impact of enzymatic digestion and internal standard selection on method performance. *Anal. Chem.*, 85 (2013) 9528–9535.
4. D. Wilffert, R. Donzelli, A. Asselman, J. Hermans, N. Govorukhina, N.H. ten Hacken, W.J. Quax, N.C. van de Merbel, R. Bischoff. Quantitative antibody-free LC-MS/MS analysis of sTRAIL in sputum and saliva at the sub-ng/mL level. *J. Chromatogr. B*, 1032 (2016) 205–210.
5. N.C. van de Merbel. Sample preparation for LC-MS bioanalysis of proteins, in: *Sample preparation in LC-MS bioanalysis*, First Edition, W. Li, W. Jian and Y. Fu (Eds), John Wiley and Sons, 2019, pp 304–318.
6. F. Klont, S.D. Pouwels, P. Bults, N.C. van de Merbel, N.H.T. ten Hacken, P. Horvatovich, R. Bischoff. Quantification of surfactant protein D (SPD) in human serum by liquid chromatography-mass spectrometry (LC-MS). *Talanta* 202 (2019) 507–513.
7. P. Bults, R. Bischoff, H. Bakker, J.A. Gietema and N.C. van de Merbel. LC-MS/MS based monitoring of in vivo protein biotransformation: quantitative determination of trastuzumab and its deamidation products in human plasma. *Anal. Chem.*, 88 (2016) 1871–1877
8. I. van den Broek, W.D. van Dongen. LC-MS-based quantification of intact proteins: perspective for clinical and bioanalytical applications. *Bioanalysis* 7(15), 1943–1958 (2015).
9. H. Liu, A.V. Manuilov, C. Chumsae, M.L. Babineau, E. Tarcsa. Quantitation of a recombinant monoclonal antibody in monkey serum by liquid chromatography-mass spectrometry. *Anal. Biochem.* 414 (2011) 147–153.
10. W. Jian, L. Kang, L. Burton, N. Weng. A workflow for absolute quantitation of large therapeutic proteins in biological samples at intact level using LC-HRMS. *Bioanalysis* 8 (2016) 1679–1691.
11. C. Lanshoeft, S. Cianferani, O. Heudi. Generic hybrid ligand binding assay liquid chromatography high-resolution mass spectrometry-based workflow for multiplexed human immunoglobulin G1 quantification at the intact protein level: application to preclinical pharmacokinetic studies. *Anal. Chem.* 89 (2017) 2628–2635.
12. P. Bults, B. Spanov, O. Olaleye, N.C. van de Merbel, R. Bischoff. Intact protein bioanalysis by liquid chromatography – high-resolution mass spectrometry. *J. Chromatogr. B* 1110–1111 (2019) 155–167.
13. X. Qiu, L. Kang, M. Case, N. Weng, W. Jian. Quantitation of intact monoclonal antibody in biological samples: comparison of different data processing strategies. *Bioanalysis* 10, 1055–1067 (2018).
14. P. Bults, M. Meints, A. Sonesson, M. Knutsson, R. Bischoff, N.C. van de Merbel. Improving selectivity and sensitivity of protein quantitation by LC-HR-MS/MS: determination of somatropin in rat plasma. *Bioanalysis* 10 (2018) 1009–1021.
15. S. Kaur, L. Liu, D.F. Cortes, J. Shao, R. Jenkins, W.R. Mylott Jr, K. Xu. Validation of a biotherapeutic immunoaffinity-LC-MS/MS assay in monkey serum: ‘plug-and-play’ across seven molecules. *Bioanalysis* 8 (2016) 1565–1577.
16. K. Wright, D. Dufield. Minimalistic sample preparation strategies for LC-MS quantification of large molecule biopharmaceuticals: a case study highlighting alpha-1 antitrypsin protein. *Bioanalysis* 6 (2014) 1813–1825.

17. K.J. Bronsema, R. Bischoff, N.C. van de Merbel. Internal standards in the quantitative determination of protein biopharmaceuticals using liquid chromatography coupled to mass spectrometry. *J. Chromatogr. B* 893-894 (2012) 1-14.
18. J.T. White, L.E. Bonilla. Free and total biotherapeutic evaluation in chromatographic assays: interference from targets and immunogenicity. *Bioanalysis* 4 (2012) 2401-2411.
19. G. Karlsson, P. Gellefors, A. Persson, B. Noren, P.O. Edlund, C. Sandberg, S. Birnbaum. Separation of oxidized and deamidated human growth hormone variants by isocratic reversed-phase high-performance liquid chromatography. *J. Chromatogr. A* 855 (1999) 147-155.

SUPPORTING INFORMATION FOR:

Intact Protein Quantification in Biological Samples by Liquid Chromatography – High-Resolution Mass Spectrometry: Somatropin in Rat Plasma

Content

- Figure S-1: Amino acid sequence of somatropin with intra-molecular disulfide bridges indicated.
- Figure S-2: Deconvolution parameters.
- Table S-1: Overview of experimental parameters optimized for the immunocapture step.
- Table S-2: Summary of accuracy and precision results (n=18) for all tested detection settings.

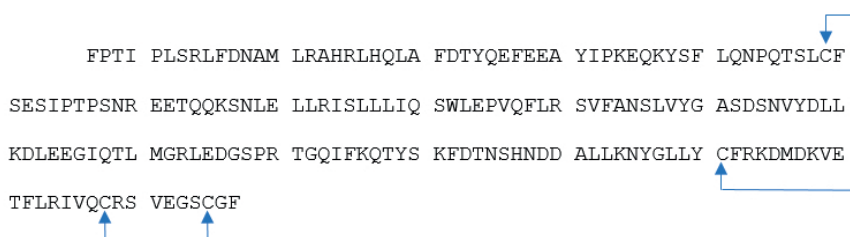


Figure S-1: Amino acid sequence of somatotropin with intra-molecular disulfide bridges indicated.

Data Type:	Mass
XIC:	
Expected RT:	9.48 min
Ret. Time Window:	0.4 min
Peak Selection:	
Expected Mass:	22124.00 Da
Mass Window:	10.0 Da
<input checked="" type="checkbox"/> Report Largest Peak (else closest)	
MQL Peak Integration:	
Peak Splitting:	2 pts
Noise Percentage:	40.0 %
Baseline Sub. Window:	1000.0 Da
Peak Filtering:	
Minimum Peak Width:	3 pts

Figure S-2: Deconvolution parameters.

Table S-1: Overview of experimental parameters optimized for the immunocapture step.

Parameter	Test range/condition	Optimum
Plate coating		
Molar ratio somatropin : Antibody	1:1 / 1:2 / 1:3	1:3
Magnetic beads amount (μL)	15 / 25 / 35	15
Binding sequence	1. Antibody + rhGH (sample) → Antibody complex + Beads 2. Beads + Antibody → Bead complex + rhGH (sample)	1.
Incubation duration, Antibody + sample (minutes)	30 / 60 / 90 / 120	60
Incubation temperature (°C)	37 / 45	45
Capture duration, Antibody complex + beads (minutes)	30 / 60 / 90 / 120	
Capture temperature (°C)	37 / 45	45
Bead Washing after capture		
Wash buffer cycles followed by water	1 / 2 / 3	2
Detergent addition	None / 0.1% Tween-20	None
Bead elution		
Elution buffer	1. 0.1% Formic acid in water 2. 1.0% Formic acid in water 3. 0.1M citric acid in water 4. 0.1M citric acid in water : acetonitrile (90 : 10, v/v))	4.
Elution time (minutes)	5 / 10 / 15 / 20	15
Elution temperature (°C)	RT / 37 / 45	45

Table S-2: Summary of accuracy and precision results (n=18) for all tested detection settings.

Charge State(s)	MEW (Da)	Nominal somatropin concentration (ng/mL)	Mean somatropin concentration (ng/mL)	CV (%)	Accuracy (%)
17	1.00	10.0	8.51	11.0	85.1
16	1.00	10.0	8.54	11.9	85.4
15	1.00	10.0	8.57	11.6	85.7
14	1.00	10.0	8.77	8.9	87.7
17 - 16	1.00	10.0	8.54	12.0	85.4
17 - 15	1.00	10.0	8.68	11.0	86.8
17 - 14	1.00	10.0	8.74	10.7	87.4
16 - 15	1.00	10.0	8.61	11.8	86.1
16 - 14	1.00	10.0	8.73	10.1	87.3
15 - 14	1.00	10.0	8.66	9.8	86.6
17 - 16 - 15	1.00	10.0	8.59	10.8	85.9
17 - 16 - 14	1.00	10.0	8.64	9.5	86.4
17 - 15 - 14	1.00	10.0	8.74	10.3	87.4
16 - 15 - 14	1.00	10.0	8.73	11.1	87.3
17 - 16 - 15 - 14	1.00	10.0	8.61	10.6	86.1
17 - 16 - 15 - 14	0.250	10.0	8.71	11.4	87.1
17 - 16 - 15 - 14	0.0625	10.0	8.70	10.6	87.0
Deconvoluted	N.a.	10.0	ND	-	-

Charge State(s)	MEW (Da)	Nominal somatropin concentration (ng/mL)	Mean somatropin concentration (ng/mL)	CV (%)	Accuracy (%)
17	1.00	30.0	25.0	15.8	83.3
16	1.00	30.0	27.6	13.4	92.1
15	1.00	30.0	27.8	12.6	92.6
14	1.00	30.0	26.2	12.2	87.5
17 - 16	1.00	30.0	26.8	14.1	89.5
17 - 15	1.00	30.0	26.9	13.6	89.7
17 - 14	1.00	30.0	26.0	13.5	86.5
16 - 15	1.00	30.0	27.5	12.9	91.6
16 - 14	1.00	30.0	27.0	12.4	90.0
15 - 14	1.00	30.0	27.2	12.3	90.7
17 - 16 - 15	1.00	30.0	27.1	13.4	90.4
17 - 16 - 14	1.00	30.0	26.7	13.6	88.9
17 - 15 - 14	1.00	30.0	26.8	13.0	89.5
16 - 15 - 14	1.00	30.0	27.3	12.4	90.9
17 - 16 - 15 - 14	1.00	30.0	26.9	13.1	89.7
17 - 16 - 15 - 14	0.250	30.0	27.7	12.5	92.3
17 - 16 - 15 - 14	0.0625	30.0	27.5	13.0	91.7
Deconvoluted	N.a.	30.0	26.9	12.0	89.8

Charge State(s)	MEW (Da)	Nominal somatropin concentration (ng/mL)	Mean somatropin concentration (ng/mL)	CV (%)	Accuracy (%)
17	1.00	100	97.8	7.7	97.8
16	1.00	100	103.9	7.0	103.9
15	1.00	100	104.0	7.3	104.0
14	1.00	100	103.0	8.2	103.0
17 - 16	1.00	100	102.2	7.2	102.2
17 - 15	1.00	100	102.7	7.4	102.7
17 - 14	1.00	100	101.6	7.8	101.6
16 - 15	1.00	100	103.6	7.0	103.6
16 - 14	1.00	100	103.4	7.2	103.4
15 - 14	1.00	100	104.0	7.5	104.0
17 - 16 - 15	1.00	100	102.8	7.0	102.8
17 - 16 - 14	1.00	100	102.3	7.2	102.3
17 - 15 - 14	1.00	100	102.9	7.5	102.9
16 - 15 - 14	1.00	100	103.6	7.2	103.6
17 - 16 - 15 - 14	1.00	100	102.9	7.2	102.9
17 - 16 - 15 - 14	0.250	100	103.5	6.8	103.5
17 - 16 - 15 - 14	0.0625	100	103.5	6.6	103.5
Deconvoluted	N.a.	100	107.0	11.2	107.0

Charge State(s)	MEW (Da)	Nominal somatropin concentration (ng/mL)	Mean somatropin concentration (ng/mL)	CV (%)	Accuracy (%)
17	1.00	500	543.1	11.9	108.6
16	1.00	500	524.2	14.4	104.8
15	1.00	500	519.3	15.9	103.9
14	1.00	500	536.3	14.2	107.3
17 - 16	1.00	500	532.1	13.4	106.4
17 - 15	1.00	500	530.5	14.1	106.1
17 - 14	1.00	500	540.5	13.0	108.1
16 - 15	1.00	500	521.9	14.9	104.4
16 - 14	1.00	500	528.0	14.4	105.6
15 - 14	1.00	500	526.5	15.4	105.3
17 - 16 - 15	1.00	500	528.8	14.0	105.8
17 - 16 - 14	1.00	500	533.5	13.5	106.7
17 - 15 - 14	1.00	500	532.3	14.2	106.5
16 - 15 - 14	1.00	500	524.9	14.8	105.0
17 - 16 - 15 - 14	1.00	500	529.7	14.0	105.9
17 - 16 - 15 - 14	0.250	500	507.9	18.3	101.6
17 - 16 - 15 - 14	0.0625	500	505.3	18.7	101.1
Deconvoluted	N.a.	500	531.8	8.1	106.4

CHAPTER VIII

Summary

The development of protein-based drugs has grown extensively over the past twenty years and this has resulted in the availability of a broad range of so-called biopharmaceuticals for the treatment of a wide variety of diseases. Along with the growing interest for biopharmaceutical drugs and their potential, there has been an increasing need for reliable analytical methods to accurately quantify their concentrations in samples of biological origin. Compared to the quantitative bioanalysis of traditional, small-molecule drugs, the quantification of the large and structurally complex biopharmaceuticals is by no means straightforward.

Historically, ligand binding assays (LBAs) have developed into the gold standard for the analysis of these biomolecules. Despite a number of clear advantages, like their high specificity, sensitivity and ease of use, there are also several down-sides to the use of LBAs, such as the limited possibility to quantify more than one analyte at the same time, the relatively limited linear dynamic ranges and, especially, the need for (expensive) critical reagents which may be difficult or even impossible to obtain and regularly suffer from poor lot-to-lot consistency. To overcome some of these limitations, liquid chromatography-mass spectrometry (LC-MS) has emerged and matured as a complementary technique for the quantification of biopharmaceuticals in biological matrices over the past ten years. This technology has been the cornerstone of small-molecule bioanalysis for over 25 years and, with some adaptations, it is also very suitable for the quantitative determination of protein concentrations in biological samples. Over the last decade there has been much attention for the technical aspects of protein quantification by LC-MS and this has resulted in the typical approach of extensive sample cleanup in combination with digestion of a protein analyte into a set of peptides and the selection of (at least) one of these for detection by LC with a triple quadrupole mass spectrometer. Although this often results in reliable bioanalytical assays, some aspects of biopharmaceutical analysis have been somewhat neglected and deserve more attention. This thesis aims at contributing to the field of biopharmaceutical quantification by focusing on some of these aspects.

After a short general introduction in Chapter I, the first part of the thesis, consisting of chapters II – IV, addresses some conceptual aspects of protein bioanalysis and pays attention to the biotransformation of biopharmaceuticals and its impact on the quantitative results obtained using different bioanalytical technologies. Part two of the thesis, chapters V – VII, is more technically and instrumentally oriented and focuses on the possibilities of protein analysis using high-resolution mass spectrometry.

Unlike the current situation for small-molecule drugs, the biotransformation of biopharmaceuticals is a largely unexplored field. Although much attention is paid to (the prevention of) degradation and structural alteration of protein-based drugs in pharmaceutical formulations, almost nothing is known about what happens to such a drug once it is dosed to a patient. An important reason for this is the fact that it is virtually impossible to investigate biotransformation using LBAs, because they typically cannot distinguish unchanged and biotransformed versions of the drug. With the increasing use of LC-MS/MS for protein quantification, it is now becoming more and more evident that *in vivo* chemical and enzymatic reactions of biopharmaceuticals are very common. Pharmacologically, biotransformation may affect the activity of a protein drug and, from an analytical perspective, it can also have a large influence on the concentration result that is reported. Chapters II to IV aim at providing more information about these aspects of biopharmaceutical analysis.

Chapter II gives an overview of the origin of protein heterogeneity and of possible biotransformation reactions within proteins, and it compares the analytical performance of the two main approaches for protein quantification: LBA and LC-MS in the selected reaction monitoring (SRM) mode. Both LC-MS (based on trypsin digestion and subsequent signature peptide analysis) and LBA methods, by nature of the techniques, only look at specific parts of a protein analyte. In addition, unlike a small molecule, a protein often is not a single, well-defined molecular species but rather a series of closely related isoforms, all of which may or may not give a response in an analytical method. *In vivo* protein biotransformation, caused by chemical or enzymatic reactions, and interaction with endogenous binding partners such as circulating targets and anti-drug antibodies further complicate the situation. Each analytical technique will therefore give information about one or a limited number of the many aspects of the protein of interest. Depending on the question that needs to be answered and on the underlying principle of the analytical approach, either LC-MS or LBA will give the most relevant and meaningful readout. A discrepancy between results obtained by LBA and LC-MS is, therefore, not uncommon and should not be seen as a disqualification of either technique; it should be realized that two different LC-MS assays or two different LBA's for a protein analyte may very well also give different results, as shown for a number of examples from the scientific literature in this chapter. It is concluded that LC-MS will likely be increasingly used in the bioanalysis of biopharmaceuticals and biomarkers, providing a richer chemical knowledge about these molecules, their *in vivo* fate and the relation between activity and concentration.

Chapter III takes a deeper look into biotransformation reactions occurring *in vitro* and *in vivo* and specifically into the deamidation of the biopharmaceutical monoclonal antibody (mAb) trastuzumab at a crucial position in its complementarity determining region (CDR). The amino acid asparagine at position 55 (Asn55), located in the CDR2 of the heavy chain of trastuzumab, is potentially deamidation sensitive, but since Asn55 deamidation does not appear to occur to a large extent in pharmaceutical preparations, it has not been studied as closely as other reactions. Because of the central position of Asn55 in the CDR2 of trastuzumab, its conversion to aspartic acid (Asp55) or iso-aspartic acid (isoAsp55) may very well affect receptor binding affinity and ultimately the pharmacological activity of trastuzumab. In this chapter, a multiplexed LC-MS/MS assay is described that allows the simultaneous quantitation of five molecular species derived from trastuzumab after tryptic digestion: a stable signature peptide (FTISADTSK), a deamidation-sensitive signature peptide (IYPTNGYTR), its deamidated products (IYPTDGYTR and IYPTisoDGYTR) and a succinimide intermediate (IYPTsuccGYTR). Digestion of a 50 μ L plasma sample is performed at pH 7.0 for three hours at 37°C, which combines a reasonable (>80%) digestion efficiency with a minimal (<1%) formation of deamidation products during digestion. Rapid *in vitro* deamidation was observed at higher pH values, leading to a (large) overestimation of the concentrations of deamidation products in the original plasma sample. The LC-MS/MS method was validated in accordance with international bioanalytical guidelines over the clinically relevant range of 0.5 to 500 μ g/mL. Also, an ELISA method was developed and validated for the determination of trastuzumab in plasma samples with a range of 60 to 4000 ng/mL, which allowed analysis of the same samples after dilution with blank plasma. Both methods were used to analyze samples from a 56-day *in vitro* forced degradation study and deamidation of trastuzumab was observed by LC-MS/MS: while the concentration of the stable peptide remained unchanged, the deamidation-sensitive peptide levels dropped by up to 37%. The ELISA results decreased exactly two-fold faster than the LC-MS/MS results for the deamidation-sensitive peptide, which was concluded to be due to the occurrence of two IYPTNGYTR sequences within the trastuzumab molecule. Since the sandwich ELISA uses two anti-idiotypic antibodies, it is very likely that both IYPTNGYTR sequences need to remain intact to form a detectable immune-complex with trastuzumab. To further investigate deamidation of trastuzumab, both the LC-MS/MS and ELISA methods were applied to plasma samples obtained from breast cancer patients during treatment with the drug for several months. LC-MS/MS analysis revealed up to 25% deamidation and isomerization of Asn55, while the concentrations found by ELISA were

more than two-fold lower than the total trastuzumab concentrations by LC-MS/MS. Since the degree of deamidation also varied considerably between patients, it is clear that protein biotransformation is complicated and that more research is needed to fully understand the *in vivo* fate of biopharmaceuticals and the consequences for their pharmacological activity. In this respect, properly designed analytical methods and notably multiplexed LC-MS/MS will be indispensable.

Nowadays, trastuzumab is often co-administered with the monoclonal antibody pertuzumab as a first-line therapy for some forms of breast cancer. Pertuzumab and trastuzumab bind to different sites on the same receptor (HER2) without competition and their combination gives enhanced antitumor activity as compared to single mAb treatment. As pertuzumab also contains a deamidation-sensitive asparagine in a CDR of the heavy chain, the deamidation of this biopharmaceutical protein could also lead to loss of efficacy. Therefore, in Chapter IV, we describe the results of a further investigation into the occurrence and pharmacological consequences of *in vitro* and *in vivo* deamidation of trastuzumab and pertuzumab, at the positions HC-Asn55 and HC-Asn54, respectively. Both protein analytes were enzymatically digested by trypsin into series of peptides and several of these were subsequently quantified by multiplexed LC-MS/MS as a surrogate for the intact forms. By quantifying the peptides comprising HC-Asn55 or HC-Asn54, a measure is obtained for the (remaining) amount of trastuzumab or pertuzumab which is non-deamidated at that position. In addition, the total concentration of the protein analytes is estimated by reference to peptides from a part of the protein which does not undergo any known *in vivo* modification. Using a plasma volume of just 10 μ L and a 2-hour digestion at pH 7.0, concentrations between 2 and 1000 μ g/mL can be determined for the various protein forms. A validation of the method showed values for bias and CV below 15% and no unacceptable deamidation taking place during sample storage or analysis. A large difference between the total and non-deamidated concentrations, and thus a substantial degree of deamidation, was observed in plasma for both trastuzumab and pertuzumab *in vitro* and *in vivo*. After a 56-day forced degradation test 40% of trastuzumab and 68% of pertuzumab was deamidated, while trastuzumab and pertuzumab showed up to 47% and 35% of deamidation, respectively, in samples collected from a clinical study in breast cancer patients during treatment with a combination of both drugs. Next to this LC-MS method, a receptor binding assay was also developed and validated to study the binding of the non-deamidated and deamidated forms of the protein analytes to the HER2 receptor. The analytical principle of the receptor binding assay is that trastuzumab or pertuzumab

is captured by a recombinant form of the extracellular domain of the HER2 receptor and subsequently detected using a generic human IgG-directed detection antibody. It should be noted that, in contrast to the LC-MS/MS method, the receptor binding assay does not provide separate read-outs for the two analytes, since both are captured by the HER2 receptor and both are also recognized by the detection antibody. Therefore, it cannot be used for samples that contain both analytes, such as plasma collected from patients after combined dosing with these biopharmaceuticals.

The trastuzumab and pertuzumab concentrations in the plasma samples from the *in vitro* degradation test, as obtained by the receptor binding assay, correlated quite well with the concentrations found using the LC-MS assay for the deamidation-sensitive peptides, which seems to imply that once trastuzumab is deamidated at HC-Asn55 and pertuzumab at HC-Asn54 the mAbs no longer give a response in the receptor binding assay and therefore, very likely, do not bind to the recombinant extracellular domain of the HER2 receptor anymore. The pharmacological consequences of deamidation for the efficacy of both mAbs were assessed by a cell viability assay with the human HER2-positive breast cancer cell line BT474. While unmodified trastuzumab effectively inhibited the growth of these breast cancer cells, it was found that the deamidated form lost its capability to do so, suggesting that there could be a relation between the degree of deamidation and the loss of pharmacological activity. In contrast, cultivation of this breast cancer cell line in the presence of unmodified pertuzumab did not result in any decrease of cell survival in our hands and was not suitable to assess the biological activity of pertuzumab. Concluding, for monitoring purposes in patients, LC-MS/MS measurement of the remaining non-deamidated concentration at HC-Asn55 and HC-Asn54 of trastuzumab and pertuzumab is likely to give the best representation of the pharmacologically active drug fraction. As other structural modifications very probably also occur, future studies should address those as well to obtain a more detailed picture of the *in vivo* biotransformation of these biopharmaceutical proteins and LC-MS/MS with proper surrogate peptides is a straightforward and reliable way of doing this in a multiplexed assay.

In Chapters V-VII we look at biopharmaceutical analysis from a more technical and instrumental point of view. So far, most protein LC-MS methods are being performed using triple-quadrupole mass spectrometry after sample digestion and further sample processing. This type of mass spectrometry has unit-mass resolution and its use for protein quantification essentially is an extension of the typical approach for small-molecule analysis. Very little is known about the quantitative possibilities of other high-resolution

mass spectrometry (HRMS) approaches for biopharmaceuticals. HRMS is extensively used for qualitative purposes, such as the structural elucidation or confirmation of both small and large molecules, because of its high mass accuracy, but it also offers the option for quantitative analysis and extensive data re-processing. It can thus be used as an alternative detection technique for digested protein analysis with improved selectivity compared to unit-mass MS and it also is capable of quantifying intact proteins, which is virtually impossible on triple-quadrupole instrumentation.

In Chapter V, a second review paper is presented which explores the (theoretical) options for intact protein quantification by HRMS. This field is still clearly in its infancy and although the first reports have started to appear, many aspects need to be further developed, from sample preparation to the separation of protein species and the use and interpretation of the highly complex mass spectra. Some key-points are that enrichment strategies for intact proteins are typically based on selectively capturing the protein of interest with an affinity ligand such as an antibody, receptor or another affinity binder. More generic enrichment techniques, such as solid-phase extraction (SPE) using electrostatic or hydrophobic interactions, immobilized metal affinity columns (IMAC) or fractionated protein precipitation can also be applied but they require careful optimization based on the physical-chemical properties of the target protein to obtain sufficient selectivity. The sample preparation for intact protein analysis by LC-MS, and specifically affinity-based enrichment, depends on the specificity of the affinity ligand. Monoclonal-, polyclonal- or engineered recombinant antibodies as well as biological receptors are widely used as capturing agents. For each type of ligand, it is important to know against which part of the protein analyte it is directed and which proteoform of the protein is captured, to allow proper interpretation of the results. Another challenge and point of interest is the setup of the liquid chromatography part of the assay. Due to their large size, intricate higher order structure and heterogeneity, chromatographic separation of proteins is extremely challenging. While sample preparation is a crucial and indispensable step to achieve sensitivity and selectivity in protein bioanalysis, it would not be possible to address protein heterogeneity to any appreciable extent without efficient LC separation prior to mass spectrometry. Recent improvements have been made by analytical column manufactures with regards to stationary phase composition/chemistry and particle sizes. Examples are organic polymer-based monolithic columns, higher temperature resistant stationary phases, titanium column bodies and wide pore (>300 Å) core-shell particles. Also the addition of so-called superchargers and other additives to the mobile phases improved

selectivity and sensitivity of intact protein analysis. In the field of mass-spectrometry, most widely used are triple quadrupole instruments, which initially focused on the analysis of small molecules. More recent developments and advances in the field of HRMS have opened new possibilities in the field of protein analysis. Most commonly used HRMS-systems are based on quadrupole time-of-flight (QTOF) and Orbitrap mass analyzers combined with 'soft ionization' modes like electrospray ionization (ESI) and matrix-assisted laser desorption ionization (MALDI). Recently the use of ion mobility spectrometry (IMS) has entered the field of protein analysis. IMS may be described as 'gas-phase electrophoresis' and introduces an extra separation dimension after the LC separation and ahead of the actual mass analyzer. Separation is based on the physical characteristics of proteins such as lipophilicity, shape and charge. IMS is of utmost interest for the field of 'native' mass spectrometry.

In Chapter VI, we describe the development and evaluation of a quantitative LC-HR-MS/MS method for the determination of the 22-kDa biopharmaceutical protein somatropin (recombinant human growth hormone, rhGH)) in rat plasma. To achieve good sensitivity and selectivity on a triple-quadrupole mass spectrometer extensive sample clean-up is needed to remove interfering tryptic peptides that appear in the chromatograms of the signature peptide, because of a rather wide mass extraction window (MEW) of 0.7 Da that is used to select analyte ions for detection. The high mass resolution of HRMS allows the application of a much narrower MEW, which can considerably reduce the number of tryptic peptides that are extracted during data processing. For an extensive evaluation of the applicability of HRMS for the analysis of plasma digests, we set up an LC-HR-MS/MS method on a QTOF instrument with which we quantified three peptides, originating from rhGH after trypsin digestion: LFDNMLR (amino acids 9-16), SNLELLR (71-77) and FDTNSHNDDALLK (146-158). After selecting the peptide precursor ions using a quadrupole with unit-mass resolution and subsequent collision induced dissociation, fragment ions were selected during data processing, on which the MEW was reduced from 0.5 to 0.01 Da. The number and intensity of interfering peaks in the extracted ion chromatograms was considerably reduced upon decreasing the MEW, which facilitated the determination of the three different signature peptides. Detection sensitivity was further enhanced by the summation of the responses of multiple product ions for each of the signature peptides. This allowed quantitation with acceptable accuracy and precision down to levels corresponding to 25 ng/mL of the intact protein somatropin in rat plasma, which is four-fold lower than on a triple-quadrupole mass spectrometer at unit-mass resolution. The conditions for

optimal selectivity and sensitivity varied from peptide to peptide and, in general, the MEW settings as well as the summation of responses have to be optimized for any given signature peptide and product ion. In conclusion, while the absolute instrument sensitivity of a triple quadrupole MS typically is better, the possibility of removing interfering peaks from the chromatograms by narrowing the MEW on HRMS may finally result in better sensitivity. This opens up the possibility to perform protein analysis with less rigorous sample preparation and it may prevent the need to use of extraction materials and reduce the time used for sample preparation.

The possibility to quantify intact rhGH in plasma by LC-HRMS is the subject of Chapter VII. It compares quantitation based on the generation of extracted-ion chromatograms (EICs), which are recorded by using the detection responses at one or more m/z values for the charged protein analyte, to those of the deconvolution approach, which constructs a theoretical uncharged mass spectrum as the basis for quantitation. In addition, the effect of the width of the MEW around each of the selected m/z values on method sensitivity and selectivity is evaluated. To this end, rat plasma samples spiked with somatropin at four levels (10.0, 30.0, 100 and 500 ng/mL) were analyzed and chromatograms recorded with different detection settings. EIC responses were determined for each of the four most intense charge states (14^+ , 15^+ , 16^+ and 17^+) of somatropin alone and for two, three and four charge states combined. In all cases, a MEW of 1.0 Da was used which corresponds to the inclusion of nearly all different isotopologues per charge state. When summing the four most abundant charge states, chromatograms were also recorded for MEW values reduced to 0.25 Da (corresponding to the four most intense ions of each charge state) and to 0.0625 Da (corresponding to only the most intense single ion per charge state). Although the absolute detection response increased when more charge states were included and when the MEW was larger, the signal-to-noise ratio in the chromatograms was essentially unaffected, indicating that along with more analyte signal more background noise is also extracted. With optimized instrumental and processing settings, the method was validated for the EIC approach and these results show that method performance in terms of selectivity, obtainable concentration sensitivity, accuracy and precision is independent of the MEW and the number of charge states used. Deconvolution of the same data to a reconstructed mass spectrum of the neutral protein (22124 Da) was also used as the analytical approach. The results for accuracy and precision show that its performance is comparable to using EICs, but the detection sensitivity is less favorable: 30 ng/mL as an acceptable LLOQ against 10 ng/mL for the EIC approach. Both methods of data processing

were subsequently used for the analysis of samples originating from a pre-clinical study and showed that both approaches are suitable for intact protein analysis with a good correlation ($R^2 > 0.97$) between the two. Altogether, this shows that intact protein quantification by LC-HRMS has the potential of even better sensitivity than digested protein analysis, if it is used in combination with a thorough sample clean-up by immunocapture extraction.

CHAPTER IX

Nederlandse samenvatting

List of publications

Curriculum vitae

Acknowledgments

NEDERLANDSE SAMENVATTING

De ontwikkeling van eiwitten voor de toepassing als geneesmiddel is in de afgelopen twintig jaar enorm toegenomen en dit heeft geleid tot de beschikbaarheid van een groot aantal zogenaamde biofarmaceutica voor de behandeling van zeer diverse ziektebeelden. Deze groeiende interesse voor biofarmaceutica gaat gepaard met een eveneens toenemende behoefte aan betrouwbare analytische methoden om de concentraties van deze eiwitten nauwkeurig te kunnen bepalen in monsters van biologische oorsprong. Vergeleken met de kwantitatieve bioanalyse van de traditionele kleine moleculen als geneesmiddel, is het meten van de concentraties van eiwitten zeker niet eenvoudig, mede vanwege hun grootte en structurele complexiteit. Van oudsher worden hiervoor ligand-binding assays (LBA's) gebruikt. Ondanks een aantal duidelijke voordelen, zoals gebruiksgemak en een hoge specificiteit en gevoeligheid, hebben LBA's zeker ook tekortkomingen, b.v. de beperkte mogelijkheid om meer dan één analiet tegelijk te meten, het relatief korte lineair dynamische bereik en vooral de afhankelijkheid van (dure) kritische reagentia die moeilijk of soms zelfs onmogelijk te verkrijgen zijn en waarvan de kwaliteit niet altijd gegarandeerd is. Om deze nadelen te omzeilen is er in de afgelopen tien jaar veel aandacht besteed aan de ontwikkeling van vloeistofchromatografie met massaspectrometrische detectie (LC-MS) als een alternatieve meetmethode voor biofarmaceutica in complexe biologische monsters. Deze technologie is al meer dan 25 jaar de hoeksteen van de bioanalyse van kleine moleculen en, met enige aanpassingen, is zij ook zeer geschikt voor het meten van eiwitconcentraties. Er is in die tien jaar vooral veel aandacht geweest voor de technische aspecten van eiwitkwantificering en dit heeft geleid tot een standaardaanpak waarbij het monster grondig wordt opgezuiverd en het eiwit wordt gedigesteerd (geknipt) tot een serie peptiden waarvan er (tenminste) één wordt geselecteerd voor detectie door middel van een combinatie van LC met een triple-quadrupole massaspectrometer. Hoewel dit vaak leidt tot betrouwbare bioanalytische methoden, zijn er toch enkele aspecten van deze manier van eiwitkwantificatie onderbelicht gebleven. Dit proefschrift heeft als doel een bijdrage te leveren aan het veld van de analyse van biofarmaceutica door enkele van deze aspecten nader te onderzoeken.

Na een korte algemene inleiding in hoofdstuk I, richt het eerste deel van het proefschrift (hoofdstukken II t/m IV) zich op de biotransformatie van biofarmaceutica en de betekenis daarvan voor de kwantitatieve resultaten van diverse analytische methoden. Deel

twee (hoofdstukken V t/m VII) hebben een meer technische focus en beschrijven de mogelijkheden van hoge-resolutie massaspectrometrie voor eiwitanalyse.

In tegenstelling tot de situatie voor kleine moleculen als geneesmiddel is de biotransformatie van biofarmaceutica een grotendeels onontgonnen terrein. Hoewel veel aandacht wordt besteed aan (het voorkómen van) degradatie en structurele veranderingen van deze eiwitten in farmaceutische formuleringen is er vrijwel niets bekend over wat er gebeurt als zo'n geneesmiddel wordt toegediend aan een patiënt. Een belangrijke reden hiervoor is het feit dat het zo goed als onmogelijk is om met een LBA biotransformatie te onderzoeken, aangezien deze techniek geen onderscheid maakt tussen de onveranderde en de omgezette vormen van het geneesmiddel. Door het toenemende gebruik van LC-MS/MS voor eiwitkwantificering wordt het steeds duidelijker dat biofarmaceutica ook *in vivo* chemische en enzymatische reacties ondergaan. Vanuit farmacologisch oogpunt kan dit betekenen dat de activiteit van het geneesmiddel verandert en, analytisch gezien, kan het ook een grote invloed hebben op het concentratieresultaat dat uiteindelijk wordt gerapporteerd. De hoofdstukken II tot IV hebben als doel meer informatie over dit fenomeen te geven.

Hoofdstuk II geeft een overzicht van de oorzaken van de heterogeniteit van eiwitten en van de mogelijke biotransformatiereacties in eiwitten, en vergelijkt de analytische prestaties van de twee belangrijkste kwantitatieve meetmethoden voor eiwitten: LBA en LC-MS in de zogenaamde selected reaction monitoring (SRM) modus. Zowel LBA als LC-MS zijn gericht op slechts een gedeelte van een eiwit (als deze laatste techniek gebruik maakt van digestie en kwantificatie van een signature peptide). Daarnaast is het zo dat, in tegenstelling tot een klein molecuul, een eiwit geen enkelvoudige, goed-gedefinieerde moleculaire structuur is, maar eerder een serie van structureel verwante isovormen. *In vivo* biotransformatie van een eiwit, door chemische of enzymatische reacties, en interactie met endogene bindingseiwitten, zoals receptoren of zogenaamde anti-drug antilodies, compliceren de situatie nog verder. Elke analytische techniek geeft daarom informatie over slechts één of een beperkt aantal van de vele aspecten van het eiwit van interesse. Afhankelijk van de vraag die moet worden beantwoord en van het onderliggende principe van de analytische meettechniek, zal ofwel LC-MS ofwel LBA het meest relevante en betekenisvolle resultaat geven. Een verschil in het resultaat verkregen met LC-MS of met LBA is daarom niet ongewoon en ook niet perse een teken dat één van beide resultaten incorrect is. Ook twee verschillende LC-MS methoden of twee verschillende LBA's kunnen verschillende resultaten geven, zoals in dit hoofdstuk wordt geïllustreerd aan de hand van een aantal voorbeelden uit de wetenschappelijke literatuur. De conclusie van dit hoofdstuk

is dat LC-MS waarschijnlijk in toenemende mate zal worden gebruikt voor de bioanalyse van biofarmaceutica, omdat het meer gedetailleerde chemische kennis kan verschaffen over deze moleculen, hun *in vivo* lotgevallen en de relatie tussen activiteit en concentratie.

In hoofdstuk III wordt in meer detail gekeken naar biotransformatiereacties die optreden *in vitro* en *in vivo*, en specifiek naar de deamidatie van het biofarmaceutische monoclonale antilichaam trastuzumab op een cruciale positie in zijn zogenaamde complementarity determining region (CDR). Het aminozuur asparagine op positie 55 (Asn55) in het CDR2 van de zware keten van trastuzumab is potentieel deamidatiegevoelig, maar omdat Asn55 deamidatie niet veel lijkt voor te komen in farmaceutische preparaten is er minder studie naar gedaan dan naar sommige andere reacties. Vanwege de centrale positie van Asn55 in CDR2 van trastuzumab, zou omzetting naar aspartaat (Asp55) of iso-aspartaat (isoAsp55) de binding van trastuzumab aan zijn receptor kunnen beïnvloeden en uiteindelijk ook de farmacologische activiteit. In dit hoofdstuk wordt daarom een multiplex LC-MS/MS methode beschreven, die de gelijktijdige kwantificatie mogelijk maakt van vijf peptiden die gevormd kunnen worden na digestie van trastuzumab: een stabiel peptide (FTISADTSK), het deamidatiegevoelige peptide met daarin Asn55 (IYPTNGYTR), de gedeamideerde producten (IYPTDGYTR en IYPTisoDGYTR) en een succinimide intermediair (IYPTsuccGYTR). Digestie van 50 µl plasma wordt uitgevoerd bij pH 7 gedurende drie uur bij 37°C, hetgeen resulteert in een goede digestie-opbrengst (>80%) en tegelijk een minimale (<1%) vorming van de deamidatieproducten tijdens de digestie. Bij hogere pH-waarden werd een snelle *in vitro* deamidatie gezien, leidend tot een (soms grote) overschatting van de oorspronkelijke concentraties van de gedeamideerde peptiden. De LC-MS/MS methode is gevalideerd volgens de meest recente internationale bioanalytische richtlijnen over het klinisch relevante bereik 0.5 tot 500 µg/ml. Ook werd een ELISA methode ontwikkeld en gevalideerd voor de bepaling van trastuzumab in plasma met een bereik van 60.1 tot 4000 ng/ml, wat analyse van dezelfde monsters mogelijk maakt na een verdunning. Beiden methoden werden toegepast om plasmamonsters te meten afkomstig van een 56-daagse geforceerde degradatiestudie, en deamidatie van trastuzumab trad inderdaad op: terwijl de concentratie van de stabiele peptide gelijk bleef daalde de spiegels van het deamidatiegevoelige peptide met 37%. De ELISA resultaten namen precies twee keer zo snel af, hetgeen waarschijnlijk verklaard kan worden door het voorkomen van twee IYPTNGYTR-sequenties in trastuzumab. Aangezien de sandwich ELISA twee anti-idiotypische antilichamen gebruikt, is het heel waarschijnlijk dat er twee niet-gedeamideerde IYPTNGYTR-sequenties nodig zijn voor het vormen van een detecteerbaar immuuncomplex met trastuzumab. Voor verder onderzoek

naar de deamidatie van trastuzumab werden de LC-MS/MS en de ELISA methode gebruikt voor het analyseren van plasmamonsters, afgenomen van borstkankerpatiënten tijdens behandeling met trastuzumab gedurende meerdere maanden. LC-MS/MS analyse liet zien dat in die periode tot wel 25% deamidatie en isomerisatie van Asn55 optreedt, terwijl een zelfs sterkere reductie van de trastuzumab concentraties werd verkregen met ELISA dan verwacht op basis van de *in vitro* experimenten. Ook verschilde de mate van Asn55 deamidatie sterk tussen patiënten, wat benadrukt dat biotransformatie een complex proces is en dat meer onderzoek nodig is voor het volledig begrijpen van de *in vivo* lotgevallen van biofarmaceutica en de consequenties voor hun farmacologische activiteit. In dat opzicht zijn goede bioanalytische methoden en zeker ook LC-MS/MS een nuttig hulpmiddel.

Tegenwoordig wordt trastuzumab vaak gecombineerd met een ander monoclonaal antilichaam, pertuzumab, als standaardbehandeling van sommige vormen van borstkanker. Pertuzumab en trastuzumab binden in het lichaam aan dezelfde receptor (HER2) en het combineren van deze twee eiwitten geeft een betere anti-tumor werking dan de toediening van één van beide. Aangezien ook pertuzumab een deamidatie gevoelige asparagine bevat in een CDR in de zware keten zou deamidatie ook voor dit biofarmaceuticum kunnen leiden tot een verlies aan activiteit. In hoofdstuk IV beschrijven we daarom de resultaten van een nader onderzoek naar het vóórkomen en de farmacologische consequenties van de *in vitro* en *in vivo* deamidatie van trastuzumab en pertuzumab, en wel op posities Asn55 resp. Asn54 in de zware ketens. Hiertoe worden beide eiwitten gedigesteerd met trypsine en een aantal van de gevormde peptiden vervolgens gekwantificeerd met een multiplex LC-MS/MS methode, als surrogaat voor de beide intacte eiwitten. De peptiden, die Asn55 resp. Asn54 bevatten, zijn een maat voor de (resterende) concentratie trastuzumab of pertuzumab wat niet is gedeamideerd. Daarnaast geeft een peptide uit een ongemodificeerd deel van elk eiwit de totale concentratie van trastuzumab of pertuzumab weer. Met een plasmavolume van slechte 10 µl en een 2-uur durende digestie bij pH 7.0 kunnen concentraties tussen 2 en 1000 µg/ml worden bepaald voor de verschillende eiwitvormen. Tijdens een formele validatie werden waarden voor bias en CV van beneden de 15% gevonden en aangetoond dat geen onacceptabele deamidatie plaatsvindt tijdens opslag of analyse van de monsters. Een groot verschil tussen de totale en niet-gedeamideerde concentraties voor trastuzumab en pertuzumab werd gezien zowel *in vitro* als *in vivo*. Na een 56-daagse geforceerde degradatie *in vitro* was 40% van trastuzumab en 68% van pertuzumab gedeamideerd, terwijl tot 47% resp. 35% deamidatie werd gevonden in plasma van borstkankerpatiënten tijdens behandeling met een combinatie van beide geneesmiddelen. Naast de LC-MS methode werd

ook een receptorbindingsassay opgezet en gevalideerd om de binding van de gedeamideerde en niet-gedeamideerde vormen van de beide biofarmaceutica aan de HER2 receptor te bestuderen. Het analytische principe is dat trastuzumab of pertuzumab wordt gebonden aan een recombinante vorm van het extracellulaire domein van de HER2 receptor, en vervolgens gedetecteerd met een generiek humaan IgG-gericht detectie-antilichaam. Deze methode kan daarom niet worden gebruikt voor monsters waar beide analieten tegelijk in voorkomen, zoals plasma afkomstig van patiënten die een combinatietherapie met beide biofarmaceutica krijgen. De trastuzumab en pertuzumab concentraties in plasmamonsters van de *in vitro* degradatietest, verkregen met de receptorbindingsassay, vertoonden een goede correlatie met de concentraties van de deamidatiegevoelige peptiden zoals bepaald met LC-MS. Dit suggereert dat, zodra trastuzumab of pertuzumab zijn gedeamideerd op Asn55 resp. Asn54, deze eiwitten geen respons meer geven in de receptorbindingsassay en daarom waarschijnlijk niet meer binden aan het (recombinante) extracellulaire domein van de HER2 receptor. De farmacologische consequenties van de deamidatie voor de werking van de beide mAbs zijn verder onderzocht m.b.v. een cell viability assay met de humane HER2-positieve borstkankercellijn BT474. Hierbij werd gevonden dat ongemodificeerd trastuzumab de groei van deze tumorcellen effectief remde, terwijl de gedeamideerde vorm dit niet langer kon, hetgeen erop wijst dat er mogelijk een relatie is tussen de mate van deamidatie en het verlies van farmacologische activiteit. Voor ongemodificeerd pertuzumab werd door ons met deze cellijn overigens geen remming van de tumorcelgroei gevonden. Concluderend, de LC-MS/MS meting van de resterende ongedeamideerde concentratie Asn-55 voor trastuzumab en Asn-54 voor pertuzumab geeft waarschijnlijk het beste beeld van de farmacologisch actieve fracties van deze geneesmiddelen in plasma van patiënten. Omdat er ongetwijfeld ook andere structurele modificaties plaatsvinden is het van belang dat hier in toekomstige studies verder naar wordt gekeken, om een gedetailleerd beeld te krijgen van de *in vivo* biotransformatie van deze biofarmaceutica. LC-MS/MS met goed gekozen surrogaatpeptiden biedt hiervoor een eenduidige en betrouwbare mogelijkheid.

In de hoofdstukken V tot VII kijken we naar biofarmaceutische analyse vanuit een meer technisch en instrumenteel oogpunt. Tot nu toe worden de meeste LC-MS methoden uitgevoerd met triple-quadrupole massaspectrometrie na digestie en verdere monsteropwerking. Dit type massaspectrometrie heeft unit-mass resolutie en het gebruik voor eiwitkwantificering is eigenlijk een uitbreiding van de typische aanpak voor het meten van kleine moleculen. Er is verder weinig kennis over de kwantitatieve mogelijkheden van hoge-resolutie massaspectrometrie (HRMS) voor biofarmaceutica. Vanwege de

hoge massa-accuraatheid wordt HRMS veel gebruikt voor kwalitatieve doeleinden, zoals structuuropheldering of -bevestiging van zowel kleine als grote moleculen, maar het biedt ook mogelijkheden voor kwantitatieve analyse. Het kan worden gebruikt als alternatieve detectietechniek voor eiwitanalyse na digestie en kan dan een betere selectiviteit geven dan unit-mass MS. Tevens kunnen er ook intacte eiwitten mee worden gekwantificeerd, wat vrijwel onmogelijk is op een triple-quadrupole instrument.

In hoofdstuk V wordt een tweede overzichtsartikel gepresenteerd waarin de (theoretische) mogelijkheden worden beschreven voor de analyse van intacte eiwitten met HRMS. Dit veld staat duidelijk nog in de kinderschoenen en hoewel de eerste rapporten zijn verschenen moeten veel aspecten nog verder worden ontwikkeld, van monsteropwerking tot de scheiding van eiwitten en het gebruik en de interpretatie van de zeer complexe massaspectra die bij deze aanpak worden verkregen. Een belangrijk punt van aandacht is dat de succesvolle verrijking van eiwitten vooral plaatsvindt door de selectieve extractie uit het monster met een affiniteitsligand zoals een antilichaam, receptor of andere bindingspartner. Generieke verrijkingsmethoden zoals vaste-fase extractie (SPE) op basis van elektrostatische of hydrofobe interacties, geïmmobiliseerde metalen (IMAC) of gefractioneerde neerslagreacties kunnen ook worden gebruikt, maar deze vereisen een zorgvuldige optimalisering om voldoende selectiviteit te verkrijgen. Een andere uitdaging is de opzet van het vloeistofchromatografische (LC) deel van de methode. Vanwege hun grootte en complexe, heterogene structuur is een goede chromatografische scheiding van eiwitten uiterst uitdagend. Al is de monsteropwerking een cruciale stap om voldoende selectiviteit en gevoeligheid te verkrijgen in de bioanalyse van eiwitten, zonder een efficiënte LC scheiding zou het onmogelijk zijn eiwitheterogeniteit te bestuderen. Recente ontwikkelingen in de samenstelling en eigenschappen van stationaire fases betreffen b.v. monolytische kolommen op basis van organische polymeren, hittebestendige fasen en deeltjes met wijdere poriën. Ook de toevoeging van zogenaamde superchargers en andere additieven aan mobiele fasen dragen bij aan de verbetering van de gevoeligheid en selectiviteit van intacte eiwit analyse. Op het gebied van de massaspectrometrie worden triple-quadrupole instrumenten het meest gebruikt, maar recente ontwikkelingen in HRMS hebben nieuwe mogelijkheden geschapen voor het kwantificeren van intacte eiwitten, zoals het gebruik van quadrupole time-of-flight (QTOF) en Orbitrap massa-analysatoren, in combinatie met 'zachte ionisatie' technieken zoals electrospray ionisatie (ESI) en matrix-assisted laser desorptie ionisatie (MALDI). Recent is ook ionmobiliteitsspectrometrie (IMS) geïntroduceerd voor eiwitanalyse. IMS kan worden gezien als gas-fase elektroforese en voegt een extra scheidingsdimensie toe

na de LC en voor de eigenlijke MS detectie. Vanwege de scheiding op basis van de fysische eigenschappen van een eiwit zoals lipofiliciteit, vorm en lading is IMS zeer interessant voor de analyse van eiwitten in hun natieve vorm.

In hoofdstuk VI beschrijven we de ontwikkeling en evaluatie van een kwantitatieve LC-HR-MS/MS methode voor de bepaling van het 22-kDa grote biofarmaceutische eiwit somatropine (recombinant humaan groeihormoon, rhGH) in rattenplasma. Om op een triple-quadrupole massaspectrometer een goede gevoeligheid en selectiviteit te verkrijgen is een grondige monsteropwerking nodig om interfererende tryptische peptiden te verwijderen die in de chromatogrammen van het signature peptide verschijnen vanwege het tamelijke wijde massa-extractie window (MEW) van 0.7 Da dat wordt gebruikt om ionen te selecteren voor detectie. De hogere massa-resolutie van HRMS maakt het gebruik mogelijk van een veel nauwer MEW, wat het aantal tryptische peptiden dat wordt geselecteerd in de massaspectrometer sterk kan beperken. Voor een uitvoerige evaluatie van de toepasbaarheid van HRMS voor de analyse van plasmadigesten hebben we een LC-HR-MS/MS methode opgezet op een QTOF instrument waarmee we drie peptiden kwantificeerden na digestie van somatropine met trypsine: LFDNMLR (aminozuren 9-16), SNLELLR (71-77) and FDTNSHNDDALLK (146-158). Na selectie van de precursorionen van deze peptiden door een quadrupool met unit-mass resolutie en daarna fragmentatie, werden de productionen softwarematig geselecteerd uit het opgenomen spectrum, waarmee we het MEW verkleinden van 0.5 tot 0.01 Da. Het aantal en de intensiteit van de interfererende pieken in de chromatogrammen werd daarmee sterk gereduceerd, hetgeen de bepaling van de drie signature peptides duidelijk vergemakkelijkte. De detectiegevoeligheid kon verder worden verbeterd door de meetsignalen van meerdere productionen van elk signature peptide te sommeren. Dit maakte kwantificering met acceptabele accuraatheid en precisie mogelijk tot 25 ng/ml somatropine in rattenplasma, wat vier keer lager is dan met een vergelijkbare methode op een triple-quadrupole MS. De omstandigheden voor optimale selectiviteit en gevoeligheid varieerden van peptide tot peptide en in zijn algemeenheid moet de MEW instellingen en ook de sommering van meetsignalen worden geoptimaliseerd voor ieder nieuw signature peptide en bijbehorende product ionen. Samenvattend, hoewel de absolute instrumentele detectiegevoeligheid op een triple-quadrupole MS vaak beduidend beter is, kan het gebruik van HRMS toch leiden tot een gevoeliger methode, vanwege de mogelijkheid om interfererende peptiden uit de chromatogrammen te verwijderen door een nauwere MEW. Dit schept mogelijkheden om eiwitanalyse uit te voeren met een minder

uitgebreide monsteropwerking en kan de noodzaak tot het gebruik van extractiematerialen voorkomen en de benodigde tijd voor monstervoorbereiding reduceren.

De mogelijkheid om intact somatropine in plasma te kwantificeren met LC-HRMS is het onderwerp van hoofdstuk VII. Het vergelijkt kwantificering m.b.v. extracted-ion chromatogrammen (EIC's), die worden opgenomen met de detectieresponses van één of meerdere m/z waarden van het geladen eiwit, met deconvolutie: het construeren van een theoretisch ongeladen massaspectrum als basis voor de kwantificering. Tevens wordt de waarde van de MEW rond elk van de gekozen m/z waarden geëvalueerd. Hiertoe werd rattenplasma gespiket met somatropine op vier niveaus (10.0, 30.0, 100 en 500 ng/ml), de monsters geanalyseerd en chromatogrammen opgenomen met verschillende detectie-instellingen. EIC signalen werden bepaald voor elk van de vier meest intense ladingstoestanden (14+, 15+, 16+ and 17+) van somatropine alleen en voor de combinaties van twee, drie en vier ladingstoestanden. In alle gevallen werd hier een MEW gebruikt van 1.0 Da, wat overeenkomt met de inclusie van vrijwel alle isotopologen per ladingstoestand. Bij het gebruik van de som van de vier ladingstoestanden werd de MEW ook gereduceerd tot 0.25 Da (overeenkomend met de vier meest intense ionen) en tot 0.0625 Da (alleen het meest intense ion per ladingstoestand). Hoewel de absolute detectierespons het hoogste was als alle ladingstoestanden werden gebruikt en als de MEW het grootst was, bleek de signaal-ruis verhouding in alle gevallen ongeveer gelijk, wat betekent dat naast meer meetsignaal voor de analiet ook meer achtergrondruis wordt meegenomen. Bij de optimale instellingen werd de methode gevalideerd voor de EIC aanpak en de resultaten lieten zien dat de selectiviteit, gevoeligheid, accuraatheid en precisie van de methode onafhankelijk zijn van de MEW en het aantal gebruikte ladingstoestanden. Het deconvolueren van dezelfde data naar een gereconstrueerd massaspectrum van het neutrale eiwit (22124 Da) werd gebruikt als alternatieve aanpak. De resultaten voor precisie en accuraatheid lieten zien dat de prestatie van deze aanpak vergelijkbaar is met die van het gebruik van EIC's, maar dat de detectiegevoeligheid minder goed is: 30 ng/ml als acceptabele LLOQ tegenover 10 ng/ml voor de EIC aanpak. Beide methoden werden vervolgens gebruikt voor de analyse van plasmamonsters uit een preklinisch onderzoek en toonden aan dat ze beide bruikbaar zijn voor intacte-eiwitanalyse, met een goede correlatie ($R^2 > 0.97$) tussen de twee. Al met al laat dit onderzoek zien dat de kwantificering van intacte eiwitten met LC-HRMS potentieel zelfs gevoeliger kan zijn dan de analyse van eiwitten na digestie, als het wordt toegepast in combinatie met immunocapture als opwerkingstechniek.

LIST OF PUBLICATIONS

First author publications

P Bults, NC van de Merbel, R Bischoff

Quantification of biopharmaceuticals and biomarkers in complex biological matrices: a comparison of liquid chromatography coupled to tandem mass spectrometry and ligand binding assays.

Expert review of proteomics, 12 (4), 355-374, 34, 2015

P Bults, R Bischoff, H Bakker, JA Gietema, NC van de Merbel

LC-MS/MS-Based Monitoring of In Vivo Protein Biotransformation: Quantitative Determination of Trastuzumab and Its Deamidation Products in Human Plasma.

Analytical Chemistry, 88 (3), 1871-1877, 54, 2016

P Bults, M Meints, A Sonesson, M Knutsson, R Bischoff, NC van de Merbel

Improving selectivity and sensitivity of protein quantitation by LC-HR-MS/MS: determination of somatropin in rat plasma.

Bioanalysis, 10 (13), 1009-1021, 5, 2018

P Bults, B Spanov, O Olaleye, NC van de Merbel, R Bischoff

Intact protein bioanalysis by liquid chromatography-high-resolution mass spectrometry.

J Chromatogr B Analyt Technol Biomed Life Sci, 1110 (1111), 155-167, 12, 2019

P Bults, A Sonesson, M Knutsson, R Bischoff, NC van de Merbel

Intact protein quantification in biological samples by liquid chromatography-high-resolution mass spectrometry: somatropin in rat plasma.

Journal of Chromatography B, 1144, 122079, 2020

P Bults, A van der Voort, C Meijer, GS Sonke, R Bischoff, NC van de Merbel

Analytical and pharmacological consequences of the in vivo deamidation of trastuzumab and pertuzumab.

Analytical and Bioanalytical Chemistry (2022)

Other publications

C Liu, P Bults, R Bischoff, J Crommen, Q Wang, Z Jiang

Separation of deamidated peptides with mixed-mode chromatography using phospholipid-functionalized monolithic stationary phases.

Journal of Chromatography A, 1603, 417-421, 4, 2019

F Klont, SD Pouwels, P Bults, NC van de Merbel, NHT Ten Hacken, P Horvatovich, R Bischoff
Quantification of surfactant protein D (SPD) in human serum by liquid chromatography-mass spectrometry (LC-MS).

Talanta, 202, 507-513, 4, 2019

CURRICULUM VITAE

Peter Bults was born on September 15th 1977 in Borger, The Netherlands. He received his primary education in Borger, Bovensmilde and again in Borger. Also in Borger his MAVO diploma was obtained at the Esdal College in 1993. After finishing high school, Peter went to the Drenthe College and subsequently the Hogeschool Drenthe in Emmen to obtain his Bachelor's degree in analytical chemistry in the year 2004. His research project focused on evaluating the differences in protein content between several starch potato species by comparing their gel-electrophoreses patterns and subsequent chemometric data-analysis. After obtaining his Bachelor's degree Peter's first job was as an intern within the Analyst Development Program of the recruitment office Checkmark (Gouda, The Netherlands). He moved to Haarlem, Rotterdam and Weesp to work at several laboratories to work for three of the ADP partner companies over a three-year period. The first partner was the pharmaceuticals manufacturer TEVA Pharmachemie in Haarlem. Within this company he worked at the Quality Control laboratory doing product release testing using a variety of analytical techniques. The second partner were the SHELL Refineries in Rotterdam. Here his job was partly performing QC checks on "crude" oil products and their refined counterparts and partly it consisted of R&D-work with regards to waste water management. Techniques used here were mainly gas chromatography based. The final, and third, partner was the manufacturing site of Abbott, based in Weesp and world leading pharmaceutical company. Peter was responsible for the development of liquid chromatography coupled to mass spectrometry (LC-MS) methods used to support pre-clinical drug trials.

As of the 1st of October 2007, Peter moved to Assen and started his job at his current employer. Over the years, the company changed its name from Pharma Bio-Research (PBR) to PRA Health Sciences and just recently to ICON. Here, Peter started as a Technician, was promoted to Senior Technician and at the present moment fulfils the role of Scientist 1. As a Scientist, his role is to develop LC-MS methods, in close collaboration with colleagues and clients, supporting clinical trials. These methods vary from so-called "small" molecules to peptides and proteins analysis using an array of sample processing techniques and (high resolution) mass spectrometry as detection coupled to LC-systems.

In 2015 he got the opportunity to start with a PhD program at the University of Groningen, under supervision of Prof. dr. Nico van de Merbel and Prof. dr. Rainer Bischoff within the department of Analytical Biochemistry. This research project focused on two areas within the field of biomolecule analysis. The first part of his research focused

on the *in vivo* biotransformations that a biopharmaceutical may undergo and on the consequences this has for the results obtained and determined by LBA and LC-MS. The second part focused more on the technical and instrumental aspects of biopharmaceutical analysis and specifically on the use and capabilities of high resolution mass spectrometry. Peter completed his PhD project in the winter of 2021 and the outcomes of his project are presented in this Thesis.

ACKNOWLEDGMENTS

Several years were spent in the lab, performing the research that lead to this thesis. Speaking in terms applicable to one of my hobbies (track marshal at car and motorcycle events); “this was not a sprint race but an endurance race” and it might even be compared with a few seasons of endurance racing. As with racing, I started out as a so-called “rookie” and worked my way up the ranks with increasing experience. It was a race that I would not have finished without the help of many others on my team and with the necessary comments and “flag” signals from race control and team managers. Leaving behind the Geert Timmer corner and heading for the finish, I would like to use the next few pages for expressing my gratitude. I’m bound to forget to mention some people in the following chapter, so upfront my apologies for this and if you were in any way or form involved with me, in my live and work, thank you.

A year prior to the start of my PhD a fellow colleague at PRA Health Sciences, Kees Bronsema, was performing the last research experiments for his thesis at the Rijks Universiteit Groningen. Within the department of analytical biochemistry there was a close collaboration between Kees and Nico van de Merbel (PRA Health Sciences/ICON) and Rainer Bischoff, head of the department at the university. The scientific papers they’ve written where the first steps within the area of protein (bio)analysis for our lab and a big contribution to protein bioanalysis in general with a few papers considered as key papers by colleagues in the industry. While still at the university, Kees returned several times to the lab in Assen to share his knowledge regarding protein analysis based on protein digestion and subsequent peptide analysis. This would be my acquaintance with the subject of protein analysis and Nico had some thoughts on a project regarding this subject, to be performed at PRA Health Sciences. In hind sight, the experiments performed then and there, would be the bases for my first paper and for the invitation by Nico, with support of Peter Ketelaar, to start with a PhD project after Kees had successfully defended his thesis.

I am grateful for the opportunity given to me by Nico, Rainer and Peter to start and finish a PhD project with 6 published papers as a first author. Nico and Rainer, I am very grateful to have you both as my supervisors and sparring partners. Over the course of the last years, we had many discussions regarding protein analysis, ranging from sample preparation to biotransformation, on a philosophical level or more technically oriented. This resulted into new insights and many more experiments. The learning curve was quit steep, but you gave me time to grow and get a better understanding of performing research

at an academic level. Not realizing, at the start of the project, writing a scientific paper is an art form. This is mastered by Nico and Rainer and this was absolutely noticeable after sharing my first draft paper. Being quite confident, it was somewhat of a shock to receive the revised paper. Who would of thought, for example, the same conclusions could be summarized in one page instead of the three pages I needed to conclude all the experiments and results. Besides the writing and choice of words, they also thought me how to prepare figures and tables, which can easily be understood by a person with less knowledge regarding the subject at matter. This was extremely helpful when I had to present our work to foreign colleagues, students and researchers. It, overall, made me a more confident scientist who likes to share his work with others, made possible with the tools you all taught me. Also, without the prior knowledge, shared by Kees, I doubt it if we would have published these 6 papers within the same timeframe. So Kees, even if you are not mentioned as an author on the published papers, you still are one of the important colleagues who has made this research possible.

With this project being finished, it is also nearly the finish line for Rainer, who will retire soon and can look back at a great academic career with many outstanding papers, presentations and classes taught. As a person Rainer welcomed me with open arms into his research group and had always a listening ear and good advice. Besides that, we had nice conversations with topics as (winter)sports, holidays and the occasional beer preferences. I wish you all the best for your retirement and hope you will have many long and healthy hiking- and cycling trips with your wife and family.

Nico, I hope we will continue to be colleagues for many more years here at ICON, formerly PRA Health Sciences. We, as in the science team at ICON, have a scientific director who still has the same enthusiasm as 10-15 years ago and loves to teach and guide us through difficult method developments. Within the global bioanalytical community you have become one of the pillars regarding “industrial” bioanalysis. We, as a team, can contribute a lot more over the coming years, with the ultimate goal to help as much patients as possible with access to newly developed medicine. Besides the professional relation, on a personal notice, we’ve had some great times outside of the lab with the Christmas parties, new years drinks and summer BBQ’s as highlights. Always time for a nice chat and a listening ear. Recently you started to take an extra day off work, ones every two weeks. For you, a nice chance to enjoy some spare time with Trudy and the kids. Well deserved.

This research would also not be possible without the collaboration with my co-authors and I would like to thank you all for your contribution, discussions and input into the 6

papers we've published together. Both reviews were written in a collaboration between PRA and the RUG (Baubek Spanov, Oladapo Olaleye, Rainer and Nico). The first paper regarding biotransformation was prepared with the help of colleagues and fellow researchers of the pharmacy and the oncology department at the UMCG (Jourik Gietema). Our second paper on biotransformation was a collaboration between PRA, the RUG, the division of medical oncology at the Netherlands Cancer Institute (Anna van der Voort, Gabe Sonk, Elise van Leeuwen and Susan van den Berg) and again the oncology department at the UMCG (Jourik Gietema and Coby Meijer). Both papers regarding hr-MS were the end products of a close collaboration between PRA, the RUG and Ferring Pharmaceuticals (Magnus Knutsson and Anders Sonesson).

The results of chapter 3 and 4 would not have been as meaningful as they are now, without the informed consent of patients enrolled into the clinical studies of which we have analyzed several hundreds of plasma samples. Ultimately, they are the reason why we do research into new bioanalytical techniques, both instrumental and sample preparation wise. With new insights into biotransformation, emerging techniques such as hr-MS, capillary electrophoreses coupled to MS, intact protein analysis and a combination of immunocapture based sample preparation combined with LC-MS analysis, we hope to help and speed-up the development of new medicine so patients can be treated better and more efficiently. I hope the experimental treatments were and still are successful for the patients who enrolled into these studies, although we know this is not always the case, and we thank you for participating in clinical research trails.

Chapter 6 and 7 are also the result of a close collaboration with SCIEX and we thank Roddy Poodt, René van Wissen, Bertram Nieland, Kerstin Pohl, Dries Vrielink and their entire support team for the opportunity to analyze samples using their SCIEX Triple-TOF 6600. I have learned so much regarding high resolution mass spectrometry from all of you and this definitely helped me a lot in the research and experiments performed with regards to the two hr-MS papers. We've got some great value out of the two years we were allowed to use, on loan basis, the hr-MS-system. Due to the experience and practical knowledge gained at the university, ICON has decided to purchase a hr-MS (SCIEX 6600 Triple TOF) and at the moment it is fully used to support LC-MS method development for both small and large molecules. It will be used for many more years as it is an excellent platform for method development, trouble shooting and analyzing samples which have chromatographic interferences on different systems.

Dear members of the assessment committee, I would like to thank you all for the time and effort you've spend reading and assessing this thesis. While writing these acknowledgements, I'm wondering what kind of questions I will need to answer during my defense, a few months away from now. Your all experts in different areas and I hope we can have some nice discussions during and after my thesis defense. I hope, in the end, you all will be satisfied with my answers and wave the checkered flag.

During the past 4 years, spend at the University of Groningen, I've met quite a number of new colleagues and inters. You've all been very helpful with introducing me to new equipment, a new lab, setting up new experiments and relieving some inevitable stress. As members of the staff of the department; Jos, Marcel, Hjalmar, Peter, Natalia, Annie, Margot, Jan Willem, Ydwine and Walid, you were always willing to help and lend a hand with theoretical and practical issues. Not only for me, but also for all other students that passed through the department over the past years. The casual chats during the coffee breaks and lunch will be missed. Jolanda, I thank you for the time and effort you dedicated to making me acquainted with all the bureaucratic rules and regulations within the university and make them work for me. In these years there were also other contributors to my research. Within several projects I had the pleasure of supervising great students who performed extra experiments needed for the research papers. Marcel, Lisa, Naomi, Hedwich, Robin and Andrea thank you for all your help and you've all got great potential for a future career in science. My fellow PhD students and colleagues, who became more than colleagues: Frank, Andres, Turhan, Marcel and Naomi. Thank you for your friendship and the good company during my time in Groningen at the University and in the evenings, in the local pubs, for some epic nights of beer tasting, talks and having fun.

Within the science department small molecules of ICON, I have a number of awesome colleagues, who make work very enjoyable. Always time for a laugh, chat, occasional dance and always working together as a team. Sharing experiences varying from easy to the difficult method developments. Sharing new insights gained and helping with new problems and issues encountered. On occasion trying to trigger one of my odd personal quirks and have fun besides work. So, many thanks to: Remco, Kees, Henk, Roderik, Frank, Steven, Peter, Harry and Sanne.

During my project, I also had a few encounters with some medical professionals, not related to my experimental work. In this period I had surgeries on my stomach and on a badly inflamed elbow, from both I've recovered completely. In the final period, while writing my final paper and this thesis, I've had a quite severe car crash, which resulted in

a broken breastbone, ribs, a broken back (vertebra) and some other issues. While writing this, I'm still recovering and I am optimistic in a full recovery. Thus, I would like to offer my sincere gratitude to the hospital staff at the ISALA in Zwolle, WZA in Assen and the UMCG in Groningen for fixing me and slowly upgrading me to Peter 2.0.

A big thank you goes out to my family: Herman, Jelly, Gerd-Jan, Ayla, Joas, Jan, Jantje († 2021) and Jan-Tinus. You were always there when needed. Helping when moving houses during the past few years, 3 times up until now. Visiting the race track together and going abroad to follow our idols, racing in the Moto3, Moto2 and MotoGP. It definitely helped me to get my thoughts cleared and go back to work with a refreshed mind. Herman also was one of my fellow marshals at the TT race track in Assen. This year, 2022, will be the last year we are together behind the guardrails because you will retire from marshalling. Lets make it a year to remember.

Also the fishing trips with Peter, Peter, Albert, Andre, Dennis, Henko, Jurjen, Johan and Sievert to Norway and Sweden were, and still are, a great way to relax, have fun, BBQ, have some beers and fish. I look back on all our holidays with great pleasure and will have some awesome stories to reflect on when we are "old". And hopefully we have many more trips in the future.

My final thoughts go out to my Jeanine. During the past years working on this thesis, writing and performing experiments, you were there to take care of all little chores in and around the house. Giving me time to do some extra work in weekends and evenings. With the PhD reaching its end, we will have more time to spent with each other, the cats (Sam, Jacky and Dani), our dog Mick and family and friends. The last few years we've had ups and downs in with regards to our health. I'm nearly recovered from my latest car crash and you are still recovering from a fall down the stairs during a holiday break. We could not have foreseen what kind of an impact that would have on our lives and especially on yours. I will support you with all choices that will be made and hopefully lead to living a normal live without the headaches, fatigue and frustrations. It will be a long road, but I will try to support you as much as you have supported me. It will make our bond even stronger and I can't wait to see and experience what the future has in store for us.

With these words being said, it is time to conclude this chapter and thank you all once more. Cheers!